Production of 3-hydroxypropionate-containing polymers by engineered *Cupriavidus necator* H16

Callum Stewart McGregor (BSc)

Thesis submitted to the University of Nottingham for the degree of Doctor of Philosophy

October 2020

Declaration

Unless otherwise acknowledged, the work presented in this thesis is my own. No part has been submitted for another degree at the University of Nottingham or any other institute of learning.

Callum Stewart McGregor, October 2020

Abstract

Alternative materials are needed to replace traditional plastics, since their production and recalcitrance in nature have negative effects on the environment. Polyhydroxyalkanoates (PHAs) are bacterially synthesised polymers which are potential alternatives to plastic on account of their availability from renewable sources, plastic-like properties and biodegradability.

Cupriavidus necator H16 is a model organism for PHA production and is also capable of using CO_2 as a carbon source. Therefore, an opportunity exists for producing biodegradable plastics and other valuable chemicals from CO_2 using engineered strains of *C. necator* H16. However, the PHA which is produced by *C. necator* H16, polyhydroxybutyrate (PHB), does not possess properties which are ideal for the manufacture of plastic products.

PHA copolymers, which consist of more than one type of monomer, can often exhibit better properties than PHA homopolymers, such as PHB. Therefore, in this study, the primary goal was to produce the PHA copolymer poly(3-hydroxybutyrate-*co*-3-hydroxypropionate (poly(3HB-*co*-3HP) using engineered *C. necator* H16. In comparison to PHB, poly(3HB-*co*-3HP) is less crystalline, has a lower melting temperature, and a lower glass transition temperature than PHB, which significantly improves its processability. Through plasmid engineering, medium alteration, and suppression of 3HB-CoA formation, it was possible to produce poly(3HB-*co*-3HP) containing a 3HP molar fraction of between 0 and 91 mol% 3HP using *C. necator* H16. Previously, the highest 3HP molar fraction reported

in a poly(3HB-*co*-3HP) copolymer produced by an engineered strain of *C. necator* H16 was 1 mol%.

While PHAs are the most studied biodegradable polymer, a more recent development in the field of biobased materials is the production of polymers containing β-methyl-Δ-valerolactone (βMΔVL). βMΔVL is derived from mevalonate, and can be used in the synthesis of homopolymers or reacted with other compounds to produce copolymers. Mevalonate can be synthesised by engineered *C. necator* H16, and other mevalonate-derived compounds have been produced from *C. necator* H16 from CO_2. Therefore an opportunity to produce novel biodegradable polymer precursors from CO_2 arises. To attempt to stabilize mevalonate biosynthesis in a bioreactor, a plasmid addiction system was also tested. Using a metabolism-based plasmid addiction system it was possible to co-produce approximately 14 g/L mevalonate and over 10 g/L PHB from CO_2 in autotrophic batch fermentation. However, during autotrophic continuous fermentation the plasmid addiction system did not support stable mevalonate production.

The results presented in this thesis indicate several directions for future research to continue developing a poly(3HB-*co*-3HP)-producing strain of *C. necator* H16. It was also found that *C. necator* H16 could be engineered to produce significant quantities of mevalonate from CO_2, although further work is required to implement a stable plasmid for use in high-density autotrophic cultivation of this organism.

Acknowledgements

Firstly I would like to thank my supervisors, Katalin Kovács and Nigel Minton. After encouraging me to apply for a PhD through the BBSRC DTP, their support, guidance, and expertise has been constant during my work on this PhD.

I would also like to thank the countless people who have given invaluable advice, friendship, and assistance during my time in CBS. This PhD and my time in Nottingham would not have been the experience it was without their contributions.

Special thanks must go to my family, who have given me so much to be grateful for. Thank you for all of your love and support, and for always encouraging me to work hard and to the best of my abilities.

Finally, I would like to thank Mariya Konstantinova for the joy, inspiration, and excitement she brings into my life.

Table of Contents

List of Figures

List of Tables

Abbreviations

3HB	3-hydroxybutyrate
3HB-CoA	3-hydroxybutyryl-CoA
3HHx	3-hydroxyhexanoate
3HP	3-hydroxypropionate
3HP-CoA	3-hydroxypropionyl-CoA
3HV	3-hydroxyvalerate
4HB	4-hydroxybutyrate
bp	base pair
CDW	cell dry weight
DNA	deoxyribonucleic acid
EBI	European Bioinformatics Institute
eyfP	enhanced yellow fluorescent protein
FOA	Fluoroorotic acid

g	gram
GCMS	gas chromatography-mass spectrometry
Gm	gentamicin
HA	hydroxyalkanoate
HPLC	high-performance liquid chromatography
KEGG	Kyoto Encyclopedia of Genes and Genomes
L	litre
LB	lysogeny Broth
LSLB	low salt lysogeny broth
m	metre
mL	millilitre
mm	millimetre
mM	millimolar
MM	minimal medium
NCBI	National Center for Biotechnology Information
nm	Nanometre
OD	optical density
PBS	phosphate-buffered saline

PCR	polymerase chain reaction
PHA	polyhydroxyalkanoate
PHB	polyhydroxybutyrate
pmol	picomol
RBS	ribosome binding site
rpm	revolutions per minute
SGMM	sodium gluconate minimal medium
TAE	Tris-acetate-EDTA buffer
Tet	tetracycline
v/v	volume/volume
w/v	weight/volume
µg	microgram
µl	microlitre
Mm	micrometer
°C	degrees Celsius

Chapter 1: Introduction

1.1 General Introduction

Modern life is heavily dependent on the exploitation of fossil reserves to manufacture everyday chemicals, materials and fuels. This is particularly the case for plastic production. This reliance poses numerous problems for a world in which concerns about climate change are continuing to grow. Firstly, fossil reserves are finite. Therefore, the feedstock for plastic production is limited. Additionally, plastic production is highly polluting and results in significant carbon dioxide (CO_2) release. Furthermore, fossil-fuel derived plastics are recalcitrant in nature, leading to accumulation in and damage to the environment. Based on this, it is evident that alternatives to traditional plastics are required.

Polyhydroxyalkanoates (PHAs) are a polymeric storage compound accumulated by numerous bacteria in response to nutrient-limiting conditions. While bacteria use PHAs as a carbon and energy source, PHAs can also be extracted and purified from the bacteria to form a material with properties similar to plastic. Since bacteria are capable of growing on a range of carbon sources, this presents the opportunity of producing alternatives to plastic without the need for fossil fuels. Another advantage of PHAs is that they are biodegradable. PHAs are therefore a promising candidate for replacing fossil fuel-derived plastics.

A major challenge of replacing traditional plastics with PHAs is ensuring properties of the polymer are able to closely match those of traditional plastics. The properties of PHAs can be modulated by changing the composition of the polymer such that more than one monomer species is present, resulting in a copolymer. The properties of the copolymer can be

further influenced by the ratio of the monomers relative to one another. It is therefore possible to produce biodegradable plastics with controllable properties.

Cupriavidus necator H16 (*C. necator* H16) is a Gram-negative betaproteobacterium found in soil and freshwater, first identified in 1961. *C. necator* H16 is widely regarded as the model organism for PHA production, as it naturally accumulates a species of PHA known as polyhydroxybutyrate (PHB). Additionally, *C. necator* H16 is capable of growing and producing PHB using CO_2 and hydrogen (H_2) as sole carbon and energy sources, highlighting a route for biodegradable plastic production from CO_2. While *C. necator* H16 is capable of accumulating large quantities of PHB, the properties of PHB are not ideally suited for plastic product manufacturing. Therefore it is necessary to improve the properties of PHB by including a second monomer. It has been shown that inclusion of 3-hydroxypropionate (3HP), a three-carbon compound, in PHB results in improved polymer properties. The main aim of this project therefore was to engineer *C. necator* H16 such that it is capable of producing poly(3-hydroxybutyrate-*co*-3-hydroxypropionate) with a range of 3-hydroxypropionate content, with the intention of producing such polymers from CO_2 in the future. Recently, biodegradable polymers containing mevalonate-derived compounds have been described. Therefore, second goal of this work was to produce mevalonate from CO_2 using *C. necator* H16, thereby expanding the range of polymers available from *C. necator* H16.

1.2 Background

1.2.1 Traditional plastics – pollution from production

Fossil fuels are currently consumed in vast quantities to provide energy for electricity, heating, and transportation. More than 80% of energy consumed in 2017 was derived from oil, gas, or coal (1). However, heavy dependence on fossil fuels poses serious problems for the future of the planet. Firstly, fossil fuels are a finite resource. At current consumption levels, it is expected that known oil, gas, and coal reserves could last another 50, 51, and 132 years respectively (2)**.** A second major issue is the level of pollution caused by fossil fuel consumption. It is estimated that almost 33,000 million tonnes of CO_2 were released into the atmosphere in 2017 (1)**.** More than 99% of this CO_2 was released due to consumption of oil, gas, and coal. CO_2 is a greenhouse gas, and therefore known to contribute to global warming. Expected effects of continued global warming include changing weather patterns and more frequent extreme weather events, both of which will affect global food supply (3,4)**.**

Replacement of fossil fuels with alternative feedstocks will also mean finding other ways of producing countless fossil fuel-derived goods. For example, fossil fuel provide the precursor chemicals for many products essential to everyday life, including tyres, fertilizers, and plastics (5). Plastics in particular constitute an essential global commodity, and are used in virtually every aspect of day to day life, including packaging, the automotive, construction, and medical sectors, as well as in household and sporting goods. Numerous beneficial traits of plastics have led to their widespread proliferation in society. They are extremely cheap to produce,

highly durable, easy to process and manufacture, and exhibit a very wide range of properties, from hard plastics to elastic films, allowing them to be used for a multitude of functions.

In order to fulfil the thousands of roles in which plastics are involved, a huge amount of plastic must be produced, and a significant amount of fossil fuel is required for this. Between four and eight percent of all oil produced is devoted to the manufacture of plastics (6). A recent report estimated that this resulted in the production of 380 million tonnes of plastic in 2015, up from only two million tonnes in 1950 (7). The same report calculated that the total amount of plastic ever produced is around 8300 million tonnes.

This gives cause for concern, as the process of plastic production is highly polluting. Transporting oil from the well to refinery alone, prior to any refining or plastic production, accounts for significant quantities of CO_2 emission. Global extraction and transport of oil to refineries resulted in the release of approximately 1.7 Gt of CO_2 into the atmosphere in 2015 (8). Considering that between four and eight percent of oil is destined for use in plastic production, between 68 and 136 million tonnes of CO_2 can be attributed to the extraction and transport of oil for plastic production. Due to the diverse ways in which plastics are manufactured, it is difficult to accurately assess the emissions of the plastic production process after this stage. It is estimated, however, that the production of one tonne of plastic will result in the production of around 1.89 tonnes of CO_2 (9)**.** Despite the environmental concerns associated with emissions from fossil fuel-derived plastics, production is unlikely to decrease soon. The American Chemistry

Council have predicted an increase in US plastic sales from USD 6.5 billion in 2014 to USD 21.5 billion by 2030 due to newly discovered shale gas reserves (10), while analysis by Material Economics estimates that increasing demand for plastic in Asia and Africa could drive global plastic production up to approximately 800 million tonnes per year by 2050 (11).

1.2.2 Traditional plastics – recalcitrance in nature

A second concern is that plastics are highly durable, and do not readily biodegrade in nature. In certain roles, non-biodegradability of the plastic is essential. For instance, plastics used in building and construction materials, or those used in the automotive or engineering sectors are typically expected to undergo several years or even decades worth of use. The property of non-biodegradability becomes a more serious problem when plastics are applied in single use applications, such as in packaging. It has been estimated that a PET bottle remains intact and robust in seawater for at least 15 years before any signs of decomposition begin to appear (12). A second report calculated that a PET bottle buried in landfill, where conditions for decomposition are much less favourable, may have a half-life of around 2500 years (13). Recalcitrance of plastic in the environment coupled with the amount of plastic entering the environment has several negative consequences for fish, animals, and humans.

The majority of discarded plastic ends up entering landfills or the natural environment (7). While recycling and incineration are end of life options for plastics, only around 7% and 10% of plastics have been treated by these means, respectively. On the other hand, 60% of all plastic ever produced is estimated to be in landfills or the natural environment (7). A

considerable amount of discarded plastic also ends up in oceans; it is thought that as much as 12.7 million tonnes of plastic may have entered the ocean in 2015 alone (14). Evidence that plastic could be detected at all ocean levels, including discovery of a plastic bag at the bottom of the Mariana Trench almost 11km beneath the surface, highlights the extent to which plastic pollutes the environment (15).

Such ubiquitous plastic pollution poses significant risk to animals and fish, as well as humans. Animals and fish can become trapped in plastic, or consume it, potentially resulting in death. Another factor to consider is the increasing presence of microplastics in the natural environment. As larger single plastic items break down, they release smaller particles of plastic, termed "microplastics" (16). The effects of microplastics on human health are not yet understood, and studies are currently limited (17). Studies using test organisms however indicate potential for disrupted metabolism, effects on bone density, and induction of the inflammatory response (18–20). Since microplastics are believed to be present in numerous common food items, their consumption by humans is highly likely (17). Furthermore, the global economic damage resulting from lost tourism, disruption to fisheries, and clean-up operations amongst other factors, is predicted to be around USD 0.5-2.5 trillion per year (21).

Single use plastics, such as those used in packaging, are major contributors to plastic pollution. It is estimated that roughly 40% of all plastic produced is used in packaging, the majority of which is made of polypropylene (PP), polyethylene (PE), and polyethylene terephthalate (PET) (22). Given that 380 million tonnes of plastic were produced in 2015,

it can be estimated that around 150 million tonnes of plastic packaging was produced in the same year. Plastic packaging is predicted to have a mean lifespan of less than one year; the plastic is produced, sold, used, and disposed of in that time (7). As a result, plastic packaging is estimated to have resulted in the generation of around 140 million tonnes of plastic waste in 2015 (7). While there are no estimates on how much plastic in the environment is derived specifically from plastic packaging, it is likely that a significant amount of plastic pollution can be traced to plastic used for packaging. The reasons for this are three-fold: 1) 40% of all plastic produced is used for packaging; 2) plastic packaging is typically produced, sold, used, and discarded within one year, generating a substantial amount of plastic waste, and; 3) plastic is far more likely to end up in landfill or the environment than it is to be recycled or incinerated (7,22).

The recalcitrance of plastics is a desirable property during the life time of a plastic product, however, becomes problematic once that plastic is disposed of, since most discarded plastic ends up in the environment. The large amounts of plastic environment have several negative consequences and potentially many as-yet unknown effects. To combat the vast amounts of plastic pollution, biodegradable alternatives are needed, particularly in sectors such as packaging.

1.3 Current alternatives to traditional plastics

As the effect of plastics on the environment has garnered more attention, so too has interest in the production of materials which can replace plastics without the associated disadvantages. The finite nature of fossil fuel also necessitates adoption of alternative materials. An alternative

material would ideally be derived from renewable and sustainable feedstocks, in order to avoid the need to extract and refine fossil fuels. Such a material would also be biodegradable, to avoid dangerous accumulation of plastic in the environment. As a result, research interest has been growing in the field of bioplastics. In the last 20 years, the number of scientific publications related to bioplastic has been increasing **[Figure 1.1]**.

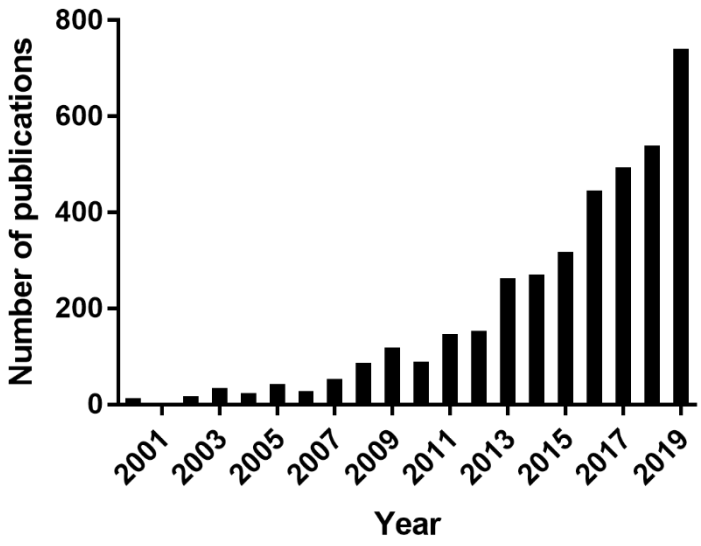

Figure 1.1 – Increasing discussion about "bioplastic" over the last two decades. Publications containing the keyword "bioplastic" have increased from 13 in the year 2000, to 740 in 2019. Data obtained by searching keyword "bioplastic" using scientific search engine ScienceDirect.

The term "bioplastic" has a broad definition, and can be considered to mean a plastic which is derived from renewable material, or a plastic which is biodegradable or compostable. Certain bioplastics are both renewable and biodegradable or compostable. This definition also means however that biodegradable materials can be made from unsustainable feedstocks, such as fossil fuels, and still be considered bioplastics **[Figure 1.2].**

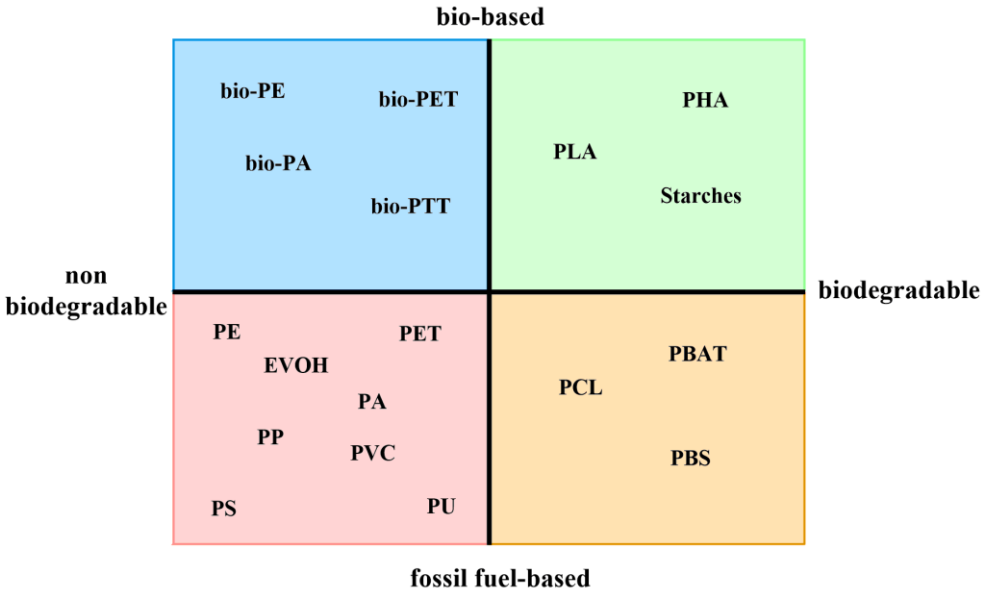

Figure 1.2 – Grouping of selected plastic and bioplastic materials based on feedstock and biodegradability. Traditional plastics are derived from fossil fuels and are non-biodegradable (red quadrant). More than 60% of bioplastics are bio-based, but non-biodegradable. While the raw materials are taken from renewable sources (e.g. biomass), the chemical composition is identical to that of traditional plastic (blue quadrant). Almost 14% of bioplastics are biodegradable, but use starting materials derived from fossil fuels (orange quadrant). Approximately 25% of bioplastics are both bio-based and biodegradable (green quadrant). PLA (polylactic acid), PHA (polyhydroxyalkanoate), PE (polyethylene), PET (polyethylene terephthalate), EVOH (ethylene vinyl alcohol), PA (polyamide) PP (polypropylene), PVC (polyvinyl chloride), PS (polystyrene), PU (polyurethane), PCL (polycaprolactone), PBAT (polybutylene adipate-*co*-butylene terephthalate), PBS (polybutylene succinate). Data for percentages, plastic/bioplastic names, and information on feedstock source and biodegradability were taken from (23–31).

The production of bioplastics represents less than 1% of global plastic production. Whereas in 2015 approximately 380 million tonnes of fossil fuel-based plastic was produced, only around 2.03 million tonnes of bioplastic was produced in the same year (32). Nonetheless, data from 2018

shows gradually increasing production of bioplastics, as global production increased to 2.61 million tonnes (23).

Unfortunately there are drawbacks to many bioplastics which limit their effectiveness at reducing damage to the environment. For instance, more than 61% of all bioplastics produced in 2018 were non-biodegradable (23). In these cases, the bioplastic is identical to traditional plastics, but the starting feedstocks have been derived from sources other than fossil fuels. For example, the most produced bioplastic in 2018 was bio-polyethylene terephthalate (bio-PET), a bio-based version of traditional PET, which accounted for more than 40% of all bioplastic produced (23). Whereas PET is traditionally produced from ethene and terephthalic acid derived from fossil fuels, bio-PET uses conversion of sugars or starch to acquire ethene. The terephthalic acid used for bio-PET is almost always fossil fuel-derived (33). Furthermore, regardless of how the bio-PET is produced, the chemical composition of PET and bio-PET is the same. Since PET is not biodegradable, bio-PET is also non-biodegradable. Thus bioplastics such as bio-PET fail to fulfil the requirements for an ideal alternative to traditional plastics, as they are non-biodegradable and persist in the environment.

As mentioned previously, a material can also be described as a bioplastic if the material is biodegradable or compostable. Approximately 39% of bioplastics produced in 2018 were considered biodegradable or compostable (23). However, a significant proportion of these biodegradable plastics are derived from fossil fuels. For instance, PBAT and PCL, which are biodegradable plastics produced from fossil fuels, currently occupy around 14% of the total bioplastic market (23). Such plastics are not a viable

alternative to traditional plastics due to dwindling fossil fuels resources, as outlined previously.

Currently, there are relatively few choices available which are both bio-based and biodegradable. These include polylactic acid (PLA), starch-based polymers, and polyhydroxyalkanoates (PHAs). PLA and starch-based polymers accounted for approximately 14 and 7% of all bioplastics produced in 2018 respectively, whereas about 4% could be attributed to PHAs (23). Due to their individual properties, different roles are ascribed to each of these types of polymer. PLA is composed of L-lactic acid and/or D-lactic acid, which are typically derived from microbial fermentation of sugars derived from foodstuffs such as sugarbeet or corn (34). Altering the ratio of lactic acid stereoisomers in the polymer influences the properties of the polymer, and expands the range of applications for PLA polymers. As a result of its biocompatibility and resorbability, PLA is commonly used in medical applications (35). Large-scale application of PLA in roles such as packaging are currently hindered, however as PLA is typically brittle, and biodegrades very slowly under non-ideal conditions (36,37). Alternatively, starch represents a low cost and abundant feedstock for polymer production, and is an attractive material for use in packaging as a result. Since the processability and properties of natural starch are limited, downstream treatment of starch is required to enhance the properties. Following treatment, the starch is typically more flexible, has a lower glass transition temperature, and more extensible (38,39). Despite this, starch-based polymers are brittle and are highly hydrophilic, and so cannot be used for packaging of wet products (38,40). Nonetheless, starch-based polymers

have applications as trays and films, and the ability of starch to form foams means it is capable of replacing polystyrene as loose-fill or packaging (40).

Unlike PLA and starch-based polymers, PHAs are a class of polymer produced in bacteria. PHAs have great potential as biodegradable polymers owing to the immense diversity of hydroxyalkanoate (HA) monomers which are available for incorporation into the polymer; more than 160 HA monomers have been identified to date (41). This diversity is reflected in the range of properties that PHAs can exhibit. PHAs can be brittle or flexible, transparent or opaque, and some have adhesive properties, depending on the composition of the polymer. On account of the biocompatibility, biodegradability, and varied properties shown by PHAs, they currently have applications in medical and packaging roles. As is the case with PLA and starch-based polymers, various drawbacks limit the widespread application of PHAs as biodegradable plastics. These limitations are largely associated with cost of production of the polymers *via* fermentation. Use of expensive starting substrates or precursors, and extraction of the polymer from cells increases costs, while low PHA content of the cells also negatively affects the economics of the process (42).

The large-scale production of PLA, starch-based polymers, and PHAs currently relies on sugars and starches derived from plants. These sugars and starches are converted by chemical and/or biological means into carbon compounds which can be polymerized to produce bioplastics. Food crops such as corn, wheat, sugarcane, or sugar beet are used to provide the biomass for production of these bioplastics in the vast majority of cases. The use of food materials as a feedstock is a controversial issue as it increases

pressure on already strained food supplies, and significant quantities of land and water are required for growing sufficient biomass (43). A preferable alternative would be to use waste materials as a source of carbon compounds for polymer production. Bacteria are capable of growing on a range of carbon sources including low purity, "dirty", or waste carbon sources, rather than refined sugars, which can be exploited to produce compounds and materials without encroaching on food supplies. Given that PHAs can be produced entirely in bacteria, are biodegradable, exhibit plastic-like properties, and are very diverse, it is valuable to investigate the possibility of producing PHAs from waste carbon sources using bacteria as cellular factories.

1.4 Bio-based and biodegradable plastics - Polyhydroxyalkanoates

Polyhydroxyalkanoates (PHAs) are a storage compound which certain bacteria accumulate in response to nutrient-limiting conditions **[Figure 1.3]**. PHAs were first described in 1926 by Maurice Lemoigne, who identified white granular deposits inside cells of *Bacillus megaterium* as poly(3-hydroxybutyrate) (PHB), a PHA composed of repeating units of 3-hydroxybutyrate (3HB) (44)**.**

Relatively little was known about the properties of PHAs until a 1958 study by Williamson and Wilkinson, which described dried PHB extracted from *Bacillus* species as having an appearance "somewhat reminiscent of plastic sheeting", and a melting temperature of approximately 170°C (45). The biodegradability of PHB by extracellular enzymes secreted from a species of *Pseudomonas* was later shown (46). The plastic-like appearance and biodegradability of PHB generated interest in

large-scale production of biodegradable plastic. In the early 1960s, patents for the extraction and use of PHB were filed (47,48). Later, Imperial Chemical Industries (ICI) attempted to commercialize the process for the purpose of large-scale manufacturing of biodegradable plastic products, however found the performance of PHB-based products was not a satisfactory replacement for plastics such as PP and PET (49). This is due to certain properties of PHB being sub-optimal. For instance, rapid thermal degradation of the polymer occurs at temperatures very close to the melting temperature. Kunioka and Doi showed that, while PHB exhibited a melting temperature of approximately 177°C, thermal degradation occurred within minutes at 175-180°C (50). Furthermore, PHB was found to have a crystallinity of approximately 60% (51). Higher crystallinity is associated with increased brittleness (52). As a result, PHB is a brittle polymer with low impact resistance (53). Due to the combination of these factors, PHB is not yet an ideal replacement for traditional plastics.

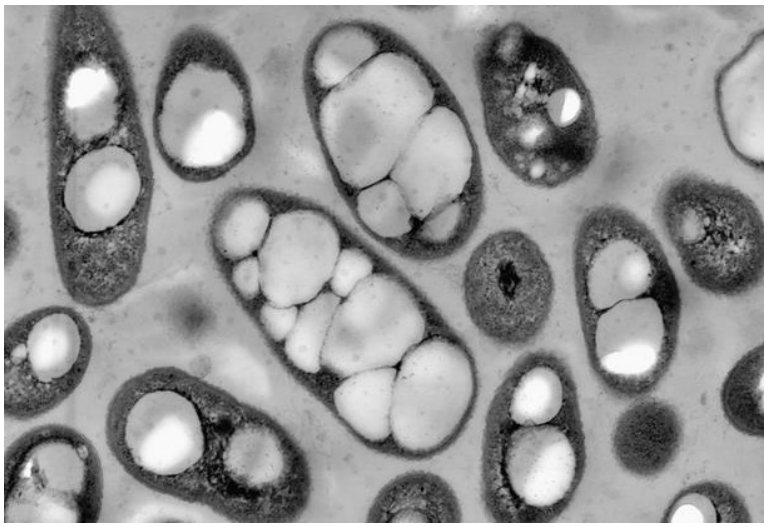

Figure 1.3 – Electron microscopy reveals the accumulation of PHB inside cells of *C. necator* H16. Image adapted from Koller *et al*. 2011 (54).

As the 100th anniversary of the discovery of PHAs approaches, PHAs have been found in at least 300 different microorganisms, and more than 160 HA monomers have been identified (41,55). **Table 1.1** highlights a selection of organisms which can natively accumulate PHAs, as well as the range of carbon sources from which PHAs were produced in these organisms.

Table 1.1 – Selection of organisms with native ability to accumulate PHAs

Organism	Substrate	PHA produced	Ref.
Cupriavidus necator H16	Fructose	PHB	(56)
	Gluconate	PHB	(57)
	CO_2	PHB	(58)
	Syngas	PHB	(59)
	Spent coffee grounds	PHB	(60)
Pseudomonas putida	Oleic acid	MCL-containing copolymers	(61)
Pseudomonas aeruginosa	Gluconate	MCL-containing copolymers	(62)
Bacillus megaterium	Sugarcane molasses	PHB	(63)
Alcaligenes latus	Sucrose	PHB	(64)
Haloferax mediterranei	Various	PHB	(65)
Methylosinus trichosporium OB3	Methane	PHB	(66)
Methylocystis parvus OBBP	Methane	PHB	(67)
Methylobacterium organophilum	Methane	PHB	(68)
Methylocystis spp.	Methane*	PHB	(69)
Rhodosporillum rubrum	Syngas	PHB	(70)
Azotobacter vinelandii	Beet molasses	PHB	(71)
Synechococcus sp. MA19	CO_2	PHB	(72)

Burkholderia sacchari	Wheat straw	PHB	(73)
Aeromonas caviae	Olive oil	poly(3HB-*co*-3HHx)	(74)
Aeromonas hydrophila	Various	poly(3HB-*co*-3HHx)	(75)
Chromobacterium sp. USM2	Various	PHB, poly(3HB-*co*-3HV)	(76)
Zooglea ramigera	Glucose	PHB	(77)
Chloroglea fritschii	Various	PHB	(78)
Synechocystis sp. PCC6803	Various	PHB	(79)
Rhodobacter sphaeroides	Various	PHB	(80)
Nostoc muscorum	Various	PHB	(81)

*****Methane was sourced from landfill and anaerobic digester gas.

From **Table 1.1** it can be seen that a range of organisms including hydrogen-oxidizing bacteria, methanotrophs, cyanobacteria, and microalgae have been shown to naturally accumulate PHAs and can do so using a variety of carbon sources, from sugars, to oils, to gases. While the range of microorganisms found to accumulate PHAs is broad, the best studied PHA biosynthetic pathway is that used by the chemolithoautotroph *C. necator* H16, which is also considered the model organism for PHA accumulation. The biosynthesis of PHB in *C. necator* H16 proceeds by a three-gene pathway described as the *phaCAB* operon (82). The first step is the condensation of two molecules of acetyl-CoA by the β-ketothiolase (PhaA), producing acetoacetyl-CoA. NADPH-dependent reduction of acetoacetyl-CoA to 3-hydroxybutyryl-CoA (3HB-CoA) is catalysed by an acetoacetyl-CoA reductase (PhaB). The polymerization of 3HB-CoA is facilitated by PHA synthase (PhaC) **[Figure 1.4]**.

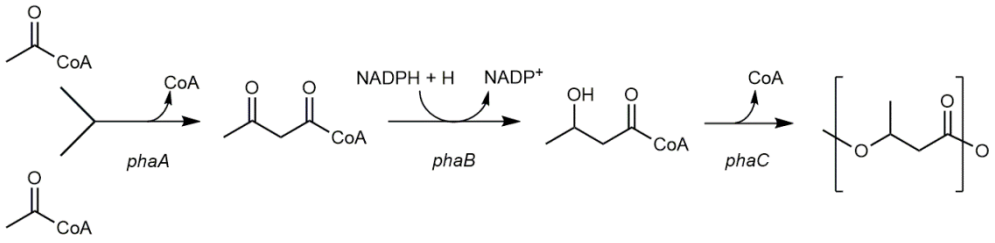

Figure 1.4 – The PHB biosynthesis pathway of *C. necator* H16, the model organism for PHA accumulation.

PHA synthases are the key enzymes of PHA biosynthesis, catalysing the incorporation of HA monomers into growing PHA chains. Generally PHA synthases have substrate specificity for short-chain-length (SCL) HA monomers of 3 – 5 carbons in length, or medium-chain-length (MCL) monomers of 6 – 14 carbons in length (83). For instance, the PHA synthase of *C. necator* H16 preferentially uses SCL HA monomers as substrates, while the PHA synthase of *Pseudomonas aeruginosa* has specificity for MCL HA monomers. Due to the relatively broad specificity of PHA synthases, and the wide range of HA monomers available, it is possible to produce PHAs consisting of more than one type of HA monomer.

The advent of metabolic and genetic engineering combined with an understanding of how PHA biosynthesis can occur has led to significant efforts to produce PHAs using microorganisms which do not natively accumulate PHAs and to engineer both natural and non-natural PHA producers to accumulate more varied PHAs, such as copolymers. **Table 1.2** highlights numerous studies describing the engineering of microorganisms for the production of diverse PHAs. Furthermore, a range of strategies

employed to confer, enhance, and alter PHA production is indicated in **Table 1.3.**

Table 2.2 – Engineering of organisms for production of diverse PHAs

PHA composition	Organism	Genes expressed	Carbon source	Ref.
Poly(2HB)	*E. coli*	pct_{Me}, $phaC1_{Ps}$	Glucose, sodium 2HB	(266)
Poly(3HB)	*E. coli*	$phaCAB_{Cn}$	LB + glucose	(267)
	C. autoethanogenum	$phaCAB_{Cn}$	Syngas	(268)
Poly(4HB)	*E. coli*	$phaC_{Cn}$, $orfZ_{Ck}$	Glucose, 4HB	(269)
Poly(3HP)	*E. coli*	$dhaB12_{Cb}$, $pduP_{Se}$, $phaC_{Cn}$	Glycerol	(106)
	K. pneumoniae	$dhaB123_{Kp}$, $gdrAB_{Kp}$, $aldH_{Ec}$, $prpE_{Ec}$, $phaC_{Cn}$	Glycerol	(115)
Poly(LA)	*E. coli*	pct_{Cp}, $phaC1_{Ps}$	Glucose	(270)
Poly(3HV)	*A. caviae*	vgb_{V}, $fadD_{Ec}$	Undecanoic acid	(271)
Poly(LA-*co*-3HB)	*E. coli*	pct_{Cp}, $phaAB_{Cn}$, $phaC1_{Ps}$	Glucose	(270)
Poly(3HB-*co*-4HB)	*E. coli* *****	$sucD_{Ck}$, $4hbd_{Ck}$, $orfZ_{Ck}$, $phaCAB_{Cn}$	Glucose	(272)
Poly(3HB-*co*-3HP)	*E. coli*	$dhaB_{Kp}$, $pduP_{Kp}$, $phaCAB_{Cn}$	Glycerol	(109)
	C. necator H16	mcr_{Ca}, acs_{Ca}	Various	(100)
	S. blattae	$aldD_{Pp}$, $dhaT_{Pp}$, pct_{Cp}, $phaCAB_{Cn}$	Glycerol	(117)

Poly(3HB-*co*-3HV)	*E. coli* Δ*prpC* Δ*scpC*	$cimA_{Mj}$, $leuBCD_{Ec}$, $poxB_{Ec}$, $prpE_{Cn}$, $phaCAB_{Cn}$	Glucose	(186)
	M. extorquens AM1 Δ*phaAC*	$bktB_{Cn}$, $phaJ1_{Pa}$, $phaC2_{Ra}$	Formate	(273)
	R. rubrum	$udhA_{Ec}$, $pntAB_{Ec}$, $phaB_{Cn}$	Syngas	(202)
Poly(3HB-*co*-3HHx)	*C. necator* NSDG **	-	Soybean oil	(274)
	C. necator NSDG	Ccr_{Me}, $phaJ4a_{Cn}$, emd_{Mm}	Fructose	(212)
	E coli	$orf1_{Ah}$, $phaJ_{Ah}$, $phaB_{Cn}$, $phaC_{Ac}$	Dodecanoic acid	(275)
Poly(3HB-*co*-4HB)	*H. bluephagenesis* ***	$orfZ_{Ck}$	Glucose	(276)
Poly(3HB-*co*-3HV-*co*-3HHx)	*C. necator* PHB¯4	$phaC_{Cs}$	CKPO + propionate/valerate	(200)
	C. necator Δ*phaB123*	$phaJ_{Pa}$, $phaA_{Pa}$, $phaC2_{Ra}$	Fructose + butyrate, propionate	(277)
Poly(3HB-*co*-3HHx-*co*-3HO)	*P. putida* Δ*phaC*	$phaC_{A\ sp.}$	Sodium heptanoate, oleic acid	(278)
Poly(MCL-3HA)	*P. putida* Δ*gcd*	-	Glucose	(279)

*****CRISPRi was also employed in order to downregulate genes involved in succinate metabolism. ******_C. necator_ NSDG is a mutant strain in which the native *phaC* gene has been replaced by an engineered PHA synthase from *A. caviae*. *******Promoter engineering was also employed to increase the 4HB molar fraction. 2HB – 2(hydroxybutyrate), LA – lactic acid, MCL – medium-chain-length, CKPO – crude palm kernel oil. *Ac*; *Aeromonas caviae*, *Ah*; *Aeromonas hydrophila*, *A.* sp.; *Alcaligenes* sp., *Ca*; *Chloroflexus aurantiacus*, *Cb*, *Clostridium butyricum*, *Ck*; *Clostridium kluyveri*, *Cn*;*Cupriavidus necator*, *Cp*; *Clostridium propionicum*, *Cs*; *Chromobacterium* sp. USM2, *Ec*; *Escherichia coli*, *Kp*; *Klebsiella pneumoniae*, *Me*; *Megasphera elsdenni*, *Mj*; *Methanococcus jannaschii*, *Mm*; *Mus musculus*, *Pa*; *Pseudomonas aeruginosa*, *Pp*; *Pseudomonas putida*, *Ps*; *Pseudomonas stutzeri* , *Ra*; *Rhodococcus aetherivorans*, *Se*; *Salmonella enterica* , *V*; *Vitreoscilla*

Table 1.3 – Methodologies employed for the production of PHAs

Approaches	PHA produced	Example	Ref.
Gene overexpression	PHB	*E. coli* engineered to produce PHB by overexpression of $phaCAB_{Cn}$	(267)
	Poly(3HB-*co*-3HP)	Overexpression of $phaCAB_{Cn}$ and $prpE_{St}$ genes in *E. coli* was employed to produce PHB and facilitate activation of exogenously supplied 3HP to 3HP-CoA, resulting in biosynthesis of copolymer	(119)
Gene deletion	Poly(3HB-*co*-3HV)	Deletion of numerous β-ketothiolases from the genome of *C. necator* H16 resulted in increasing molar fraction of 3HV.	(207)
	Poly(3HB-*co*-3HHx)	Deletion of *phaB1* and *fadB* resulted in increasing molar fraction of 3HHx monomer	(274)
Gene downregulation	Poly(3HB-*co*-4HB)	CRISPRi was employed to downregulate genes involved in metabolism of succinate. This approach successfully increased the molar fraction of 4HB in the copolymer by maintaining higher levels of succinate, a precursor to 4HB, in the cell.	(272)
Cell morphology engineering	Poly(LA-*co*-3HB)	Deletion of *mtgA* from the genome of engineered *E. coli* resulted in increased polymer accumulation.	(280)
Enzyme engineering	PLA, Poly(LA-*co*-3HB)	A propionyl-CoA transferase and PHA synthase were engineered to better accept lactic acid (LA) as a substrate, resulting in LA-containing copolymer	(281)

Promoter engineering	Poly(3HB-*co*-4HB)	Generation of a promoter library through saturation mutagenesis of the promoter core region was used to enhance the 4HB molar fraction and PHA content of the cells.	(276)
RBS engineering	PHB	Alteration of the RBS preceding each gene of the *phaCAB* operon in engineered *E. coli* was used to balance enzyme activity and resulted in *E. coli* strains which accumulated PHB contents of between 0% and 92%.	(282)
Block copolymer synthesis	Poly(3HB-*co*-4HB)	Selectively timing supplementation of HA precursors allowed generation of block copolymer.	(283)
Carbon source alteration	Poly(3HB-*co*-3HP)	Cultivation of *A. latus* in sucrose-containing medium resulted in a PHB homopolymer. Supplementation of the medium with 3HP was shown to result in biosynthesis of a copolymer, poly(3HB-*co*-3HP).	(51)
	Poly(3HB-*co*-3HV)	Cultivation of *C. necator* H16 in medium containing valerate as the only carbon source resulted in biosynthesis of poly(3HB-*co*-3HV), whereas only PHB was produced if only octanoate or oleate was available.	(207)
Two-step	Poly(3HB-*co*-3HP)	Cells of *S. blattae* were first cultivated in an anaerobic environment to facilitate the biosynthesis of 1,3-propanediol from glycerol. In a second step, cultivation mode was switched to aerobic conditions to convert 1,3-propanediol to 3HP which was subsequently incorporated into the PHA.	(100)
Co-culture	PHB	*C. necator* H16, which cannot use glucose as a carbon source, was co-cultured with *L. delbrueckii* to produce PHB. Glucose was metabolized to lactate by *L. delbrueckii*, which was then metabolized to PHB by *C. necator* H16.	(284)

1.5 Polyhydroxyalkanoates – The effect of altering monomer composition

As can be seen from **section 1.4**, a diverse range of PHA-producing organisms, both natural and non-natural, have been described. Additionally, these organisms have been shown to produce copolymers beyond simply PHB. The value of producing PHA copolymers is that inclusion of a second monomer results in a polymer with altered properties compared to the original homopolymer. Furthermore, the ratio of the two monomers can be modulated. In this manner it is possible to produce a range of polymers with different properties by varying the amount of one monomer present in the copolymer.

Frequently incorporated secondary HA monomers include 3-hydroxypropionate (3HP), 3-hydroxyvalerate (3HV), 3-hydroxyhexanoate (3HHx), and 4-hydroxybutyrate (4HB). As one of the most popular copolymers, the properties of poly(3HB-*co*-3HV) are relatively well described. As 3HV content increases to approximately 45 mol%, the melting temperature of the copolymer decreases from around 170°C down to near 60°C. As 3HV fraction increases further, melting temperature begins to rise again, reaching around 110°C when 3HV content is close to 100 mol% (50). On the other hand, the glass transition temperature decreases consistently as 3HV content increases (84). The decrease in melting temperature is beneficial for processing, as it means copolymers of poly(3HB-*co*-3HV) can be melted at temperature ranges far below that of thermal degradation, reducing the risk of polymer loss. However, increasing 3HV content has minimal effect on copolymer crystallinity, and higher

molar fractions of 3HV in a poly(3HB-*co*-3HV) copolymer are even shown to result in higher crystallinity than exhibited by PHB (85).

Copolymers of poly(3HB-*co*-3HHx) display unique mechanical and physical properties due to the combination of SCL and MCL monomers. At 3HHx content of around 30 mol%, poly(3HB-*co*-3HHx) is highly elastic and ductile (86). These properties make it similar to low-density polyethylene (LDPE). Interestingly, poly(3HB-*co*-3HHx) with 3HHx content above 70 mol% has been shown to be a gluey and sticky polymer, and as such has potential roles as an adhesive compound.

Another PHA copolymer displaying interesting properties depending on monomer ratio is poly(3HP-*co*-4HB). As well as exhibiting much greater elasticity and lower melting temperatures in comparison to PHB, poly(3HP-*co*-4HB) copolymers also possess interesting optical properties. By altering the 4HB content of the polymer it was possible to produce copolymers with different levels of transparency. For instance, poly(3HP-*co*-4HB) with 67 mol% 4HB was completely transparent, while copolymers with more or less 4HB were seen to be opaque (87). **Table 1.4** shows the thermal and mechanical properties of a range of PHAs compared to those of traditional plastics. The wide range of properties that can be achieved through diversifying PHA composition means PHAs can be used in a broad range of generic applications, including packaging, utensils, and containers, as well as more specialist applications such as scaffolds for tissue engineering, surgical sutures, and as drug delivery systems (88–90).

Table 3.4 – Comparison of the properties of traditional plastics with select PHAs

Material	**T_m (°C)**	**T_g (°C)**	**ΔH_m (J/g)**	**Crystallinity (%)**	***E* (MPa)**	**σ_t (MPa)**	**ε_b (%)**	**Ref.**
PP	170 – 176	-10 – -20	148	50 – 70	0.6 – 1.7	27 – 38	400 – 900	(90,285,286)
LDPE	88 – 130	-30 – -36	-	20 – 50	0.05 – 0.3	10 – 78	126 – 620	(90,285,286)
HDPE	112 – 135	-	216.94	75	0.4 – 1.0	18 – 33	12 – 700	(90,286,287)
PET	262	-	-	-	-	56	7300	(286)
PHB	177	4	97	61	1470	18	3	(51,288)
Poly(3HB-*co*-7% 3HP)	160	3	71	43	-	-	-	(51)
Poly(3HB-*co*-20% 3HP)	143	-1	18	28	-	-	-	(51)
Poly(3HB-*co*-77.5% 3HP)	73	-20	48	-	-	-	-	(101)
Poly(3HP)	78	-17.85 – -21	53.6	37	327.9 – 2889.3	21.54 – 26.5	497.6 – 583	(51,87,107)
Poly(3HB-*co*-20% 3HV)	145	-1	-	-	2.9	-	50	(289)
Poly(3HB-*co*-55% 3HV)	77	-10	-	-	-	16	>1200	(289)

Poly(3HB-*co*-71% 3HV)	83	-13	-	-	-	11	5	(289)
Poly(3HV)	106.2	-15.7	-	-	390	6.6	3.5	(288)
Poly(3HP-*co*-11.86% 4HB)	61.68	-24.42	-	-	3.9	48.82	1248.3	(87)
Poly(3HP-*co*-37.89% 4HB)	63.46	-36.14	-	-	4.4	0.54	1611.0	(87)
Poly(3HP-*co*-67% 4HB)	64.77	-41.87	-	-	1.8	0.34	429.2	(87)
Poly(4HB)	61	-47	-	-	180.9	34.66	696.6	(87)
Poly(3HB-*co*-10% 3HHx	127	-1	77	34	-	21	400	(290)
Poly(3HB-*co*-17% 3HHx	120	-2	34	26	-	20	850	(290)

Note; HDPE; high-density polyethylene, LDPE; low-density polyethylene, PET; polyethylene terephthalate, PP; polypropylene, T_m; melting temperature, T_g; glass transition temperature, ΔH_m; enthalpy of fusion, E; Young's Modulus, σ_t; tensile strength, ε_b; elongation at break

Based on the evidence presented above, PHA copolymers clearly have potential as a replacement for traditional plastics. A wide range of thermal and mechanical properties can be obtained, and other factors, such as transparency, can also be controlled. Additionally, PHAs can be produced from a range of carbon sources. Another copolymer which has been shown to exhibit promising properties is poly(3-hydroxybutyrate-*co*-3-hydroxypropionate) (poly(3HB-*co*-3HP).

1.5 Poly(3-hydroxybutyrate-*co*-3-hydroxypropionate)

1.5.1 Properties of poly(3-hydroxybutyrate-*co*-3-hydroxypropionate

Poly(3HB-*co*-3HP) can be produced if both 3HB and 3HP monomers are available for polymerization by PHA synthase. If 3HB is not available, it is also possible to produce a homopolymer of 3HP; poly(3HP). Biosynthesis of these polymers has required supplementation of the medium with 3HP or use of an artificial pathway. The development of engineered pathways now facilitates the biosynthesis of 3HP-containing polymers from various different carbon sources.

Nakamura and coworkers first reported the bacterial biosynthesis of poly(3HB-*co*-3HP) in 1991 by feeding *C. necator* H16 with 3HP. While only 7 mol% 3HP was included in the copolymer, the melting temperature was seen to decrease by almost 30°C, and the enthalpy of fusion also decreased, suggesting a concomitant decrease in crystallinity (91). Considering that high melting temperature and crystallinity are major drawbacks of PHB, the potential for a polymer more amenable to processing was clear. Subsequently it was shown that *Alcaligenes latus* (now known as

Azohydromonas lata (92)) was capable of incorporating greater amounts of 3HP into the polymer than *C. necator* H16. Studies in the 1990s and early 2000s therefore used *Alcaligenes latus* to produce poly(3HB-*co*-3HP) with higher 3HP molar fractions, allowing further characterization of the effect of increasing 3HP content (51,93–99). Additional studies of the thermal properties of poly(3HB-*co*-3HP) were later made by Fukui *et al.*, and Wang *et al.*, who used engineered *C. necator* H16 and *E. coli* to produce the polymer respectively (100,101). Compiling data from some of these publications, it can be seen that increasing 3HP molar fraction of the polymer has significant effects on the thermal properties of the polymer **[Figure 1.5]**. Glass transition temperature decreases consistently as 3HP molar fraction increases. On the other hand, crystallinity, melting temperature, and enthalpy of fusion decrease before increasing again as 3HP molar fraction increase. Since PHB is known to possess properties which are not ideal for manufacture of biodegradable plastics, addition of 3HP into the polymer results in a material with greater potential than PHB.

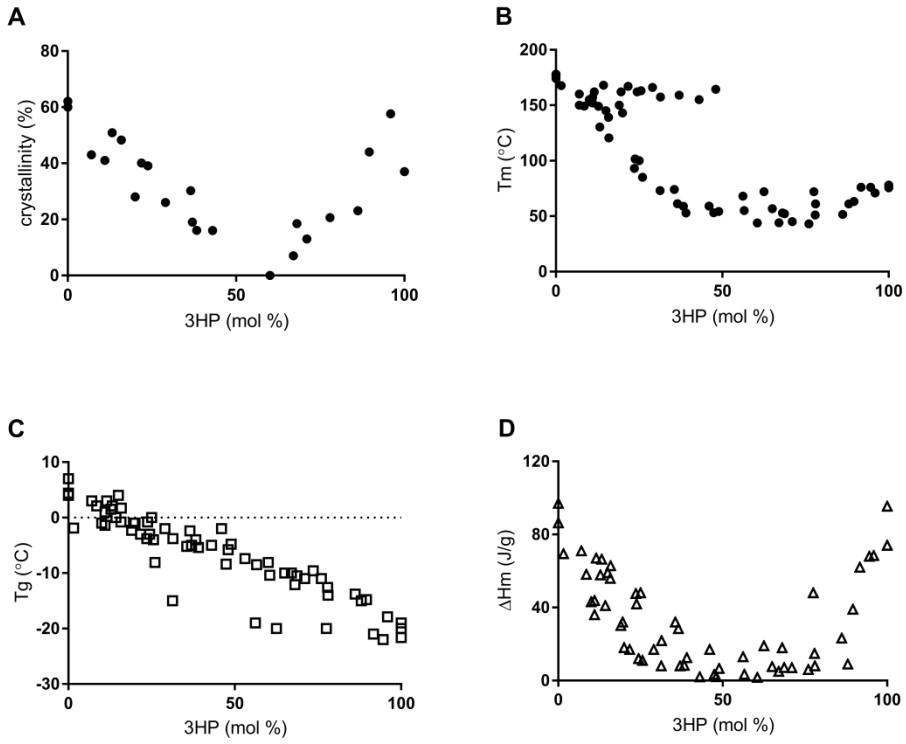

Figure 1.5 –Effect of changing 3HP molar fraction on the thermal properties of poly(3HB-*co*-3HP). The change in crystallinity (**A**), melting temperature (**B**), glass transition temperature (**C**), and enthalpy of fusion (**D**) are shown. Data was compiled from (51,91,93,96,97,99–101)**.**

The 3HP molar fraction has also been shown to influence the biodegradability of the polymer. The breakdown of poly(3HB-*co*-3HP) has been investigated by directly exposing the copolymer to purified PHA depolymerases, and also by environmental degradation. Shimamura *et al.* investigated the degradation of PHB and poly(3HB-*co*-3HP) by the PHA depolymerase from *Alcaligenes faecalis* (51)**.** Samples of PHB and poly(3HB-*co*-3HP) were incubated with the PHA depolymerase for 2 hours at 37°C. Their results showed that after 2 hours, only 0.3mg of PHB had been degraded, copolymers with a molar fraction of between 7 and 43 mol% had lost between 1 and 1.6mg of their weight. Studies by Cao *et al.*

investigated the degradation of both PHB and poly(3HB-*co*-3HP) in river water (102). PHB and copolymers containing a 3HP molar fraction of up to 95.9 mol% 3HP were observed to be degraded in the river water, and increased 3HP molar fraction was associated with faster degradation. However, degradation of poly(3HP) in the river water was not observed. Several other studies however have shown degradation of poly(3HP). Degradation of poly(3HP) could be achieved by numerous purified PHA depolymerases, and by microorganisms from a range of different environments including various water and soil sources (103–105).

In these early studies describing biosynthesis of poly(3HB-*co*-3HP), the polymer was produced by feeding bacteria with 3HP as a sole carbon source, or the 3HP was provided alongside sucrose or 3HB. In order to avoid feeding with 3HP and to use cheaper, more abundant carbon sources as precursors to 3HP, recombinant bacteria can be used. In line with advances in metabolic engineering, several pathways have been described which lead to production of the 3HP monomer.

1.5.2 Pathways to the 3HP monomer

Engineering of bacteria for the production of polymers containing 3HP, including poly(3HB-*co*-3HP), poly(3HP-*co*-4HB), and poly(3HP), has been described in numerous publications. While the focus of this thesis is on the production of poly(3HB-*co*-3HP), at this point it is important to consider 3HP-containing polymers in general, as various different pathways have been designed which lead to the 3HP monomer. The range of pathways and

carbon sources used to produce the 3HP monomer are reviewed below, and depicted in **Figure 1.6**.

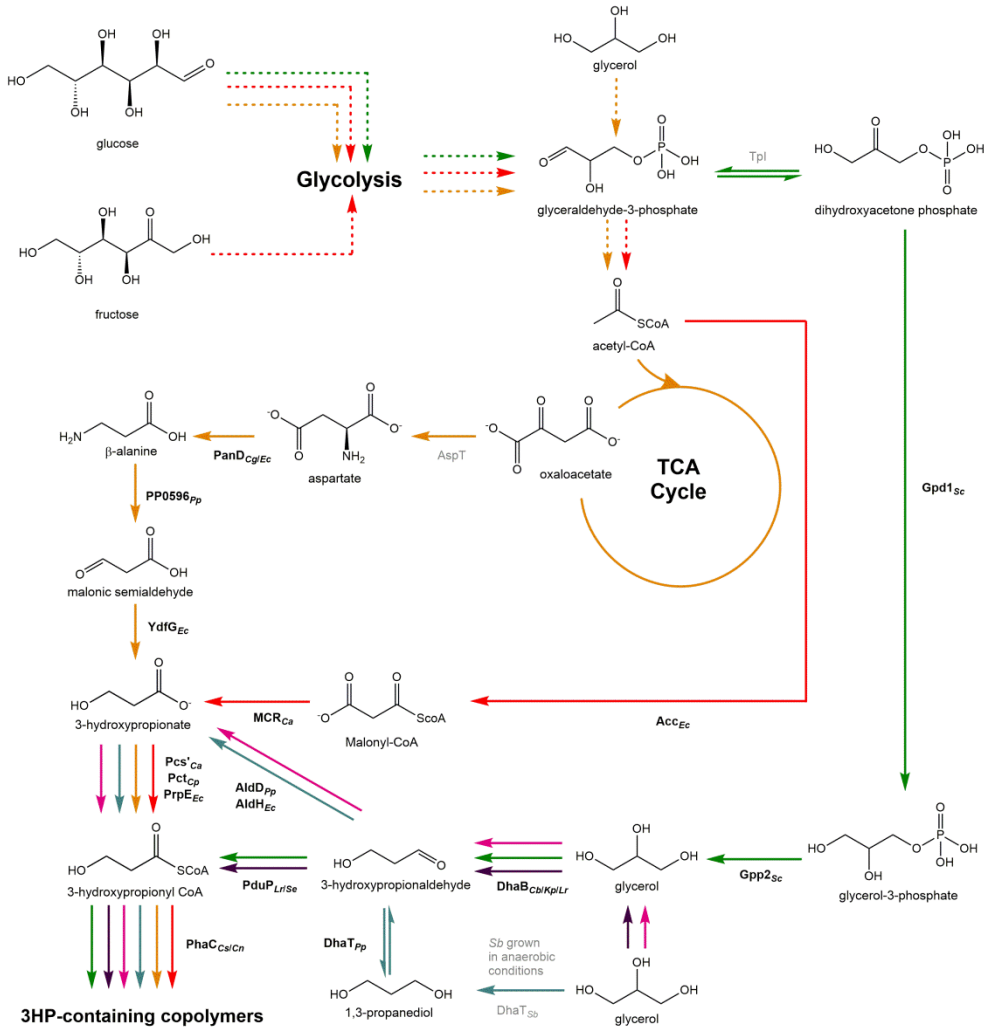

Figure 1.6 – Engineered pathways for the production of 3HP-containing copolymers using various carbon sources including glucose, fructose, glycerol, and 1,3-propanediol. Coloured lines indicate distinct routes by which the 3HP-CoA monomer has been produced. Orange line – β-alanine route, red line – malonyl-CoA route, green line – glycerol-3-phosphate route, Pink and teal lines – 3HP route from 1,3-propanediol and glycerol respectively, Purple line – PduP route. Acc_{Ec} – acetyl-CoA carboxylase (*Escherichia coli*); $AldD_{Pp}$ – aldehyde dehydrogenase (*Pseudomonas putida* KT 2442); $AldH_{Ec}$ – aldehyde dehydrogenase; AspT – aspartate aminotransferase; $DhaB_{Cb/Kp/Lr}$ – glycerol dehydratase (*Clostridium butyricum*/*Klebsiella pneumoniae*/*Lactobacillus reuteri*); $DhaT_{Pp/Sb}$ – 1,3-propanediol dehydrogenase (*Pseudomonas putida* KT 2442/*Shimwellia blattae*); $Gpd1_{Sc}$ – glycerol-3-phosphate dehydrogenase (*Saccharomyces cerevisiae*); $Gpp2_{Sc}$ – glycerol-3-phosphate phosphatase (*Saccharomyces cerevisiae*); MCR_{Ca} – malonyl-CoA reductase (*Chloroflexus aurantiacus*); $PanD_{Cg/Ec}$ – L-aspartate decarboxylase (*Corynebacterium*

glutamicum/*Escherichia coli*); Pcs'$_{Ca}$ – acyl-CoA synthetase domain of propionly-CoA (*Chloroflexus aurantiacus*); Pct$_{Cp}$ – propionyl-CoA transferase (*Clostridium propionicum* X2); PduP$_{Lr/Se}$ – propionaldehyde dehydrogenase (*Lactobacillus reuteri*/*Shimwellia blattae*); PhaC$_{Cn/Cs}$ – (*Cupriavidus necator* H16/*Chromobacterium* sp. USM2) PP0596$_{Pp}$ – β-alanine pyruvate aminotransferase (*Pseudomonas putida* KT 2442); PrpE$_{Ec}$ – propionyl-CoA synthetase (*Escherichia coli*) YdfG$_{Ec}$ – NADP-dependent 3-hydroxyacid dehydrogenase (*Escherichia coli*); Tpi – triosephosphate isomerase. Genes which are black and bold have been overexpressed for the production of 3HP-containing copolymers. Genes in gray are part of the indicated pathway but were not overexpressed. Dashed lines indicate multiple steps. Figure was constructed using pathways from (87,100,113–118,101,106–112).

The first example of engineering a bacteria to produce poly(3HB-*co*-3HP) was reported in 2000, however, addition of 3HP to the media was still required (119). *E. coli* was engineered to produce poly(3HB-*co*-3HP) using a two plasmid system in which one plasmid contained the *phaCAB* operon of *C. necator* H16 for synthesis of the 3HB monomer and expression of the PHA synthase. A second plasmid carried genes encoding one of three CoA-addition mechanisms; either propionyl-CoA synthetase from *Salmonella typhimurium*, acetyl-CoA synthetase from *C. necator* H16, or acetyl-CoA:4-hydroxybutyryl-CoA transferase from *Clostridium propionicum*. Since PHA synthases can only polymerise substrates with a CoA moiety attached, expression of a CoA-addition mechanism was essential to facilitate addition of CoA to 3HP, resulting in 3HP-CoA. It was shown that bacteria could be engineered to produce poly(3HB-*co*-3HP), even those which do not natively accumulate PHAs, such as *E. coli*. In this case the authors were able to produce poly(3HB-*co*-3HP) with 91 mol% 3HP using the propionyl-CoA synthetase from *Salmonella typhimurium* to facilitate addition of CoA to 3HP.

To avoid addition of 3HP to the media, Fukui *et al*. engineered *C. necator* H16 and JMP134 to produce 3HP from the central metabolism through a route termed the malonyl-CoA route. While the 3HB monomer was produced through the native PHB metabolism of *C. necator* H16, the 3HP monomer was synthesised using an arabinose-inducible plasmid-based pathway containing the malonyl-CoA reductase and the 3HP-CoA synthase domain of propionyl-CoA synthase from the 3-hydroxypropionate cycle of *Chloroflexus aurantiacus* (*C. aurantiacus*) (100). Feeding with fructose and inducing with L-arabinose, poly(3HB-*co*-3HP) was produced in both strains, though the molar fractions were low; 1 mol% 3HP in *C. necator* H16, and 2.1 mol% in *C. necator* JMP134. The authors suggested the low amounts of 3HP in the polymer could be due to low activity of the 3HP-CoA synthase domain used to a CoA moiety to 3HP. Since 3HP must first be activated to 3HP-CoA before incorporation into the polymer, inefficiency at this step would limit the amount of 3HP available to the PHA synthase. A variation of the malonyl-CoA route was also used to produce the homopolymer poly(3HP) from glucose using *E. coli* as the host organism (108). To increase the malonyl-CoA pool, acetyl-CoA carboxylase was overproduced to enhance conversion of acetyl-CoA to malonyl-CoA. To facilitate production and incorporation of 3HP into the polymer, a second plasmid carried genes coding for malonyl-CoA reductase from *C. aurantiacus*, propionyl-CoA synthetase from *E. coli*, and PHA synthase of *C. necator* H16. Without expression of the *phaCAB* operon, no 3HB was available. With only 3HP available, rather than 3HB and 3HP, a homopolymer was produced. Though the study described the biosynthesis

of poly(3HP) from a structurally unrelated carbon source, the yield was very low; PHA content of the cells was less than 1%. Low activity of malonyl-CoA reductase, due to suboptimal temperature, was cited as a reason for the low yield. The authors also described significant plasmid loss as a contributing factor.

One of the most popular routes to production of the 3HP monomer is the pduP route. The pduP route describes a pathway by which glycerol is first converted to 3-hydroxypropionaldehyde by glycerol dehydratase using vitamin B12 as a cofactor. The 3-hydroxypropionaldehyde is subsequently converted to 3HP-CoA by propionaldehyde dehydrogenase. The pathway takes its name from the propionaldehyde dehydrogenase, which is encoded by the *pduP* gene (120). Since the pathway results in production of 3HP-CoA, rather than 3HP, a CoA-addition mechanism is not required. The pduP route has been used for the production of poly(3HP) and poly(3HB-*co*-3HP) (101,106,109,112,114). A variation of the pduP route, here termed the glycerol-3-phosphate route, proceeds by a slightly longer pathway than that of the pduP route. A 2015 study by Meng *et al.* used glucose as the sole carbon source for production of 3HP-containing polymers (116). In this case, dihydroxyacetone phosphate available from glycolysis is converted to glycerol by the action of glycerol-3-phosphate dehydrogenase and glycerol-3-phosphate phosphatase from *S. cerevisiae*. With glycerol now available to the cell, the genes of the pduP route facilitate production of 3HP-CoA. While the pduP route allows use of cheap glycerol for the biosynthesis of 3HP-CoA, one drawback is that most bacteria do not synthesise vitamin B12 naturally (121). As mentioned above, glycerol dehydratase facilitates

the conversion of glycerol to 3-hydroxypropionaldehyde in a vitamin B12-dependent reaction. Therefore, supplementation with vitamin B12 is often required when glycerol is used to produce 3HP-containing polymers.

Another common pathway is the 3HP route, so named as 3HP is an intermediate in the pathway. Like the pduP route, variations of the 3HP route exist. The most common variation uses 1,3-propanediol (1,3-PDO), supplied in the medium, as the precursor molecule to 3HP. Firstly, the 1,3-PDO is converted to 3-hydroxypropionaldehyde by action of 1,3-propanediol dehydrogenase. This is subsequently converted to 3HP in a reaction catalysed by aldehyde dehydrogenase. Since this reaction forms 3HP, rather than 3HP-CoA, a CoA-addition mechanism is required. This pathway was used in a series of publications describing the production of poly(3HP) and poly(3HP-*co*-4HB) (87,107,122). One major drawback of producing 3HP in this manner is that 1,3-PDO is an expensive compound and other carbon sources, such as glycerol are cheaper. In order to avoid using 1,3-PDO, several studies have used *Shimwellia blattae* (*S. blattae*) grown in glycerol as their production platform (110,111,117). The advantages of producing 3HP-containing polymers using *S. blattae* are that it naturally accumulates 1,3-PDO from glycerol when grown in anaerobic conditions and also synthesises vitamin B12. As a result, neither 1,3-PDO nor vitamin B12, both of which are costly, need to be exogenously supplied. By cultivating *S. blattae* in anaerobic conditions for 24 hours, it was possible to convert glycerol to 1,3-PDO inside the cells. Following a switch to aerobic conditions, the 3HP production pathway was induced by addition of isopropyl thio-β-D-galactoside (IPTG). One disadvantage of this pathway

was that cells of *S. blattae* began to secrete 1,3-PDO into the supernatant in the anaerobic conditions, resulting in not all of the substrate being converted into poly(3HP). Nonetheless, using this two-step process, poly(3HP) and poly(3HB-*co*-3HP) were produced. A final variation of the 3HP route made use of *Klebsiella pneumoniae* (*K. pneumoniae*) as the host strain, and used glycerol as the carbon source (115). Like *S. blattae*, *K. pneumoniae* is capable of producing vitamin B12 and 1,3-PDO from glycerol. In this case, glycerol was converted to 3-hydroxypropionaldehyde, as is common in the pduP pathway, but the resulting 3-hydroxypropionaldehyde is then converted to 3HP by aldehyde dehydrogenase, rather than to 3HP-CoA by propionaldehyde dehydrogenase. This process allowed a one step, fully aerobic pathway.

A more recently developed pathway for the production of 3HP-containing polymers is the β-alanine route. This route relies on drawing carbon from intermediates in the TCA cycle towards 3HP *via* β-alanine, and has been used for the production of 3HP and poly(3HP) (113,118,123). Several genes are required to facilitate the production of 3HP-containing polymers from the TCA cycle. Firstly, L-aspartate derived from oxaloacetate must be converted to β-alanine by an aspartate decarboxylase. Conversion of β-alanine to 3HP occurs in two steps; transamination of β-alanine by a β-alanine pyruvate aminotransferase produces malonic semialdehyde, which is then reduced to 3HP by a 3-hydroxyacid dehydrogenase. 3HP is then activated to 3HP-CoA before being polymerized by PHA synthase. In the first study to produce poly(3HP) using the β-alanine route, poly(3HP) was produced using glucose and glycerol,

and PHA content of the cell reached 10% (113). To further improve this, a second study used an aspartate decarboxylase from *Corynebacterium glutamicum* to increase conversion of aspartate to β-alanine (118). Use of the β-alanine pathway provides several advantages over other pathways: it is redox neutral, does not require additional cofactors and, since the precursor is drawn from the TCA, a wide range of carbon sources can be used. However the yield from the pathway is relatively low. As a result, significant work is required to improve yield using the β-alanine route.

The descriptions above highlight the numerous pathways and carbon sources used to produce 3HP-containing polymers. Each pathway has advantages and disadvantages. For the production of poly(3HB-*co*-3HP) in *C. necator* H16, a suitable carbon source and pathway must be chosen. Carbon sources such as 1,3-PDO are not ideal, as they are expensive and are useful compounds in their own right (124). On the other hand, glycerol is a cheap and widely available carbon source. However, use of glycerol to produce 3HP-containing polymers typically requires addition of vitamin B12 to maintain the function of glycerol dehydratase. It has been shown that *C. necator* H16 does not possess the necessary pathway for biosynthesis of vitamin B12 (125). Therefore, the use of glycerol to produce 3HP-containing polymers using *C. necator* H16 would require supplementation of expensive vitamin B12. The malonyl-CoA pathway suffers due to low activity of malonyl-CoA reductase on account of its high optimum temperature of around 55°C, whereas the β-alanine route requires more pathway optimization. Nevertheless, the malonyl-CoA and β-alanine routes both allow production from a range of carbon sources, since they use

intermediates of the central metabolism as precursors. The malonyl-CoA route has been shown to be more strongly oxygen-dependent than the β-alanine route, and to have a lower predicted yield than the β-alanine route (123). Therefore, the β-alanine route was chosen as the pathway for the production of 3HP-containing polymers.

1.6 *Cupriavidus necator* H16 – chemolithoautotrophic chassis

Cupriavidus necator H16 (*C. necator* H16) is a Gram-negative, non-pathogenic betaproteobacterium found in soil and freshwater (126). It is both a facultative chemolithoautotroph, and a facultative anaerobe, allowing use of organic and inorganic carbon as growth substrates, and the use of oxygen, nitrate, or nitrite as the final electron acceptor (127). The versatile metabolism of *C. necator* H16 is reflected by a relatively large genome; the organism possesses two chromosomes and a megaplasmid (pHG1), constituting a total of 6626 coding sequences (125,128). Previously, *C. necator* H16 has been known by several names; *Hydrogenemonas eutropha*, *Alcaligenes eutrophus*, *Wautersia eutropha*, and *Ralstonia eutropha* (129). Nowadays the organism is referred to as *Ralstonia eutropha* H16 or *Cupriavidus necator* H16. As outlined below, the metabolic versatility of *C. necator* H16 has led to significant research and industry interest with the aim of exploiting it for biotechnological applications.

1.6.1 Brief history of *C. necator* H16 research

C. necator H16 was first discovered in the early 1960s, and was shown to grow and accumulate PHB in chemolithoautotrophic conditions (130). Possible applications for *C. necator* H16 were investigated soon after this discovery. Several subsequent studies examined the possibility of using

C. necator H16 in space as a food source during long space missions. For cultivation in space, carbon dioxide would be produced through respiration of the astronauts, oxygen and hydrogen would be derived from electrolysis of water, and nitrogen would be available from compounds found in urine (131–133)**.** The results of these studies provided information on the growth rate and gas consumption characteristics of *C. necator* H16 in continuous chemolithoautotrophic cultivation and showed that a wide range of compounds could be used as a nitrogen source. At the same time, further study into the accumulation of PHB was underway (134). Schlegel *et al*. reported in their 1961 publication that PHB accumulation occurred under nitrogen and phosphate limitation (130). In the 1970s it was found that magnesium and sulphate limitation also induced PHB accumulation, the minimum nutrient concentrations required for unrestricted growth of *C. necator* H16 were elucidated (135). This information was then used in an accompanying publication in which *C. necator* H16 was grown to a high cell density of 25 g/L in chemolithoautotrophic growth conditions, the highest cell density reported at the time (136). By this point the potential of PHB as a bioplastic was being explored. The ability to accumulate significant amounts of PHB and achieve high cell densities led ICI to begin their large-scale fermentations for the production of PHB using *C. necator* H16. Although ICI subsequently ceased their PHB production efforts, research and industry interest in *C. necator* H16 has continued. The availability of a fully sequenced genome and necessary genomic tools have allowed in depth study of the organism's metabolism. As such *C. necator* H16 has become not only a model organism for PHB accumulation and

chemolithoautotrophic growth, but also a target of metabolic engineering for the production of industrially relevant chemicals and polymers.

1.6.2 Overview of *C. necator* H16 metabolism

The metabolism of *C. necator* H16 is unique in that a wide variety of carbon sources can be assimilated as biomass and PHB, but certain common carbon sources are not consumed. For instance, wild-type *C. necator* H16 cannot use glucose due to numerous absent enzymes, including a major facilitator for glucose transport into the cell (57). Cultivation in glycerol is also slow, and results in upregulation of stress-related enzymes (137). Genetic engineering and adaptive evolution can be employed to overcome these barriers however (57,138,139). Instead fructose or gluconate are used as common carbon sources, which are metabolised *via* the Entner-Duodoroff pathway, since key enzymes of the Embden-Meyerhof-Parnas, and oxidative pentose phosphate pathway are absent **[Figure 1.7]**.

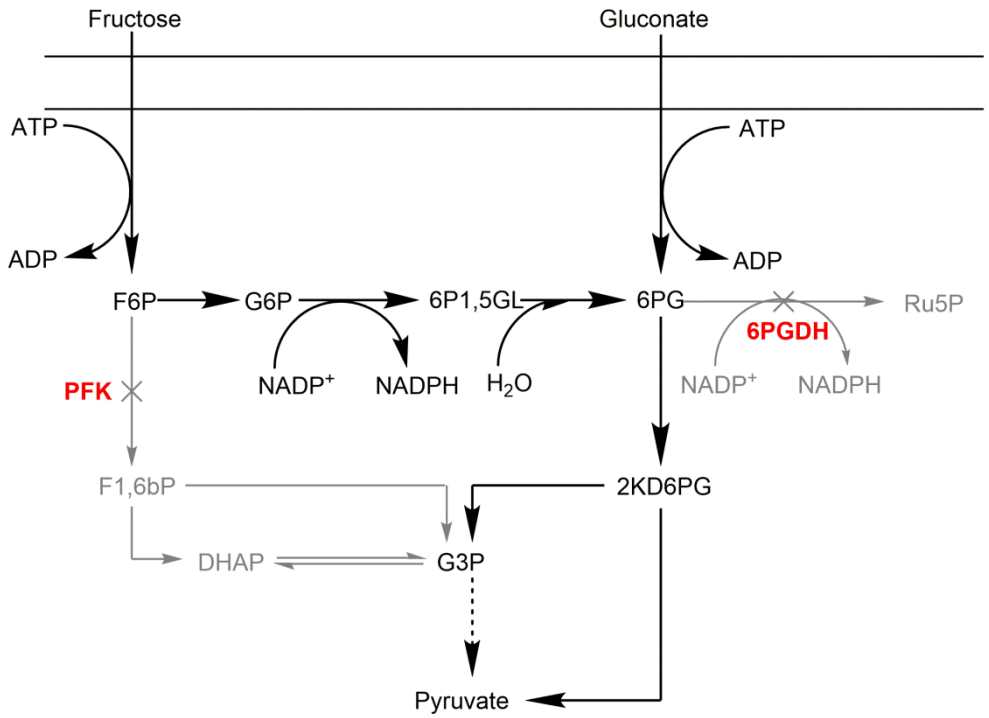

Figure 1.7 – Metabolism of fructose and gluconate proceeds through the Entner-Duodoroff pathway in *C. necator* H16. Key enzymes of the Embden-Meyerhof-Parnas pathway and oxidative pentose phosphate pathway, PFK and 6PGDH respectively, are absent. Missing genes are indicated in red. Missing pathways are indicated in grey. Dashed lines indicate multiple steps. PFK – phosphofructokinase, 6PGDH – 6-phosphogluconate dehydrogenase.

Beyond these, *C. necator* H16 can make use of a range of other carbon sources including fatty acids, aromatic compounds, amino acids, and TCA intermediates (125). Additionally, as a facultative chemolithoautotroph, *C. necator* H16 is capable of using the Calvin-Benson-Bassham (CBB) cycle for growth, using CO_2 and H_2 as sole carbon and energy sources.

The genes for the CBB cycle are encoded in duplicate operons in the case of *C. necator* H16; one operon is located on chromosome 2, while a second operon is located on the megaplasmid (125). Each operon also possesses a transcriptional regulator, encoded by *cbbR*, however only the copy present on chromosome 2 is active. The key enzyme of the CBB cycle

is ribulose-1,5-bisphosphate carboxylase/oxygenase (RuBisCO) facilitates the fixation of CO_2, adding it to ribulose-1,5-bisphosphate (Ru1,5BP) to produce two molecules 3-phosphoglycerate (3PG). One of these molecules of 3PG enters the central metabolism through pyruvate, while the second is regenerated to Ru1,5BP in order to continue the cycle (140). Molecular hydrogen is oxidized to provide reducing equivalents and ATP through oxidative phosphorylation. In *C. necator* H16, the cleavage of molecular hydrogen is facilitated by three Ni-Fe hydrogenases which are encoded on the megaplasmid (128,141).

1.6.3 Metabolic engineering of *C. necator* H16

Since *C. necator* H16 can metabolise a wide range of carbon sources, efforts have been made to utilise this for the production of valuable or useful compounds. The natural ability of *C. necator* H16 to accumulate PHA has been exploited as a means of producing PHAs beyond PHB. On the other hand, as *C. necator* H16 is capable of directing large amounts of carbon towards PHB, the PHB biosynthesis pathway can be deleted, with the aim of redirecting the carbon towards other products. These include various PHAs, cyanophycin, alcohols, alkanes, fatty acids, and ketones (142,143).

In order to produce a variety of products from *C. necator* H16, genetic engineering has been utilised. This has allowed the redirection of metabolic flux for the biosynthesis of a desired product, competing pathways can be removed, interesting native pathways can be upregulated, or entirely novel pathways can be expressed. Fortunately, a robust range of genetic tools is available for use in *C. necator* H16. While early studies on

C. necator H16 made use of Tn*5* mutagenesis for gene knockouts, the availability of homologous recombination alongside a fully annotated genome allows for targeted deletion of desired genes (129). Furthermore, a range of plasmids and promoters allows expression and fine-tuning of a given pathway to optimise production (144–146).

The ability of *C. necator* H16 to grow chemolithoautotrophically leads to the interesting possibility of producing valuable chemicals and compounds from CO_2. Several compounds have already been produced using autotrophically grown *C. necator* H16 as the microbial chassis including PHB, humulene, and isopropanol (58,147,148). The potential for production of PHAs beyond PHB using CO_2 is also an area of interest. It has previously been shown that *C. necator* H16 supplemented with various fatty acids during growth on CO_2 is capable of synthesising copolymers containing 3HV, 3HHx, 3HHp, and 3HO (149). With the aim of producing PHAs with improved properties from CO_2 in the future, efforts were made to construct a strain of *C. necator* H16 capable of incorporating 3HP into PHB, resulting in a copolymer of poly(3HB-*co*-3HP).

1.7 Synthesis of novel polymer precursors from CO_2 by *C. necator* H16

C. necator H16 is best known for its ability to accumulate large amounts of PHB when grown under nutrient-limiting conditions. While this capability is one of the major reasons for interest in the microorganism, *C. necator* H16 has also been used for non-PHA polymers, and for the biosynthesis of compounds which can act as precursors to other non-PHA compounds. For instance, several publications describe the biosynthesis of cyanophycin, a polymer consisting of a polyaspartic acid backbone with

arginine side chains attached, by engineered *C. necator* H16 (150–153). Cyanophycin is a biodegradable compound which exhibits properties similar to polycarboxylates, and can be used in a range of applications including laundry detergents, washing detergents, and as a water treatment chemical (154). Additionally, *C. necator* H16 has been engineered to produce and secrete 2-hydroxyisobutyrate, which can be used as a precursor to polymers such as poly(methylmethacrylate) (155,156).

A more recent development in the field of biodegradable materials is the use of mevalonate-derived compounds as a monomer in the production of polymers (157,158). Similarly to PHAs, polymers and copolymers containing the mevalonate-derived compounds have been shown to exhibit a range of properties depending on the composition, from stiff and tough plastics to soft and extendable materials, depending on their composition. Briefly, the publications by Xiong et al and Zhang et al show that mevalonate, synthesised from glucose by *E. coli*, can be enzymatically or chemically converted to β-methyl-Δ-valerolactone (βMΔVL). In the enzymatic process, mevalonate is first converted to anhydromevalonyl-CoA by acyl-CoA ligase (SidI) and enoyl-CoA hydratase (SidH). The anhydromevalonyl-CoA is then converted to βMΔVL by enoate reductase, Oye2. In contrast, the chemical process involves purification of mevalonate from the fermentation broth, dehydration of mevalonate to form anhydromevalonyl-CoA, and reaction over a palladium catalyst to form βMΔVL. It was finally shown that βMΔVL could be polymerized via ring-opening transesterification polymerization to form a homopolymer, and could even be reacted with lactide, a cyclic di-ester of lactic acid, to produce

a copolymer. Recently, mevalonate was shown to be synthesised from fructose by engineered *C. necator* H16 by members of the SBRC, and α-humulene, a mevalonate-derived compound, has also been synthesised from CO_2 by *C. necator* H16 by other researchers (147,159).

Given that the focus of this work was biodegradable polymers, it was envisioned that a strain of *C. necator* H16 could be engineered to overproduce mevalonate from CO_2, which could then be processed to produce βMΔVL-containing polymers. Furthermore, it was estimated that the production cost of βMΔVL from glucose by *E. coli* would be around \$2 kg^{-1} (157). Using carbon dioxide as the carbon source, particularly from a waste source, could potentially reduce the cost of βMΔVL production even further, thereby increasing the range of possible applications. Such a strain would represent a novel application of the autotrophic capabilities of *C. necator* H16.

During the course of this work, a DASGIP® bioreactor system was installed in the SBRC at the University of Nottingham, which allowed for autotrophic cultivation of *C. necator* H16 in working volumes of up to 750 mL. While this offered an opportunity to cultivate *C. necator* H16 to higher cell density than was previously possible in autotrophic conditions, it presented a challenge in maintenance of the biosynthetic mevalonate pathway, as is discussed below.

1.7.1 Plasmid stability in high-density fermentation

High titre of the desired product is essential in any industrial process. This is also the case when considering bacterial fermentation for

the production of chemicals. Numerous factors can be considered when aiming to increase product titres in bacterial fermentation. For instance, competing metabolic pathways can be deleted in order to direct as much flux as possible towards the desired product. Deletion of the *phaCAB* operon in *C. necator* H16 has been used to direct carbon towards other products (152,160,161). Additionally, the biosynthetic pathway can be optimally expressed, noting that organization of an operon can have a large influence on efficacy of the pathway (111,162,163). Another factor which must be taken into account is the manner in which the pathway is expressed. The two options available for bacterial fermentation are genomic integration of the pathway, or plasmid-based expression. Each option, however, comes with advantages and disadvantages. At high-density fermentation, as is often required for maximum product titre, genetic stability of plasmids decreases, affecting productivity (164). Typically, plasmids can be maintained by addition of antibiotics. In industrial fermentation, antibiotic addition is not feasible. The large amounts of antibiotic needed and their removal from the final product both contribute to the cost of the fermentation (164–166). Another factor to consider is that plasmid loss has been noted to occur even in the presence of antibiotics (167). Thus, in the case of large-scale fermentation, addition of antibiotics is not practical.

The alternative option of genomic integration has the advantage of genetic stability; the pathway is not plasmid based, therefore cannot be lost due to plasmid loss. Conversely, however, only one copy of the pathway is present per cell. Several genomic integrations can be carried out, though this requires identification of neutral sites in the genome which will not affect

cell viability if disrupted and is a cumbersome process. Compared to plasmid-based systems, in which there are often tens of copies of the production pathway per cell, genomic integration therefore typically results in a reduced capacity for product formation (152).

Choosing between genomic integration and a plasmid-based system therefore represents a choice between increased pathway stability but low product formation, versus increased product formation with the likelihood of reduced pathway stability and decreasing productivity. Another option to explore is plasmid addiction, a method of antibiotic-free plasmid retention.

Plasmid addiction can be described as a method of ensuring stable plasmid retention and maintenance in cells. Numerous mechanisms by which plasmid addiction can be facilitated have been described in literature, and these fall broadly into three categories: toxin/antitoxin, metabolic, and operator/repressor systems (164). Each option differs in the mechanism by which the plasmid is maintained. Toxin/antitoxin systems rely on the simultaneous expression of a toxic protein in the genome and an antitoxin, which counteracts the effect of the toxin, is expressed on the plasmid containing the biosynthetic pathway of choice. In order to abrogate the effects of the toxin, the antitoxin must be present. Since the gene coding for the antitoxin is present on the plasmid, the plasmid must be retained in order for the antitoxin protein to be formed (168). A second, less common mechanism of plasmid addiction is the operator/repressor system. In this case, a genomic copy of an essential gene is placed under the control of a repressor, while the operator is placed on a plasmid. To release the repression of the target gene, the operator must be present. Therefore cells

which lose the plasmid cannot grow, leaving only plasmid-containing cells in the fermentation (164). A third mechanism relies on the deletion of a gene from the genome and replacement of that gene on a plasmid containing the product biosynthetic pathway. More specifically, the target gene must be essential for the function of the bacteria, such that the bacteria cannot survive without it. By placing the target gene on the plasmid, and deleting it from the genome, the plasmid must be retained in order for the bacteria to survive. Since the plasmid is forcibly retained, the biosynthetic pathway is also retained. The resulting high-copy number of the plasmid within cells allows higher titres of product than genomic integration, while maintaining genetic stability of the pathway **[Figure 1.8]**. This type of plasmid addiction system typically targets a gene involved in an essential metabolic reaction, such as the breakdown of a specific metabolite, or the biosynthesis of an amino acid. This type of system is referred to as a metabolism-based addiction system.

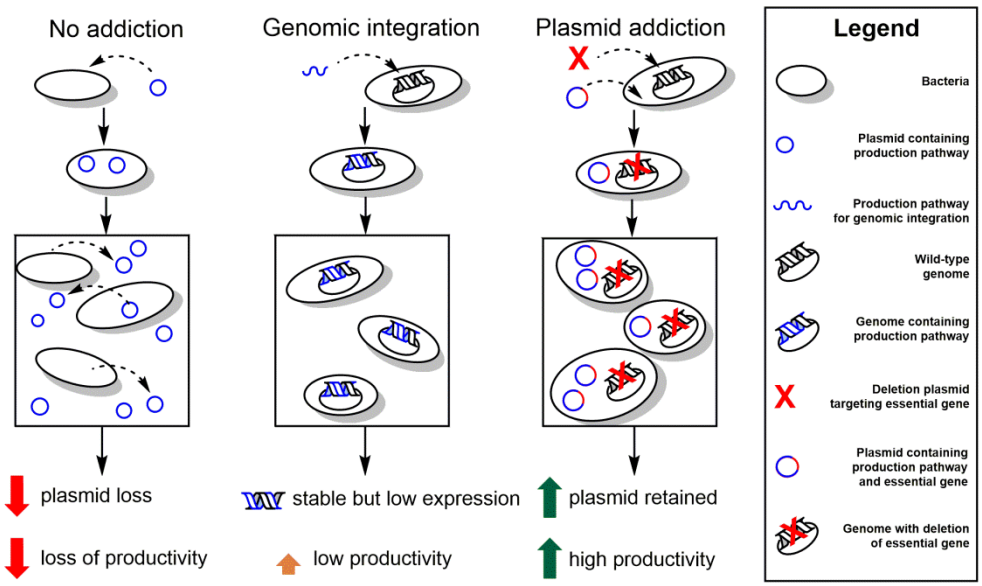

Figure 1.8 – Depiction of different methods of plasmid maintenance in large-scale fermentation. Without antibiotics as an option, plasmid loss can be expected. This leads to low production pathway expression, and loss of productivity. Genomic integration allows increased pathway stability, but due to the low copy number, productivity is also likely to be low. Plasmid addiction forces the cell to retain the plasmid for cell viability. By forcing plasmid retention, the production pathway is also maintained, resulting in high productivity.

Numerous examples of metabolism-based plasmid addiction are described in the literature. These examples fall into two further categories: catabolism- and anabolism-based addiction. In the case of catabolism-based addiction, a gene responsible for the breakdown of a specific metabolite is deleted. One of the first examples of an addiction system based on catabolism was utilised in *C. necator* H16 to produce cyanophycin (152). The authors found low cyanophycin contents of between 4.6 and 6.2% in 30L fermentations of engineered *C. necator* H16, and attributed this to plasmid loss due to the absence of antibiotics. To stabilize expression, the cyanophycin production pathway was then integrated into the genome. However, the low copy number resulted in similarly low titres of around 2.2

and 7.7%. A plasmid addiction system based on the catabolism of fructose and gluconate was then developed. As described previously, *C. necator* H16 metabolises fructose and gluconate through the Entner-Duodoroff pathway. One of the metabolites of this pathway is 2-keto-3-deoxy-6-phosphogluconate (KDPG), which is converted to pyruvate and glyceraldehyde-3-phosphate and pyruvate by KDPG-aldolase, encoded by the gene *eda*. The gene product of *eda* is the only enzyme capable of catalysing this reaction. Therefore, loss of *eda* renders the mutant unable to grow using fructose or gluconate. To facilitate plasmid retention for the production of cyanophycin, *eda* was deleted from the genome and instead expressed on a plasmid containing the cyanophycin biosynthetic pathway. The plasmid-addicted strain was again cultivated in a 30L fermenter, this time achieving cyanophycin contents of up to 36% even in the absence of antibiotics. Further scale up to 500L resulted in cyanophycin contents up to 32%, demonstrating the efficacy of the plasmid addiction system.

Anabolism-based addiction systems target a gene involved in the biosynthesis of a metabolite. Amino acids and nucleobases are common targets for the development of an anabolic addiction system and have been used in several instances for the production of polymers in bacteria. Cyanophycin production was carried out using *Pichia pastoris* GS115, a strain which is a histidine auxotroph. Absence of the *his4* gene prevents conversion of L-histidinol to L-histidine, and as a result strain GS115 cannot grow without supplementary histidine. Stabilization of the plasmid-based cyanophycin production pathway was achieved when the *his4* gene from *S. cerevisiae* also expressed on the plasmid, resulting in cyanophycin

content up to 23% in a 2L batch fermenter (169). Proline auxotrophy, achieved by deletion of the pyrroline-5-carboxylate reductase encoded by *proC*, has been exploited for the production of poly(3HB-*co*-3HHx) in *C. necator* H16 in two separate publications. It was firstly shown that a strain using plasmid addiction to maintain plasmid stability accumulated poly(3HB-*co*-3HHx) to similar levels and composition as a strain which used antibiotics to maintain the plasmid (170). In a second publication, the same strain was used in a high-density batch fermentation to produce poly(3HB-*co*-3HHx) from palm oil without the need for antibiotics (171). More recently, uracil auxotrophic *Halomonas bluephagenesis* was used as a host strain for the production of PHB. Orotidine 5'-phosphate decarboxylase, encoded by *pyrF*, is responsible for the conversion of orotidine 5'-monophosphate to uridine 5'-monophosphate in the uracil biosynthesis pathway. Deletion of *pyrF* from the genome resulted in uracil auxotrophy. Expression of *pyrF* on a plasmid containing the PHB biosynthetic operon of *C. necator* H16 resulted in a strain capable of accumulating up PHA content of up to 95% in flask cultivation, and almost 80% in 7L batch fermentation without the need for antibiotics (172).

The above examples indicate the ability of plasmid addiction to provide stable plasmid maintenance in larger scale fermentations without the addition of antibiotics. Since the aim of this section was to produce mevalonate from CO_2 in high-density cultivation, it was also chosen to test the applicability of a plasmid addiction system in stabilizing mevalonate biosynthesis.

1.8 Aims of the project

Various factors make *C. necator* H16 an interesting host organism for biotechnological applications. It is genetically amenable, non-pathogenic, and can grow on a range of carbon sources, including carbon dioxide. Therefore, an opportunity arises for the production of valuable and useful chemicals from waste carbon sources. In particular, it is possible to use *C. necator* H16 for the synthesis of biodegradable plastics in the form of PHAs. This attractive trait can be further enhanced if the PHA produced by *C. necator* H16 can be altered to contain a second monomer, such as 3-hydroxypropionate. The properties of poly(3HB-*co*-3HP) are superior to those of PHB, making the copolymer the more attractive compound for the manufacture of biodegradable plastic products.

There was also interest in developing *C. necator* H16 as a chassis for the biosynthesis of mevalonate from CO_2, as this compound has recently been used in the biosynthesis of novel biodegradable polymers and copolymers. Since the option was available to use a bioreactor for the biosynthesis of mevalonate from CO_2, it was also hypothesised that a plasmid addiction system could help stabilize production of mevalonate, since the pathway instability associated with larger scale cultivation can negatively affect bioprocesses.

The overall aims of the project therefore were as follows:

- To facilitate conversion of exogenous β-alanine to 3HP using an engineered pathway.

- To increase the ability of *C. necator* H16 to incorporate 3HP into a growing polymer chain
- To investigate the effect of altering medium composition and the genomic makeup of the background strain on 3HP incorporation into the polymer.
- To facilitate biosynthesis of mevalonate, a precursor to biodegradable polymers, from CO_2.
- To investigate the stabilization of the mevalonate biosynthesis pathway using a plasmid addiction system.

Chapter 2: Materials and Methods

2.1 Preparation of Growth Media

2.1.1 Lysogeny broth

Standard lysogeny broth (LB) medium was prepared with 20 g/L sodium chloride, 10 g/L yeast extract and 20 g/L tryptone. For LB agar, 15 g/L technical agar no. 3 was added to the broth. LB medium and agar were both sterilized by autoclaving.

2.1.2 Low salt lysogeny broth

Low salt lysogeny broth (LSLB) was prepared with 2.5 g/L sodium chloride, 5 g/L yeast extract, and 10 g/L tryptone. LSLB medium was sterilized by autoclaving.

2.1.3 LSLB + 15% sucrose

LSLB was prepared as above then 15% sucrose (w/v) was added. For LSLB + 15% sucrose agar, 15 g/L technical agar no. 3 was added to the broth. LSLB +15% sucrose medium and agar were both sterilized by autoclaving.

2.1.4 Hanahan's broth

Hanahan's broth was prepared according to the manufacturer's instructions. Hanahan's broth was sterilized by autoclaving.

2.1.5 Minimal medium

Minimal medium (MM) was prepared with 9 g/L Na_2HPO_4 x 12 H_2O, 1.5 g/L KH_2PO_4, 0.5 g/L NH_4Cl, 0.2 g/L $MgSO_4$ x 7 H_2O, 20 mg/L $CaCl_2$ x 2 H_2O, 1.2 mg/L Fe(III)NH_4-citrate, and trace element solution (SL7) 1 mL/L. SL7 was prepared to the following composition; 25% (w/v) HCl 1.3 mL/L, H_3BO_3 62 mg/L, $CoCl_2$ x 6 H_2O 190 mg/L, $CuCl_2$ x 2 H_2O 17 mg/L, $MnCl_2$

x 4 H_2O 100 mg/L, Na_2MoO_4 x 2 H_2O 36 mg/L, $NiCl_2$ x 6 H_2O 24 mg/L, and $ZnCl_2$ 70 mg/L. The pH was adjusted to 6.9.

For sodium gluconate minimal medium (SGMM), 2% sodium gluconate (w/v) was added. SGMM was sterilized by filter sterilization.

For SGMM agar, 15 g/L technical agar no. 3 was added to the broth. SGMM agar was sterilized by autoclaving.

2.2 Cultivation and Storage of Bacteria

2.2.1 Storage of *E. coli* and *C. necator* H16 strains

All strains were stored at -80 °C in Microbank vials. To prepare a Microbank vial containing a culture of interest, cultures of the strain were grown overnight in LB medium supplemented with the appropriate antibiotics. A loop of cells taken from a streak on an LB agar plate supplemented with the appropriate antibiotics was used to inoculate the overnight cultures. The following day, culture from the overnight cultivation was pipetted into three Microbank vials for storage. Approximately 1mL of culture was used per vial.

2.2.2 General cultivation of *E. coli* and *C. necator* H16

Liquid cultures of *E. coli* were grown aerobically at 37 °C in a shaking incubator at 200 rpm. Approximately 5 mL of LB medium was inoculated with a single bead from a Microbank vial, or with a single colony taken from an LB agar plate. If antibiotics were required, for instance in the case of plasmid maintenance, the following concentrations were used; chloramphenicol 12.5 μg/mL, tetracycline 15 μg/mL.

Liquid cultures of *C. necator* H16 were grown aerobically at 30 °C in a shaking incubator at 200 rpm. Approximately 5 mL of LB medium was inoculated with a single bead from a Microbank vial, or with a single colony taken from an LB agar plate. In strains of *C. necator* H16 not containing a plasmid, 10 μg/mL of gentamicin was added. If antibiotics were required, for instance in the case of plasmid maintenance, they were used in the following concentrations: chloramphenicol 50 μg/mL, tetracycline 15 μg/mL.

2.2.3 Conditions for PHA production

PHA production by *C. necator* H16 was carried out in a shaking incubator set at 200 rpm and 30 °C. Cultivations were carried out in 250 mL Erlenmeyer flasks containing 30 mL of SGMM supplemented with varying amounts of β-alanine, as described in the text. On one occasion, 2 mM cysteine was also added to the medium. An overnight culture of *C. necator* H16 was used to inoculate the flasks to a starting OD_{600} of 0.05. For plasmid maintenance, tetracycline was added to the medium at a concentration of 15 μg/mL.

2.2.3 Strains

Table 2.1 – List of strains used in this study

Strain	Genotype	Source
E. coli		
DH5-α	F- φ80*lac*ZΔM15 Δ(*lac*ZYA-*arg*F)U169 *deo*R *rec*A1 *end*A1 *hsd*R17(rk-, mk+) *pho*A *sup*E44 *thi*-1 *gyr*A96	
S17-1	*recA*, *thi*, *pro*, *hsdR*-M+RP4: 2-Tc:Mu:Km Tn*7* *λpir*, Tp^R Sm^R	
***C. necator* H16**		

H16	Wild type	DMS 428
Δ3	H16 derivative; Δ*mmsA1*Δ*mmsA2*Δ*mmsA3*	(173)
Δ3A	H16 derivative; Δ*mmsA1*Δ*mmsA2*Δ*mmsA3*Δ*phaA*	This study
Δ3B1	H16 derivative; Δ*mmsA1*Δ*mmsA2*Δ*mmsA3*Δ*phaB1*	This study
Δ3AB1	H16 derivative; Δ*mmsA1*Δ*mmsA2*Δ*mmsA3*Δ*phaA*Δ*phaB1*	This study
ΔpanC	H16 derivative; Δ*panC*	This study
ΔpanCΔphaCAB	H16 derivative; Δ*panC*Δ*phaCAB*	This study (Marco Garavaglia)
ΔphaCAB::phaA_mvaES	H16 derivative;	This study (Marco Garavaglia)
ΔpyrE	H16 derivative; Δ*pyrE*	This study
ΔpanD	H16 derivative; Δ*panD*	This study

2.3 DNA manipulation

2.3.1 Plasmids

Table 2.2 – List of plasmids used in this study

Plasmid	Description*	Source
pMTL71301	Broad host range plasmid; pBBR1 origin of replication, Tet^r	Muhammad Ehsaan
pBBR1_PphaC-CvBAPAT-EcydfG	pBBR1 derivative; P$phaC_{Cn}$, $BAPAT_{Cv}$, $ydfG_{Ec}$	Katalin Kovacs
pBBR1_PphaC-CvBAPAT-EcydfG-Cnpct	pBBR1 derivative; P$phaC_{Cn}$, $BAPAT_{Cv}$, $ydfG_{Ec}$, pct_{Cn}	This study
pMTL71101_PphaC-CvBAPAT-EcydfG-Cnpct	pMTL71101 derivative; P$phaC_{Cn}$, $BAPAT_{Cv}$, $ydfG_{Ec}$, pct_{Cn}	This study
pMTL71101_PphaC	pMTL71101 derivative; P$phaC_{Cn}$	Katalin Kovacs

pMTL71301_PphaC	pMTL71301 derivative; P*phaC*$_{Cn}$	Alex van Hagen
pCNCM_eyfP	pMTL71301 derivative; P*phaC*$_{Cn}$, eyfP	Katalin Kovacs
pCNCM0	pMTL71301 derivative; P*phaC*$_{Cn}$, *BAPAT*$_{Cv}$, *ydfG*$_{Ec}$	Katalin Kovacs
pCNCM1	pMTL71301 derivative; P*phaC*$_{Cn}$, *BAPAT*$_{Cv}$, *ydfG*$_{Ec}$, *prpE*$_{Cn}$	This study
pCNCM2	pMTL71301 derivative; P*phaC*$_{Cn}$, *BAPAT*$_{Cv}$, *ydfG*$_{Ec}$, *pct*$_{Cn}$	This study
pCNCM3	pMTL71301 derivative; P*phaC*$_{Cn}$, *BAPAT*$_{Cv}$, *ydfG*$_{Ec}$, *prpE*$_{Ec}$	This study
pCNCM4	pMTL71301 derivative; P*phaC*$_{Cn}$, *BAPAT*$_{Cv}$, *ydfG*$_{Ec}$, *atoAD*$_{Ec}$	This study
pCNCM5	pMTL71301 derivative; P*phaC*$_{Cn}$, *BAPAT*$_{Cv}$, *ydfG*$_{Ec}$, *ptb-buk*$_{Ca}$	This study
pCNCM6	pMTL71301 derivative; P*phaC*$_{Cn}$, *BAPAT*$_{Cv}$, *prpE*$_{Cn}$, *ydfG*$_{Ec}$	This study
pCNCM7	pMTL71301 derivative; P*phaC*$_{Cn}$, *BAPAT*$_{Cv}$, *pct*$_{Cn}$, *ydfG*$_{Ec}$	This study
pCNCM8	pMTL71301 derivative; P*phaC*$_{Cn}$, *BAPAT*$_{Cv}$, *prpE*$_{Ec}$, *ydfG*$_{Ec}$	This study
pCNCM9	pMTL71301 derivative; P*phaC*$_{Cn}$, *BAPAT*$_{Cv}$, *atoAD*$_{Ca}$, *ydfG*$_{Ec}$	This study
pCNCM10	pMTL71301 derivative; P*phaC*$_{Cn}$, *BAPAT*$_{Cv}$, *ydfG*$_{Ec}$, *phaC*$_{Cn}$	This study
pCNCM11	pMTL71301 derivative; P*phaC*$_{Cn}$, *BAPAT*$_{Cv}$, *ydfG*$_{Ec}$, *phaC*$_{Cs}^{\text{RBS}_{\text{SL}}}$	This study
pCNCM12	pMTL71301 derivative; P*phaC*$_{Cn}$, *BAPAT*$_{Cv}$, *ydfG*$_{Ec}$, *rrnBT1T2*$_{Ec}$, *prpE*$_{Cn}$, P*trp*$_{Ec}$	This study
pCNCM13	pMTL71301 derivative; P*phaC*$_{Cn}$, *BAPAT*$_{Cv}$, *ydfG*$_{Ec}$, *rrnBT1T2*$_{Ec}$, *pct*$_{Cn}$, P*trp*$_{Ec}$	This study
pCNCM14	pMTL71301 derivative; P*phaC*$_{Cn}$, *BAPAT*$_{Cv}$, *ydfG*$_{Ec}$, *rrnBT1T2*$_{Ec}$, *prpE*$_{Ec}$, P*trp*$_{Ec}$	This study
pCNCM15	pMTL71301 derivative; P*phaC*$_{Cn}$, *BAPAT*$_{Cv}$, *ydfG*$_{Ec}$, *rrnBT1T2*$_{Ec}$, *atoAD*$_{Ec}$,	This study

	$\underline{Ptrp_{Ec}}$	
pCNCM16	pMTL71301 derivative; P*phaC*$_{Cn}$, *BAPAT*$_{Cv}$, *ydfG*$_{Ec}$, *rrnBT1T2*$_{Ec}$, $\underline{phaC_{Cn1}}$, $\underline{prpE_{Cn}}$, $\underline{Ptrp_{Ec}}$	This study
pCNCM17	pMTL71301 derivative; P*phaC*$_{Cn}$, *BAPAT*$_{Cv}$, *ydfG*$_{Ec}$, *rrnBT1T2*$_{Ec}$, $\underline{phaC_{Cn1}}$, $\underline{pct_{Cn}}$, $\underline{Ptrp_{Ec}}$	This study
pCNCM18	pMTL71301 derivative; P*phaC*$_{Cn}$, *BAPAT*$_{Cv}$, *ydfG*$_{Ec}$, *rrnBT1T2*$_{Ec}$, $\underline{phaC_{Cn1}}$, $\underline{prpE_{Ec}}$, $\underline{Ptrp_{Ec}}$	This study
pCNCM19	pMTL71301 derivative; P*phaC*$_{Cn}$, *BAPAT*$_{Cv}$, *ydfG*$_{Ec}$, *rrnBT1T2*$_{Ec}$, $\underline{phaC_{Cn1}}$, $\underline{atoAD_{Ec}}$, $\underline{Ptrp_{Ec}}$	This study
pCNCM20	pMTL71301 derivative; P*phaC*$_{Cn}$, *BAPAT*$_{Cv}$, *ydfG*$_{Ec}$, *rrnBT1T2*$_{Ec}$, $\underline{phaC_{Cs1}}$, $\underline{prpE_{Cn}}$, $\underline{Ptrp_{Ec}}$	This study
pCNCM21	pMTL71301 derivative; P*phaC*$_{Cn}$, *BAPAT*$_{Cv}$, *ydfG*$_{Ec}$, *rrnBT1T2*$_{Ec}$, $\underline{phaC_{Cs1}}$, $\underline{pct_{Cn}}$, $\underline{Ptrp_{Ec}}$	This study
pCNCM22	pMTL71301 derivative; P*phaC*$_{Cn}$, *BAPAT*$_{Cv}$, *ydfG*$_{Ec}$, *rrnBT1T2*$_{Ec}$, $\underline{phaC_{Cs1}}$, $\underline{prpE_{Ec}}$, $\underline{Ptrp_{Ec}}$	This study
pCNCM23	pMTL71301 derivative; P*phaC*$_{Cn}$, *BAPAT*$_{Cv}$, *ydfG*$_{Ec}$, *rrnBT1T2*$_{Ec}$, $\underline{phaC_{Cs1}}$, $\underline{atoAD_{Ec}}$, $\underline{Ptrp_{Ec}}$	This study
pMTL70641	Suicide vector used for gene knockouts in *C. necator* H16. Contains *sacB* counter-selection marker and confers tetracycline resistance	Muhammad Ehsaan
pMTL70641_phaA	pMTL70641 derivative; carries *phaA* deletion cassette	This study
pMTL70641_phaB1	pMTL70641 derivative; carries *phaB1* deletion cassette	This study
pLO3_phaAB1	pLO3 derivative; carries *phaAB1* deletion cassette	Giorgia Tibaldero
pMTL70641_pyrE	pMTL70641 derivative; carries *pyrE* deletion cassette	This study
pMTL70641_panC	pMTL70641 derivative; carries *panC*	Muhammad

	deletion cassette	Ehsaan
pMTL70641_panD	pMTL70641 derivative; carries *panD* deletion cassette	This study
pMTL70641::ΔphaCAB-KI araC-Pbad-mvaES	pMTL70641 derivative; carries *mvaES* expression cassette, integrates at the *phaCAB* locus	Marco Garavaglia
pCNCMpanC	pMTL71301 derivative; $panC_{Cn}$	This study
pCNCM_eyFP_panC	pCNCM_eyfP derivative; P$phaC_{Cn}$, eyfP $panC_{Cn}$	This study
p71301_mvaES	pMTL71301 derivative; P*BAD*, *mvaES*	Marco Garavaglia
p71301_mvaES_panC	pMTL71301 derivative; P*BAD*, *mvaES*, $panC_{Cn}$	Marco Garavaglia
p71301_phaA_ mvaES_panC	pMTL71301 derivative; P*BAD*, *phaA*, *mvaES*, $panC_{Cn}$	Marco Garavaglia
pCNCMpyrE	pMTL71301 derivative; $pyrE_{Cn}$	This study
p71301_phaA_ mvaES_pyrE	pMTL71301 derivative; P*BAD*, *phaA*, $mvaES_{Ef}$, $pyrE_{Cn}$	Marco Garavaglia
pUC57_phaCCs USM2	pUC57 derivative; $phaC_{Cs}$	This study (purchased from Genscript)

2.3.2 Primers

Table 2.3 – List of primers used in this study

Primer name	**Sequence (5' – 3')**	**Function**
	tctagaaggagacagcaatgaaggtgatcaccgcacgcga	Construction of pBBR1_PphaC-CvBAPAT-EcydfG-Cnpct
	Gcgatcgttacaggtgcaggggcccggcctg	Construction of pBBR1_PphaC-CvBAPAT-EcydfG-Cnpct

Fw HiFi – CnprpE – CNCM1	ccaccgtcagtaaactagttctagacagac gcggaggagacagacatgacggcaagcc atgccgtgcatgcccg	Construction of pCNCM1
Rev HiFi – CnprpE – CNCM1	Caaatgcaggcttcttatttttatgctagccta gcctttcagcgctgcctgcaactgttccagc gcacc	Construction of pCNCM1
Fw HiFi – EcprpE – CNCM3	ccaccgtcagtaaactagttctagacaacag gagagcattatgtc	Construction of pCNCM3
Rev HiFi – EcprpE – CNCM3	Gcaggcttcttatttttatgctagcctactctt ccatcgcctg	Construction of pCNCM3
Fw HiFi – EcAtoAD – CNCM4	aatgtccaccgtcagtaaactagttctagatg tatgcaagagggataaaaaatg	Construction of pCNCM4
Rev HiFi – EcAtoAD – CNCM4	caaatgcaggcttcttatttttatgctagctcat aaatcaccccgttg	Construction of pCNCM4
Fw HiFi – Captbbuk – CNCM5	ccaccgtcagtaaactagttctagacagac gcggaggagacagacatgattaagagtttt aatgaaattatcatgaagg	Construction of pCNCM5
Rev HiFi – Captbbuk – CNCM5	caaatgcaggcttcttatttttatgctagcttat ttgtattccttagctttttcttctcctcttaaaact ctaagtccac	Construction of pCNCM5
Fw HiFi – CvBAPAT – CNCM6	agtgacggcagagagacaatcaacatatg aaccacccgctcaccacc	Construction of pCNCM6
Rev HiFi – CvBAPAT – CNCM6	Tctcctccgcgtctgtcaggccagcttggc cagcg	Construction of pCNCM6
Fw HiFi – CnprprE – CNCM6	Caagctggcctgacagacgcggaggaga cagac	Construction of pCNCM6
Rev HiFi – CnprpE – CNCM6	Gggtatatctcctctagcctttcagcgctgc ct	Construction of pCNCM6
Fw HiFi – EcydfG – CNCM6	Gctgaaaggctagaggagatatacccatg gccg	Construction of pCNCM6
Rev HiFi – EcydfG – CNCM6	agaggatccccgggtaccgagctcgaattc ttactgacggtggacattcag	Construction of pCNCM6

Fw HiFi – CvBAPAT – CNCM7	agtgacggcagagagacaatcaacatatg aaccacccgctcaccacc	Construction of pCNCM7
Rev HiFi – CvBAPAT – CNCM7	Cattgctgtctcctcaggccagcttggcca gcg	Construction of pCNCM7
Fw HiFi – Cnpct – CNCM7	caagctggcctgaggagacagcaatgaag gtgatcaccg	Construction of pCNCM7
Rev HiFi – Cnpct – CNCM7	Gggtatatctcctttacaggtgcaggggcc cgg	Construction of pCNCM7
Fw HiFi – EcydfG – CNCM7	Cctgcacctgtaaaggagatatacccatgg ccg	Construction of pCNCM7
Rev HiFi – EcydfG – CNCM7	agaggatccccgggtaccgagctcgaattc ttactgacggtggacattcag	Construction of pCNCM7
Fw HiFi – CvBAPAT – CNCM8	agtgacggcagagagacaatcaacatatg aaccacccgctcaccacc	Construction of pCNCM8
Rev HiFi – CvBAPAT – CNCM8	Tgctctcctgttgtcaggccagcttggcca gcg	Construction of pCNCM8
Fw HiFi – EcprprE – CNCM8	Caagctggcctgacaacaggagagcatta tgtcttttag	Construction of pCNCM8
Rev HiFi – EcprpE – CNCM8	Gggtatatctcctctactcttccatcgcctgg c	Construction of pCNCM8
Fw HiFi – EcydfG – CNCM8	Gatggaagagtagaggagatatacccatg gccg	Construction of pCNCM8
Rev HiFi – EcydfG – CNCM8	agaggatccccgggtaccgagctcgaattc ttactgacggtggacattcag	Construction of pCNCM8
Fw HiFi – CvBAPAT – CNCM9	agtgacggcagagagacaatcaacatatg aaccacccgctcaccacc	Construction of pCNCM9
Rev HiFi – CvBAPAT – CNCM9	Cctcttgcatacatcaggccagcttggcca gcg	Construction of pCNCM9
Fw HiFi – EcAtoAD – CNCM9	Caagctggcctgatgtatgcaagagggat aaaaaatg	Construction of pCNCM9
Rev HiFi – EcAtoAD – CNCM9	Gggtatatctccttcataaatcaccccgttgc g	Construction of pCNCM9
Fw HiFi – EcydfG –	Gggtgatttatgaaggagatatacccatgg	Construction of pCNCM9

CNCM9	ccg	
Rev HiFi – EcydfG – CNCM9	agaggatccccgggtaccgagctcgaattc ttactgacggtggacattcag	Construction of pCNCM9
Fw HiFi – CnphaC – CNCM10	aatgtccaccgtcagtaaactagttctagaa gtgacggcagagagacaatc	Construction of pCNCM10
Rev HiFi – CnphaC – CNCM10	caaatgcaggcttcttatttttatgctagctcat gccttggctttgac	Construction of pCNCM10
Fw HiFi – CsphaC – CNCM11	Aatgtccaccgtcagtaaactagttctagaa atccctattaaaatcaatatctcacaaaggag gtttttatg	Construction of pCNCM11
Rev HiFi – CsphaC – CNCM11	caaatgcaggcttcttatttttatgctagctca gttcaaggcggcggc	Construction of pCNCM11
Fw HiFi – rrnBT1T2 – CNCM12	Ccaccgtcagtaaactagttctagaatcaaa taaaacgaaaggctc	Construction of pCNCM12
Rev HiFi – rrnBT1T2 – CNCM12	gaaaggctaggtagaaacgcaaaaaggc	Construction of pCNCM12
Fw HiFi – CnprpE – CNCM12	gcgtttctacctagcctttcagcgctgc	Construction of pCNCM12
Rev HiFi – CnprpE – CNCM12	gcaggcttcttatttttatgctagcctgttgac aattaatcatcgaactagttaactagtacgca atgacggcaagccatgcc	Construction of pCNCM12
Fw HiFi – rrnBT1T2 – CNCM13	ccaccgtcagtaaactagttctagaatcaaa taaaacgaaaggctc	Construction of pCNCM13
Rev HiFi – rrnBT1T2 – CNCM13	gcacctgtaagtagaaacgcaaaaaggc	Construction of pCNCM13
Fw HiFi – Cnpct – CNCM13	gcgtttctacttacaggtgcaggggccc	Construction of pCNCM13
Rev HiFi – Cnpct – CNCM13	gcaggcttcttatttttatgctagcctgttgac aattaatcatcgaactagttaactagtacgca atgaaggtgatcaccgcacg	Construction of pCNCM13
Fw HiFi – rrnBT1T2 –	ccaccgtcagtaaactagttctagaatcaaa	Construction of pCNCM14

CNCM14	taaaacgaaaggctc	
Rev HiFi – rrnBT1T2 – CNCM14	ggaagagtaggtagaaacgcaaaaaggc	Construction of pCNCM14
Fw HiFi – CnprpE – CNCM14	gcgtttctacctactcttccatcgcctg	Construction of pCNCM14
Rev HiFi – CnprpE – CNCM14	gcaggcttcttatttttatgctagcctgttgac aattaatcatcgaactagttaactagtacgca atgtcttttagcgaattttatcag	Construction of pCNCM14
Fw HiFi – rrnBT1T2 – CNCM15	ccaccgtcagtaaactagttctagaatcaaa taaaacgaaaggctc	Construction of pCNCM15
Rev HiFi – rrnBT1T2 – CNCM15	tgatttatgagtagaaacgcaaaaaggc	Construction of pCNCM15
Fw HiFi – EcAtoAD – CNCM15	gcgtttctactcataaatcaccccgttg	Construction of pCNCM15
Rev HiFi – EcAtoAD – CNCM15	Gcaggcttcttatttttatgctagcctgttgac aattaatcatcgaactagttaactagtacgca atgaaaacaaaattgatgacattac	Construction of pCNCM15
Fw HiFi – rrnBT1T2 – CNCM16	ccaccgtcagtaaactagttctagaatcaaa taaaacgaaaggctc	Construction of pCNCM16
Rev HiFi – rrnBT1T2 – CNCM16	caaggcatgagtagaaacgcaaaaaggc	Construction of pCNCM16
Fw HiFi – CnphaC – CNCM16	gcgtttctactcatgccttggctttgac	Construction of pCNCM16
Rev HiFi – CnphaC – CNCM16	gaaaggctaggaatagtgacggcagagag	Construction of pCNCM16
Fw HiFi – CnprpE – CNCM16	gtcactattcctagcctttcagcgctgc	Construction of pCNCM16
Rev HiFi – CnprpE – CNCM16	gcaggcttcttatttttatgctagcctgttgac aattaatcatcgaactagttaactagtacgca atgacggcaagccatgcc	Construction of pCNCM16
Fw HiFi – rrnBT1T2 – CNCM17	ccaccgtcagtaaactagttctagaatcaaa taaaacgaaaggctc	Construction of pCNCM17
Rev HiFi – rrnBT1T2 –	caaggcatgagtagaaacgcaaaaaggc	Construction of pCNCM17

CNCM17		
Fw HiFi – CnphaC – CNCM17	gcgtttctactcatgccttggctttgac	Construction of pCNCM17
Rev HiFi – CnphaC – CNCM17	gcacctgtaagaatagtgacggcagagag	Construction of pCNCM17
Fw HiFi – Cnpct – CNCM17	gtcactattcttacaggtgcaggggccc	Construction of pCNCM17
Rev HiFi – Cnpct – CNCM17	gcaggcttcttatttttatgctagcctgttgac aattaatcatcgaactagttaactagtacgca atgaaggtgatcaccgcacg	Construction of pCNCM17
Fw HiFi – rrnBT1T2 – CNCM18	ccaccgtcagtaaactagttctagaatcaaa taaaacgaaaggctc	Construction of CNCM18
Rev HiFi – rrnBT1T2 – CNCM18	caaggcatgagtagaaacgcaaaaaggc	Construction of CNCM18
Fw HiFi – CnphaC – CNCM18	gcgtttctactcatgccttggctttgac	Construction of CNCM18
Rev HiFi – CnphaC – CNCM18	Ggaagagtaggaatagtgacggcagaga g	Construction of pCNCM18
Fw HiFi – EcprpE – CNCM18	gtcactattcctactcttccatcgcctg	Construction of pCNCM18
Rev HiFi – EcprpE – CNCM18	gcaggcttcttatttttatgctagcctgttgac aattaatcatcgaactagttaactagtacgca atgtcttttagcgaattttatcag	Construction of pCNCM18
Fw HiFi – rrnBT1T2 – CNCM19	ccaccgtcagtaaactagttctagaatcaaa taaaacgaaaggctc	Construction of pCNCM19
Rev HiFi – rrnBT1T2 – CNCM19	caaggcatgagtagaaacgcaaaaaggc	Construction of pCNCM19
Fw HiFi – EcAtoAD – CNCM19	gcgtttctactcatgccttggctttgac	Construction of pCNCM19
Rev HiFi – EcAtoAD – CNCM19	tgatttatgagaatagtgacggcagagag	Construction of pCNCM19
Fw HiFi – EcAtoAD – CNCM19	gtcactattctcataaatcaccccgttg	Construction of pCNCM19
Rev HiFi – EcAtoAD –	gcaggcttcttatttttatgctagcctgttgac aattaatcatcgaactagttaactagtacgca	Construction of pCNCM19

CNCM19	atgaaaacaaaattgatgacattac	
Fw HiFi – rrnBT1T2 – CNCM20	ccaccgtcagtaaactagttctagaatcaaataaaacgaaaggctc	Construction of pCNCM20
Rev HiFi – rrnBT1T2 – CNCM20	Cgccttgaactgagtagaaacgcaaaaagc	Construction of pCNCM20
Fw HiFi – CsphaC – CNCM20	tttgcgtttctactcagttcaaggcggcggc	Construction of pCNCM20
Rev HiFi – CsphaC – CNCM20	cagagagacaatcaaatcatgcagcagtttgtcaattccctg	Construction of pCNCM20
Fw HiFi – CnprpE – CNCM20	caaactgctgcatgatttgattgtctctctgccgtcactattcctagcctttcagcgctgc	Construction of pCNCM20
Rev HiFi – CnprpE – CNCM20	caaatgcaggcttcttatttttatgctagcctgttgacaattaatcatcgaactagttaactagtacgcaatgacggcaagccatgcc	Construction of pCNCM20
Fw HiFi – rrnBT1T2 – CNCM21	ccaccgtcagtaaactagttctagaatcaaataaaacgaaaggctc	Construction of pCNCM21
Rev HiFi – rrnBT1T2 – CNCM21	Cgccttgaactgagtagaaacgcaaaaagc	Construction of pCNCM21
Fw HiFi – CsphaC – CNCM21	tttgcgtttctactcagttcaaggcggcggc	Construction of pCNCM21
Rev HiFi – CsphaC – CNCM21	cagagagacaatcaaatcatgcagcagtttgtcaattccctg	Construction of pCNCM21
Fw HiFi – Cnpct – CNCM21	caaactgctgcatgatttgattgtctctctgccgtcactattcttacaggtgcaggggccc	Construction of pCNCM21
Rev HiFi – Cnpct – CNCM21	caaatgcaggcttcttatttttatgctagcctgttgacaattaatcatcgaactagttaactagtacgcaatgaaggtgatcaccgcacg	Construction of pCNCM21
Fw HiFi – rrnBT1T2 – CNCM22	ccaccgtcagtaaactagttctagaatcaaataaaacgaaaggctc	Construction of pCNCM22
Rev HiFi – rrnBT1T2 – CNCM22	Cgccttgaactgagtagaaacgcaaaaagc	Construction of pCNCM22
Fw HiFi – CsphaC – CNCM22	tttgcgtttctactcagttcaaggcggcggc	Construction of pCNCM22

Rev HiFi – CsphaC – CNCM22	cagagagacaatcaaatcatgcagcagtttgtcaattccctg	Construction of pCNCM22
Fw HiFi – EcprpE – CNCM22	caaactgctgcatgatttgattgtctctctgccgtcactattcctactcttccatcgcctg	Construction of pCNCM22
Rev HiFi – EcprpE – CNCM22	caaatgcaggcttcttatttttatgctagcctgttgacaattaatcatcgaactagttaactagtacgcaatgtcttttagcgaattttatcag	Construction of pCNCM22
Fw HiFi – rrnBT1T2 – CNCM23	ccaccgtcagtaaactagttctagaatcaaataaaacgaaaggctc	Construction of pCNCM23
Rev HiFi – rrnBT1T2 – CNCM23	Cgccttgaactgagtagaaacgcaaaaagc	Construction of pCNCM23
Fw HiFi – CsphaC – CNCM23	tttgcgtttctactcagttcaaggcggcggc	Construction of pCNCM23
Rev HiFi – CsphaC – CNCM23	cagagagacaatcaaatcatgcagcagtttgtcaattccctg	Construction of pCNCM23
Fw HiFi – EcAtoAD – CNCM23	caaactgctgcatgatttgattgtctctctgccgtcactattctcataaatcaccccgttg	Construction of pCNCM23
Rev HiFi – EcAtoAD – CNCM23	caaatgcaggcttcttatttttatgctagcctgttgacaattaatcatcgaactagttaactagtacgcaatgaaaacaaaattgatgacattac	Construction of pCNCM23
phaA LHA Fw HiFi	catgattacgaattcgagctcttgcgcgaggccacgctgggcggc	Amplification of phaA left homology arm
phaA LHA Rev HiFi	aacccttcctgtgtagtcctttcaatggaaacgggagggaacctgcaggcc	Amplification of phaA left homology arm
phaA RHA Fw HiFi	Ggactacacaggaaggggttttccggggccgcgc	Amplification of phaA right homology arm
phaA RHA Rev HiFi	atggacgcgtgacgtcgactctagaacgacaaccaggcgcagatcgaggc	Amplification of phaA right homology arm
phaA ext Fw	gcttgcatgagtgccggcgtgc	External screening primer for phaA KO
phaA ext Rev	ggcttcgttatcgtcgccgggtcc	External screening primer for phaA KO
phaA int Fw	caagccggagcaggtg	Internal screening primer for phaA KO

phaA int Rev	ccgttcacattgaccttggag	Internal screening primer for phaA KO
phaB1 LHA Fw HiFi	catgattacgaattcgagctccatcacacgc gaggcgcaggatga	Amplification of phaB1 left homology arm
phaB1 LHA Rev HiFi	Ggccggcagggtccactccttgattggctt cgttatcgtc	Amplification of phaB1 left homology arm
phaB1 RHA Fw HiFi	Aggagtggaccctgccggcctggttcaac cagtc	Amplification of phaB1 right homology arm
phaB1 RHA Rev HiFi	atggacgcgtgacgtcgactctagagcctg gatgttcttttccaggtaggtgc	Amplification of phaB1 right homology arm
phaB1 ext Fw	gcgcggacccggcgacgataacg	External screening primer for phaB1 KO
phaB1 ext Rev	ccgcgctggctgcaccgcaatac	External screening primer for phaB1 KO
phaB1 int Fw	gcattgcgtatgtgaccggc	Internal screening primer for phaB1 KO
phaB1 int Rev	cgagaaaccggactcctccgac	Internal screening primer for phaB1 KO
phaAB1 LHA Fw HiFi	agatccttttaattcgagctcccatgtgcagtt gcgcgaggccac	Amplification of phaAB1 left homology arm
phaAB1 LHA Rev HiFi	ggccggcaggtgtgtagtcctttcaatggaa acgggaggg	Amplification of phaAB1 left homology arm
phaAB1 RHA Fw HiFi	Ggactacacacctgccggcctggttcaac cagtc	Amplification of phaAB1 right homology arm
phaAB1 RHA Rev HiFi	tttaaacagtcgactctagagtcgatgaagg cctggatgttcttttccag	Amplification of phaAB1 right homology arm
phaAB1 ext Fw	gatcaacgtgctcggcttctgcgt	External screening primer for phaAB1 KO
phaAB1 ext Rev	gcatgttcatgaactgcgaccacatg	External screening primer for phaAB1 KO
phaAB1 int Fw	gccatgaccatcaacaaggtgtgc	Internal screening primer for phaAB1 KO
phaAB1 int Rev	cgtcgatcacctgcttggtgacgt	Internal screening primer for phaAB1 KO

panC LHA Fw	atggcggccatgctgatcgagatcaag	Amplification of panC left homology arm
panC LHA Rev	catctgccttggtgtgctggtcg	Amplification of panC left homology arm
panC RHA Fw	tgagcggcagcgccgcaccaggc	Amplification of panC right homology arm
panC RHA Rev	tgttgctgaccacgctggtgggcgtg	Amplification of panC right homology arm
panC ext Fw	ccgcaggacctgtacatcc	External screening primer for panC KO
panC ext Rev	gtatatcggcctgagccttg	External screening primer for panC KO
panC int Fw	caactgcgcggccagaac	Internal screening primer for panC KO
panC int Rev	ccagcttggcggcagtcag	Internal screening primer for panC KO
panD LHA Fw	Catgattacgaattcgagctcgccgcgcac cactaccag	Amplification of panD left homology arm
panD LHA Rev	agcaaacccgggtgatacgtccttatatttg atgcaaaagc	Amplification of panD left homology arm
panD RHA Fw	cgtatcacccgggtttgctcccctctcc	Amplification of panD right homology arm
panD RHA Rev	atggacgcgtgacgtcgactctagaatcag gaccagcgtggtc	Amplification of panD right homology arm
panD ext Fw	tctcggcctgcctgatgtgca	External screening primer for panD KO
panD ext Rev	gatcaggttgatcaccgtgtggttca	External screening primer for panD KO
panD int Fw	ggcggacctcaactacg	Internal screening primer for panD KO
panD int Rev	cgttcaccaggatgaccttg	Internal screening primer for panD KO
pyrE LHA Fw HiFi	Catgattacgaattcgagctccttgtagatc	Amplification of pyrE left

	gagcaaag	homology arm
pyrE LHA Rev HiFi	Atcaacggttcatttctctctgaattcaaaatt tc	Amplification of pyrE left homology arm
pyrE RHA Fw HiFi	gagagaaatgaaccgttgatggcaaggg	Amplification of pyrE right homology arm
pyrE RHA Rev HiFi	atggacgcgtgacgtcgactctagaggtcg aagtcggcaaaac	Amplification of pyrE right homology arm
pyrE ext Fw	ggtatcggcgatcttcg	External screening primer for pyrE KO
pyrE ext Rev	cgtagaagctgacatggc	External screening primer for pyrE KO
pyrE int Fw	gcagaaaccgcccgcgggtgccgatctc	Internal screening primer for pyrE KO
pyrE int Rev	cgtagcgctgacgataggccgccaccgc	Internal screening primer for pyrE KO
Fw HiFi pyrE	caggcttcttatttttatggcgcgcctcgggg aaattttgaattcagagagaaatgatgacg	pyrE complementation plasmid Fw
Rev HiFi pyrE	tctggcgctcctgcggccggccgccgcgc tcctgccgatt	pyrE complementation plasmid Rev
Fw HiFi panC	caggcttcttatttttatggcgcgcccccacc cgcgctgcgggg	panC complementation plasmid Fw
Rev HiFi panC	tctggcgctcctgcggccggccaaaaagc aggccgccggcctgc	panC complementation plasmid Rev
Fw HiFi panC	Caggcttcttatttttatggcgcgcccccac ccgcgctgcgggg	PphaC_eyfP panC complementation plasmid
Rev HiFi panc	tctggcgctcctgcggccggccaaaaagc aggccgccggcctgc	PphaC_eyfP panC complementation plasmid
ara_fwd	ctacaatttttttatcaggaaacagctatgacc gcggccgcttaagcagaaggccatcc	Construction of p71301_mvaES_panC
ara_rev	aatcaccacggttttcatatgtatatctccttct taaaagatctttg	Construction of p71301_mvaES_panC
mvae_fwd	Taagaaggagatatacatatgaaaaccgtg gtgattattg	Construction of p71301_mvaES_panC

mvae_rev	Ttattttgtcgctaatcattactgtttacgcag atcattc	Construction of p71301_mvaES_panC
mvas_fwd	Gatctgcgtaaacagtaatgattagcgaca aaataaataac	Construction of p71301_mvaES_panC
mvas_rev	tatttttatgctagttgatcagttatctagatcc ggtggatccttaattacgatagctacgc	Construction of p71301_mvaES_panC
mvas_REV2	gagatctccatggacgcgtgacgtcgactc tagaggatccttaattacgatagctacgc	Construction of p71301_mvaES
ara-phac_fwd	gttcgaatagtgacggcagagagacaatca aatcccatggttaagcagaaggccatcc	Construction of pMTL70641::ΔphaCAB-KI araC-Pbad-mvaES
mvas-phab_rev	ccgcgaaacgggcggcgaaacgaaacgc ccgccgccatggttaattacgatagctacgc	Construction of pMTL70641::ΔphaCAB-KI araC-Pbad-mvaES

2.3.3 Synthesised PHA synthase from *Chromobacterium* sp. USM2

The synthesised PHA synthase was ordered from Genscript and was provided in the pUC57 vector as lyophilised DNA. DNA was resuspended according to the manufacturer's instructions before being transformed into *E. coli*. Codon optimization was not used.

The DNA sequence of the PHA synthase of *Chromobacterium* sp. USM2 is indicated below;

ATGCAGCAGTTTGTCAATTCCCTGTCGCTCGGCCAGGACCAGTCCGATGCCCCC
CATCCGCTGACCGGCGCCTGGTCGCAGCTGATGAGCCAGACCAATCAGCTCTTG
CAGCTGCAATCCAGCCTCTACCAACAGCAATTGGGCTTGTGGACGCAATTCCTC
GGCCAAACCGCCGGCAACGACGCTTCCGCGCCGTCGGCCAAGCCGAGCGACCG
CCGCTTCGCCTCGCCGGAGTGGGATGAGCATCCGTTCTACAGCTTCCTCAAGCA
GAGCTATCTGCAAACCTCCAAGTGGATGATGGAGCTGGTGGACAAGACCCAGA
TCGACGAAAGCGCTAAGGACAAGCTGTCCTTCGCCACTCGCCAGTACCTGGAT
GCCATGGCGCCCAGCAACTTCATGCTGACCAACCCCGACGTGGTCAAACGCGC

CATCGAAACCCAGGGCGAAAGCCTGGTGGAAGGCATGAAGAACATGATGGAG
GACATCCAGAAGGGCCATATCTCGATGTCCGACGAGAGCAAGTTCCAAATCGG
CAAAAACCTGGTGGTGACGCCGGGCGAGGTGGTGTTCCGCAATGAACTGATCG
AGCTGATCCAGTACACGCCGACCACCGAAAAAGTCCACGAAAAGCCCTTGCTG
TTTGTCCCGCCGTGCATCAACAAGTACTACCTGATGGATCTGCAGCCGGACAAC
TCCATGGTGCGCCACTTCGTCGGCCAGGGTTACCGCGTTTTCCTGGTCAGCTGG
CGTTCCGCCGTGCCCGAGATGAAGAACTTCACTTGGGAGACCTACATCGAGAA
AGGCGTGTTCGCCGCGGCCGAAGCGGTTCAGAAGATCACCAAGCAGCCGACCA
TGAACGCGCTGGGCTTCTGCGTGGGCGGCGTGATCCTCACTACCGCGCTGTGCG
TGGCCCAGGCCAAGGGTCTGAAATACTTCGACTCCGCCACCTTCATGACGTCGC
TGATCGACCACGCCGAACCGGGCGAGATCTCCTTCTTCATCGACGAGGCGCTG
GTAGCCAGCCGCGAAGCCAAAATGGCGGCCGGCGGCATCATCAGCGGCAAGG
AAATCGGACGCACTTTCGCCAGCCTGCGCGCCAACGACCTGGTGTGGAACTAC
GTCGTCAACAACTACCTGCTGGGCAAGACCCCGGCGCCGTTCGACCTGCTGTAC
TGGAACAACGACGCGGTGGACCTGCCGCTGCCGATGCACACCTTCATGCTGCG
GCAGTTCTACATCAACAACGCGCTGATCACCCCGGGCGCCATTACGCTGTGCGG
CGTCCCGATCGACATCTCCAAGATCGACATCCCGGTGTATATGTTCGCCGCGCG
CGAAGACCACATCGTGCTGTGGAGTTCCGCCTACTCCGGCCTGAAATATCTGAG
CGGCACGCCAAGCCGCCGCTTTGTCCTGGGCGCATCCGGCCACATCGCCGGCTC
GATCAACCCCGTCACCAAGGATAAGCGCAACTACTGGACCAACGAGCAGCTGC
CGGTGAATCCGGAAGAATGGCTGGAGGGCGCGCAAAGCCATCCAGGCAGCTG
GTGGAAGGACTGGGACGCCTGGCTGGCCCCGCAATCTGGAAAACAGGTTCCGG
CGCCCAAGATGCTGGGCAGCAAGGAGTTCCCCCCGCTGCAGCCTGCGCCGGGC
AGCTATGTGCTCGCCAAGGCGATGCCTCCCGTCGCCGCCGCCTTGAACTGA

2.3.4 Isolation of plasmid DNA

Plasmid DNA isolation was performed using the Monarch Plasmid Miniprep Kit (New England BioLabs Inc. (NEB)) according to the manufacturer's instructions using 5 mL of an overnight culture.

2.3.5 Isolation of chromosomal DNA

Genomic DNA isolation was performed using the GenElute Bacterial Genomic DNA Kit (Sigma-Aldrich) according to the manufacturer's instructions using 1 mL of an overnight culture.

2.3.6 PCR analysis of DNA

All primers designed during the course of this study were ordered from Sigma-Aldrich. Lyophilized oligonucleotides were resuspended in sterile de-ionised water to a final concentration of 100 pmol/µl.

PCR was performed using GoTaq, Q5, or Phusion polymerases according to the manufacturer's instructions. Taq polymerase was used for screening of colonies for successful plasmid transformation or gene deletion. Q5 polymerase was used to amplify genes for cloning into overexpression vectors, and to amplify homology arms used in the generation of knockout cassettes. Phusion was used to amplify the pantothenate synthetase gene (*panC*) and of *C. necator* H16.

2.3.7 Restriction analysis of plasmid DNA

Restriction enzymes from two sources were used; NEB and "FastDigest" from Fermentas (ThermoFisher Scientific). Each was used according to the manufacturer's instructions. Restriction digestion reactions typically contained 1 µl of the relevant restriction enzymes, 0.5-1 µg DNA, 2 µl of 10x buffer and nuclease-free water up to 20 µl. The digestions were performed at 37 °C for two hours and analysed by agarose gel electrophoresis.

2.3.8 Agarose gel electrophoresis

A 1% agarose gel solution was prepared by mixing 1 g agarose powder with 100 mL 1x TAE buffer (40mM Tris-acetate, 1mM EDTA). The agarose gel solution was poured into a casting tray and 10 µl SYBR Safe DNA Gel Stain (ThermoFisher Scientific) was added.

Approximately 20 µl of the relevant sample (restriction digest or PCR product) was loaded per well. Restriction digestions using NEB enzymes or PCR mixtures using either Q5 or Phusion polymerases were mixed with 4µl loading dye (Gel Loading Dye, Purple (6x)) prior to loading of the sample. The reaction mixture of restriction digests using FastDigest enzymes or PCR reactions using GoTaq contained green dye and could be loaded directly into the gel.

2.3.9 Gel extraction and purification

Fragments of DNA amplified by PCR and relevant digestion bands were excised from agarose gels and recovered using a Monarch DNA Gel Extraction Kit (NEB) in accordance with the manufacturer's instructions.

2.3.10 Quantification of DNA

Quantification of DNA was carried out using a SimpliNano microvolume spectrophotometer (GE Healthcare Life Sciences).

2.3.11 Ligation of plasmid DNA

Ligation reactions were performed using T4 DNA ligase (NEB). Samples of digested vector and insert were mixed, at a ratio of 1:3, with 1 µl T4 DNA ligase, 2 µl T4 ligation buffer, and nuclease-free water in a total volume of 20 µl. The reaction mixture was incubated overnight at room temperature.

The following day, the reaction mixture was transformed into *E. coli* using the method outlined in **section 2.4.2**.

2.4 Transformation of bacterial strains

2.4.1 Preparation of chemically competent *E. coli* cells

An overnight culture of *E. coli* cells was diluted 1:100 in 100 mL LB at 37 °C and 200 rpm until OD_{600} of approximately 0.8 was reached. The culture was then cooled on ice for approximately 20 minutes. The culture was centrifuged at 5000 rpm for 6 minutes at 4 °C to collect the cells. The pellet was resuspended in 100 mL of ice-cold 0.1 M calcium chloride and centrifuged again under the same conditions as before. The cells were again collected, and then resuspended in 50 mL of ice-cold calcium chloride + 15% (v/v) glycerol, before being centrifuged again as before. The cells were collected again and resuspended in 5 mL of ice-cold calcium chloride + 15% (v/v) glycerol. The final cell suspension was divided into 50 µl aliquots in pre-chilled Eppendorf tubes, and immediately used or frozen at -80 °C.

2.4.2 Transformation of chemically competent *E. coli* cells

A single aliquot (50 µl) of chemically competent *E. coli* cells was mixed with 5 µl of a solution containing 50-100 ng DNA and incubated in ice for one hour. The cells were heat-shocked for two minutes at 42 °C in a water bath, and 950 µl SOC was added immediately after removal from the water bath. The cells were then incubated at 37 °C for approximately 90 minutes. The cells were then collected by centrifugation at 4000 rpm for 5 minutes at room temperature, and resuspended in 100-200 µl of LB, before being

plated on LB agar plates containing the appropriate antibiotic. The plates were then incubated overnight at 37 °C.

2.4.3 Preparation of electrocompetent *C. necator* H16 cells

An overnight culture of *C. necator* H16 was used to inoculate 50 mL of Hanahan's broth to an OD_{600} of approximately 0.05. The culture was grown at 30 °C /200 rpm until OD_{600} 0.2-0.3 was reached. Cells were then collected by centrifugation at 7000 rpm for 10 minutes at 4 °C. The cells were resuspended in 20 mL of 1 mM HEPES (pH 7.0) and centrifuged again as before. The wash was repeated again with 10 mL of 1mM HEPES (pH 7.0), and cells centrifuged as before. The cells were collected again and resuspended in 2 mL of 1 mM HEPES + 10% glycerol (v/v). The final cell suspension was divided into 50 µl aliquots in pre-chilled Eppendorf tubes and used immediately.

2.4.4 Transformation of electrocompetent *C. necator* H16 cells

A single aliquot (50 µl) of electrocompetent *C. necator* H16 cells were mixed with 5 µl of a solution containing 100-500 ng DNA in a pre-chilled electroporation cuvette with a 0.2 cm gap width and incubated on ice for 5 minutes. After incubation on ice, the cell suspension was subjected to electroporation at 2.5 kV, 200 Ω, and 25 µF, using a MicroPulser Electroporator (Bio-Rad). Immediately after electroporation, 950 µl SOC was added to the cell suspension, followed by incubation at 30 °C /200 rpm for approximately two hours. The cells were then collected by centrifugation at 4000 rpm for 5 minutes at room temperature, and resuspended in 100-200 µl of LB, before being plated on LB agar plates containing the appropriate antibiotic. The plates were then incubated for 48 hours at 30 °C.

2.4.5 Conjugative plasmid transfer into *C. necator* H16

E. coli S17-1 was incubated overnight in LB containing the appropriate antibiotic at 37 °C/200 rpm. *C. necator* H16 was incubated overnight in LSLB containing the appropriate antibiotic at 30 °C/200 rpm. The following day, 1 mL of each culture was separately centrifuged for 4 minutes at 5000 rpm to collect cells. The cell pellets were individually resuspended in 1 mL of LB and centrifuged as before. The cell pellets were resuspended in 500 µL the mixed together. The cells were centrifuged as before. The cell pellet was resuspended in 30 µl LB and spotted on an LB agar plate for mating. Mating was allowed to occur at 30 °C for at least 6 hours, up to a maximum of 24 hours. After mating, cells were collected from the plate using a sterile loop and resuspended in 200 µl PBS. The cell suspension was then plated on SGMM + tetracycline (15 µg/mL) agar plates. Transconjugants appeared after 48-72 hours of incubation at 30 °C. Tetracycline-resistant colonies were picked and purified by streaking again on SGMM + tetracycline (15 µg/mL) agar plates. This process was repeated a second time to purify *C. necator* H16 transconjugants and eliminate any remaining *E. coli* S17-1 donor cells.

2.5 Construction of plasmids

2.5.1 Construction of expression vectors

With the exception of plasmids pBBR1_PphaC-CvBAPAT-EcydfG-Cnpct, pMTL71101_PphaC-CvBAPAT-EcydfG-Cnpct, and pCNCM2 (described below), all other expression plasmids in this study were designed using the NEBuilder Assembly Tool and constructed using HiFi DNA Assembly Kit (NEB) following the manufacturer's protocol. Following amplification of

the target insert(s) and digestion of the target plasmid with the appropriate restriction enzymes, the vector and insert were analysed by gel electrophoresis and extracted from the gel according to **sections 2.3.8** and **2.3.9**. The vector and insert(s) were then mixed in a 1:2 ratio along with 5 µl of 2x NEBuilder DNA HiFi Assembly Master Mix, and nuclease-free water added to a final volume of 10 µl. The mixture was incubated at 50 °C for one hour to facilitate ligation of insert and vector. The resulting assembly was transformed into *E. coli* using the procedure described in **section 2.4.2**.

Plasmid pBBR1_PphaC-CvBAPAT-EcydfG-Cnpct was constructed using traditional cloning. Propionyl-CoA transferase from *C. necator* H16 (Cnpct) was amplified with primers containing restriction sites for XbaI (5') and PvuI (3'). Plasmid pBBR1_PphaC-CvBAPAT-EcydfG and the Cnpct insert were digested by XbaI/PvuI. The digested vector and insert were analysed by gel electrophoresis and extracted from the gel according to **sections 2.3.8** and **2.3.9,** then ligated according to the method described in **section 2.3.11**.

Plasmid pMTL71101_PphaC-CvBAPAT-EcydfG-Cnpct was constructed by ligation of linearised pMTL71101_PphaC and the CvBAPAT-EcydfG-Cnpct fragment from plasmid pBBR1_PphaC-CvBAPAT-EcydfG-Cnpct. Using the restriction enzymes NdeI/PvuI, pMTL71101_PphaC was linearised, while digestion of plasmid pBBR1_PphaC-CvBAPAT-EcydfG-Cnpct released the CvBAPAT-EcydfG-Cnpct fragment. The digested vector and insert were analysed by gel electrophoresis and extracted from the gel according to **sections 2.3.8** and **2.3.9,** then ligated according to the method described in **section 2.3.11**.

Plasmid pCNCM2 was constructed by ligation of linearised pMTL71301_PphaC and the CvBAPAT-EcydfG-Cnpct fragment from plasmid pBBR1_PphaC-CvBAPAT-EcydfG-Cnpct. Using the restriction enzymes NdeI/NheI, was pMTL71301_PphaC was linearised, while digestion of plasmid pMTL71101_PphaC-CvBAPAT-EcydfG-Cnpct released the CvBAPAT-EcydfG-Cnpct fragment. The digested vector and insert were analysed by gel electrophoresis and extracted from the gel according to **sections 2.3.8** and **2.3.9,** then ligated according to the method described in **section 2.3.11**.

2.5.2 Construction of deletion vectors

Gene deletions in *C. necator* H16 were carried out using either the pLO3 or pMTL70641 suicide vectors. These plasmids both contain a tetracycline resistance marker and encode the *sacB* gene that allows for counter-selection in sucrose.

The suicide vector was digested with SacI/XbaI, and 750 bp upstream and downstream of the target gene were amplified by PCR. The amplified flanking regions of the target gene and the digested vector were analysed by gel electrophoresis and extracted from the gel according to **sections 2.3.8** and **2.3.9**. The digested vector and amplified flanking regions were then mixed in a 1:2 ratio along with 5 µl of 2x NEBuilder DNA HiFi Assembly Master Mix, and nuclease-free water added to a final volume of 10 µl. The mixture was incubated at 50 °C for one hour to facilitate ligation of insert and vector. The resulting assembly was transformed into *E. coli* using the procedure described in **section 2.4.2**.

2.5.3 Construction of ORF deletions in *C. necator* H16

Suicide vectors containing the target gene sequence and *sacB* gene were transferred from *E. coli* S17-1 to *C. necator* H16 by conjugation as described in **section 2.4.5.** Transconjugants resistant to tetracycline after two streaks on SGMM + tetracycline were used to inoculate 5 mL of LSLB + 15% sucrose. These cultures were grown overnight at 30 °C/200 rpm. The cultures were then serially diluted and 100 µl of dilutions 10^{-4} - 10^{-6} were spread on LSLB + 15% sucrose agar plates and incubated at 30 °C. Sucrose-resistant colonies appeared 48-72 hours of incubation. These colonies were picked and purified in LB agar plates, after first streaking in LB + tetracycline agar plates to confirm loss of the suicide vector. Clones were screened by colony PCR to identify strains of *C. necator* H16 with the gene deletion.

2.5.4 Construction of putatively auxotrophic strains of *C. necator* H16

To construct the Δ*panD*, Δ*panC*, and Δ*pyrE* strains, the conjugation and ORF deletion protocols described in **sections 2.4.5** and **2.5.3** respectively were used as before, but with modifications to account for the potentially auxotrophic phenotype of the resulting knockout strains.

Following resuspension in 200 µl PBS described in **section 2.4.5**, cells were subsequently plated on SGMM + tetracycline (15 µg/mL) agar plates supplemented with the metabolite for which the knockout strains were putatively auxotrophic. Metabolite supplementation was used for all remaining steps of the conjugation protocol. Metabolite supplementation was also used in all steps of the ORF deletion protocol, with the exception of the LB + tetracycline plates.

During the construction of strain Δ*panD*, 1 mM β-alanine was supplemented. During the construction of strain Δ*panC*, 1mM pantothenate was supplemented. During the construction of strain Δ*pyrE*, 20 μM uracil was supplemented.

2.5.5 Evaluation of strains Δ*panD*, Δ*panC*,and Δ*pyrE* for auxotrophy

To determine whether the Δ*panD*, Δ*panC*,and Δ*pyrE* strains were auxotrophs, each strain was spread on SGMM with and without supplementation of the appropriate metabolite.

The concentration of the supplemented metabolites was the same as described in **section 2.5.4**.

2.5.6 Plasmid stability assay

To analyse the stability of the plasmid addiction system, samples were withdrawn from the reactors approximately every 24 hours throughout the fermentation. These samples were first spread on LB plates containing gentamicin and incubated for 24-48 hours at 30 °C. Following appearance of colonies on this plate, 100 colonies were chosen at random and restreaked on LB plates containing no antibiotic and LB plates containing tetracycline. These plates were incubated for another 24-48 hours at 30 °C. The plates were then compared to identify the proportion of cells which had failed to grow on LB containing tetracycline (indicating plasmid loss).

2.6 Bioinformatics

2.6.1 Plasmid map analysis

Sequence alignment, restriction site analysis, and design of plasmids was conducted using Benchling (https://benchling.com/)

2.6.2 Sequence databases

Nucleotide and peptide sequences of genes of interest were investigated using the National Center for Biotechnology Information (NCBI) database. Functional information of proteins was investigated using UniProt. Metabolic pathways and associated genes were investigated using the Kyoto Encyclopedia of Genes and Genomes (KEGG). The sequence for the PHA synthase of *Chromobacterium* sp. USM2 was taken from the European Bioinformatics Institute (EBI) database.

2.6.3 Identification of ribosome binding sites

The Salis Lab ribosome binding site (RBS) calculator was used to identify the RBS of genes of interest, and to construct a synthetic RBS for the synthesised PHA synthase from *Chromobacterium* sp. USM2.

2.6.4 Data presentation and figure construction

Figures presenting data were constructed using Graphpad Prism. Figures presenting metabolic pathways or biological concepts were constructed using ChemBioDraw Ultra 14.0.

2.7 Detection and analysis of compounds

2.7.1 HPLC detection of gluconate and 3HP

Culture samples were centrifuged at 14,000 rpm for 2 minutes. The supernatant was filtered through a 0.2 μm filter. The cell pellet was kept for GCMS to analyse PHA content and composition. Approximately 150 μl of filtered supernatant was added to 150 μl of mobile phase and vortex to ensure sufficient mixing. The mobile phase was a solution of 5 mM H_2SO_4 supplemented with 50 mM valerate as an internal standard.

Samples were run at a flow rate of 0.5 mL min^{-1} at 35 °C for 30 minutes. A Dionex UltiMate 3000 HPLC system (ThermoFisher Scientific), Rezex ROA-Organic Acid H+ (8%) 150 mm x 4.6 mm x 8 μm column (Phenomex), and a Diode Array detector (UV-VIS 210 nm) were used. When required, an Aminex HPX-87H 300 nm x 7.8 mm x 9 μm column (Bio-Rad) was used to better separate peaks.

2.7.2 HPLC detection of mevalonate

Culture samples were centrifuged at 14,000 rpm for 2 minutes. The supernatant was filtered through a 0.2 μm filter. Approximately 150 μl of filtered supernatant was added to 150 μl of mobile phase and vortex to ensure sufficient mixing. The mobile phase was a solution of 5 mM H_2SO_4 supplemented with 50 mM valerate as an internal standard.

The mobile phase was composed of 0.005 M H_2SO_4. The mix was passed through a membrane filter with a pore size of 0.22 μm. Samples were analysed using a Dionex 3000 HPLC system (Thermo Fisher Scientific) equipped with a Rezex ROA-organic acid H+ (8%)

150 mm × 7.8 mm × 8 µm column (Phenomex) and a diode array detector (UV-VIS 210 nm). The column was operated at 35 °C with a flow rate of 0.5 mL/min. Samples were run for 30 min and the injection volume was 20 µl.

2.7.3 Freeze drying of cell pellets

Cell pellets were retained after centrifugation of culture at 14,000 rpm for 2 minutes. Samples were washed three times with water. Eppendorf tubes containing the washed samples were then covered with aluminium foil. The foil covering the opening of the Eppendorf tube was pierced to allow moisture to leave during freeze drying. Prior to freeze drying, samples were frozen at -80 °C to prevent bubbling of the sample during freeze drying. Samples were freeze dried for approximately 24 hours using a Micromodulyo Freeze Dryer (ThermoFisher Scientific).

2.7.4 Extraction of PHA from cells

Freeze dried sample of a known weight was added to a glass centrifuge tube. In a fume cupboard, 100 µl of 1 mg/mL benzoic acid in 1-propanol was added to the sample, followed by 2 mL of 25% concentrated hydrochloric acid in 1-propanol, followed by 2 mL chloroform. The screw cap tube was closed, and samples were incubated in a dry block heater at 100 °C for 2 hours.

After heating, the samples were removed from the dry block heater and allowed to cool to room temperature. In a fume hood, 4 mL of de-ionised water was added to the samples. Samples were vortexed for 30 seconds and set aside for 5 minutes to allow for phase separation. Following phase

separation, the upper aqueous layer was removed and discarded. Another 4 mL of de-ionised water was added to the samples. Samples were again vortexed for 30 seconds and set aside for 5 minutes to allow for phase separation. Following phase separation, the upper aqueous layer was removed and discarded again.

Approximately 1 mL of the sample was transferred to a GC vial and the cap closed. Samples were then taken for analysis.

2.7.5 Analysis of PHAs by GCMS

Samples were run at a flow rate of 0.6 mL min^{-1} at 250 °C using H_2 as a carrier gas. An Agilent 6890N GC with 5973N MSD (Conquer Scientific) and an Agilent HP-INNOWAX 20 m x 0.18 mm x 0.18 μm column (Conquer Scientific). During samples analysis, the oven was held at 50 °C for 4 minutes, ramped to 240 °C at 19 °C/min, and held at 240 °C for 6 minutes.

2.8 Gas fermentation

2.8.1 Gas fermentation media

Seed cultures were incubated in 50 mL Hanahan's broth in 250 mL flasks at 30°C 200 rpm for 24 hours. A modified version of the DSMZ 81 medium was used for batch and continuous autotrophic cultivation. In the modified medium, the standard vitamin solution and $NaVO_3$ are left out, and KH_2PO_4 is replaced with $Na_3P_3O_9$. L-arabinose was added to a final concentration of 2 g/L (0.2% w/v) to induce cultures.

2.8.2 Gas fermentation reactor setup

Gas fermentation was carried out using a DASGIP® bioreactor system according to the protocols described by Bommareddy *et al*. (174).

Briefly, autotrophic fermentations were carried out in 1L bioreactors with a 750 mL working volume. Gas composition during fermentation was maintained at 78% H_2, 3% CO_2, and 19% air. The rate of gas flow into the reactor was maintained by mass flow controllers [M13 mini CORI-FLOW Coriolis Mass Flow Meter – Bronkhorst]. Agitation was facilitated by two Rushton impellers. Stirring speed was controlled at between 400 rpm and 1600 rpm. Gas sparging was facilitated by two spargers, one for CO_2 and air, and the other for H_2. The pH was monitored by a pH probe [Mettler Toledo] and the dissolved oxygen measured by an optical probe [Mettler Toledo]. To ensure the gas composition was maintained outside explosive limits, the DASware® software was programmed to halt the flow of CO_2, air, and H_2, and flood the reactor with N_2 if the O_2 concentration in the off gas rose above 5%.

2.8.3 Autotrophic culture inoculation, maintenance, and sampling

For cultivation initiation, gas fermentation medium in the reactor was inoculated using the 50 mL preculture. Agitation was initially set at 400 rpm and was controlled by the DASware® software such that low dissolved oxygen resulted in accelerated agitation, up to a maximum of 1600 rpm, in order to facilitate increased oxygenation of the culture medium. The pH was maintained at approximately pH 6.9 by the DASware® software using aqueous NH_3.

Batch fermentations lasted approximately 8 days. Following inoculation, no additional medium was provided. Induction with arabinose was carried out after 48-72 hours of growth.

Continuous cultivations lasted approximately 14 days. Feeding with medium containing arabinose began after 48-72 hours of growth. The initial rate for the feeding rate was 7.5 mL/h^{-1}, and the initial dilution rate was set at 0.01 h^{-1}. During continuous cultivation, the level of the cultivation was maintained at a maximum of 750 mL by the level probe.

During both batch and continuous cultivation, samples were withdrawn from the reactor approximately every 24 hours. Optical density was measured using a spectrophotometer at 600 nm. The samples were used to collect cells for the plasmid stability assay, to determine the PHB concentration, and to determine the concentration of mevalonate.

Chapter 3: Engineering of *C. necator* H16 for the production of 3HP-containing polymers

3.1 Introduction

To date, the biosynthesis of poly(3HB-*co*-3HP) copolymers has been described in several publications, as mentioned in **Chapter 1 (Introduction)**. The biosynthesis of this copolymer by *C. necator* H16 has only also been reported on two occasions. In both instances, however, the 3HP molar ratio of the copolymer accumulated by the cells was very low. In the first instance, *C. necator* H16 was cultivated with various amounts – between 5 and 30 g/L – of 3HP added to the cultivation media, achieving a maximum 3HP molar fraction of 7 mol% (91). Subsequently, Fukui *et al*. reported the engineering of *C. necator* H16 for *de-novo* synthesis of 3HP and production of the copolymer from fructose, however the 3HP molar fraction was even lower, 1 mol% (100). This work aimed to engineer *C. necator* H16 to produce poly(3HB-*co*-3HP) with much higher 3HP molar fraction, as this was shown to improve its thermal and physical properties.

Of the numerous pathways which have been described to produce poly(3HB-*co*-3HP), the pathway proceeding *via* β-alanine was chosen based on advantages over other pathways, as described in **Chapter 1 (introduction)**. In previous studies, 3HP and poly(3HP) have been produced using the β-alanine route (113,118,123,175**).**

The β-alanine pathway can be split into two sections. The overproduction of β-alanine from central metabolism is referred to as the "upstream" part, while conversion of β-alanine to 3HP is referred to as the "downstream" part. Previous studies indicate that implementation of the β-alanine route, particularly the upstream part of the pathway, requires extensive pathway and strain engineering. For instance, in the study by

Borodina *et al*., the integration of a five gene pathway into the genome of *S. cerevisiae* was required to produce 3HP *via* the β-alanine route (123). Notably, sufficient flux towards β-alanine required multiple integrations of the gene encoding aspartate decarboxylase, the role of which is the conversion of aspartate to β-alanine. On the other hand, only a single integration was required for genes forming the downstream part of the pathway (123). Production of 3HP *via* the β-alanine pathway in *E. coli* also required expression of a five gene pathway, though in this case using a two-plasmid system was used rather than genome integration (175). In a previous study, the same group had described a strain in which six genome deletions had been made in order to increase flux towards β-alanine (176). Using the same strain in a subsequent study for production of 3HP using the β-alanine pathway, promoter engineering was also employed to further increase flux towards β-alanine (175). Moreover, the conversion of β-alanine to 3HP in these studies requires only two steps, whereas production of β-alanine from the central metabolism requires three steps.

The pathway by which poly(3HB-*co*-3HP) could be produced is shown below **[Figure 3.1]**. Starting from β-alanine, conversion of β-alanine to 3HP *via* malonate semialdehyde is facilitated by a β-alanine-pyruvate aminotransferase (*BAPAT*) and an NADP-dependent 3-hydroxyacid dehydrogenase (*ydfG*). Next, 3HP is activated to 3HP-CoA by a CoA-addition mechanism. This step is essential as PHA synthases can only catalyse the polymerization of hydroxyacyl-CoA substrates (83). Engineering is not required to supply the 3HB-CoA monomer, since it is provided by the activity of the genes of the *phaCAB* operon natively present

in *C. necator* H16. The β-ketothiolase encoded by *phaA* condenses two molecules of acetyl-CoA to produce acetoacetyl-CoA, which is then reduced by the acetoacetyl-CoA reductase encoded by *phaB1* to form 3HB-CoA. The final step in the pathway is incorporation of the 3HB-CoA and 3HP-CoA monomers into the polymer, which is catalysed PHA synthase, encoded by *phaC*.

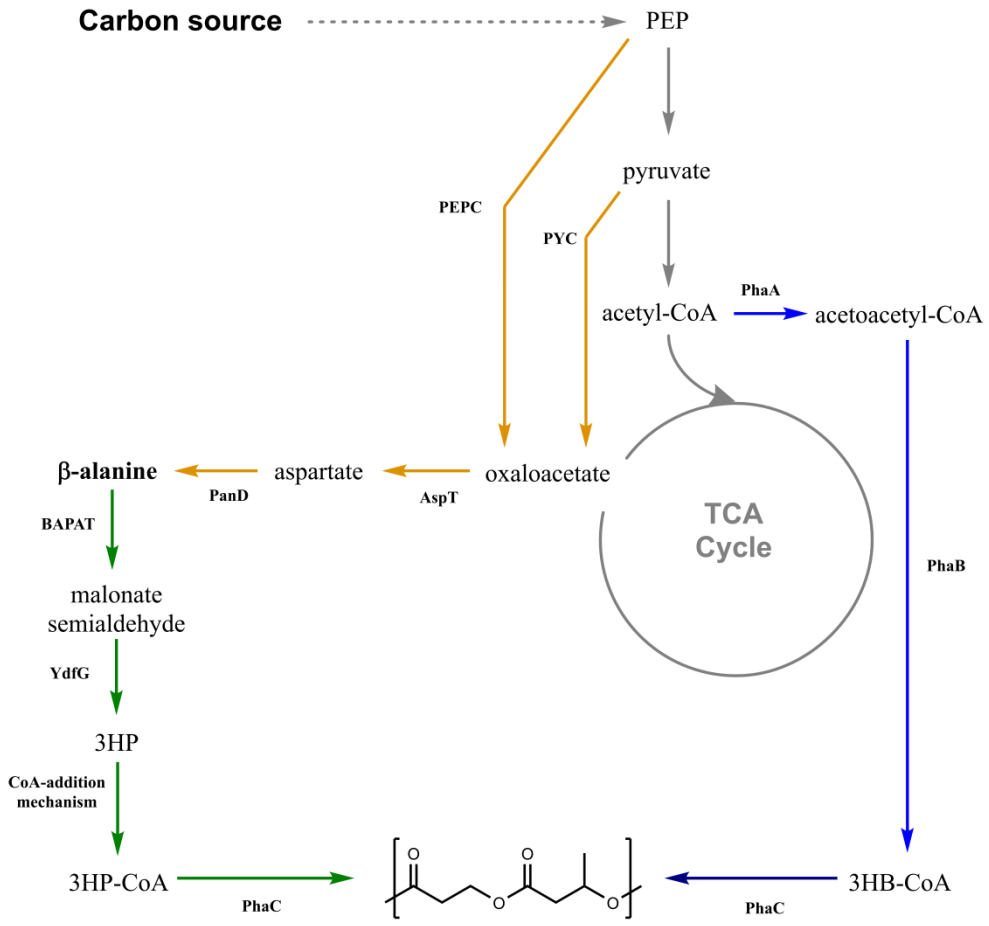

Figure 3.1 – Schematic for the biosynthesis of poly(3HB-*co*-3HP) by engineered *C. necator* H16. The 3HP monomer can be provided from the central metabolism by expression of the β-alanine pathway. The β-alanine pathway can be split into two parts: an upstream part and a downstream part. The upstream part of the β-alanine pathway results in overproduction of β-alanine from the central metabolism (indicated by orange lines). Genes such as *PEPC* and *PYC* can be overexpressed to increase flux towards oxaloacetate, which is then converted to β-alanine *via* aspartate. The resulting β-alanine is converted to 3HP and

incorporated into the polymer in the downstream part of the pathway (indicated by green lines). β-alanine is converted to malonate semialdehyde by BAPAT. Malonate semialdehyde is subsequently reduced to 3HP by YdfG. The 3HP is then activated to 3HP-CoA by a CoA-addition mechanism, before being incorporated into the copolymer by PHA synthase, encoded by *phaC*. 3HB-CoA is provided and incorporated into the copolymer by the genes of the *phaCAB* operon of *C. necator* H16. For the purposes of this work, the focus was on the downstream part of the pathway, and excess β-alanine was supplied exogenously. AspT – aspartate decarboxylase, BAPAT - β-alanine pyruvate aminotransferase, PhaA – β-ketothiolase, PhaB – acetoacetyl-CoA reductase, PhaC – PHA synthase, PEP – phosphoenolpyruvate, PEPC- PEP carboxylase, PYC – pyruvate carboxylase, YdfG – NADP-dependent 3-hydroxyacid dehydrogenase.

Currently, biosynthesis of 3HP using the β-alanine pathway has not been described in *C. necator* H16. Establishment of the upstream part of the pathway required substantial work even in model organisms such as *S. cerevisiae* and *E. coli*. Equally, the studies of Nakamura *et al*. and Fukui *et al*. showed that *C. necator* H16 does not efficiently incorporate 3HP into the polymer, suggesting that significant optimisation would also be needed there. Since the primary goal was to improve the ability of *C. necator* H16 to incorporate 3HP into the polymer, work carried out first focused on the downstream part of the β-alanine pathway. For the purposes of this work, the downstream part of the β-alanine pathway is considered as conversion of β-alanine to 3HP and incorporation of 3HP into the polymer.

Rather than attempt to construct the entire pathway at once, a systematic approach was adopted. This allowed us to more easily identify bottlenecks associated with any given step. Firstly, a previously constructed pathway for conversion of β-alanine to 3HP was tested. Next, enhanced

activation of 3HP to 3HP-CoA by expression of a CoA-addition mechanism was tested. The effect of overexpressing a PHA synthase was also tested, since the PHA synthase of *C. necator* H16 does not have high activity towards 3HP-CoA compared to 3HB-CoA (177). Finally, the effects of separating the enzymes involved in conversion of β-alanine to 3HP from those involved in incorporation of 3HP into the polymer were tested, such that 3HP production and integration of 3HP into the polymer were controlled by different promoters. In total, five different CoA-addition mechanisms and two different PHA synthases were tested in various combinations and operon structures. A summary of all plasmids tested for the production of poly(3HB-*co*-3HP) in this study is shown in **Figure 3.2** and **Table 3.1**.

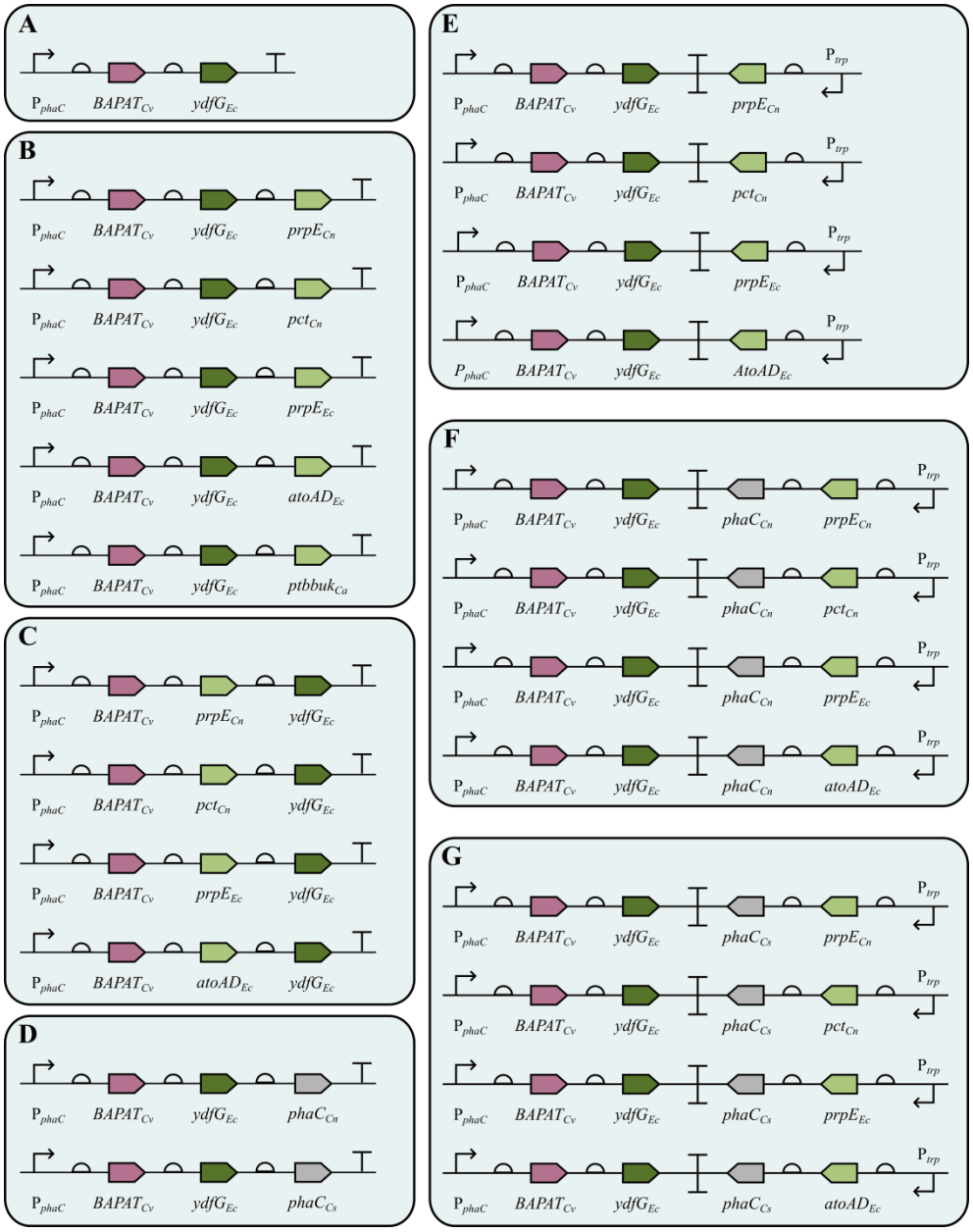

Figure 3.2 – Depiction of all plasmid structures tested for production of poly(3HB-*co*-3HP) in this chapter. Gene names and the function of the enzymes they encode are depicted by the following colours; purple, $BAPAT_{Cv}$ – conversion of β-alanine to malonic semialdehyde; dark green, $ydfG_{Ec}$ – conversion of malonic semialdehyde to 3HP; pale green, CoA-addition mechanisms – activation of 3HP to 3HP-CoA; grey, PHA synthases – incorporation of 3HP into the polymer. Various different combinations of genes and operon structures were tested. (**A**) Plasmid pCNCM0, (**B**) plasmids pCNCM1-5, (**C**) plasmids pCNCM6-9, (**D**) plasmids pCNCM10 and 11, (**E**) plasmids pCNCM12-15 (**F**) plasmids pCNCM16-19 (**G**) plasmids pCNCM20-23. Coloured, pointed boxes indicate genes. Arrows indicate

promoters. T-shapes (T) indicate terminators. Semi-circles indicate ribosomal binding site (RBS). *Cn* – *Cupriavidus necator* H16, *Cs* – *Chromobacterium* sp. USM2, *Cv* – *Chromobacterium violaceum*, *Ec* – *Escherichia coli*, P_{phaC} – *phaC* promoter, P_{trp} – *trp* promoter, *BAPAT* – β-alanine-pyruvate aminotransferase, *ydfG* – NADP-dependent 3-hydroxyacid dehydrogenase, *prpE* – propionyl-CoA synthetase, *pct* – propionyl-CoA transferase, *atoAD* – acetyl-CoA acetyltransferase, *ptb-buk* – phosphotransbutyrylase-butyrate kinase, *phaC* – PHA synthase.

Table 3.1 – Plasmid names and description of genes encoded on each plasmid.

Plasmid	Plasmid Description
pCNCM0	pMTL71301 derivative; P$phaC_{Cn}$, $BAPAT_{Cv}$, $ydfG_{Ec}$
pCNCM1	pMTL71301 derivative; P$phaC_{Cn}$, $BAPAT_{Cv}$, $ydfG_{Ec}$, $prpE_{Cn}$
pCNCM2	pMTL71301 derivative; P$phaC_{Cn}$, $BAPAT_{Cv}$, $ydfG_{Ec}$, pct_{Cn}
pCNCM3	pMTL71301 derivative; P$phaC_{Cn}$, $BAPAT_{Cv}$, $ydfG_{Ec}$, $prpE_{Ec}$
pCNCM4	pMTL71301 derivative; P$phaC_{Cn}$, $BAPAT_{Cv}$, $ydfG_{Ec}$, $atoAD_{Ec}$
pCNCM5	pMTL71301 derivative; P$phaC_{Cn}$, $BAPAT_{Cv}$, $ydfG_{Ec}$, $ptb\text{-}buk_{Ca}$
pCNCM6	pMTL71301 derivative; P$phaC_{Cn}$, $BAPAT_{Cv}$, $prpE_{Cn}$, $ydfG_{Ec}$
pCNCM7	pMTL71301 derivative; P$phaC_{Cn}$, $BAPAT_{Cv}$, pct_{Cn}, $ydfG_{Ec}$
pCNCM8	pMTL71301 derivative; P$phaC_{Cn}$, $BAPAT_{Cv}$, $prpE_{Ec}$, $ydfG_{Ec}$
pCNCM9	pMTL71301 derivative; P$phaC_{Cn}$, $BAPAT_{Cv}$, $atoAD_{Ca}$, $ydfG_{Ec}$
pCNCM10	pMTL71301 derivative; P$phaC_{Cn}$, $BAPAT_{Cv}$, $ydfG_{Ec}$, $phaC_{Cn}$
pCNCM11	pMTL71301 derivative; P$phaC_{Cn}$, $BAPAT_{Cv}$, $ydfG_{Ec}$, $phaC_{Cs}{}^{RBS}{}_{SL}$
pCNCM12	pMTL71301 derivative; P$phaC_{Cn}$, $BAPAT_{Cv}$, $ydfG_{Ec}$, $rrnBT1T2_{Ec}$, $prpE_{Cn}$, Ptrp_{Ec}
pCNCM13	pMTL71301 derivative; P$phaC_{Cn}$, $BAPAT_{Cv}$, $ydfG_{Ec}$, $rrnBT1T2_{Ec}$, pct_{Cn}, Ptrp_{Ec}
pCNCM14	pMTL71301 derivative; P$phaC_{Cn}$, $BAPAT_{Cv}$, $ydfG_{Ec}$, $rrnBT1T2_{Ec}$, $prpE_{Ec}$, Ptrp_{Ec}

pCNCM15	pMTL71301 derivative; P*phaC*$_{Cn}$, *BAPAT*$_{Cv}$, *ydfG*$_{Ec}$, *rrnBT1T2*$_{Ec}$, *atoAD*$_{Ec}$, P*trp*$_{Ec}$
pCNCM16	pMTL71301 derivative; P*phaC*$_{Cn}$, *BAPAT*$_{Cv}$, *ydfG*$_{Ec}$, *rrnBT1T2*$_{Ec}$, *phaC*$_{Cn}$, *prpE*$_{Cn}$, P*trp*$_{Ec}$
pCNCM17	pMTL71301 derivative; P*phaC*$_{Cn}$, *BAPAT*$_{Cv}$, *ydfG*$_{Ec}$, *rrnBT1T2*$_{Ec}$, *phaC*$_{Cn}$, *pct*$_{Cn}$, P*trp*$_{Ec}$
pCNCM18	pMTL71301 derivative; P*phaC*$_{Cn}$, *BAPAT*$_{Cv}$, *ydfG*$_{Ec}$, *rrnBT1T2*$_{Ec}$, *phaC*$_{Cn}$, *prpE*$_{Ec}$, P*trp*$_{Ec}$
pCNCM19	pMTL71301 derivative; P*phaC*$_{Cn}$, *BAPAT*$_{Cv}$, *ydfG*$_{Ec}$, *rrnBT1T2*$_{Ec}$, *phaC*$_{Cn}$, *atoAD*$_{Ec}$, P*trp*$_{Ec}$
pCNCM20	pMTL71301 derivative; P*phaC*$_{Cn}$, *BAPAT*$_{Cv}$, *ydfG*$_{Ec}$, *rrnBT1T2*$_{Ec}$, *phaC*$_{Cs}$, *prpE*$_{Cn}$, P*trp*$_{Ec}$
pCNCM21	pMTL71301 derivative; P*phaC*$_{Cn}$, *BAPAT*$_{Cv}$, *ydfG*$_{Ec}$, *rrnBT1T2*$_{Ec}$, *phaC*$_{Cs}$, *pct*$_{Cn}$, P*trp*$_{Ec}$
pCNCM22	pMTL71301 derivative; P*phaC*$_{Cn}$, *BAPAT*$_{Cv}$, *ydfG*$_{Ec}$, *rrnBT1T2*$_{Ec}$, *phaC*$_{Cs}$, *prpE*$_{Ec}$, P*trp*$_{Ec}$
pCNCM23	pMTL71301 derivative; P*phaC*$_{Cn}$, *BAPAT*$_{Cv}$, *ydfG*$_{Ec}$, *rrnBT1T2*$_{Ec}$, *phaC*$_{Cs}$, *atoAD*$_{Ec}$, P*trp*$_{Ec}$

Earlier work showed that *C. necator* H16 is capable of using 3HP as a carbon source (173). Since the goal of this work was to incorporate 3HP into the copolymer, this trait was undesirable. It was shown that a triple mutant, in which three methylmalonate semialdehyde dehydrogenases encoded by *mmsA1*, *mmsA2*, and *mmsA3* have been deleted, is unable to grow using 3HP as a carbon source (173). This strain, hereafter referred to as Δ3, was used as the background strain in all experiments described in this chapter.

3.2 Results

3.2.1 Production of 3HP from β-alanine

Previous work had resulted in construction of a plasmid in which a putative β-alanine pyruvate aminotransferase (BAPAT) from *Chromobacterium violaceum* and NADP-dependent 3-hydroxyacid dehydrogenase (YdfG) from *E. coli* were cloned downstream of the

constitutive *phaC* promoter (P_{phaC}) from *C. necator* H16 [source; Katalin Kovács]. This plasmid was termed plasmid pCNCM0. Transformation of this plasmid into strain Δ3 resulted in strain Δ3_CNCM0. Flask cultivation experiments showed that growing strain Δ3_CNCM0 in SGMM with 50mM β-alanine resulted in presence of approximately 40mM 3HP in the supernatant. The control strains Δ3, containing no plasmid, and Δ3_eyfP, containing a plasmid pCNCM_eyfP in which *eyfP* is expressed under P_{phaC}, produced trace or no 3HP respectively **[Figure 3.3]**.

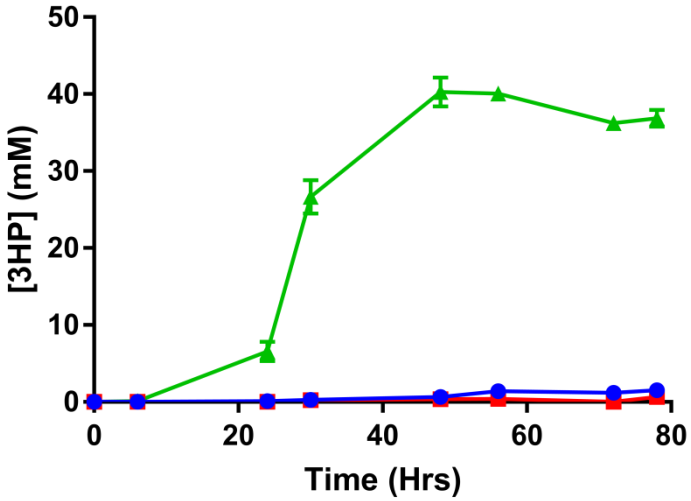

Figure 3.3 - 3HP produced by strains Δ3, Δ3_eyfP, and Δ3_CNCM0 following flask cultivation in SGMM supplemented with 50mM β-alanine. A peak of approximately 40mM 3HP was detected in the supernatant after 48hrs cultivation. (●) – Δ3, (■) – Δ3_eyfP, (▲) – Δ3_CNCM0. Experiments were performed triplicate.

Approximately 40mM 3HP was detected in the supernatant, suggesting the pathway for conversion of β-alanine to 3HP was functional. Control strains Δ3 and Δ3_eyfP produced trace and no 3HP, respectively.

Since large quantities of 3HP were detected in the supernatant of strain Δ3_CNCM0, this suggested minimal incorporation of 3HP into the copolymer. This was confirmed by GCMS analysis **[Table 3.2]**.

Table 3.2 – PHA composition of strains Δ3, Δ3_eyfP, and Δ3_CNCM0 following flask cultivation in SGMM supplemented with 50mM β-alanine. Experiments were performed in triplicate.

Strain	CDW (g/L)	PHA (%wt)	PHA (g/L)	3HB mol%	3HP mol%
Δ3	4.70	66.72	3.14	100	0
Δ3_eyfP	3.86	62.38	2.41	100	0
Δ3_CNCM0	2.00	17.74	0.35	98.73	1.27

Only 1.27 mol% 3HP was detected in the polymer extracted from strain Δ3_CNCM0. Both control strains were unable to produce 3HP from β-alanine, and a PHB homopolymer was produced. The results showed that while conversion of β-alanine to 3HP was enabled by the plasmid-based expression of $BAPAT_{Cv}$ and $ydfG_{Ec}$, *C. necator* H16 has insufficient ability to integrate this 3HP into a growing polymer chain. Furthermore, without expression of $BAPAT_{Cv}$ and $ydfG_{Ec}$ no significant quantities of 3HP were seen.

3.2.2 Expression of CoA-addition mechanism

In order to improve the incorporation of 3HP into the polymer, five genes with the ability to add a CoA moiety to compounds were selected for testing. These genes were a propionyl-CoA synthetase ($prpE_{Cn}$) and a propionyl-CoA transferase (pct_{Cn}) from *C. necator* H16, a propionyl-CoA synthetase ($prpE_{Ec}$) and an acetyl-CoA acetyltransferase ($atoAD_{Ec}$) from *E. coli*, and a phosphotransbutyrylase and butyrate kinase gene pair ($ptb\text{-}buk_{Ca}$)

from *Clostridium acetobutylicum*. Each gene was cloned individually downstream of $ydfG_{Ec}$ in plasmid pCNCM0, yielding five plasmids (pCNCM1-5). Transformation of these plasmids into the *C. necator* H16 background strain Δ3 resulted in strains Δ3_CNCM1-5. These strains were cultivated in SGMM supplemented with 50mM β-alanine as before.

The results of the cultivation of strains Δ3_CNCM1-5 are shown below in **Figure 3.4** and **Table 3.3**. HPLC analysis showed that different amounts of 3HP were detected in the supernatant depending on which CoA-addition mechanism was used **[Figure 3.4]**. A significant amount of 3HP was detected in the supernatant taken from strains Δ3_CNCM1 and Δ3_CNCM3, which encoded the propionyl-CoA synthetases of *C. necator* H16 and *E. coli* respectively. After 48 hours of cultivation, 44mM of 3HP could be detected in the supernatant taken from strain Δ3_CNCM1. However, this decreased to 35mM by the end of the cultivation. 3HP production by strain Δ3_CNCM3 also peaked at 48 hours, and 48mM of 3HP was detected in the supernatant. In this case however the concentration of 3HP did not decrease. Very little 3HP was detected in the supernatant of strains Δ3_CNCM2 and Δ3_CNCM4, which used propionyl-CoA transferase from *C. necator* H16 and acetyl-CoA acetyltransferase from *E. coli* respectively. Production of 3HP by these strains only began at around 72 hours, and the maximum 3HP produced by both strains was approximately 5mM. The strain using the *ptb-buk* gene pair as the CoA-addition system, strain Δ3_CNCM5, produced no 3HP at any point during the cultivation.

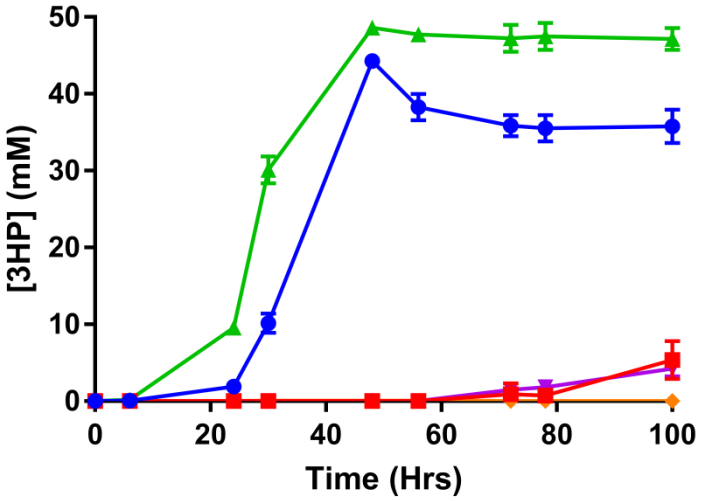

Figure 3.4 – 3HP produced by strains Δ3_CNCM1-5 following flask cultivation in SGMM supplemented with 50mM β-alanine. (●) – Δ3_CNCM1, (■) – Δ3_CNCM2, (▲) – Δ3_CNCM3, (▼) – Δ3_CNCM4, (♦) – Δ3_CNCM5. Experiments were performed triplicate.

Analysis of the copolymers produced by strains Δ3_CNCM1-5 is shown below in **Table 3.3**. Inclusion of a CoA-addition mechanism downstream of the 3HP-production operon increased 3HP molar fraction in the polymer 3-4-fold in all strains in comparison to strain Δ3_CNCM0, with the exception of strain Δ3_CNCM5. In the case of Δ3_CNCM5, no 3HP was detected in the polymer.

Table 3.3 – PHA composition of strains Δ3_CNCM1-5 following flask cultivation in SGMM supplemented with 50mM β-alanine. Experiments were performed in triplicate.

Strain	CDW (g/L)	PHA (%wt)	PHA (g/L)	3HB mol%	3HP mol%
Δ3_CNCM1	1.8	13.84	0.25	96.63	3.37
Δ3_CNCM2	0.80	2.50	0.02	96.52	3.48
Δ3_CNCM3	3.91	20.54	0.80	96.21	3.79
Δ3_CNCM4	0.74	3.12	0.02	95.98	4.02
Δ3_CNCM5	2.00	29.67	0.59	100	0

The results shown in **Table 3.3** suggest that conversion of 3HP to 3HP-CoA is a bottleneck for the synthesis of poly(3HB-*co*-3HP) in *C. necator* H16. While each strain tested was an improvement upon strain Δ3_CNCM0, the highest 3HP molar fraction achieved was by strain Δ3_CNCM4, at 4.02 mol% 3HP. Since strain Δ3_CNCM5, expressing *ptb-buk* from *C. acetobutylicum* as the CoA-addition mechanism, produced a polymer which contained no 3HP, further experiments with this gene were not carried out.

3.2.3 Alteration of operon structure

The results of **section 3.2.2** suggested that improving the ability of *C. necator* H16 to produce 3HP-CoA resulted in poly(3HB-*co*-3HP) with increased 3HP molar fraction. In order to further test this, the structure of the operon was altered such that the gene used for CoA-addition was now located in the second position. This gene rearrangement was expected to increase the expression of the CoA-addition mechanism, and therefore enhance 3HP-CoA synthesis. To test the effect of operon structure on the ability to incorporate 3HP into the polymer, the operons described in **section 3.2.2** were reorganised such that the gene used for CoA-addition was placed between $BAPAT_{Cv}$ and $ydfG_{Ec}$. The resulting plasmids were termed pCNCM6-9, and once transformed into background strain Δ3; this resulted in strains Δ3_CNCM6-9. These strains were cultivated in SGMM supplemented with 50mM β-alanine.

The results of the cultivation of strains Δ3_CNCM6-9 are shown below in **Figure 3.5** and **Table 3.4**. The amount of 3HP detected in the supernatant of strains expressing the altered operons was very similar to that

observed previously by strains expressing the original operons, as can be seen in **Figure 3.5**. Changing the operon structure had virtually no effect on 3HP production by the two strains expressing propionyl-CoA synthetases, Δ3_CNCM6 and Δ3_CNCM8, except that the strain expressing propionyl-CoA synthetase from *E. coli* no longer showed a peak in 3HP production at 48 hours. A more pronounced effect was observed following the change in operon structure with strains expressing pct_{Cn} or $atoAD_{Ec}$ as the CoA addition mechanism. While Δ3_CNCM2 and Δ3_CNCM4 produced around 5mM 3HP, strains Δ3_CNCM7 and Δ3_CNCM9 only produced around 2mM 3HP. However, 3HP production still only began after around 72 hours of cultivation.

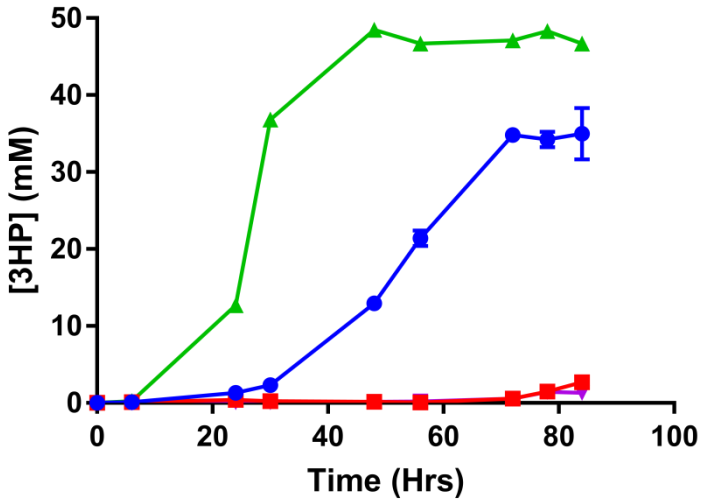

Figure 3.5 – 3HP produced by strains Δ3_CNCM6-9 following flask cultivation in SGMM supplemented with 50mM β-alanine. (●) – Δ3_CNCM6, (■) – Δ3_CNCM7, (▲) – Δ3_CNCM8, (▼) – Δ3_CNCM9. Experiments were performed triplicate.

The effect of altering operon structure on copolymer composition is shown in **Table 3.4**. All strains showed increased 3HP molar fraction compared to those expressing operons in the original structure. The strains

endowed with pct_{Cn} and $atoAD_{Ec}$, Δ3_CNCM7 and Δ3_CNCM9, were particularly improved by the operon reorganization, as both strains produced a copolymer containing approximately 8 mol% 3HP, the highest 3HP molar fraction achieved in this work so far. Strains Δ3_CNCM6 and Δ3_CNCM8 also showed an increase in 3HP molar fraction, though not as significant as Δ3_CNCM7 and Δ3_CNCM9.

Table 3.4 – PHA composition of strains Δ3_CNCM6-9 following flask cultivation in SGMM supplemented with 50mM β-alanine. Experiments were performed in triplicate.

Strain	CDW (g/L)	PHA (%wt)	PHA (g/L)	3HB mol%	3HP mol%
Δ3_CNCM6	3.55	14.90	0.53	94.37	5.63
Δ3_CNCM7	3.35	10.05	0.33	92.21	7.79
Δ3_CNCM8	3.93	18.00	0.70	95.87	4.13
Δ3_CNCM9	3.03	6.21	0.19	91.95	8.05

The results of the cultivation following plasmid reorganization showed that increasing the expression of the CoA-addition mechanism improved incorporation of 3HP into the polymer. While an increase in 3HP molar fraction was seen in all constructs, strains Δ3_CNCM7 and Δ3_CNCM9 produced copolymer with 7.79 and 8.05 mol% 3HP, the highest molar fractions of 3HP seen so far in the course of these experiments. However, these strains still required several days to begin producing 3HP, and the amount produced was low. Overall the increase in 3HP molar fraction for strains Δ3_CNCM6, 7, 8, and 9, was 67%, 124%, 9%, and 100% respectively, in comparison to the corresponding strains described in **section 3.2.2.**

3.2.4 Expression of PHA synthases

A second option for improving 3HP incorporation into the polymer was to increase the amount of PHA synthase available for carrying out the polymerization reaction. To facilitate this, genes encoding the PHA synthases from *C. necator* H16 and *Chromobacterium* sp. USM2 (*C.* sp. USM2) were cloned downstream of *ydfG* in plasmid pCNCM0, resulting in plasmids pCNCM10 and pCNCM11. Since genomic DNA of *C.* sp. USM2 was not available, the PHA synthase from this organism was synthesised, and a synthetic ribosomal binding site (RBS) designed using the Salis Lab RBS calculator was placed upstream of the start codon. Transformation of pCNCM10 and pCNCM11 into Δ3 resulted in strains Δ3_CNCM10 and Δ3_CNCM11. The results of the cultivation are shown below in **Table 3.5**.

Table 3.5 – PHA composition of strains Δ3_CNCM10-11 following flask cultivation in SGMM supplemented with 50mM β-alanine. Experiments were performed in triplicate.

Strain	CDW (g/L)	PHA (%wt)	PHA (g/L)	3HB mol%	3HP mol%
Δ3_CNCM10	2.13	15.25	0.32	97.13	2.87
Δ3_CNCM11	2.21	16.09	0.35	91.4	8.60

The effects of overexpressing a PHA synthase downstream of $ydfG_{Ec}$ differed between strains Δ3_CNCM10 and Δ3_CNCM11. While strain Δ3_CNCM10, expressing the PHA synthase from *C. necator* H16 showed an approximately 2-fold increase in 3HP molar fraction compared to strain Δ3_CNCM0, strain Δ3_CNCM11 carrying the PHA synthase from *C.* sp. USM2 exhibited an almost 7-fold increase in 3HP molar fraction over strain Δ3_CNCM0. At 8.6 mol% 3HP, strain Δ3_CNCM11 further increased the maximum incorporation of 3HP achieved so far.

3.2.5 Expression of CoA-addition mechanism and PHA synthase genes under a separate promoter

Taken together, the results from **sections 3.2.2**, **3.2.3**, and **3.2.4** showed that: 1) inclusion of a CoA-addition mechanism was beneficial for 3HP incorporation; 2) increasing the expression of the CoA-addition mechanism further improved incorporation, and; 3) overexpression of a PHA synthase also had a positive effect on the ability of the engineered strains to incorporate 3HP into the polymer. It was hypothesised that a combination of these three factors would lead to a further increase in 3HP molar fraction. In order to test this, another three sets of plasmids were generated.

3.2.5.1 Expression of CoA-addition mechanism under P_{trp}

In the first set of these three sets of plasmids, the CoA-addition mechanisms tested in **section 3.2.3** were cloned and placed under the control of the *trp* promoter (P_{trp}). The CoA-addition mechanism and P_{trp} were transcribed in the reverse orientation, and the rrnbT1T2 double terminator from *E. coli* was placed between *ydfG* and the gene used for the CoA-addition mechanism. The resulting plasmids were termed pCNCM12-15. Transformation into Δ3 yielded strains Δ3_CNCM12-15.

The results of the cultivation of strains Δ3_CNCM12-15 are shown below in **Figure 3.6** and **Table 3.6**. Strains Δ3_CNCM12 and Δ3_CNCM14 produced around 45mM 3HP. Previously, strains expressing pct_{Cn} had shown a long lag phase before production of 3HP began, and very low amounts of 3HP were produced. However, in this case the strain encoding pct_{Cn}, Δ3_CNCM13, was found to produce 3HP after 24 hours and a maximum of 35mM 3HP was detected in the supernatant of this strain after

48 hours of cultivation. By the end of the cultivation of strain Δ3_CNCM13, around 29mM 3HP was detected in the supernatant. On the other hand, strain Δ3_CNCM15 failed to grow.

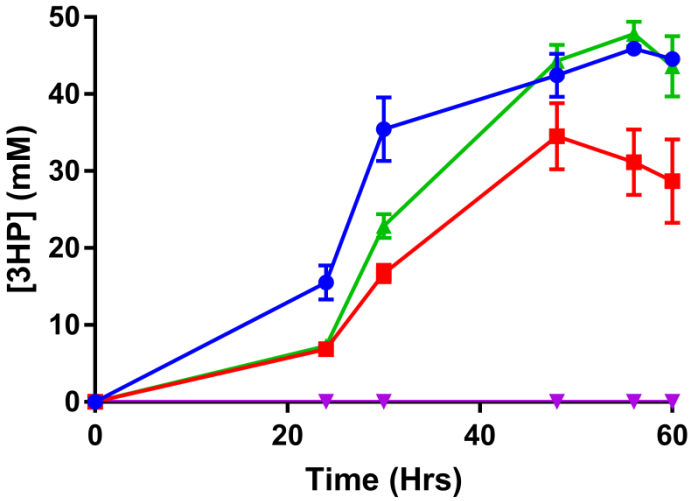

Figure 3.6 – 3HP produced by strains Δ3_CNCM12-15 following flask cultivation in SGMM supplemented with 50mM β-alanine. (●) – Δ3_CNCM12, (■) – Δ3_CNCM13, (▲) – Δ3_CNCM14, (▼) – Δ3_CNCM15. Experiments were performed triplicate.

The composition of the copolymers produced by strains Δ3_CNCM12-15 is shown in **Table 3.6**. Strain Δ3_CNCM14 produced a copolymer containing 11.5 mol% 3HP, the highest 3HP molar fraction observed so far. On the other hand strains Δ3_CNCM12 and Δ3_CNCM14 did not benefit from increased expression of $prpE_{Cn}$ or $prpE_{Ec}$, and 3HP molar fraction was only around 2 mol% 3HP. Since strain Δ3_CNCM15 failed to grow, no polymer analysis was carried out.

Table 3.6 – PHA composition of strains Δ3_CNCM12-15 following flask cultivation in SGMM supplemented with 50mM β-alanine. Experiments were performed in triplicate.

Strain	CDW (g/L)	PHA (%wt)	PHA (g/L)	3HB mol%	3HP mol%
Δ3_CNCM12	4.20	36.00	1.50	98.1	1.90
Δ3_CNCM13	2.78	11.23	0.31	88.5	11.50
Δ3_CNCM14	4.60	36.62	1.68	98.40	1.60
Δ3_CNCM15	-	-	-	-	-

The results from strains expressing the CoA-addition mechanism under P_{trp} showed that pct_{Cn} outperformed the other strains, producing a copolymer with 11.5 mol% 3HP, the highest molar fraction seen so far. Interestingly, it was also seen that the constructs containing $atoAD_{Ec}$, which was previously capable of achieving a high molar fraction of 3HP, failed to grow. Furthermore, the two strains containing propionyl-CoA synthetases had a reduced capacity for 3HP incorporation compared to previous constructs used in **sections 3.2.2** and **3.2.3**.

3.2.5.2 Expression of CoA-addition mechanism and $phaC_{Cn}$ under P_{trp}

In the next series of plasmids, the *C. necator* H16 PHA synthase gene and its native RBS were cloned downstream of the CoA-addition mechanism. These plasmids were termed pCNCM16-19, and their transformation into Δ3 resulted in strains Δ3_CNCM16-19.

HPLC analysis of supernatants taken during the cultivation of strains Δ3_CNCM16-19 is shown below **[Figure 3.7]**. Strains Δ3_CNCM16 and Δ3_CNCM18 both produced more than 40mM 3HP, as had previous versions of these strains. Δ3_CNCM18 produced less 3HP than the previous iteration of this strain; by the end of the cultivation only 21mM 3HP was detected in the supernatant. While the previous iteration of the $atoAD_{Ec}$-

expressing strain, Δ3_CNCM15, was unable to grow, strain Δ3_CNCM19 showed weak growth. However, only around 2mM 3HP was detected in samples taken during the cultivation of this strain.

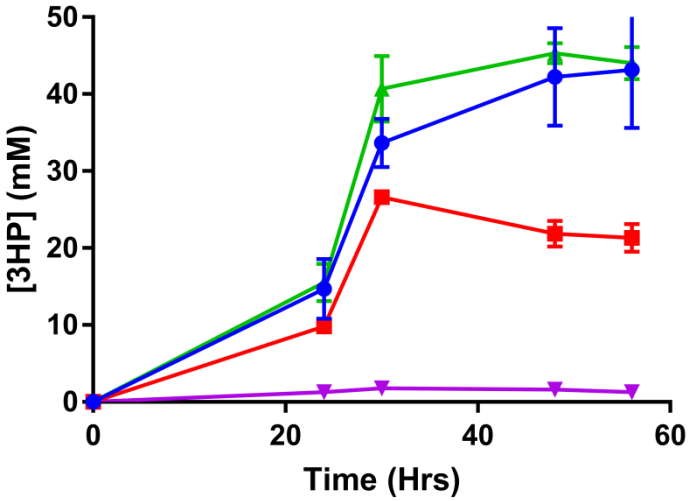

Figure 3.7 - 3HP produced by strains Δ3_CNCM16-19 following flask cultivation in SGMM supplemented with 50mM β-alanine. (●) – Δ3_CNCM16, (■) – Δ3_CNCM17, (▲) – Δ3_CNCM18, (▼) – Δ3_CNCM19. Experiments were performed triplicate.

The effect of overexpressing *phaC*$_{Cn}$ downstream of the CoA-addition mechanisms on copolymer composition is shown below **[Table 3.7]**. An increase in 3HP molar fraction was observed in strains Δ3_CNCM16 and Δ3_CNCM18 in comparison to strains Δ3_CNCM12 and Δ3_CNCM14. However, only around 7 mol% 3HP was achieved. Conversely, the copolymer produced by strain Δ3_CNCM17 had a dramatically increased 3HP content compared to all previous strains, as the copolymer contained approximately 77 mol% 3HP. Surprisingly, the copolymer produced by strain Δ3_CNCM19 contained even more 3HP, at around 89 mol% 3HP.

Table 3.7 – PHA composition of strains Δ3_CNCM16-19 following flask cultivation in SGMM supplemented with 50mM β-alanine. Experiments were performed in triplicate.

Strain	CDW (g/L)	PHA (%wt)	PHA (g/L)	3HB mol%	3HP mol%
Δ3_CNCM16	2.81	30.75	1.23	93.91	6.81
Δ3_CNCM17	3.33	14.30	0.47	22.60	77.40
Δ3_CNCM18	3.36	26.17	0.94	93.63	6.73
Δ3_CNCM19	0.35	16.16	0.05	11.28	88.72

Strains Δ3_CNCM17 and Δ3_CNCM19 both produced copolymers with a high molar fraction of 3HP. However, HPLC analysis showed that more 3HP could be detected in the supernatant of strain Δ3_CNCM17. Furthermore, strain Δ3_CNCM17 had shown much stronger growth than strain Δ3_CNCM19. While strain Δ3_CNCM17 achieved a maximum OD_{600} of approximately 9, strain Δ3_CNCM19 grew to an OD_{600} of less than 2 **[Figure 3.8]**.

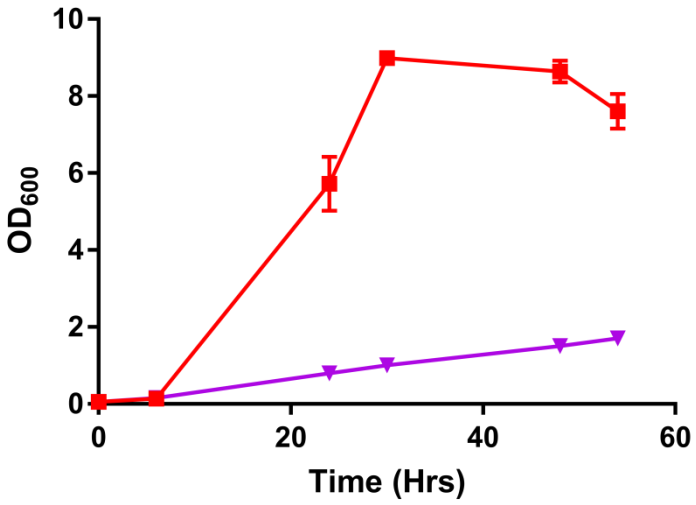

Figure 3.8 - Comparison of growth profiles from strains Δ3_CNCM17 and Δ3_CNCM19. Strains were cultivated in SGMM + 50mM β-alanine. (■) – Δ3_CNCM17, (▼) – Δ3_CNCM19. Experiments were performed in triplicate.

Since strain Δ3_CNCM19 exhibited weak growth, the cell dry weight was also low. It was reasoned that this would result in a low PHA titre in comparison to strain Δ3_CNCM17. Further analysis revealed that both cell dry weight (CDW) PHA titre of strain Δ3_CNCM19 was approximately 10 times less than strain Δ3_CNCM17 **[Table 3.8]**.

Table 3.8 – Comparison of poly(3HB-*co*-3HP) production by strains Δ3_CNCM17 and Δ3_CNCM19. Strains were cultivated in SGMM supplemented with 50mM β-alanine. Experiments were performed in triplicate.

Strain	CDW (g/L)	PHA (%wt)	PHA (g/L)	3HB mol%	3HP mol%
Δ3_CNCM17	3.33	14.30	0.47	22.60	77.40
Δ3_CNCM19	0.35	16.16	0.05	11.28	88.72

In summary, overexpression of both a CoA-addition mechanism and $phaC_{Cn}$ had greatly increased the ability of strains Δ3_CNCM17 and Δ3_CNCM19 to incorporate 3HP into the copolymer. However, due to weak growth, strain Δ3_CNCM19 produced very little copolymer.

3.2.5.3 Expression of CoA-addition mechanism and $phaC_{Cs}$ under P_{trp}

In the final series of vectors, the PHA synthase gene from *C. necator* H16 used in plasmids pCNCM 16-19 was replaced by the PHA synthase gene of *C.* sp. USM2. In order to better compare results of constructs containing the different PHA synthases, the synthetic RBS originally used for the $phaC_{Cs}$ in **section 3.2.4** was replaced by the RBS of the *C. necator* H16 PHA synthase. These plasmids were termed pCNCM20-23 and following transformation into Δ3, resulted in strains Δ3_CNCM20-23.

The analysis of strains containing the final vectors is shown below in **Figure 3.9** and **Table 3.9**. Strains Δ3_CNCM20 and Δ3_CNCM22 performed similarly to previous versions of these strains, both producing

around 40mM 3HP by the end of the cultivation. Less 3HP was detected in the supernatant of strain Δ3_CNCM21 than had been found in the supernatant of strain Δ3_CNCM17. Strain Δ3_CNCM23 was found to be unable to grow, as had its predecessor, strain Δ3_CNCM15. Therefore, no 3HP was detected in supernatant from this strain.

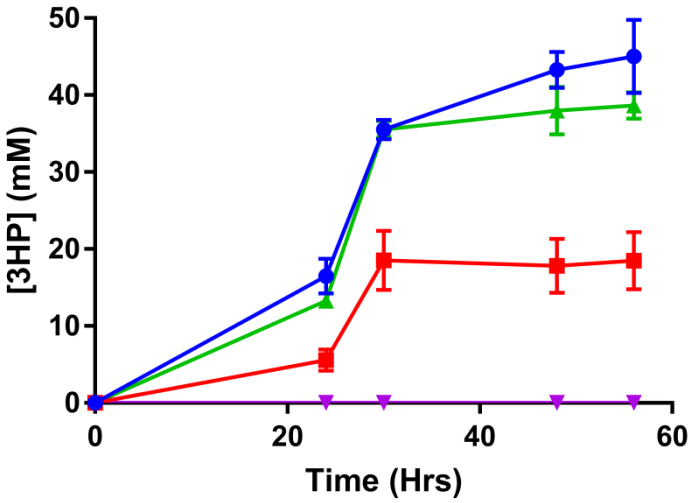

Figure 3.9 – 3HP produced by strains Δ3_CNCM20-23 following flask cultivation in SGMM supplemented with 50mM β-alanine. (●) – Δ3_CNCM20, (■) – Δ3_CNCM21, (▲) – Δ3_CNCM22, (▼) – Δ3_CNCM23. Experiments were performed triplicate.

The composition of copolymers produced by strains Δ3_CNCM20-23 is shown below **[Table 3.9]**. The best performing strain was seen to be Δ3_CNCM21, which produced a copolymer containing approximately 80 mol% 3HP. Strains Δ3_CNCM20 and Δ3_CNCM22 produced polymer with very similar composition to their predecessors, Δ3_CNCM16 and Δ3_CNCM18, while the absence of growth meant that no polymer analysis was carried out on strain Δ3_CNCM23.

Table 3.9 – PHA composition of strains Δ3_CNCM20-23 following flask cultivation in SGMM supplemented with 50mM β-alanine. Experiments were performed in triplicate.

Strain	CDW (g/L)	PHA (%wt)	PHA (g/L)	3HB mol%	3HP mol%
Δ3_CNCM20	3.23	28.46	0.91	94.90	7.10
Δ3_CNCM21	3.96	19.24	0.76	20.29	79.71
Δ3_CNCM22	4.11	26.64	1.09	90.98	9.02
Δ3_CNCM23	-	-	-	-	-

Since strains Δ3_CNCM17 and Δ3_CNCM21 had both produced copolymer with high 3HP molar fraction and had not shown any growth defects, further analysis was carried out on these strains to determine which would be most appropriate for further study. A comparison of CDW, PHA content, and PHA titre for strains Δ3_CNCM17 and Δ3_CNCM21 is shown below **[Table 3.10]**. While the only difference between the strains was the PHA synthase used, it was seen that strain Δ3_CNCM21, expressing $phaC_{Cs}$, contained approximately 35% more PHA than Δ3_CNCM17. As a result, the PHA titre of strain Δ3_CNCM21 was approximately 62% greater than strain Δ3_CNCM17, expressing $phaC_{Cn}$.

Table 3.10 – Comparison of poly(3HB-*co*-3HP) produced by strains Δ3_CNCM17 and Δ3_CNCM21. Strains were cultivated in SGMM supplemented with 50mM β-alanine. Experiments were performed in triplicate.

Strain	CDW (g/L)	PHA (%wt)	PHA (g/L)	3HB mol%	3HP mol%
Δ3_CNCM17	3.33	14.30	0.47	22.60	77.40
Δ3_CNCM21	3.96	19.24	0.76	20.29	79.71

As a result of extensive testing of numerous genes in various different operon structures, plasmid pCNCM21 was revealed to be the most appropriate plasmid for further work.

3.3 Discussion

The aim of this chapter was to produce poly(3HB-*co*-3HP) in *C. necator* with high 3HP molar fraction. Of the numerous studies describing biosynthesis of poly(3HB-*co*-3HP), only two describe the use of *C. necator* (91,100). The highest 3HP molar fraction observed in those works was 7 mol% 3HP, despite supplementation with up to 30 g/L 3HP in the medium. Initially, low 3HP content was observed in the polymer when cells were engineered to produce 3HP from β-alanine. The low incorporation into the polymer could result from a combination of two factors; that 3HP was not being effectively activated to 3HP-CoA, and that the PHA synthase of *C. necator* H16 has low affinity for 3HP-CoA. The initial experiments showed that expression of a CoA-addition mechanism was advantageous for increasing 3HP content in the copolymer, and that stronger expression of the CoA-addition mechanism resulted in further improvements. Expression of a PHA synthase was also shown to increase 3HP molar fraction. Later experiments showed that combined overexpression of a CoA-addition mechanism and PHA synthase greatly enhanced 3HP incorporation into the copolymer. Following a significant amount of plasmid engineering, it proved possible to produce poly(3HB-*co*-3HP) in *C. necator* H16 with a 3HP molar fraction of approximately 80 mol% 3HP.

The first aim of this study was to facilitate the conversion of β-alanine to 3HP. This meant that adding 3HP directly to the medium could be avoided and allowed construction of the downstream part of the β-alanine pathway to procede. Earlier studies have shown that combined production of a β-alanine pyruvate aminotransferase (BAPAT) and NADP-dependent 3-

hydroxyacid dehydrogenase (ydfG) could effectively provide 3HP from β-alanine (113,118,123,175). Following cultivation in medium supplemented with 50mM β-alanine, it was observed that around 40mM 3HP accumulated in the supernatant of strain Δ3_CNCM0, and a small amount of 3HP in the copolymer produced, suggesting at least 80% of the β-alanine was converted to 3HP **[Figure 3.3]**. However, in agreement with the studies by Nakamura *et al*. and Fukui *et al*., availability of 3HP did not lead to a copolymer with high 3HP molar fraction, as only 1.27 mol% 3HP was detected in the copolymer produced [**Table 3.2]**. It was decided to test the effect of overexpressing CoA-addition mechanisms and PHA synthases on 3HP molar fraction.

The five CoA-addition mechanisms tested were chosen based on their ability to activate 3HP to 3HP-CoA, or propionate to propionyl-CoA. The five genes which were selected encoded propionyl-CoA synthetases from *E. coli* and *C. necator* H16, propionyl-CoA transferase from *C. necator* H16, acetyl-CoA acetyltransferase from *E. coli*, and the phosphotransbutyrylase and butyrate kinase from *C. acetobutylicum*.

The propionyl-CoA synthetase from *E. coli* has been used on several occasions to produce poly(3HP), demonstrating an ability to form 3HP-CoA from 3HP (108,113,115,118). On the other hand, the propionyl-CoA synthetase from *C. necator* H16 has been used in the production of polymers containing lactic acid (LA), 2-hydroxybutyrate (2HB), and 3-hydroxyvalerate (3HV), rather than those containing 3HP (178–181). However, since LA is structurally very similar to 3HP, and production of 3HV requires activation of propionate to propionyl-CoA, it was reasoned

that the propionyl-CoA synthetase of *C. necator* H16 may be able use 3HP as a substrate as well. Furthermore, the evidence that the propionyl-CoA synthetases of *E. coli* and *S. typhimurium* (119) have been used for the production of 3HP-containing polymers suggests that propionyl-CoA synthetases in general could have activity on 3HP. Moreover, propionyl-CoA synthetases function in an ATP-dependent manner, which should be favourable for conversion of 3HP to 3HP-CoA (182).

A propionyl-CoA transferase from *C. necator* H16 has been characterized and was shown to transfer CoA from acetyl-CoA to 3HP as well as several other substrates (183,184). Despite this, the pct_{Cn} gene does not appear to have been used in the production of any compound, PHA or otherwise, at the time of writing. On the other hand, the propionyl-CoA transferase of *Clostridium propionicum* (*C. propionicum*) has been used several times in previous studies for the production of 3HP-containing polymers (110,111,117). Based on the results of these studies, it was expected that the propionyl-CoA transferase of *C. necator* H16 would be able to use 3HP as a substrate *in vivo*. While propionyl-CoA transferases do not require ATP to function, they do require a donor molecule, such as acetyl-CoA, to supply the CoA moiety (185).

The acetyl-CoA acetyltransferase from *E. coli* has so far been used for the production of poly(3HB-*co*-3HV) copolymers (186,187). The production of 3HV in these studies relied on conversion of propionate to propionyl-CoA by *atoAD*, and the gene was chosen as a possible CoA-addition mechanism due to this. Acetyl-CoA acetyltransferases function

similarly to propionyl-CoA transferases in that they do not require ATP to function, instead using a donor molecule to provide the CoA moiety (188).

Lastly, the *ptb-buk* gene pair from *C. acetobutylicum* has been used to produce CoA-thioesters of various PHA monomers, including 3HB, 3HV, 4HB, and 4HV and to activate propionate and butyrate to propionyl-CoA and butyryl-CoA for the biosynthesis of 3HV and 3-hydroxyhexanoate (3HHx) (189,190). Reports also state, however, that the enzymes encoded by *ptb-buk* are capable of performing the reverse reaction. That is, removing the CoA moiety from a given substrate (191,192). The reaction catalysing addition of CoA to a substrate uses ATP which could help to drive the reaction in the direction of CoA-addition.

It was expected that expression of a CoA-addition mechanism would positively influence 3HP content of the polymer, since activation of 3HP to 3HP-CoA is essential in order for incorporation of the monomer into the polymer (83,119). The 3HP content of the polymer produced was influenced not only by which CoA-addition mechanism was used, but also by how strongly the CoA-addition mechanism was expressed. The results of **section 3.2.2** showed that overexpression of a CoA-addition mechanism improved the ability of the cells to integrate 3HP into the polymer **[Table 3.3]**. However, in comparison to strain Δ3_CNCM0, which began producing 3HP after 24 hours, strains expressing either pct_{Cn} or $atoAD_{Ec}$ took approximately 72 hours begin producing 3HP due to a long lag phase, and the 3HP titre in these strains was much lower **[Figure 3.4]**. Additionally, 3HP production was completely abrogated in the strain expressing *ptb-buk* from *C. acetobutylicum* as the CoA-addition mechanism, and the polymer produced

by this strain contained no 3HP **[Figure 3.4, Table 3.3]**. Since expression of *ptb-buk*$_{Ca}$ had negatively affected the process, this gene was not used for further study.

In **section 3.2.3**, the operons tested in **section 3.2.2** were rearranged in order to more strongly express the CoA-addition mechanism. This resulted in further increased 3HP molar fraction. Work by Lim *et al*. showed how the structure of an operon influences the expression of genes (162). Using an operon containing three fluorescent proteins, it was shown that higher or lower fluorescence was observed if the fluorescent protein was in the first or third position in the operon respectively. This phenomenon has been exploited for biotechnological purposes. In one instance, the *phaCAB* operon of *C. necator* H16 was reorganized into six different structures to investigate the effect of gene order on PHB accumulation (193). The authors found that a gene order of *phaCBA* resulted in 57% PHA as CDW, while the native gene order of *phaCAB* resulted in 52% PHA as CDW. In a second study, Andreessen *et al.* rearranged the structure of an operon for the production of poly(3HP) from glycerol in *S. blattae* (111). Secretion of 3HP into the supernatant was observed in a previous attempt to produce poly(3HP) by the same group, who reasoned that insufficient activation of 3HP to 3HP-CoA was the cause (110). Altering the operon structure such that the CoA-addition mechanism was situated closer to the promoter increased the poly(3HP) content of glycerol-grown *S. blattae* cells from 9.8% to 14.5%. In the work undertaken here, altering the operon structure also improved the ability of the cells to incorporate 3HP into the polymer, though not all strains benefitted equally. It was seen that the strains

expressing *pct*$_{Cn}$ or *atoAD*$_{Ec}$ benefitted much more from being placed closer to the promoter than *prpE*$_{Cn}$ or *prpE*$_{Ec}$ **[Table 3.4]**. However, strain expressing either *pct*$_{Cn}$ or *atoAD*$_{Ec}$ still required several days to produce very low amounts of 3HP **[Figure 3.5]**.

The results of **sections 3.2.2** and **3.2.3** suggested that increasing expression of genes encoding the CoA-addition mechanisms also increased 3HP incorporation [**Tables 3.3, 3.4]**. Accordingly, the expression of the CoA-addition mechanism was further enhanced by placing it under a separate promoter. The strong promoter of the *E. coli trp* gene (P$_{trp}$) was chosen as it has previously been successfully employed in *C. necator* H16, and shown to be a stronger promoter than P$_{phaC}$ (194). Stronger expression of the CoA-addition mechanisms under P$_{trp}$, did not result in the same effects as seen before except in the case of the strain expressing *pct*$_{Cn}$, Δ3_CNCM13 **[Table 3.6]**. Surprisingly, stronger expression of *pct*$_{Cn}$ relieved the apparent inhibition in 3HP production that previous strains containing this gene had shown **[Figure 3.6]** Expression of the propionyl-CoA synthetases under P$_{trp}$ resulted in decreased 3HP content in the copolymer compared to previous strains containing propionyl-CoA synthetases. It is possible that the increased expression resulted in excessive production of protein which then aggregated. Alternatively the increased metabolic burden of stronger expression may have excessively drained cellular resources, leaving insufficient ATP for the propionyl-CoA synthetases to effectively catalyse the addition of CoA to 3HP. It was also observed that the strain expressing *atoAD*$_{Ec}$ under P$_{trp}$, Δ3_CNCM15, was unable to grow **[Table 3.6]**. Strains expressing the same combination of

genes had previously produced copolymer with some of the highest 3HP molar fractions **[Tables 3.3, 3.4]**. One possible reason for this is that *atoAD*$_{Ec}$ was too strongly expressed under P_{trp}, and as a result drained the acetyl-CoA pool, as it can use acetyl-CoA in addition to acetoacetyl-CoA as a CoA donor (188). A similar phenomenon was observed during the characterization of propionyl-CoA transferase isolated from *C. propionicum*. Expression of this propionyl-CoA transferase in *E. coli* resulted in severe growth defects when induced using IPTG (195). The authors suggested depletion of the acetyl-CoA pool resulted in excess interference with essential metabolic pathways. Since growth defects were not observed in the equivalent strain containing *pct*$_{Cn}$, which also draws CoA from acetyl-CoA, this may suggest that *atoAD*$_{Ec}$ has a higher activity on acetyl-CoA than *pct*$_{Cn}$. The potential of *atoAD*$_{Ec}$ in activation of 3HP to 3HP-CoA was also indicated by strain Δ3_CNCM19 in **Table 3.7** of **section 3.2.5.2**. The polymer produced by this strain contained 89 mol% 3HP, though growth was still severely inhibited. Since the results of **Tables 3.3**, **3.4**, and **3.7** showed *atoAD*$_{Ec}$ has the capacity to improve addition of 3HP to the polymer, further work could be carried out to express *atoAD*$_{Ec}$ under a weaker promoter to investigate whether or not this would alleviate the growth impairments observed in these studies. Although strain Δ3_CNCM19 was capable of producing copolymer with very high 3HP molar fraction, the heavily restricted growth and PHA titre in comparison to strain Δ3_CNCM17 meant strain Δ3_CNCM19 was not a viable choice for further experimentation.

In vitro studies have shown that the PHA synthase from *C. necator* H16 has low affinity for 3HP-CoA compared to 3HB-CoA (177,196). Therefore another possibility for improving 3HP content of the polymer was increasing the amount of PHA synthase in the cells. The work carried out in **section 3.2.4** investigated two PHA synthases; the native PHA synthase from *C. necator* H16, and the PHA synthase from *C.* sp. USM2. The PHA synthase from *C. necator* H16 has been used extensively for the production of 3HP-containing polymers from engineered microorganisms (101,106,107,112). On the other hand, the PHA synthase of *C.* sp. USM2 has only been used on one occasion for the production of a 3HP-containing polymer, in this case poly(3HP) (114). The PHA synthase of *C.* sp. USM2 was also chosen on account of the fact that it possesses a higher catalytic activity than the PHA synthase of *C. necator* H16. While the PHA synthase from *C. necator* H16 was shown to have an activity of around 40 U/mg, the activity of the PHA synthase from *C.* sp. USM2 was 238 U/mg (177)(197)**.**

The results from **section 3.2.4** suggested that overexpression of the PHA synthase gene from *C.* sp. USM2 was much more effective in increasing 3HP molar fraction than overexpression of the *C. necator* H16 PHA synthase gene **[Table 3.5]**. However, the difference could be attributed to various factors. One possibility is that the much higher activity of the *C.* sp. USM2 PHA synthase contributed to the increased 3HP molar fraction. Another possibility is due to the fact that the two constructs did not use the same ribosomal binding site (RBS). The function of the RBS is to provide a binding site for the ribosome at the 5’ end of mRNA, prior to protein

translation (198). However, changes to the sequence of the RBS affect how readily the ribosome binds to the mRNA, resulting in varied levels of expression (199). This phenomenon can be exploited for biotechnological purposes. For instance, Bi *et al*. showed that changing the RBS in a series of plasmids designed for hydrocarbon production resulted in different titres (144). In the case of plasmids Δ3_CNCM10 and Δ3_CNCM11, $phaC_{Cn}$ was cloned downstream of its native RBS, while $phaC_{Cs}$ was synthesised with a synthetic RBS. The synthetic RBS was likely stronger than that of the $phaC_{Cn}$ native RBS, leading to greater expression and therefore more PHA synthase available for incorporation of 3HP into the copolymer. While the amount of 3HP content of the copolymers produced by strains Δ3_CNCM10 and Δ3_CNCM11 differed, it was indicated that overexpression of a PHA synthase had increased the ability of the cells to incorporate 3HP into the copolymer.

The results discussed so far had shown that overexpression of either a CoA-addition mechanism or PHA synthase was beneficial for improving the ability of *C. necator* H16 to incorporate 3HP into the polymer. Plasmids pCNCM16-23 tested the effect of simultaneously overexpressing both a CoA-addition mechanism and PHA synthase. The results of **sections 3.2.5.2** and **3.2.5.3** revealed that strains Δ3_CNCM17 and Δ3_CNCM21, which expressed pct_{Cn} alongside $phaC_{Cn}$ or $phaC_{Cs}$ respectively, had a dramatically improved ability to integrate 3HP into the copolymer compared to previous strains. An interesting observation was that while both strains accumulated poly(3HB-*co*-3HP) with very similar 3HP molar fraction, the PHA content and titre between the two strains was quite different. The PHA content and

titre of strain Δ3_CNCM21 were around 35% and 60% higher than in strain Δ3_CNCM17. As mentioned above in **section 3.2.4**, the effect of overexpressing either *phaC*$_{Cn}$ or *phaC*$_{Cs}$ downstream of *BAPAT*$_{Cv}$ and *ydfG*$_{Ec}$ was tested using strains Δ3_CNCM10 and Δ3_CNCM11 respectively. In those experiments the PHA synthase gene of *C. necator* H16 was downstream of its native RBS, while the PHA synthase gene of *C.* sp. USM2 was downstream of a synthetic RBS. It is likely that strain Δ3_CNCM11 outperformed strain Δ3_CNCM10 because the synthetic RBS was stronger than the native RBS. In order to more fairly compare the effect of the different PHA synthases in **sections 3.2.5.2** and **3.2.5.3**, the RBS used in both cases was that of the *C. necator* H16 PHA synthase gene. As such this suggests that the results presented in **Table 3.10** are due to the higher activity of the *C.* sp. USM2 PHA documented by Bhubalan *et al* (197).

With the exception of strain Δ3_CNCM19, which was discussed above, no other strains in which a CoA-addition mechanism and PHA synthase were simultaneously overexpressed showed a large increase in 3HP incorporation **[Table 3.7, 3.9]**. Strains expressing a propionyl-CoA synthetase alongside a PHA synthase under P$_{trp}$ showed an increased 3HP molar fraction compared to strains only expressing a propionyl-CoA synthetase under P$_{trp}$, however the difference can likely be attributed to increased PHA synthase activity in those cells.

The results of this chapter showed that *C. necator* H16 does not readily incorporate 3HP into the polymer. However, this was remedied with sufficient overexpression of relevant genes. It was shown that the expression of *BAPAT*$_{Cv}$ and *ydfG*$_{Ec}$ under the control of P$_{phaC}$ resulted in the conversion

of 50mM β-alanine to approximately 40mM 3HP. Incorporation of 3HP into the polymer required overexpression of both a suitable CoA-addition mechanism and PHA synthase. Individual expression of either of these enzymes did not lead to significant increase in 3HP molar fraction. Furthermore it was shown that the higher activity of the PHA synthase from *C.* sp. USM2 resulted in a greater PHA titre compared to the strain overexpressing the PHA synthase of *C. necator* H16. The 79.71 mol% 3HP achieved by strain Δ3_CNCM21 represents an almost 63-fold increase in 3HP molar fraction compared to the first strain, Δ3_CNCM0, which achieved 1.27 mol% 3HP.

Chapter 4: Effect of medium composition on polymer composition and content of cells

4.1 Introduction

As highlighted in **Chapter 1**, the properties of PHAs can be modulated not only by inclusion of a second monomer, but also by changing the molar fraction of the second monomer. Data compiled from a number of studies on poly(3HB-*co*-3HP) showed how increasing 3HP molar fraction changed the properties of the copolymer (51,91,93,96,97,99–101) **[Figure 1.5 Chapter 1]**. Additional studies on copolymers such as poly(3HP-*co*-4HB) and poly(3HB-*co*-3HHx) showed that changing the ratio of the monomers can result in polymers with very diverse properties including transparency, opacity, elasticity, and adhesive qualities (86,87).

One of the most common means of producing copolymers with different monomer ratios is to cultivate the polymer-producing bacteria in medium containing varied amounts of the precursor(s) towards the desired HA monomer(s). This method was used extensively in early studies of poly(3HB-*co*-3HP). For example, by cultivating *Alcaligenes latus* with 3HP and sucrose, or 3HP and 3HB, poly(3HB-*co*-3HP) could be produced with 3HP molar fraction between 7 and 88 mol% 3HP (51). More recently, the molar fractions of 3HB, 3HV, and 3HHx in a copolymer of poly(3HB-*co*-3HV-*co*-3HHx) could be altered depending on the amounts of crude palm kernel oil, valerate, and propionate added to the medium (200). A similar approach was also used for the production of poly(3HP-*co*-4HB) by engineered *E. coli* cultivated in medium containing 1,3-propanediol (PDO) and 1,4-butanediol (BDO) as precursors to 3HP and 4HB, respectively. By altering the concentration of PDO and BDO, it was possible to produce poly(3HP-*co*-4HB) with 3HP molar fraction ranging between 16 and 88

mol%. Furthermore, cultivation in only PDO or only BDO resulted in production of poly(3HP) and poly(4HB) homopolymers respectively (87).

One unique approach employed for the production of poly(3HB-*co*-3HP) using engineered *E. coli* was to separately control the expression of pathways responsible for the biosynthesis of the 3HB and 3HP monomers with different inducers (101). The pathway for 3HB biosynthesis was controlled by an arabinose-inducible promoter, while the pathway for 3HP biosynthesis was controlled by an IPTG inducible promoter. While IPTG concentration was kept constant, different concentrations of arabinose were used to vary the expression of the 3HB biosynthetic pathway. As a result, the amount of 3HB available varied, and therefore the composition of the polymer varied. Using this method, poly(3HB-*co*-3HP) with 3HP content ranging from 11.5 to 95.6 mol% 3HP could be produced.

The work carried out in the previous chapter had resulted in the production of poly(3HB-*co*-3HP) containing a high molar fraction of 3HP. The composition of the polymers obtained, however, only covered a narrow range of 3HP molar fractions; various 3HP contents from 1 to 11.5 mol% 3HP, and high 3HP contents of around 80 and 89 mol% 3HP had been achieved. As such, no copolymer with 3HP content between 11.5 and 80 mol% 3HP had been produced. Therefore, the work of this chapter aimed to fill in these gaps, such that poly(3HB-*co*-3HP) with a range of 3HP content could be produced.

As mentioned above, supplementing PHA-producing bacteria with varying amounts of precursor is a simple and effective means of producing a

copolymer with varied composition. Accordingly, the effect of varying β-alanine concentration on 3HP molar fraction was investigated. Besides, none of the plasmids tested in **Chapter 3** contained any inducible elements; therefore, control of gene expression in this manner was not an option.

On the one hand, the results of the previous chapter showed that strain Δ3_CNCM19 had produced copolymer with the highest 3HP content, growth of this strain was severely inhibited and PHA titre was very low. On the other hand, strain Δ3_CNCM21 had exhibited a good balance of growth, PHA titre, and high 3HP molar fraction. On account of these factors, strain Δ3_CNCM21 was used in the following experiments.

4.2. Results

4.2.1 Cultivation of strain Δ3_CNCM21 in varying concentrations of β-alanine

During the plasmid engineering experiments, strains were fed with 50mM β-alanine in order to produce 3HP. The strain with the best overall performance was strain Δ3_CNCM21, producing a copolymer containing approximately 80 mol% 3HP. In order to obtain poly(3HB-*co*-3HP) with a varying 3HP molar fraction, it was reasoned that feeding strain Δ3_CNCM21 with lower amounts of β-alanine would result in lower amounts of 3HP produced, and subsequently a lower amount of 3HP in the polymer. Further, it was hypothesised that supplementing strain Δ3_CNCM21 with 2mM cysteine as well as 50mM β-alanine would further increase the 3HP molar fraction, since cysteine supplementation has previously been used in increase CoA pool (201). Strain Δ3_CNCM21 was

therefore grown in SGMM supplemented with β-alanine concentrations ranging from 0 to 40mM, and in one instance in SGMM supplemented with 50mM β-alanine + 2mM cysteine.

The results of the cultivations in different medium are shown below in **Figure 4.1** and **Table 4.1**. HPLC analysis revealed that as the amount of supplemented β-alanine increased, so did the amount of 3HP secreted by the cells **[Figure 4.1]**. For instance, when Δ3_CNCM21 was grown in SGMM supplemented with 5 or 10mM β-alanine, essentially no 3HP was detected in the supernatant. If no β-alanine was provided, no 3HP was detected. It was also noticed that different amounts of 3HP were found in the supernatant at the end of the cultivation depending on whether strain Δ3_CNCM21 was cultivated in SGMM supplemented with 50mM β-alanine, or SGMM supplemented with 50mM β-alanine + 2mM cysteine. Cultivation in SGMM supplemented with 50mM β-alanine resulted in the presence of approximately 18mM 3HP in the supernatant after 48 hours of cultivation. In contrast, only 13mM 3HP was detected after 48 hours cultivation when strain Δ3_CNCM21 was cultivated in SGMM supplemented with 50mM β-alanine + 2mM cysteine.

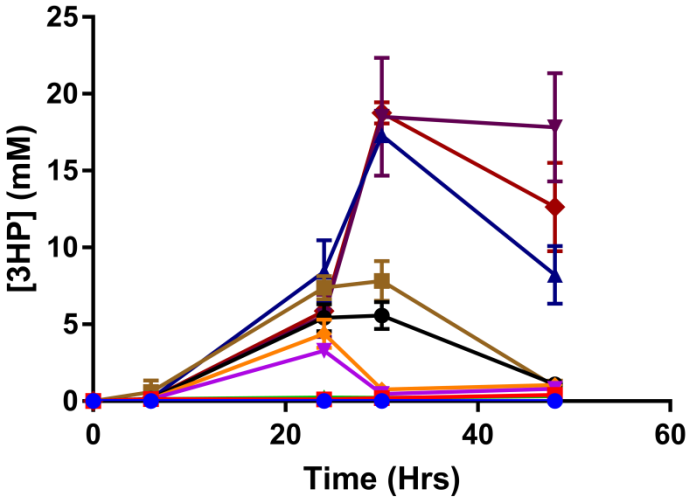

Figure 4.1 - 3HP production by strain Δ3_CNCM21following flask cultivation in different media. Cultivations were carried out in SGMM supplemented with varying millimolar amounts of β-alanine, or β-alanine and cysteine. The cultivation conditions were as follows; (●) – 0mM β-alanine, (■) – 5mM β-alanine, (▲) – 10mM β-alanine, (▼) – 15mM β-alanine, (♦) – 20mM β-alanine, (●) – 25mM β-alanine, (■) – 30mM β-alanine, (▲) – 40mM β-alanine, (▼) – 50mM β-alanine, (♦) - 50mM β-alanine + 2mM cysteine.

The results of **Figure 4.1** showed that the amount of 3HP secreted into the supernatant increased as the amount of β-alanine increased. They also showed that additional supplementation with 2mM cysteine reduced the amount of 3HP secreted into the supernatant. Based on these results, it was expected that the copolymers produced by strain Δ3_CNCM21 in each of these different conditions would show similar variation in 3HP molar content.

The results of the copolymer analysis are shown below in **Table 4.1**. It was found that the ratio between 3HB and 3HP monomers could be controlled by adjusting the amount of β-alanine in the medium. Cultivation with between 5 and 50mM β-alanine resulted in production of copolymers with a range of 3HP content; between 2 and 79 mol% 3HP was achieved. It

was also shown that supplementation with 40 or 50mM β-alanine resulted in copolymer with essentially the same 3HP molar fraction. While supplementation with 40mM β-alanine resulted in 78 mol% 3HP, supplementation with 50mM had previously resulted in 79 mol% 3HP. The HPLC analysis showed that supplementation with 50mM β-alanine and 2mM cysteine resulted in a much lower final 3HP concentration in the supernatant compared to cultivation in 50mM β-alanine alone. The results of the copolymer analysis showed that including cysteine in the medium was beneficial for 3HP incorporation into the polymer, since the 3HP molar fraction could be increased to 89 mol%.

Table 4.1 – Composition of poly(3HB-*co*-3HP) produced by strain Δ3_CNCM21 grown in different media. Cultivations were carried out in SGMM supplemented with varying millimolar amounts of β-alanine, or β-alanine and cysteine. All experiments were carried out in triplicate. Results are from samples taken at 48hrs. *** Data for cultivation with 50mM β-alanine was taken from the 48hr timepoint of the cultivation of Δ3_CNCM21 in **section 3.2.5.3**, **Table 3.8**.

β-alanine (mM)	Cysteine (mM)	CDW (g/L)	PHA (wt%)	PHA (g/L)	3HB (mol%)	3HP (mol%)
0	-	2.92	65.98	1.93	>99.9	Trace
5	-	4.41	60.18	2.64	97.76	2.24
10	-	5.10	50.77	2.59	92.89	7.11
15	-	5.31	39.24	2.08	83.4	16.60
20	-	4.99	29.91	1.49	63.28	36.72
25	-	5.16	24.03	1.23	50.17	49.83
30	-	5.03	22.16	1.11	32.99	67.01
40	-	4.14	16.97	0.70	21.37	78.63
50***	-	3.96	19.27	0.76	20.29	79.71
50	2	4.76	17.51	0.83	11.16	88.84

The results from **Table 4.1** showed that the molar fraction of 3HP could be altered by supplementing strain Δ3_CNCM21 with varied β-

alanine concentrations. By feeding strain Δ3_CNCM21 with varying amounts of β-alanine it was possible to produce poly(3HB-*co*-3HP) with molar fractions ranging from 0 to ~79 mol%. The results also revealed that the 3HP molar fraction remained essentially the same between 40 and 50mM β-alanine. This apparent upper limit could be increased by adding 2mM cysteine to strain Δ3_CNCM21 cells grown in 50mM β-alanine. Addition of cysteine increased 3HP molar fraction from approximately 79 mol% to almost 89 mol%.

4.2.2 Effect of different molar fraction of 3HP on polymer content of cells

Previous studies have indicated that as the molar fraction of 3HP in a copolymer of poly(3HB-*co*-3HP) increases, the PHA content of cells decreases (93–95,100,101). From the cultivations described in **section 4.2.1**, poly(3HB-*co*-3HP) with 10 different 3HP molar fractions had been produced, ranging from trace to 89 mol% 3HP. To determine the effect of increasing 3HP content on the cells, the PHA content and 3HP molar fraction were compared **[Figure 4.2]**.

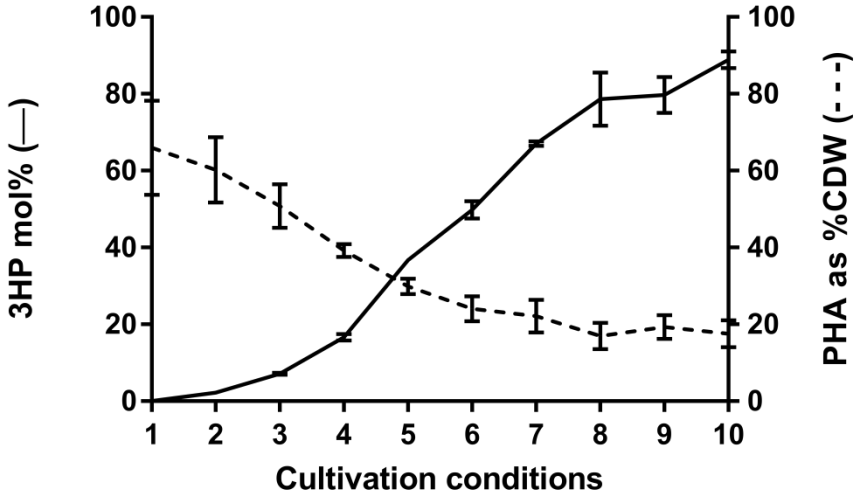

Figure 4.2 – Plot of the relationship between 3HP content of the copolymer and PHA content of the cells. 3HP content of the polymer is indicated by the solid black line. PHA content of the cells is indicated by the dashed line. Strain Δ3_CNCM21 was cultivated in SGMM supplemented with varying amounts of β-alanine, and in one instance both β-alanine and cysteine. "Cultivation conditions" indicates the amount of β-alanine or cysteine supplemented in the SGMM. Cultivation conditions were as follows; 1 – 0mM β-alanine, 2 – 5mM β-alanine, 3 – 10mM β-alanine, 4 – 15mM β-alanine, 5 – 20mM β-alanine, 6 – 25mM β-alanine, 7 – 30mM β-alanine, 8 – 40mM β-alanine, 9 – 50mM β-alanine, 10 – 50mM β-alanine + 2mM cysteine.

The results presented in **[Figure 4.2]** show that as 3HP molar fraction increases, PHA content decreases. Cultivation of strain Δ3_CNCM21 in SGMM with no additional β-alanine resulted in a cellular PHA content of approximately 66%, but only trace amounts of 3HP was detected in the copolymer. On the other hand, cultivation of Δ3_CNCM21 in SGMM supplemented with 50mM β-alanine and 2mM cysteine resulted in a copolymer containing 89 mol% 3HP, but the PHA content of the cells was drastically reduced, as only around 17% of CDW was PHA. This

represents a decrease in PHA content of over 70% between the first and last cultivation.

4.3 Discussion

In the previous chapter, *C. necator* H16 was engineered to improve its ability to incorporate 3HP into a growing PHA chain. As a result, strain Δ3_CNCM21 was generated, which could produce poly(3HB-*co*-3HP) with a 3HP molar fraction of approximately 80 mol% 3HP when cultivated in medium containing 50mM β-alanine. Production of poly(3HB-*co*-3HP) with a range of 3HP content is desirable on account of the fact that properties of the polymer change according to composition. In this chapter it was shown that the 3HP content of the copolymer can be varied by supplementing the medium different amounts of β-alanine. Accordingly, it proved possible to produce poly(3HB-*co*-3HP) with 3HP content ranging from 0 to 79 mol% when strain Δ3_CNCM21 was grown in SGMM supplemented with 0 to 50mM β-alanine **[Table 4.1]**. This has interesting implications for future poly(3HB-*co*-3HP)-producing strains of *C. necator* H16, since engineering of the upstream part of the β-alanine pathway could be tailored to provide more or less β-alanine depending on the desired polymer composition. It has been shown that engineering of *E. coli* for overproduction of β-alanine resulted in β-alanine titres of between 0.3 and 4 g/L in flask experiments (176). The β-alanine titre was influenced by various factors, including which genomic deletions had been made, which genes were overexpressed, and how strongly those genes were overexpressed. If *C. necator* H16 could be similarly engineered, combination of those strains with the downstream

pathway encoded in plasmid pCNCM21 should result in production of copolymer with a range of 3HP content.

Cultivation of strain Δ3_CNCM21 was undertaken in SGMM supplemented with both 50mM β-alanine and 2mM cysteine. It was reasoned that cysteine supplementation would increase the size of the CoA pool in the cell, leading to an increase in the amount of acetyl-CoA available. Plasmid pCNCM21 encodes pct_{Cn} as the CoA-addition mechanism, which uses CoA derived from acetyl-CoA to activate 3HP to 3HP-CoA. It was anticipated that greater availability of acetyl-CoA would mean increased ability of the cells to activate 3HP to 3HP-CoA, allowing more 3HP to be incorporated into the copolymer. Besides, the supplementation of amino acids in order to increase molar fraction of a second monomer had been tested in a previously (202). During the cultivation of *Rhodosporillum rubrum* for the production of poly(3HB-*co*-3HV), threonine supplementation was shown to significantly increase the 3HV molar fraction of the copolymer. Threonine can be metabolised to propionyl-CoA which, when condensed with acetyl-CoA, produces 3HV.

Manipulation of CoA biosynthesis has been employed in previous studies with the aim of increasing CoA and acetyl-CoA pools for the improved production of compounds. It was shown in *E. coli* that supplementation with pantothenic acid, a precursor to CoA, led to an increase in both CoA and acetyl-CoA levels (203). Subsequently it was shown that the titre of isoamyl acetate, an acetyl-CoA-derived compound, could be increased by supplementing engineered *E. coli* with pantothenic acid (204). Similarly, supplementation with cysteine was used to increase

the availability of free CoA in the production of 1-butanol by engineered *E. coli* (201). Cysteine is condensed with 4'-phosphopantothenate, forming 4'-phosphopantothenoyl-cysteine, an intermediate in CoA biosynthesis (205). Since supplementing intermediates of the CoA biosynthesis pathway has been shown to increase the levels of free CoA and acetyl-CoA, supplementation with cysteine was tested as a means of increasing the acetyl-CoA pool. Supplementation with 2mM cysteine was also clearly beneficial. Not only was less 3HP found in the supernatant at the end of the cultivation compared to cultivation with 50mM β-alanine alone, but a significantly higher 3HP molar fraction was achieved. Previous cultivation of strain Δ3_CNCM21 in 50mM β-alanine had resulted in a maximum 3HP molar fraction of approximately 80 mol% 3HP. Supplementation with both 50mM β-alanine and 2mM cysteine increased the 3HP molar fraction further, to 89 mol% 3HP. The observation that increasing CoA and acetyl-CoA levels by supplementing with cysteine was beneficial for increasing 3HP molar fraction could guide future strain engineering efforts.

Previous studies reporting biosynthesis of poly(3HB-*co*-3HP) have shown that as 3HP molar fraction increases, PHA content of the cells decreases (93–95,100,101). The same trend was observed in the studies described here [**Figure 4.2]**. A possible explanation for this is the substrate specificity of the PHA synthase. The PHA synthases of *C. necator* H16 and *C.* sp. USM2 are both considered Class I PHA synthases, meaning they preferentially polymerize short-chain-length HA monomers with carbon lengths of 3 to 5 carbons. However, previous studies have shown that the specificity of PHA synthase from *C. necator* H16 towards 3HP-CoA is low

compared to 3HB-CoA (177,196). In particular it was shown that CoA release from 3HP-CoA, indicating polymerization, was far slower than CoA release from 3HB-CoA (177). Release of CoA occurs during polymerization of HA monomers (83)**.** Since CoA release from 3HP-CoA was slower, this suggests the time required to polymerize 3HP is longer, and that the binding site of the PHA synthase is occupied for longer. If the binding site of the PHA synthase is occupied for longer, less polymer synthesis will occur and the total amount of polymer in the cells will be decreased. The substrate specificity of the PHA synthase from *C.* sp. USM2 for 3HP-CoA and 3HB-CoA has not yet been determined. However, since the PHA synthase from *C.* sp. USM2 is also a Class I PHA synthase, it is possible that the substrate specificities of the PHA synthase from *C.* sp. USM2 for 3HP-CoA and 3HB-CoA are similar to those of the PHA synthase from *C. necator* H16. If this is the case, the PHA synthase of *C.* sp. USM2 will also have low specificity for 3HP-CoA. This could explain why PHA content diminished as the 3HP molar fraction increased.

Chapter 5: Effect of *phaCAB* operon alteration on polymer composition and accumulation

5.1 Introduction

The results of the previous two chapters had shown that plasmid engineering could be used to produce poly(3HB-*co*-3HP) with high 3HP molar fraction in *C. necator* H16, and that 3HP content could be controlled by changing the concentration of β-alanine in the medium. In this chapter the effect of reduced 3HB-CoA synthesis on copolymer accumulation and composition was investigated.

Reducing the flux towards 3HB-CoA was hypothesised to confer several advantages for the production of poly(3HB-*co*-3HP) in *C. necator* H16. Firstly, suppression of 3HB-CoA biosynthesis should result in decreased 3HB content in the polymer since less 3HB-CoA will be available, thereby enhancing the 3HP molar fraction further. A similar strategy has been used for the production of copolymers containing enhanced molar fraction of second monomers including 3-mercaptopropionate (3MP) and 3-hydroxyvalerate (3HV) (206,207). Another potential advantage of reducing flux towards 3HB-CoA is that of reduced acetyl-CoA consumption. In the previous chapter cysteine was included in the PHA production medium with the aim of increasing the intracellular pool of acetyl-CoA such that activation of 3HP to 3HP-CoA was enhanced. If reducing flux towards 3HB-CoA results in increased acetyl-CoA, the increased acetyl-CoA availability should be beneficial for further increased 3HP content. This approach was employed to increase the 3HHx molar fraction during the production of poly(3HB-*co*-3HHx) by engineered *C. necator* H16 (208). Lastly, it was hypothesised that reduced 3HB-CoA might result in reduced turnover of the copolymer. The

simultaneous biosynthesis and degradation of PHAs in *C. necator* H16 was first shown in 1990 (209). As a result, the composition of PHA accumulated over time can change. For instance, it was shown that *C. necator* H16 containing PHB homopolymer would begin to accumulate poly(3HB-*co*-3HV) when transported to medium containing precursors to 3HV. Since 3HV has become available as a precursor, 3HV begins to appear in the copolymer. Similarly, when *C. necator* H16 containing poly(3HB-*co*-3HV) was transported to medium lacking precursors to the 3HV unit, the composition of the polymer changed to PHB homopolymer again, since there is no longer a supply of 3HV (209). It follows that suppressing 3HB-CoA formation would result in a copolymer composition which retains higher 3HP molar fraction throughout the course of the cultivation.

As was described earlier, PHB biosynthesis in *C. necator* H16 proceeds *via* the well-described *phaCAB* operon. The β-ketothiolase encoded by *phaA* is responsible for the production of acetoacetyl-CoA from two molecules of acetyl-CoA. Acetoacetyl-CoA is reduced to 3HB-CoA by an acetoacetyl-CoA reductase encoded by *phaB1*, and polymerization is catalysed PHA synthase encoded by *phaC* (82). A series of strains were generated with different alterations to the *phaCAB* operon **[Figure 5.1]**. The deletions were made in the Δ3 background, since previous experiments undertaken in this study had used that strain.

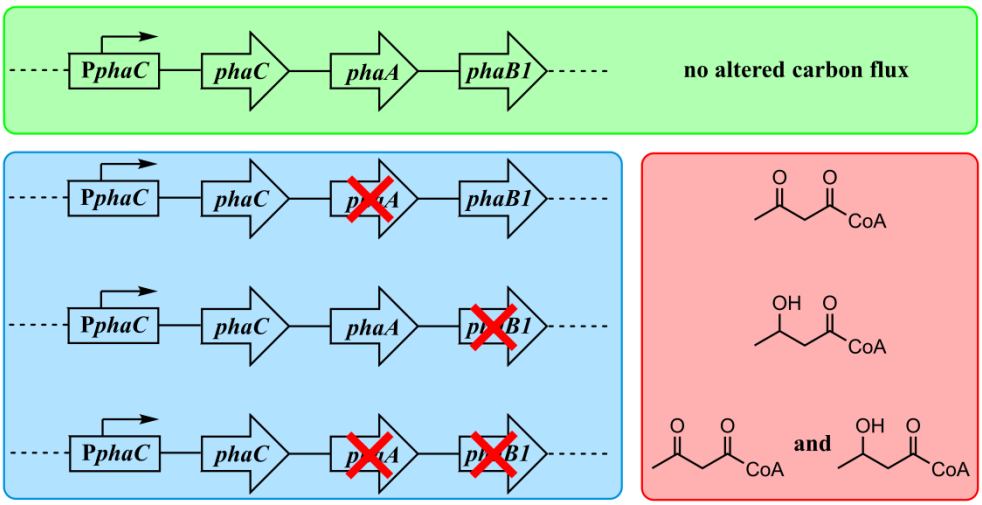

Figure 5.1 - Diagram illustrating the *C. necator* H16 *phaCAB* operon, the deletion mutants generated and described in this chapter, and the targeted metabolite. **(Green box)** Organisation of the PHB biosynthetic pathway in *C. necator* H16. Flux towards PHB is not altered in the unperturbed operon. **(Blue box)** Genes targeted in knockout studies. From top to bottom; deletion of *phaA* (β-ketothiolase), deletion of *phaB1* (NADPH-dependent acetoacetyl-CoA reductase), deletion of *phaA* and *phaB1*. **(Red box)** Knockouts were designed to reduce carbon flux towards indicated molecules. From top to bottom; *phaA* single knockout aimed to reduce carbon flux toward acetoacetyl-CoA, *phaB1* single knockout aimed to reduce flux toward 3HB-CoA, *phaAB1* double knockout aimed to reduce flux toward both metabolites.

5.2 Results

5.2.1 Generation of *phaA*, *phaB1*, and *phaAB1* knockouts strains

To reduce the carbon flux going towards PHB synthesis, a series of knockout strains were generated. The *phaA* and *phaB1* genes were knocked out individually, and then knocked out together to create a *phaAB1* double knockout strain. The deletions were made in the Δ3 background strain, resulting in strains Δ3A, Δ3B1, and Δ3AB1. The knockouts were generated according to the knockout protocol described in materials and methods.

Following screening on LB/LB tet plates, colony PCR was carried out on colonies which had lost tetracycline resistance.

5.2.2 Effect of *phaA*, *phaB1*, and *phaAB1* deletions on PHB accumulation and 3HP molar fraction

Following generation of strains Δ3A, Δ3B1, and Δ3AB1, transformation using plasmids pCNCM21 and pCNCMeyfP was carried out. This gave rise to the experimental strains Δ3A_CNCM21, Δ3B1_CNCM21, and Δ3AB1_CNCM21, and the control strains Δ3A_eyfP, Δ3B1_eyfP, and Δ3AB1_eyfP. These strains were cultivated in SGMM + 50mM β-alanine as had been used in previous experiments. The results of the cultivation are detailed below in **Table 5.1**. While the cultivation of these strains lasted 54 hours, the data presented below uses samples taken at 48 hours in order to fairly compare the results with those of previous chapters.

Table 5.1 – PHA content and composition of *phaCAB* mutant strains containing plasmid pCNCM21 or pCNCMeyfP following flask cultivation in SGMM + 50mM β-alanine. Experiments were carried out in triplicate. Data presented is from samples taken at 48hrs cultivation.

Strain	CDW (g/L)	PHA (wt%)	PHA (g/L)	3HB (mol%)	3HP (mol%)
Δ3A_CNCM21	3.48	33.15	1.15	16.44	83.56
Δ3B1_CNCM21	2.93	28.15	0.83	10.82	89.18
Δ3AB1_CNCM21	3.01	29.50	0.88	8.89	91.11
Δ3A_eyfP	3.23	72.13	2.33	100	0
Δ3B1_eyfP	2.15	18.05	0.38	100	0
Δ3AB1_eyfP	1.86	16.4	0.30	100	0

The results of **Table 5.1** revealed that native PHB accumulation was either slightly or significantly affected by the alterations made to the *phaCAB* operon, indicated by PHA content and titre of the control strains.

Deletion of *phaA* alone resulted in a minor decrease in PHA titre. Previously, cultivation of strain Δ3_eyfP resulted in a PHA titre of over 3 g/L. Under the same conditions, strain Δ3A_eyfP produced around 2.3 g/L PHA. In contrast, strains Δ3B1_eyfP and Δ3AB1_eyfP exhibited dramatic reductions in their ability to form PHB. While deletion of *phaB1* alone resulted in a polymer content of only around 18%, deletion of *phaA* and *phaB1* together reduced polymer content down to near 16%. The low PHA content corresponded to a PHA titre of only 0.38 g/L and 0.30 g/L, respectively. Deletion of *phaB1* had a much more significant effect on PHB accumulation than deletion of *phaA*.

Reducing the ability of *C. necator* H16 to form 3HB-CoA had a positive impact on 3HP molar fraction. Strain Δ3A_CNCM21 was shown to produce a copolymer with a 3HP molar fraction of approximately 84 mol% 3HP. Furthermore, the PHA content of the cells was 33%, and PHA titre was 1.15 g/L. While PHA titre of strains Δ3B1_CNCM21 and Δ3AB1_CNCM21 did not exceed 1 g/L, the poly(3HB-*co*-3HP) produced by these strains contained 89 and 91 mol% 3HP respectively, and both strains had a PHA content of almost 30%. Previously, supplementation with cysteine had been required to achieve 3HP content of above 80 mol%. Here it was shown that perturbation of the *phaCAB* operon could be used to exceed 80 mol% 3HP without the need for cysteine supplementation. Furthermore, the simultaneous deletion of *phaA* and *phaB1* resulted in a strain which could produce a copolymer containing 91 mol% 3HP, the highest 3HP molar fraction observed so far.

5.2.3 Effect of *phaA*, *phaB1*, and *phaAB1* deletions on copolymer turnover

While the differences between production and control strains showed an effect on polymer composition and content at the end of the cultivation, a difference was also observed in the composition of the polymer over time, as can be seen in **Figure 3.3**.

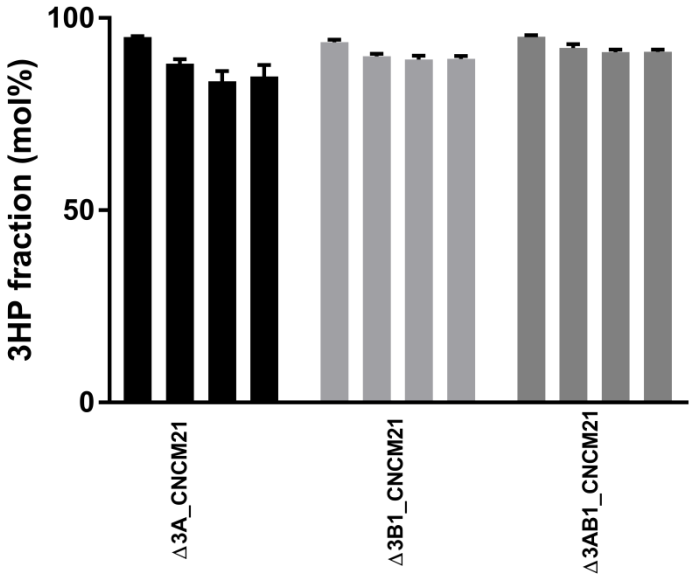

Figure 5.2 - Change in 3HP molar fraction over time. Bars for each strain represent the times at which samples were taken (From left to right; 24, 36, 48, 54 hours).

The data presented in **Figure 5.2** highlights changes in 3HP molar fraction during the course of the cultivation. It was observed that strain Δ3A_CNCM21 underwent the largest change in 3HP content. At 24hrs the 3HP molar fraction was approximately 95 mol% 3HP, and by the end of the cultivation at 54hrs the 3HP molar fraction had decreased to 85%. While a change in copolymer composition was seen in strains Δ3B1_CNCM21 and Δ3AB1_CNCM21 as well, the decrease in 3HP molar fraction was not as

significant. While strain Δ3B1_CNCM21 exhibited a decrease from approximately 93 to 89 mol% 3HP, the 3HP content of strain Δ3AB1_CNCM21 decreased from 95 to 91 mol% 3HP.

5.2.4 Effect of *phaB1* deletion on PHB accumulation

It was apparent that control strains in which *phaB1* had been deleted produced very little polymer. Thus, the polymer titres of control strains Δ3B1_eyfP and Δ3AB1_eyfP were both less than 0.4 g/L **[Table 5.1]**. This was in contrast to the polymer titre of strain Δ3_eyfP which was more than 3 g/L. *C. necator* H16 is known to possess at least three acetoacetyl-CoA reductases, encoded by *phaB1*, *phaB2*, and *phaB3* (210). The study by Budde *et al*. showed that deletion of *phaB1* resulted in minor or major inhibition of PHB biosynthesis, depending on growth conditions. It was found that under certain conditions, expression of *phaB3* was the cause of PHB accumulation in *phaB1* mutant strains. Expression of *phaB2* was not detected in any of the conditions tested.

In the experiments described here, only *phaB1* had been deleted, but PHB accumulation was severely reduced. This suggested *phaB3* was not active under the conditions tested here. To investigate whether or not *phaB3* had influenced PHB accumulation at any point during the cultivation, the data collected from the cultivation of the control strains was further analysed. Specifically, how the PHA content changed over time was analysed **[Figure 5.3]**.

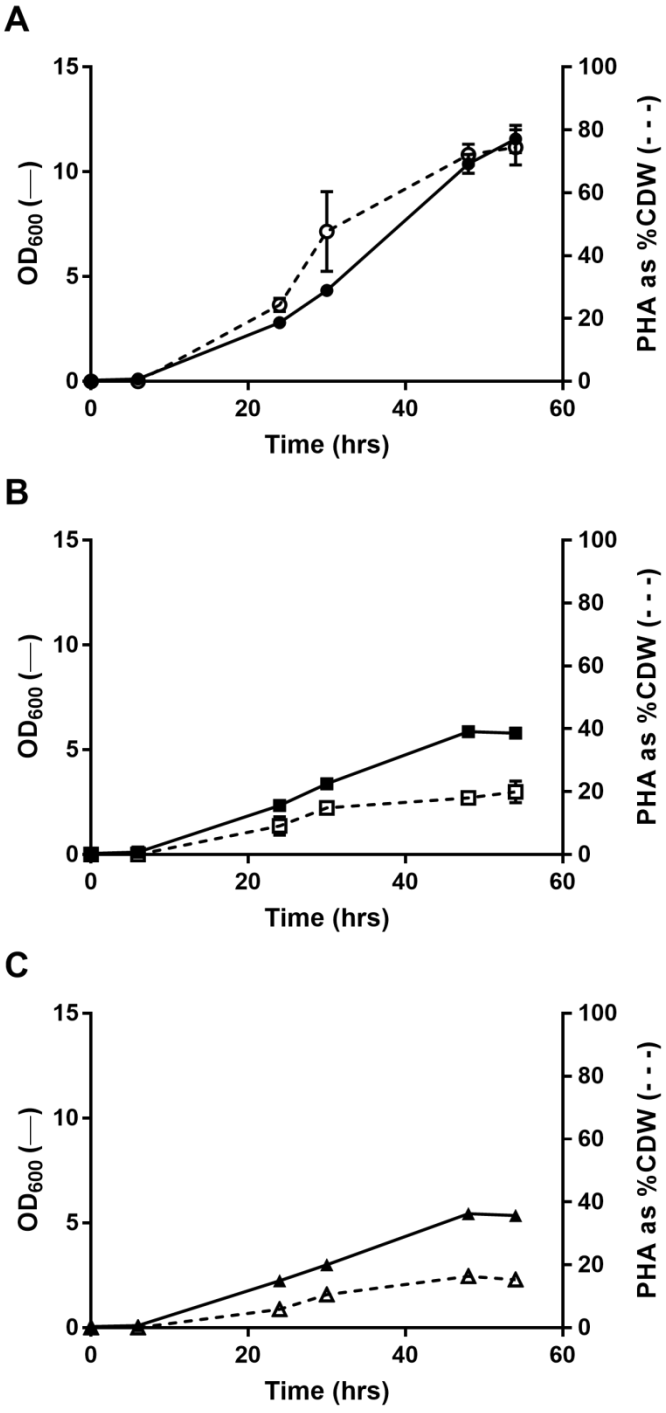

Figure 5.3 – Change in PHA content over time for *phaCAB* mutant control strains. Graphs represent data from the cultivation of **(A)** strain Δ3A_eyfP, **(B)** strain Δ3B1_eyfP, and **(C)** strain Δ3AB1_eyfP. Optical density at 600nm is indicated by a black unbroken line (─) and filled shapes. PHA content as a % of CDW is indicated by a black dotted line (- - -) and empty shapes.

The data presented in **Figure 5.3** showed that in all cases, PHA content of the cells increased linearly following the beginning of the cultivation. As previously observed, strain Δ3A_eyfP performed similarly to wild-type *C. necator* H16. The two *phaB1* deletion strains, Δ3B1_eyfP and Δ3AB1_eyfP, exhibited a markedly decreased PHB content throughout the course of the cultivation.

5.3 Discussion

In order to further increase the 3HP content of the polymer without additional plasmid engineering, a series of *phaCAB* operon mutants were constructed. The aim of these mutants was to test the effect of reducing flux towards 3HB-CoA on poly(3HB-*co*-3HP) accumulation and 3HP molar fraction.

Strain Δ3A lacked the β-ketothiolase encoded by *phaA* of the *phaCAB* operon, which is responsible for the condensation of two acetyl-CoA molecules to produce acetoacetyl-CoA, the precursor to 3HB-CoA **[Figure 5.1]**. Deletion of *phaA* was shown to have a significant effect on PHA content of the cells, copolymer composition, and titre of poly(3HB-*co*-3HP) produced. In **Chapter 3**, cultivation of Δ3_CNCM21 in SGMM supplemented with 50mM β-alanine the cells had a PHA content of approximately 18% of CDW with a 3HP molar fraction of 80 mol% 3HP, and the PHA titre was 0.76 g/L. In the case of Δ3A_CNCM21, the titre was increased to 1.15 g/L while PHA content of the cells was near 40% of CDW and 3HP molar fraction increased to 85 mol%. While it is clear that the

deletion of *phaA* was beneficial for increasing PHA content, 3HP molar fraction, and PHA titre, the deletion only resulted in a minor decrease in PHB production. Comparison of the data between strains Δ3_eyfP and Δ3A_eyfP showed that while both had PHA content of around 70%, strain Δ3_eyfP produced more than 3 g/L of PHB whereas strain Δ3A_eyfP produced only 2.33 g/L of PHB.

Analysis of the genome sequence suggested the presence of numerous genes encoding β-ketothiolases in *C. necator* H16 indicating a significant capacity for direction of flux towards 3HB-CoA (125). Therefore, subsequent studies investigated the effect of several single and multiple β-ketothiolase deletions on PHB accumulation as well as the effect on incorporation of a second monomer into the polymer (206,207). In agreement with the results obtained here, deletion of *phaA* resulted in a minor decrease in PHA titre and an increase in second monomer molar fraction. In the case of the experiments described here however, the effect on monomer composition was more pronounced. This could be because incorporation of 3HP into the polymer was enhanced due to the overexpression of pct_{Cn} and $phaC_{Cs}$ in this study, whereas in the studies undertaken by Lindenkamp *et al*. no such work was carried out. Additionally, the molar fraction of 3HV in poly(3HB-*co*-3HV) increased as more of the β-ketothiolases were deleted, such that it was almost possible to produce a poly(3HV) homopolymer in *C. necator* H16 when the cells were cultivated with valerate as the sole carbon source (207). Future work for polymer production in *C. necator* H16 could use a similar approach to attempt production of poly(3HP).

As mentioned in the introduction to this chapter, it was hypothesised that deletion of *phaA* may increase the pool of acetyl-CoA, since less acetyl-CoA will be consumed in the production of PHB. Sato *et al*. deleted *phaA* in their attempts to produce poly(3HB-*co*-3HHx) in *C. necator* H16 (208). The 3HHx monomer can be synthesised by the condensation of acetyl-CoA and butyryl-CoA. Deletion of *phaA* resulted in an increased 3HHx molar fraction, which the authors attribute to the increased amount of acetyl-CoA available. Presumably the increased pool of acetyl-CoA was also a factor in the studies described here, as more CoA would have been available for activation of 3HP to 3HP-CoA.

The effect of deleting *phaB1*, both as a single knockout and as a part of a double knockout, was also tested. The NADPH-dependent acetoacetyl-CoA reductase encoded by *phaB1* is responsible for conversion of acetoacetyl-CoA to 3HB-CoA, the substrate which PHA synthase uses to produce PHB **[Figure 5.1]**. Deletion of *phaB1* from the *C. necator* H16 genome has been used for improving the 3HHx molar fraction of poly(3HB-*co*-3HHx) (170,211–213)**.** In both the single and double knockout strains, deletion of *phaB1* dramatically reduced PHB content of the cells, indicating a major disruption of flux towards 3HB-CoA. Control strains Δ3B1_eyfP and Δ3AB1_eyfP both contained low PHA content. Consequently, the PHA titre of both strains was very low, at less than 0.4 g/L. This translated into increased 3HP molar fraction in the experimental strains Δ3B1_CNCM21 and Δ3AB1_CNCM21, which produced poly(3HB-*co*-3HP) with 3HP contents of 89 and 91 mol% 3HP, respectively **[Table 5.1]**. In the previous chapter it was observed that PHA content decreases as 3HP molar fraction

increases **[Figure 4.2]**. Considering this, it could be expected that at 91 mol% 3HP, the PHA content and titre of Δ3AB1_CNCM21 would be lower than that of Δ3_CNCM21, which produced a copolymer containing 80 mol% 3HP under the same cultivation conditions. In fact, strain Δ3AB1_CNCM21 contained almost 30% PHA and produced almost 0.9 g/L of poly(3HB-*co*-3HP), whereas strain Δ3_CNCM21 contained 20% PHA and the PHA titre was 0.76 g/L. Deletion of both *phaA* and *phaB1* in this strain therefore appeared to lessen the negative effect of very high 3HP molar fraction on PHA content and titre.

Further analysis of the data from these cultivations indicated that suppression of 3HB-CoA biosynthesis had reduced the effect of polymer turnover on copolymer composition **[Figure 5.2]**. It is known that PHB is metabolised in a cyclic nature in *C. necator* H16 (209). While the phenomenon is still not entirely understood, it is thought that the polymer is continually synthesised and broken down in a non-futile cycle which provides acetyl-CoA and NADH as limited carbon and energy sources during times of nutrient limitation (214). This has implications for copolymer composition. For instance, 3HB-CoA is continually formed by the natural metabolism of *C. necator* H16. On the other hand, many second monomers are formed by addition of precursor molecules at the beginning of the cultivation, or are otherwise not available continuously from metabolic pathways. As a result, the molar fraction of any second monomer can decrease as cultivation continues, since 3HB-CoA is being continually produced while availability of the second monomer is typically restricted. As well as the initial report by Doi and co-workers (209), the effect can be

observed in other publications. The study of Lindenkamp and co-workers showed decreasing molar fraction of 3MP in a poly(3HB-*co*-3MP) as cultivation continued, since the 3MP was only provided at the start of the cultivation (206). In addition, the studies by Jeon and co-workers (211), as well as Sato and co-workers (208), which investigated production of poly(3HB-*co*-3HHx), both showed decreasing 3HHx fraction as cultivation continued, since the butyrate required for 3HHx formation was only provided at the beginning of the cultivation. A similar trend was observed here; 3HP molar fraction decreases as cultivation progressed. This trend was less evident, however, in the two strains with a deletion of *phaB1*. While the copolymer produced by strain Δ3A_CNCM21 exhibited an almost 11% decrease in 3HP content during the course of the cultivation, the copolymer from strains Δ3B1_CNCM21 and Δ3AB1_CNCM21 showed approximately 4.7 and 4.1% decreases in 3HP molar fraction respectively. Earlier data obtained in this investigation had shown that in control strains deletion of *phaA* did not significantly affect PHB production, whereas the *phaB1* deletion strains were strongly affected **[Table 5.1]**. The slower rate of 3HP loss can presumably be attributed to the severely inhibited ability of the *phaB1* mutants to produce 3HB-CoA. With less 3HB-CoA available, it is less likely that the PHA synthase will incorporate 3HB into the polymer, thereby maintaining a higher 3HP molar fraction.

It was also of interest to explore how the deletion of *phaB1* had affected PHB accumulation in control strains Δ3B1_eyfP and Δ3AB1_eyfP, since previous work had shown that deletion of *phaB1* alone could result in minor or major inhibition of PHB accumulation depending on the growth

conditions used (210). That work had shown that during cultivation on fructose, *phaB3* was expressed and contributed to PHB biosynthesis, thereby rescuing PHB accumulation in strains lacking *phaB1*. In contrast, growth on palm oil or trioleate did not induce expression of *phaB3*, leading to strongly impaired PHB accumulation in *phaB1*-deleted strains. Other studies have also indicated expression of *phaB3* is dependent on growth conditions. For instance, it was shown that expression of *phaB3* decreases significantly when *C. necator* H16 is grown on plant oils rather than fructose (215). Additionally, increased *phaB3* expression was observed when *C. necator* H16 was cultivated in medium containing gluconate and 3,3'-thiodipropionic acid as opposed to cultivation with gluconate alone (216). More recently, a publication by Zhang and co-workers showed that *phaB1*-deleted strains of *C. necator* H16 which were engineered to grow on glycerol and glucose produced different levels of PHA depending on carbon source (213). While the PHA content of glucose- and fructose-grown cells was above 60%, glycerol-grown cells contained less than 30% PHA (213). Expression of *phaB*3, therefore, appears to be dependent on carbon source. Budde and co-workers showed that a strain in which *phaB1* and *phaB3* were deleted was unable to accumulate more than 20% PHA (210). Since in the experiments here gluconate was used as a carbon source, and low PHB contents of less than 20% in strains lacking *phaB1* were observed, it is likely that *phaB3* is not expressed when cultivated in gluconate.

The results of this chapter showed that reduction of flux towards 3HB-CoA is useful for increasing the molar fraction of a second monomer such as 3HP. Thus, deletion of *phaA* resulted in increased PHA content of

the cells, as well as a higher 3HP molar fraction in the polymer. Furthermore, the PHA titre obtained was over 1 g/L after 48 hours cultivation. Increased 3HP molar fraction could be achieved by deletion of *phaB1* either as a single knockout or as in a double knockout with *phaA*, although the PHA titre was not as high as was reached by the *phaA* single knockout. Reduction of flux towards 3HB-CoA also reduced the effect of PHA turnover on copolymer composition. Lastly, it was apparent that *phaB3* did not appear to contribute to PHB accumulation in strains grown on gluconate. Understanding the conditions in which *phaB3* is active will be useful for future strain engineering.

Chapter 6: Engineering of *C. necator* H16 for stable autotrophic biosynthesis of mevalonate, a precursor to biodegradable polymers

6.1 Introduction

As outlined in **Chapter 1**, mevalonate-derived compounds have recently been shown to have important applications in the field of biodegradable polymers. Since mevalonate has been shown to be produced by engineered *C. necator* H16, and mevalonate-derived compounds have been produced from CO_2 using *C. necator* H16, it was chosen to attempt biosynthesis of mevalonate from CO_2 for the use in biodegradable polymer synthesis.

A schematic diagram for the biosynthesis of mevalonate from carbon dioxide is shown in **Figure 6.1**. The two genes required for conversion of acetyl-CoA to mevalonate are *mvaE* and *mvaS* from the Gram-positive bacterium *Enterococcus faecalis*. The *mvaE* gene encodes an acetyl-CoA acetyltransferase/HMG-CoA reductase, and *mvaS* encodes an HMG-CoA synthase. First, two molecules of acetyl-CoA are condensed to acetoacetyl-CoA by MvaE in a reaction identical to that catalysed by PhaA from *C. necator* H16. Acetoacetyl-CoA is then converted to HMG-CoA by MvaS. Lastly, HMG-CoA is reduced to mevalonate by MvaE in an NADPH-dependent reaction. While the interest of the work carried out here was to produce mevalonate as a precursor to novel biodegradable polymers, mevalonate is also a precursor to other useful compounds including artemisinin (an anti-malarial compound) and β-carotene (a food colorant) (217,218) **[Figure 6.1]**.

Since *C. necator* H16 produces significant quantities of PHB using acetyl-CoA as a precursor, a large intracellular pool of acetyl-CoA is presumably available (219,220). As mentioned above, the PHB and

mevalonate biosynthesis pathways share several metabolites, reactions, and cofactors. For instance, both pathways use acetyl-CoA as the starting molecule. Furthermore, the reactions catalysed by MvaE and PhaA carry out the same role; condensation of two molecules of acetyl-CoA to produce one molecule of acetoacetyl-CoA. Lastly, both pathways require NADPH as the reducing cofactor. To determine how alterations to PHB metabolism might affect mevalonate production, mevalonate production was also investigated in *phaCAB*-negative deletion strains. Moreover, since PhaA and MvaE catalyse the same reaction, a plasmid was also constructed in which *phaA* was overexpressed alongside *mvaE* and *mvaS* with the aim of directing more flux towards acetoacetyl-CoA. A further strain was constructed in which the *phaCAB* operon had been replaced by a mevalonate production pathway to compare the effect of multi-copy plasmid expression versus single-copy genome expression. In all cases, the mevalonate production pathway was placed under the control of an arabinose-inducible promoter.

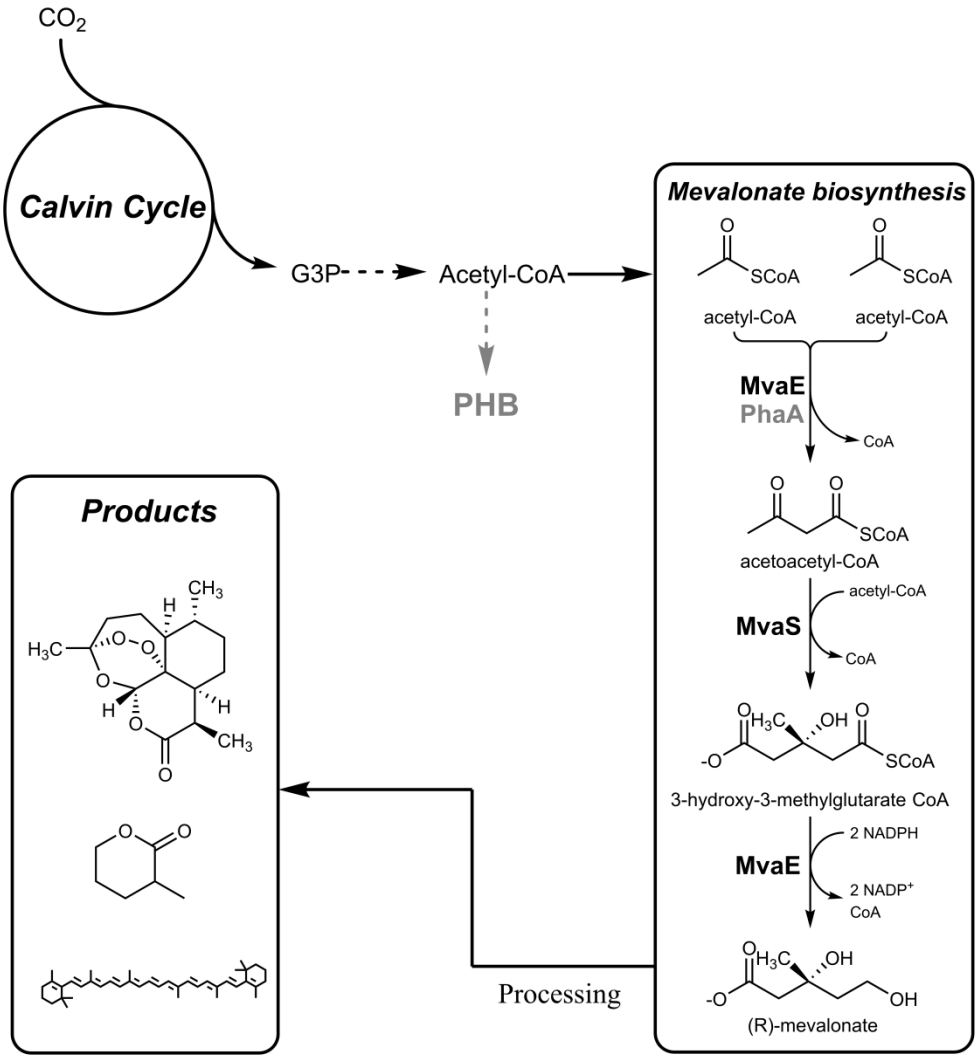

Figure 6.1 – Schematic diagram of mevalonate biosynthesis from CO_2 using *C. necator* H16 as the host organism. In the first step of the pathway, acetyl-CoA derived from CO_2 metabolism is condensed by MvaE to form acetoacetyl-CoA. The same reaction can be carried out by PhaA, indicated in grey. The acetyl-CoA is can also be directed towards PHB by the action of the *phaCAB* operon, indicated in grey. Acetoacetyl-CoA is then converted to HMG-CoA by MvaS. Lastly, HMG-CoA is reduced and CoA removed in an NADPH-dependent reaction by MvaE. Mevalonate can act as a precursor to numerous different products. Products from top to bottom; artemisinin, β-methyl-Δ-valerolactone, β-carotene. Dashed lines indicate multiple reactions.

It was also chosen to attempt construction of a plasmid-addicted strain of *C. necator* H16, in order to stabilize the plasmid during high-density autotrophic fermentation. As outlined in Chapter 1, plasmid addiction can be facilitated by various different mechanisms. For the purposes of this work, it was decided to develop a plasmid addiction system based on metabolism. To that end, various strains of *C. necator* H16 which were putatively auxotrophic for certain essential metabolites were generated.

Coenzyme A (CoA) is an essential intracellular metabolite in all known organisms. It is estimated that around 4% of all known enzymes use CoA as a cofactor (221). CoA is involved in the tricarboxylic acid (TCA) cycle, fatty acid biosynthesis and degradation, as well as the synthesis of phospholipids (205,222). Starting from L-aspartate, the biosynthesis of CoA involves seven steps. Previous studies have shown that loss of any one of the genes involved in these seven steps results in abrogated growth in *E. coli*. The first two steps of the pathway from L-aspartate involve conversion of aspartate to β-alanine by aspartate decarboxylase, encoded by *panD*, and conversion of β-alanine to pantothenate by pantothenate synthetase, encoded by *panC*. Deletion of either *panD* or *panC* has been shown to generate *E. coli* strains which cannot grow unless β-alanine or pantothenate is added to the medium (223). Footprinting studies revealed that the remaining five steps of the pathway, which facilitate conversion of pantothenate to CoA, are also essential for growth (224). However, strains in which any of these five steps are absent cannot be rescued by supplementation, since the intermediates involved are phosphorylated. Since phosphorylated

compounds cannot cross the membrane, there is no way for the cells to take up these compounds, and growth cannot be restored. Mutation of any one step of the CoA biosynthetic pathway results in *E. coli* strains with growth defects. Based on this, strains of *C. necator* H16 lacking either *panD* or *panC* were generated with the aim of producing strains auxotrophic for β-alanine or pantothenate, respectively.

Another option for generating auxotrophic strains was targeting of the uracil biosynthetic pathway. Uracil plays a critical role in the cell as one of the four bases of RNA. Two key genes of the uracil biosynthesis pathway are orotate phosphoribosyltransferase and orotidine 5'phosphate decarboxylase, encoded by *pyrE* and *pyrF*, respectively. These enzymes are responsible for facilitating the conversion of orotate to orotidine 5'phosphate, and orotidine 5'phosphate to uridine 5'phosphate (225). It has been shown that loss of *pyrE* or *pyrF* results in uracil auxotrophy in various microorganisms (226–228). Additionally, a plasmid addiction system based on complementation of *pyrF* was previously used in yeast (229). The uracil auxotrophy exhibited by *pyrE*-deleted strains has also been used as a counterselection marker in *Clostridium* (230). Therefore, generation of a *C. necator* H16 strain auxotrophic for uracil by deleting *pyrE* was also attempted.

The genomic contexts of the three genes targeted for deletion, as well as their functions in their respective pathways, are indicated in **Figure 6.2**. Deletion of these genes was hypothesised to result in auxotrophic strains of *C. necator* H16. The auxotrophy would then be exploited to facilitate plasmid addiction. A plasmid encoding the deleted gene would be

transformed into the corresponding auxotroph. Since retention of the plasmid is required to maintain growth, cells should stably maintain the plasmid, even in the absence of antibiotics.

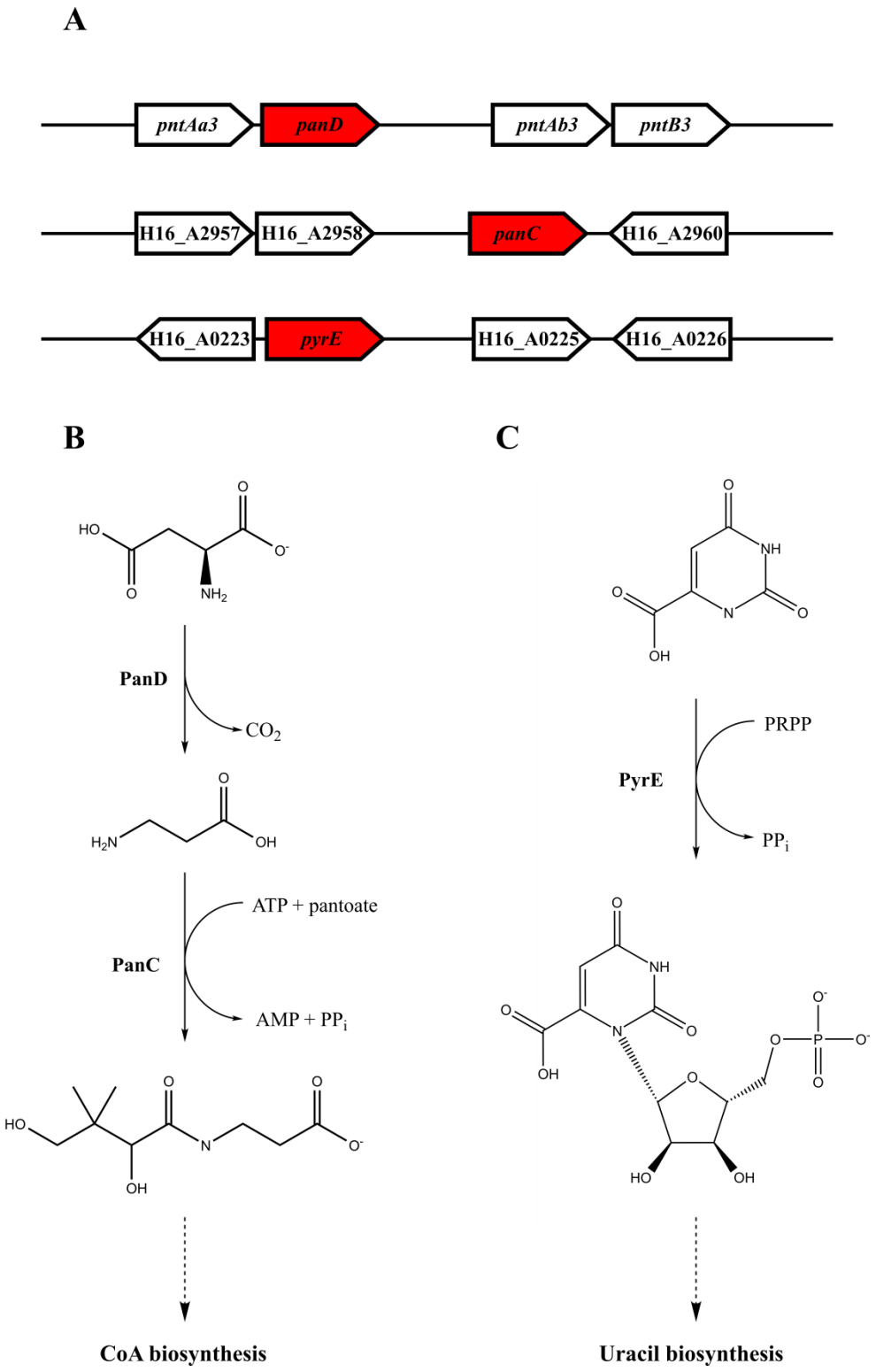

Figure 6.2 - Genomic context and function of genes targeted for generation of auxotrophic strains of *C. necator* H16. While *panD* is surrounded by genes encoding subunits of a transhydrogenase, the genes upstream and downstream of *panC* and *pyrE* have not yet been fully described in *C. necator* H16 and their functions are not yet known (A). PanD facilitates the conversion of aspartic acid to β-alanine with the release of CO_2. PanC

condenses β-alanine with pantoate in an ATP-consuming reaction, resulting in production of pantothenate. Pantothenate is then further metabolised to the essential intracellular metabolite coenzyme A (CoA) (B). PyrE catalyses the formation of orotidine 5'phosphate from phosphoribosyl pyrophosphate (PRPP) and orotic acid. Orotidine 5'phosphate is then converted to uracil (C). Dashed lines indicate multiple steps. Genes which are targeted for deletion are highlighted in red.

6.2 Results

6.2.1 Generation of *panD, panC,* and *pyrE* knockouts and testing for auxotrophy

The candidate auxotrophic strains were generated in accordance with the protocols specifically designed for each auxotroph, as described in the materials and methods.

To investigate whether the knockouts had resulted in strains auxotrophic for the target metabolite, the mutants were streaked on SGMM with and without supplementation of the target metabolite. It was observed that strains Δ*panC* and Δ*pyrE* were unable to grow on SGMM lacking pantothenate or uracil, respectively, but that growth could be rescued by supplementing the medium with the necessary compound. On the other hand, strain Δ*panD* was still able to grow on SGMM even if β-alanine or pantothenate was not added to the medium. As a result, further experiments with strain Δ*panD* were not carried out.

6.2.2 Complementation of *panC* and *pyrE* deletions

To confirm that the genomic deletions were responsible for the lack of growth exhibited by strains Δ*panC* and Δ*pyrE*, complementation studies were carried out. The *panC* and *pyrE* genes were cloned into plasmid pMTL71301, resulting in plasmids pCNCMpanC and pCNCMpyrE. The upstream intergenic region, consisting of the sequence between the target gene (*panC* or *pyrE*) and the gene upstream of the target gene, was used as the promoter sequence. Transformation of these plasmids into the auxotrophic strains resulted in strains Δ*panC*_CNCMpanC and Δ*pyrE*_CNCMpyrE. After streaking Δ*panC*_CNCMpanC onto SGMM lacking pantothenate, it was shown that growth could be restored **[Figure 6.3]**.

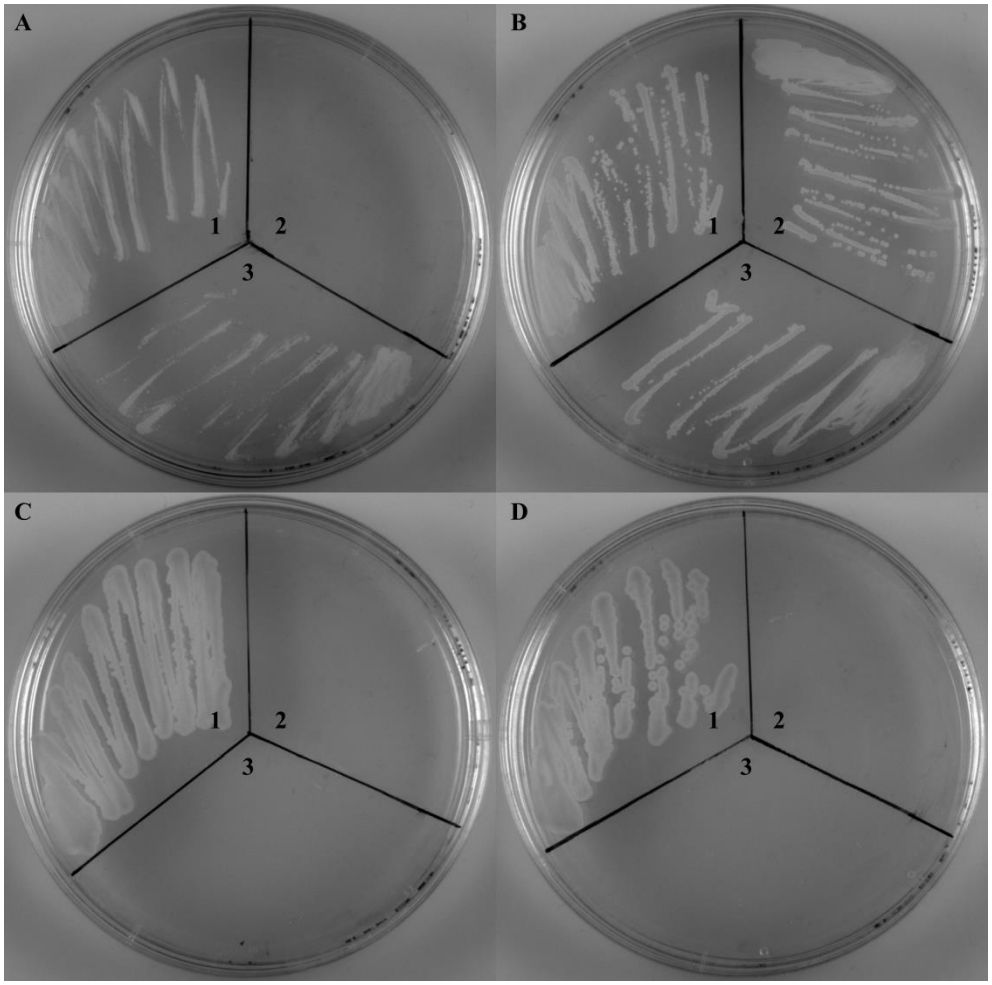

Figure 6.3 – Effect of supplementation or complementation on growth of the Δ*panC* strain. Without supplementation of pantothenate, strain Δ*panC* is unable to grow. Supplementation with pantothenate, or complementation with a plasmid encoding a functional copy of the *panC* gene restores growth. Strains are indicated by numbers; **1** = Δ*panC*_CNCMpanC, **2** = Δ*panC*, **3** = Wild-type *C. necator* H16.Plate conditions are indicated by letters; (**A**) SGMM + 10 μg/mL Gm, no pantothenate, (**B**) SGMM + 10 μg/mL Gm, 1mM pantothenate, (**C**) SGMM + 10 μg/mL Gm, 15 μg/mL Tet, no pantothenate, (**D**) SGMM + 10 μg/mL Gm, 15 μg/mL Tet, 1 mM pantothenate.

The same effect was observed using the *pyrE* mutant strain. These results confirmed that deletions of *panC* and *pyrE* were responsible for the observed auxotrophy.

6.2.3 Initial experiments using *panC*-based addiction system in continuous fermentation

The results of the complementation studies had shown that growth could be restored to the auxotrophic Δ*panC* and Δ*pyrE* strains if they were transformed with a plasmid expressing either *panC* or *pyrE*, respectively. Based on these observations it was anticipated that strains Δ*panC* and Δ*pyrE* should retain the plasmid during cultivation, since a plasmid encoding the appropriate gene was essential for growth without supplementation of pantothenate or uracil.

In the first instance, ability of strains using the *panC*-based addiction system to produce mevalonate from CO_2 was tested. Therefore, in the first set of experiments, two strains were grown simultaneously in continuous autotrophic conditions. Wild-type *C. necator* H16 was transformed with plasmid p71301_mvaES, while strain Δ*panC* was transformed with plasmid p71301_mvaES-panC. The resulting strains were termed Wt_mvaES and Δ*panC*_mvaES-panC. In these experiments optical density (OD_{600}), plasmid stability, and mevalonate production were measured. It should be noted though that the experiment was interrupted by a hydrogen shortage which affected the growth of the strains. The results of the fermentation are shown below in **Figure 6.4**.

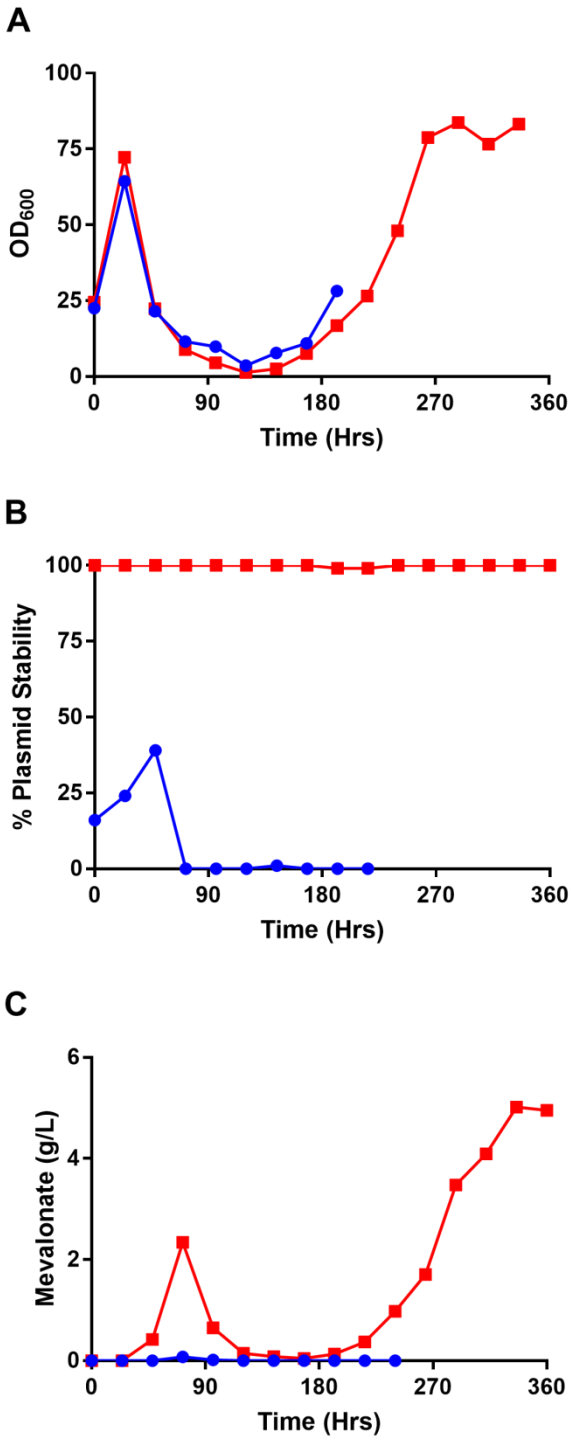

Figure 6.4 – Growth, plasmid stability, and mevalonate production by strain Wt_mvaES and strain Δ*panC*_mvaES-panC during autotrophic continuous fermentation. Graphs represent OD_{600} (**A**), plasmid stability (**B**), and mevalonate titre (**C**). Colours indicate strain Wt_mvaES (●) and strain Δ*panC*_mvaES-panC (■). Since no plasmid or mevalonate was detected after approximately 72 hours, the cultivation of strain Wt_mvaES was stopped at 216 hours. X-axis represents time since induction with L-arabinose.

Despite the disruption, the results of the above experiment indicated that the plasmid addiction system had supported the growth of the auxotrophic Δ*panC* strain and production of mevalonate during autotrophic cultivation. Strain Δ*panC*_mvaES-panC reached an OD_{600} of approximately 70 after 48 hours of cultivation, and OD_{600} of over 100 was achieved by the end of the cultivation. Furthermore, plasmid stability assays indicated that plasmid retention was completely stable through the entirety of the cultivation of strain Δ*panC*_mvaES-panC. On the other hand, severe plasmid loss was observed in strain Wt_mvaES, even at the very start of the cultivation. By 72 hours of cultivation, plasmid could no longer be detected in strain Wt_mvaES. HPLC analysis revealed that mevalonate was produced throughout the cultivation for strain Δ*panC*_mvaES-panC, even after recovery from the hydrogen shortage, although mevalonate titre was low when OD_{600} was low. More than 2 g/L of mevalonate was detected at 48 hours of cultivation in the case of strain Δ*panC*_mvaES-panC, and at later timepoints approximately 5 g/L was detected. Only trace amounts of mevalonate were detected in samples from the cultivation of strain Wt_mvaES, and only at a single timepoint. The cultivation of strain Wt_mvaES was stopped after 216 hours since no plasmid or mevalonate had been detected for several days.

6.2.4 Batch cultivation using panC-based addiction system

Although the first cultivation was interrupted by loss of hydrogen, the results indicated that *C. necator* H16 could be engineered to produce mevalonate from CO_2, and that a plasmid addiction system could be used to

facilitate this. Based on this, a range of batch fermentations were undertaken as detailed below.

6.2.4.1 Batch cultivation of strains Δ*panC*_mvaES-panC and Δ*panC*_phaA-mvaES-panC

In this experiment two strains were compared again. Strain Δ*panC*_mvaES-panC was used as before. Since PhaA catalyses the same reaction as MvaE, it was hypothesised that overexpression of *phaA* alongside *mvaE* and *mvaS* would further increases mevalonate titre. Therefore, *phaA* was cloned into plasmid p71301_mvaES-panC, upstream of *mvaE*. This resulted in plasmid p71301_phaA-mvaES-panC. Transformation of strain Δ*panC* with this plasmid resulted in a second strain, Δ*panC*_phaA-mvaES-panC. Optical density and mevalonate titre achieved by each strain is shown below in **Figure 6.5**.

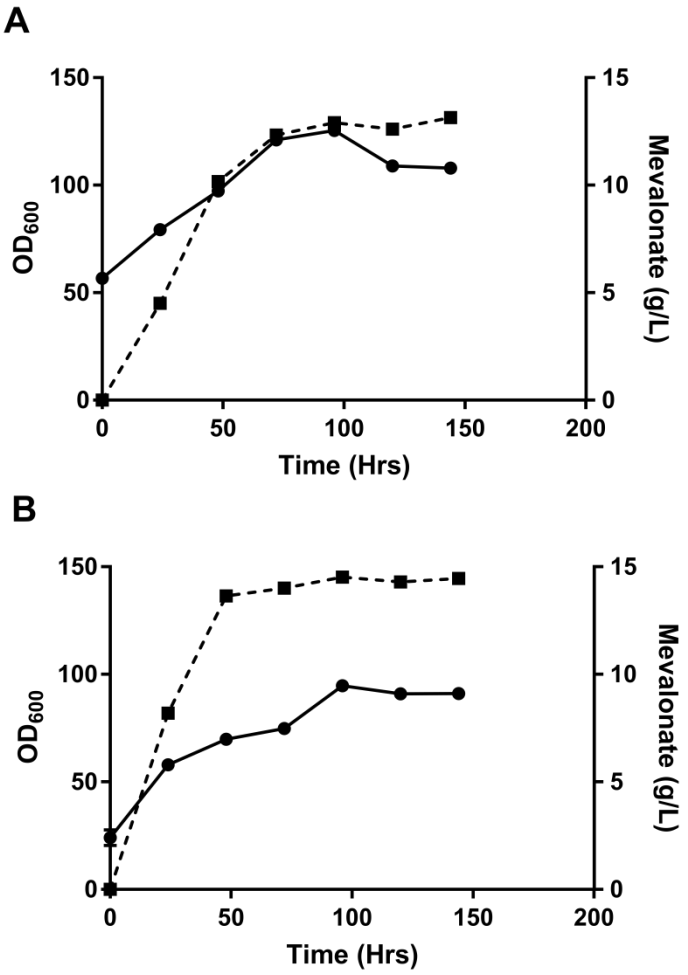

Figure 6.5 – Growth and mevalonate production by strain Δ*panC*_mvaES-panC and strain Δ*panC*_phaA-mvaES-panC during autotrophic batch fermentation. Graphs represent data obtained for strain Δ*panC*_mvaES-panC (**A**), and Δ*panC*_phaA-mvaES-panC (**B**). OD_{600} is represented by a black unbroken line (─) and filled circles. Mevalonate titre is represented by a dashed line (---) and filled squares. X-axis represents time since induction with L-arabinose.

Cultivation of the Δ*panC*_mvaES-panC and Δ*panC*_phaA-mvaES-panC strains revealed that overexpression of *phaA* had a positive influence on mevalonate titre. Whereas strain Δ*panC*_mvaES-panC produced approximately 13 g/L mevalonate, strain Δ*panC*_phaA-mvaES-panC produced 14.5 g/L mevalonate. Notably, the OD_{600} differed between the two strains. While strain Δ*panC*_mvaES-panC grew to an OD_{600} of

approximately 108 at the end of the cultivation, strain Δ*panC*_phaA-mvaES-panC grew to an OD_{600} of around 90. The yields of mevalonate from biomass for strains Δ*panC*_mvaES-panC and Δ*panC*_phaA-mvaES-panC were approximately 0.43 g/gCDW and 0.57 g/gCDW, respectively.

The effect of overexpressing *phaA* on PHB content of the cells was also investigated. GCMS analysis showed that although the PHA content of both strains was approximately 44%, strain Δ*panC*_mvaES-panC produced around 13.4 g/L PHB, whereas strain Δ*panC*_phaA-mvaES-panC produced 10.6 g/L PHB.

6.2.4.2 Batch cultivation of Δ*panC*Δ*phaCAB*_phaA-mvaES-panC

Deletion of the *phaCAB* operon is frequently employed in studies of *C. necator* H16 to redirect carbon flux away from PHB towards other target compounds (220). The *phaCAB* operon was, therefore, deleted from the genome of strain Δ*panC* to investigate the effect this would have on mevalonate production. This resulted in strain Δ*panC*Δ*phaCAB*. The results of the fermentations carried out in **section 6.2.4** suggested that overexpression of *phaA* along with *mvaE* and *mvaS* resulted in an increased mevalonate titre. Strain Δ*panC*Δ*phaCAB* was transformed with plasmid p71301_phaA-mvaES-panC, resulting in strain Δ*panC*Δ*phaCAB*_phaA-mvaES-panC. The results of the fermentation are shown below in **Figure 6.6**.

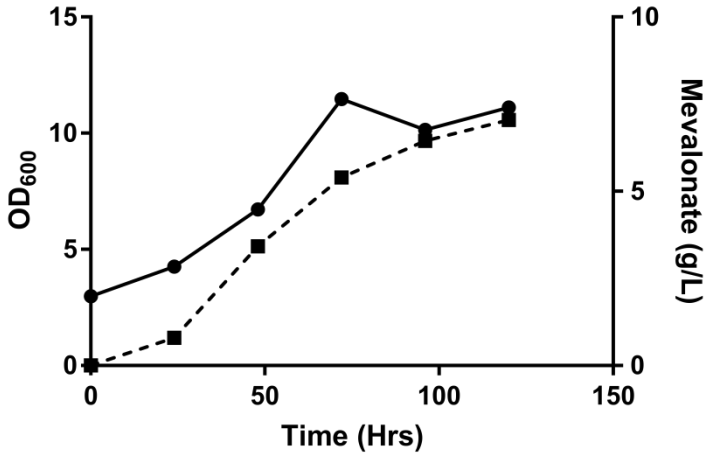

Figure 6.6 – Growth and mevalonate production by strain Δ*panC*Δ*phaCAB*_phaA-mvaES-panC during autotrophic batch fermentation. OD_{600} is represented by a black unbroken line (─) and filled circles. Mevalonate titre is represented by a dashed line (---) and filled squares. X-axis represents time since induction with L-arabinose.

Both the OD_{600} and mevalonate titre achieved by strain Δ*panC*Δ*phaCAB*_phaA-mvaES-panC were lower than those seen during the batch fermentation of strains in which the *phaCAB* operon was intact. A maximum OD_{600} of around 10 was reached and by the end of the cultivation approximately 7 g/L mevalonate was produced. However, while deletion of the *phaCAB* operon had reduced mevalonate titre, the mevalonate yield from biomass had increased to 1.56 g/gCDW, around 3-fold higher than strains Δ*panC*_mvaES-panC and Δ*panC*_phaA-mvaES-panC had achieved.

6.2.4.3 Batch cultivation of Δ*phaCAB*::*phaA-mvaES*

The experiments carried out so far in this chapter had investigated the use of a plasmid addiction system for the production of mevalonate from CO_2. Expression of a pathway from a plasmid is typically associated with greater product formation due to the larger copy number compared to genome integration. To compare genome integration versus plasmid

addiction on mevalonate production, the mevalonate production pathway was integrated into the genome of *C. necator* H16. A knock-in knock-out approach was used to replace the *phaCAB* operon with the arabinose-inducible promoter, *phaA*, *mvaE*, and *mvaS*. The resulting strain was termed Δ*phaCAB*::*phaA-mvaES*.

Strain Δ*phaCAB*::*phaA-mvaES* was cultivated autotrophically in batch mode as before. The results of the fermentation are shown below in **Figure 6.7**.

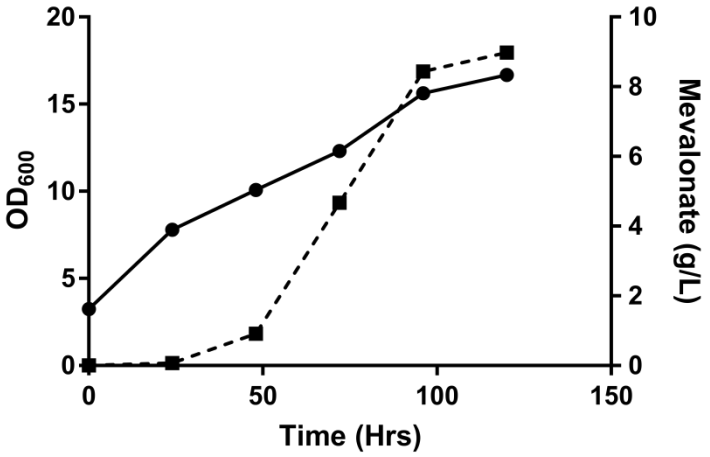

Figure 6.7 – Growth and mevalonate production by strain Δ*phaCAB*::phaA-mvaES during autotrophic batch fermentation. OD_{600} is represented by a black unbroken line (─) and filled circles. Mevalonate titre is represented by a dashed line (---) and filled squares. X-axis represents time since induction with L-arabinose.

As was observed with strain Δ*panC*Δ*phaCAB*_phaA-mvaES-panC which also lacks the *phaCAB* operon, the OD_{600} of strain Δ*phaCAB*::*phaA-mvaES* was relatively low; an OD_{600} of around 15 was achieved by the end of the cultivation. However, despite only containing a single copy of the mevalonate production pathway, strain Δ*phaCAB*::*phaA-mvaES* produced almost 9 g/L mevalonate during the cultivation. Furthermore, the

mevalonate yield from biomass was 1.43 g/gCDW, similar to that of strain Δ*panC*Δ*phaCAB*_phaA-mvaES-panC.

6.2.5 Continuous cultivation using *panC*-based addiction system

The results of the batch fermentation had shown that all strains using the *panC*-based addiction system were capable of producing mevalonate in autotrophic conditions. Furthermore, an integration strain had produced almost 9 g/L mevalonate. The initial continuous cultivation had been interrupted by loss of hydrogen. Nevertheless, the results of those cultivations had indicated that the plasmid addicted strains had retained the plasmid even through a period of very low OD_{600}, and had been capable of producing mevalonate. Following on from the batch experiments, a range of continuous cultivations were carried out using the same strains as above.

6.2.5.1 Continuous cultivation of strains Δ*panC*_mvaES-panC and Δ*panC*_phaA-mvaES-panC

Strains Δ*panC*_mvaES-panC and Δ*panC*_phaA-mvaES-panC were cultivated first. The results of the continuous cultivation of these strains are show below in **Figure 6.8**.

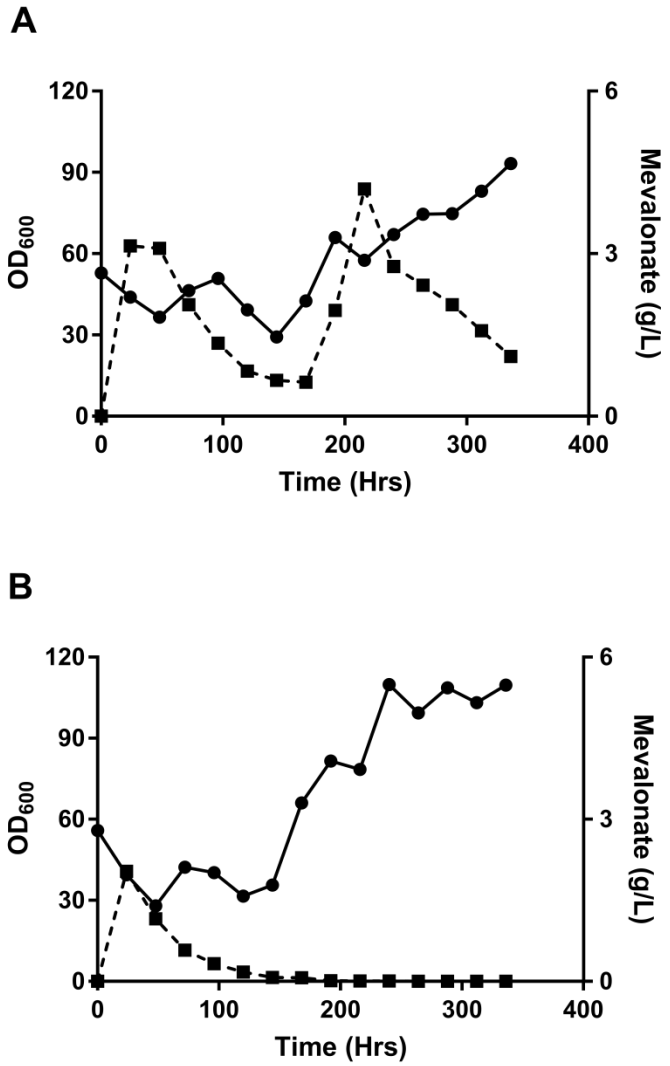

Figure 6.8 – Growth and mevalonate production by strain Δ*panC*_mvaES-panC and strain Δ*panC*_phaA-mvaES-panC during autotrophic continuous fermentation. Graphs represent data obtained for strain Δ*panC*_mvaES-panC (**A**), and Δ*panC*_phaA-mvaES-panC (**B**). OD_{600} is represented by a black unbroken line (─) and filled circles. Mevalonate titre is represented by a dashed line (---) and filled squares. X-axis represents time since induction with L-arabinose.

The production of mevalonate by the two strains differed significantly. Although the production of mevalonate by strain Δ*panC*_mvaES-panC was not stable, mevalonate was detected throughout the cultivation. After induction, around 3 g/L mevalonate could be detected,

though this dropped to less than 1 g/L after 168 hours of cultivation. Mevalonate titre then increased again to around 4 g/L; however, this peak also dropped towards the end of the cultivation, again nearer to 1 g/L. In contrast to strain Δ*panC*_mvaES-panC, it was found that strain Δ*panC*_phaA-mvaES-panC did not produce mevalonate throughout the cultivation. HPLC analysis revealed that strain Δ*panC*_phaA-mvaES-panC produced relatively little mevalonate; a peak of around 2 g/L mevalonate was observed 24 hours after induction. Mevalonate titre then steadily decreased and by 192 hours cultivation, no more mevalonate could be detected.

Growth of neither strain was a very stable, and oscillations in OD_{600} were observed. The growth pattern of each strain was very similar. At the point of induction, OD_{600} of both strains was around 53. A drop in OD_{600} to nearer 30 was observed for both strains in the days following induction. OD_{600} subsequently rose again by 100 hours of cultivation, before a second decrease in OD_{600} was observed. From here the OD_{600} of both strains continued to rise until the end of the cultivation, although minor decreases in OD_{600} were still observed.

6.2.5.2 Continuous cultivation of Δ*panC*Δ*phaCAB*_phaA-mvaES-panC

Following on from the cultivations of strains Δ*panC*_mvaES-panC and Δ*panC*_phaA-mvaES-panC, in which the PHB biosynthetic pathway is intact, cultivation of the PHB-negative strain Δ*panC*Δ*phaCAB*_phaA-mvaES-panC was carried out **[Figure 6.9]**.

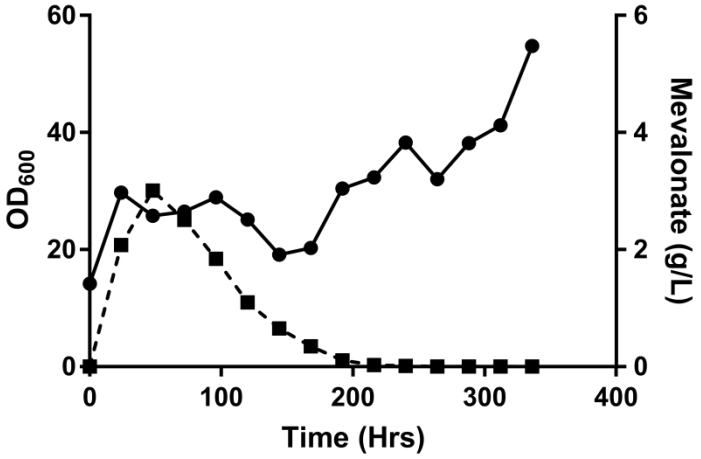

Figure 6.9 – Growth and mevalonate production by strain Δ*panC*Δ*phaCAB*_phaA-mvaES-panC during autotrophic continuous fermentation. OD_{600} is represented by a black unbroken line (─) and filled circles. Mevalonate titre is represented by a dashed line (---) and filled squares. X-axis represents time since induction with L-arabinose.

The results of the cultivation strain Δ*panC*Δ*phaCAB*_phaA-mvaES-panC were similar to those of strain Δ*panC*_phaA-mvaES-panC in the previous section. Mevalonate titre peaked at approximately 3 g/L 48 hours after induction with arabinose. Mevalonate titre then decreased until it could no longer be detected. As had been observed during the cultivation of strains Δ*panC*_mvaES-panC and Δ*panC*_phaA-mvaES-panC, strain Δ*panC*Δ*phaCAB*_phaA-mvaES-panC also exhibited some oscillatory growth.

6.2.5.3 Continuous cultivation of Δ*phaCAB*::*phaA-mvaES*

Finally, strain Δ*phaCAB*::*phaA-mvaES* was grown in continuous cultivation **[Figure 6.10]**.

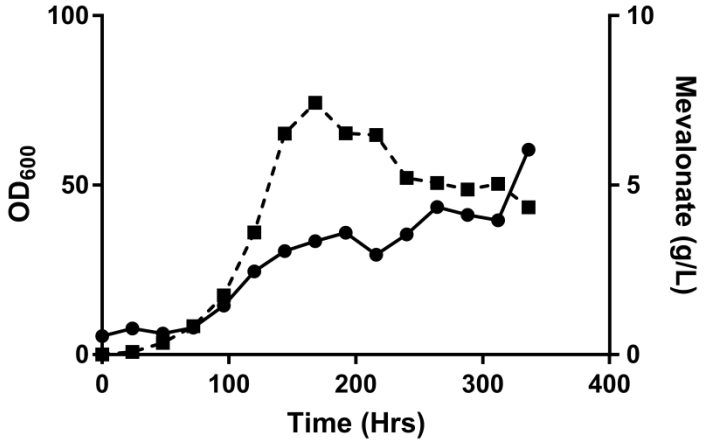

Figure 6.10 – Growth and mevalonate production by strain Δ*phaCAB*::*phaA-mvaES* during autotrophic continuous fermentation. OD_{600} is represented by a black unbroken line (─) and filled circles. Mevalonate titre is represented by a dashed line (---) and filled squares. X-axis represents time since induction with L-arabinose.

Compared to the plasmid addicted strains, the integration strain Δ*phaCAB*::*phaA-mvaES* performed well in continuous cultivation, achieving the highest peak in mevalonate production at more than 7 g/L. However, mevalonate production still decreased to approximately 4.3 g/L by the end of the cultivation. Nonetheless, mevalonate production was observed for the entirety of the cultivation. Furthermore, production was more stable in this strain than in strain Δ*panC*_mvaES-panC, which had also produced mevalonate throughout the cultivation. During the cultivation smaller oscillations in OD_{600} were observed in comparison to the plasmid addicted strains. However, at the end of the cultivation, a significant increase in OD_{600} occurred; from 40 to 60 in 24 hours.

6.2.6 Production of mevalonate using *pyrE*-based addiction system

Having explored the *panC*-based addiction system, attention turned to the *pyrE*-based system. The results of the *panC*-based addiction system studies indicated that including *phaA* in the mevalonate production pathway

had resulted in increased mevalonate titre. Accordingly, the *pyrE*-based system was tested with *phaA* included in the mevalonate production pathway. Strain Δ*pyrE* was transformed with plasmid p71301_phaA-mvaES-pyrE. The resulted in strain Δ*pyrE*_phaA-mvaES-pyrE.

Strain Δ*pyrE*_phaA-mvaES-pyrE was grown in continuous cultivation as had been used previously for the testing of the *panC*-based system. Cultivation of this strain in autotrophic conditions did not result in production of mevalonate. Furthermore, up to 0.5mM uracil could be detected in the supernatant of samples taken through the fermentation (data not shown). As a result, no further experiments were carried out using the *pyrE*-based system.

6.3 Discussion

The aim of the work in this chapter was to develop engineered strains of *C. necator* H16 for use in the production of mevalonate, a precursor to biodegradable polymers, from carbon dioxide. It was also chosen to investigate the development of plasmid addiction systems for use in larger scale autotrophic cultivation, since ultimately the use of antibiotics to maintain a mevalonate biosynthetic pathway would be infeasible for a strain of *C. necator* H16 producing mevalonate at large scale. To facilitate mevalonate biosynthesis, a plasmid in which the *mvaE* and *mvaS* genes of *E. faecalis* were cloned downstream of P_{BAD} was used. In order to generate a plasmid addicted strain, genes involved in pantothenate and uracil biosynthesis were deleted, resulting in auxotrophic strains of *C. necator* H16. Transformation of these auxotrophic strains with complementation plasmids bearing the deleted gene restored growth to the cells. Lastly, the

putative plasmid-addicted, mevalonate-producing strain was generated by cloning the deleted gene into the plasmid bearing the mevalonate biosynthesis pathway and subsequent transformation of that plasmid into the relevant auxotroph.

To investigate further possibilities for increasing mevalonate production, it was also decided to compare the effect of overexpression of *phaA* in the mevalonate biosynthetic pathway, since PhaA of the PHB biosynthetic pathway carries out the same reaction as MvaE. Additionally, to attempt to direct more carbon towards mevalonate, deletion of the *phaCAB* operon was investigated. With regard to pathway stability, in order to compare the effect of mevalonate production from a multi-copy plasmid versus the single-copy genome integration, a knock-in strain was also generated in which the *phaCAB* operon was replaced with the mevalonate biosynthesis pathway consisting of arabinose-inducible promoter, *phaA*, *mvaE*, and *mvaS*.

As described in the introduction to this chapter, three genes involved in the anabolism of essential metabolites were identified as targets which, when deleted, could potentially lead to auxotrophic strains of *C. necator* H16. Aspartate decarboxylase (*panD*), pantothenate synthetase (*panC*), and orotate phosphoribosyltransferase (*pyrE*) were deleted, generating strains Δ*panD*, Δ*panC*, and Δ*pyrE*, respectively. These enzymes are responsible for the biosynthesis of β-alanine, pantothenate, and orotidine 5'phosphate respectively.

The initial plate experiments undertaken to test for auxotrophy demonstrated that while strains Δ*panC* and Δ*pyrE* were auxotrophic for pantothenate and uracil, respectively, strain Δ*panD* was not an auxotroph, as it was capable of growing on SGMM without supplementation with β-alanine. An earlier study by Hoppensack and co-workers discusses the generation of *C. necator* strains lacking *panD* (231). Despite describing the strains as β-alanine auxotrophs, the authors showed that the *panD*-deleted strains still grew in minimal medium even in the absence of β-alanine. Based on the results obtained here and those of the study by Hoppensack and co-workers, it was concluded that *C. necator* H16 must be capable of producing β-alanine by another pathway. Alternative routes for the biosynthesis of β-alanine include the reductive pyrimidine pathway, the spermine pathway, and the acryloyl-CoA pathway (232–234). The reductive pyrimidine pathway facilitates the conversion of uracil to β-alanine *via* a three-step pathway. The enzyme required for the first part of this pathway has been identified and characterized in *C. necator* H16 (235). The subsequent steps have not been demonstrated experimentally for *C. necator* H16, although they are annotated in the organism's KEGG database entry for pyrimidine metabolism. Certain genes of the spermine and acryloyl-CoA pathways are also annotated in the KEGG database entry for *C. necator* H16, but no experimental work has shown their existence. As such, none of the alternative pathways for β-alanine synthesis have been fully described in *C. necator* H16. Therefore, further work is required to elucidate the mechanisms by which the *panD* deletion strain produces β-alanine.

Since strains Δ*panC* and Δ*pyrE* were unable to grow without supplementation with pantothenate and uracil, respectively, these strains were taken forward for plasmid addiction studies. The auxotrophy exhibited by strain Δ*panC* could be relieved by supplementation with pantothenate or complementation with a plasmid-based copy of the *panC* gene **[Figure 6.3]**. The same effect was observed if strain Δ*pyrE* was cultivated in the presence of uracil or when it was transformed with a plasmid containing the *pyrE* gene.

With regard to mevalonate biosynthesis by the engineered strains using the *panC*-based addiction system, the results were mixed. In the initial experiment, which tested the ability of the engineered strain to produce mevalonate from CO_2 and estimated plasmid stability, showed that mevalonate could be produced from CO_2 in continuous cultivation and that the *panC*-based plasmid addiction system was beneficial in supporting this. Despite the interruption to the cultivation, caused by a temporary lack of hydrogen, strain Δ*panC*_mvaES-panC recovered from the significant decrease in OD_{600} and then continued to produce mevalonate **[Figure 6.4**]**.** Strain Wt_mvaES, which lacked the addiction system, failed to produce mevalonate **[Figure 6.4]**. Furthermore, almost 15 g/L mevalonate could be achieved in batch fermentation using the *panC*-based addiction system **[Figure 6.5]**. Additionally, mevalonate and PHB could be co-produced, and overexpression of *phaA* alongside *mvaE* and *mvaS* could further increase mevalonate titre. However, later continuous cultivations showed unstable mevalonate production or complete loss of mevalonate production when the *panC*-based addiction system was used **[Figures 6.8**, **6.9]**.

In the following discussion, the batch fermentations of plasmid-addicted strains will be discussed first along with the implications of the data obtained from those experiments. Next, the data from the initial continuous cultivation and subsequent continuous cultivations of plasmid addicted strains will be examined, and possible explanations for the data obtained from those experiments presented. Lastly, the studies using the integration strain will be discussed, followed by possible directions for future work.

Through the batch experiments, the effect of overexpression of *phaA* alongside *mvaE* and *mvaS*, rather than only *mvaE* and *mvaS*, on mevalonate titre, was characterized. The effect of deleting the *phaCAB* operon on mevalonate production was also investigated. The cultivation of strains Δ*panC*_mvaES-panC and Δ*panC*_phaA-mvaES-panC showed that additionally overexpressing *phaA* increased mevalonate titre, as strain Δ*panC*_mvaES-panC produced around 13 g/L mevalonate while strain Δ*panC*_phaA-mvaES-panC produced 14.5 g/L mevalonate. Through GCMS analysis it was found that overexpressing *phaA* had an effect on the amount of PHB produced by the cells as well. While the PHB content of both cells was around 44%, the PHB titres differed. Strain Δ*panC*_mvaES-panC produced around 13 g/L PHB, and strain Δ*panC*_phaA-mvaES-panC produced nearer to 10 g/L. This could be due to two factors. Firstly, the overexpression of *phaA* increased mevalonate titre. Comparing the yields from biomass, it was seen that strain Δ*panC*_mvaES-panC produced 0.43 g/gCDW mevalonate, while strain Δ*panC*_phaA-mvaES-panC achieved 0.57 g/gCDW mevalonate. It is likely, therefore, that some carbon was

diverted away from PHB towards mevalonate. Secondly, it was seen that the OD_{600} of strain Δ*panC*_phaA-mvaES-panC was lower than that of Δ*panC*_mvaES-panC. The larger metabolic burden experienced by strain Δ*panC*_phaA-mvaES-panC could have negatively affected growth, meaning a smaller PHB titre on account of less biomass.

Next, the effect of deleting the *phaCAB* operon on mevalonate titre was tested. Deletion of the *phaCAB* operon is commonly employed in order to redirect carbon flux towards other compounds and has been used previously in the production of cyanophycin, alcohols, and fatty acids (152,160,161). In comparison to strains Δ*panC*_mvaES-panC and Δ*panC*_phaA-mvaES-panC, which produced 13 and 14.5 g/L of mevalonate, respectively, strain Δ*panC*Δ*phaCAB*_phaA-mvaES-panC produced nearer to 7 g/L. Therefore, in this example, deletion of the *phaCAB* operon reduced mevalonate titre. However, the mevalonate yield from biomass was much higher, at 1.56 g/gCDW mevalonate. A similar phenomenon was observed by Muller et al during their attempts to produce methyl ketones from fructose using a PHB-negative mutant of *C. necator* H16 (236). In this case the authors were unable to determine why deletion of the *phaCAB* operon did not improve methyl ketone titre.

In the case of the autotrophically grown cells, one possible explanation could be due to an effect of deletion of the *phaCAB* operon on the regulation of enzymes of the Calvin-Benson-Bassham (CBB) cycle. A commonly used PHB-negative strain of *C. necator* H16 is the PHB$^-$4 strain (DSM 541), generated in 1970 by treating wild-type *C. necator* H16 with the mutagen 1-nitroso-3-nitro-1-methylguanidine (NMG) (237). In this

strain, PHB biosynthesis is abrogated due to a stop codon in the *phaC* gene, introduced by a point mutation (238). As a result, the PhaC protein is truncated, and neither the *phaA* nor the *phaB1* gene is expressed. In the present study, the entire *phaCAB* operon is deleted, however, the end effect is the same; none of the genes of the *phaCAB* operon are expressed. Transcriptome analysis has shown that the genes of the CBB cycle are significantly downregulated in strain PHB$^-$4 in comparison to wild-type *C. necator* H16 (239). It is possible, therefore, that reduced capacity of the *phaCAB* knockout strain to fix carbon dioxide resulted in lower carbon uptake into the cell and, as a consequence, reduced carbon available for conversion to mevalonate.

Regarding the higher mevalonate titre achieved by strains possessing an intact *phaCAB* operon, it has also been shown that co-production of PHAs can have a positive effect on the production of a second metabolite (240,241). While this phenomenon is not yet well understood, one possible reason for this could be the effect of NADPH consumption on flux through the TCA cycle. Previously it was shown that deletion of the *zwf* gene from the *E. coli* genome increases flux through the TCA cycle (242). The reaction catalysed by G6PDH, which is encoded by *zwf*, is an NADPH-producing reaction. The authors determined that in strains lacking a functional *zwf* gene, flux through the TCA cycle was increased to maintain a sufficient intracellular concentration of NADPH. It was later hypothesised by Kang et al that this effect could be somewhat mimicked in *E. coli* which had been engineered to produce PHB (243). Since PHB is a sink for NADPH, Kang et al suggested that the engineered PHB-producing *E. coli* would also increase

flux through the TCA in order to maintain adequate quantities of NADPH in the cell. Their results showed that the NADPH/NADP+ ratio in PHB-producing and non-producing strains of *E. coli* was the same, suggesting higher carbon flux through TCA in order to maintain NADPH concentration. Since their target product was succinate, an intermediate of the TCA cycle, increased flux through the TCA was hypothesised to result in increased production of succinate. One possibility is, therefore, that removing PHB biosynthesis in *C. necator* H16 could reduce flux to the TCA cycle, reducing acetyl-CoA availability and as a consequence reduce mevalonate production. However, in this scenario it is unclear why NADPH consumption due to mevalonate production would not result in the same increased flux through the TCA cycle.

Compared to the results of the batch cultivations, the results of the continuous cultivations carried out in this chapter gave different indications of how effectively the engineered strains of *C. necator* H16 could produce mevalonate from CO_2, and of the functionality of the *panC*-based addiction system. Despite the interruption to the cultivation, the initial continuous cultivation indicated that mevalonate could be produced continuously from CO_2 by engineered *C. necator* H16. The initial continuous cultivation also suggested that the addiction system resulted in complete plasmid retention. By comparison, a strain not using an addiction system lost the plasmid rapidly, and mevalonate was not produced **[section 6.2.3]**. In contrast, later continuous cultivations using the addiction system indicated unstable mevalonate production or even loss of mevalonate production **[sections 6.2.5.1** and **6.2.5.2]**. Additionally, significant oscillations in growth were

observed during the continuous cultivations carried out in **section 6.2.5.1** and **6.2.5.2**. A large fluctuation in OD_{600} was also observed during the continuous cultivation carried out in **section 6.2.3**; however, this is due to loss of hydrogen for a period during the cultivation.

The unstable mevalonate production shown in **sections 6.2.5.1** and **6.2.5.2** could possibly be attributed to a range of causes. These include loss of pathway induction, washing out of cell culture during continuous cultivation, or issues with pathway stability and integrity.

In this work, the mevalonate pathway was placed under the control of the arabinose-inducible promoter P_{BAD}. Arabinose can be metabolized as a carbon source by many bacteria (244). Therefore, one possible reason could have been that the arabinose used to induce the mevalonate biosynthetic pathway was being consumed during the cultivation, diminishing expression of the mevalonate pathway genes. HPLC analysis however did not indicate this, as a stable level of arabinose could be detected throughout the continuous cultivations (data not shown).

A second possibility could have been that either mevalonate or the engineered cells were being washed out of the reactor. During continuous cultivation, fresh medium is continually fed into the reactor, while medium inside the reactor is removed via an outflow line, resulting in constant turnover of the medium inside the reactor. If mevalonate is produced too slowly, or the culture grows too slowly, the effect is gradual reduction of mevalonate or cell concentration in the reactor, until that concentration reaches 0. It was seen that during the continuous cultivation that OD_{600}

increased, showing that cells were not washed out of the reactor **[Figures 6.9**, **6.9]**. Therefore, loss of mevalonate production cannot be attributed to the absence of cells. The remaining option is that mevalonate was produced too slowly. However, since the cells were theoretically plasmid-addicted, increasing OD_{600} should result in increased mevalonate production, as this should mean more mevalonate-producing cells. Increasing OD_{600} but decreasing mevalonate production therefore indicates that the ability to produce mevalonate was being lost from the culture. This suggested issues with the stability or integrity of the mevalonate biosynthetic pathway itself.

Despite the use of a plasmid addiction system, plasmid loss can still occur if the addiction is dependent on a metabolite. In the experiments described here, addiction systems dependent on pantothenate or uracil auxotrophy were tested. Without the plasmid, strains lacking a genomic copy of *panC* or *pyrE* are unable to grow. Therefore, retention of a plasmid encoding a copy of *panC* or *pyrE* by these strains is essential for the cells to grow. However, if sufficient pantothenate or uracil were to become available in the growth medium, cells could use the metabolite in the medium instead of synthesising it themselves. In this scenario, the plasmid is no longer necessary for cell growth. Since the plasmid is no longer needed for growth, the plasmid can be lost.

In the systems described here the *panC* and *pyrE* genes were overexpressed on plasmids to facilitate plasmid addiction in the Δ*panC* and Δ*pyrE* strains, respectively. The base plasmid used in this work, pMTL71301, has a copy number of 30-40 per cell (M. Ehsaan, personal communication). As such, the capacity of the cells to produce pantothenate

or uracil was much higher than usual, since each gene is normally only encoded in the genome once. While pantothenate was not detected during HPLC analysis, the sole attempt at using the *pyrE*-based addiction system revealed up to 0.5mM uracil in the medium. The presence of uracil in the medium of the strain using the *pyrE*-based addiction system could then result in plasmid loss through the mechanism described in the previous paragraph. It is also highly likely that pantothenate was also overproduced and secreted into the medium in the case of strains using the *panC*-based addiction system. The process by which plasmid-addicted cells overproduce and secrete the metabolite responsible for auxotrophy thereby resulting in plasmid loss is termed "cross-feeding", and is a risk for plasmid addiction systems based on auxotrophy (245,246). In a previous study, leucine auxotrophy was exploited to facilitate plasmid addiction in *S. cerevisiae*. Cells were observed to overproduce and secrete leucine into the growth medium. Cross-feeding resulted in loss of auxotrophy and subsequently decreased xylitol production (247). Initial data obtained suggested the *panC*-based addiction system to be very stable, since the plasmid stability assay did not indicate plasmid loss in the addicted strain Δ*panC*_mvaES-panC **[Figure 6.4B]**. However, if cross-feeding was resulting in plasmid loss, it is unlikely that this could have been detected due to the conditions of the plasmid stability assay, as is discussed below.

The plasmid stability assay was carried out by taking samples throughout the cultivation and plating these on LB + Gm plates. After colonies had appeared on the plates, 100 colonies were randomly chosen, and these were restreaked on LB, and LB + Tet. Growth would only be

observed on tetracycline-containing plates if the plasmid was retained. In the case of strain Wt_mvaES, plasmid loss occurred rapidly and after 72 hours of cultivation, colonies were no longer detected on the LB + Tet plates, indicating total plasmid loss. In contrast, the plasmid stability assay indicated 100% plasmid retention for strain Δ*panC*_mvaES-panC.

One factor which was not taken into taken into account during the plasmid stability assay of the addiction system used in strain Δ*panC*_mvaES-panC was that any cells which had lost the plasmid would be eliminated when they were plated on LB + Gm, since pantothenate was not available on the plate. As a result, the conditions of the LB + Gm plate selected for plasmid-addicted cells and against plasmid-free cells. This bias would then carry over into the subsequent step in which individual cells were restreaked on LB and LB + Tet. Since the only cells which could grow on the LB + Gm plate were those retaining the plasmid, the results of restreaking onto LB and LB + Tet would indicate 100% plasmid stability. Taken together with the data of the continuous cultivations, which indicated unstable mevalonate production, it is likely that some plasmid loss was occurring due to cross-feeding. However, this would not have been detected due to the conditions of the plasmid stability assay.

Cross-feeding could also explain the unstable OD_{600} observed during the work carried out in **sections 6.2.5.1** and **6.2.5.2**. If pantothenate was secreted into the medium during cultivation of strains using the *panC*-based addiction system, it is reasonable to assume that as OD_{600} increases, the amount of pantothenate in the medium increases. Therefore, at a certain point, sufficient pantothenate is in the medium that cross-feeding can occur.

Now a population of cells can arise which have lost the plasmid and have begun using pantothenate secreted into the medium instead. At this point, both plasmid-addicted and plasmid-free cells are able to grow, resulting in increasing OD_{600}. After the pantothenate in the medium has become depleted, plasmid-free cells are no longer able to grow since they have lost the plasmid which facilitated pantothenate biosynthesis, and no pantothenate remains in the medium. As a result, these plasmid free cells are washed out of the cultivation, causing a drop in OD_{600}. The OD_{600} increases again afterwards due to the presence of cells still containing the plasmid, which are able to repopulate the cultivation. This would also explain why strain Δ*panC*_mvaES-panC recovered and was able to produce mevalonate following the hydrogen shortage which occurred in the continuous cultivation detailed in **section 6.2.3**.

A second factor affecting the stability of an engineered pathway is the presence of molecular mechanisms within the bacteria, the functions of which are to generate genetic diversity. Examples of these mechanisms include error-prone DNA polymerases, which can introduce point mutations in a gene, and insertion sequences, which can move around the genome and insert themselves into genes or operons (248). Such mechanisms are valuable in the natural environment where conditions are frequently changing, allowing bacteria to adapt to changes in order to survive. For instance, error-prone DNA polymerase can restore lactose metabolism to mutant *E. coli*, while movement of an insertion sequence into the *bgl* operon can facilitate the use of β-glucosides as carbon sources (249,250). The activity of mechanisms such as these typically increases when bacteria

encounter stresses like DNA damage, heat-shock, or nutrient starvation, amongst others (248). However, bacteria can also become stressed during fermentation due to a range of factors, including population density, oxygen availability, substrate availability (251). Plasmid maintenance and expression of genes encoded on a plasmid impose further stress on bacteria (252). As a result, these mutation-generating mechanisms can also become active during fermentation for the production of a target compound. The activation of such mechanisms during fermentation poses a significant threat to the efficacy of a biosynthetic pathway. As the mutation rate increases, so does the chance of the engineered strain acquiring mutations which are detrimental to the production of the target compound. This leads not only to loss of productivity, but also to the emergence of faster growing strains, which do not experience the full metabolic burden of non-mutated strains. These faster growing strains further reduce the productivity of the process, as they begin to outcompete slower growing strains which are still producing the target compound. Conveniently, recent work has studied the effect of these mutation-generating mechanisms on *E. coli* engineered to produce mevalonate (253). The authors of that study also observed declining mevalonate production during their cultivations. To determine whether their chosen mevalonate production pathway was affected by mutations, deep sequencing was employed. They found that as the cultivation proceeded, less and less of their sequencing reads mapped to the mevalonate production pathway. In particular, the authors found that insertion sequences had progressively disrupted the pathway, severely reducing mevalonate

production. As mevalonate production decreased, growth rate was found to increase.

Taken together, the effects of cross-feeding and mutation to the mevalonate production pathway could explain the results of the continuous cultivation of strains using the *panC*-based system. Cross-feeding would simultaneously result in increasing OD_{600} and decreasing mevalonate production. The plasmid-free cells no longer have the metabolic burden of mevalonate production and are able to grow more quickly, increasing OD_{600}. At the same time, mevalonate production decreases since fewer cells retain the plasmid. Mutation of the mevalonate biosynthesis pathway would have a similar effect. In this case, cells escape the metabolic burden of mevalonate biosynthesis due to accumulation of mutations which inactivate the mevalonate production pathway, leading to faster growth. The end result is again increased growth and decreased mevalonate production. It is likely that the performance of the batch fermentations were also limited by these effects. However, since mevalonate cannot leave the reactor during batch cultivation as there is no outflow line, loss of mevalonate production would not be so apparent in this mode of culture.

It was also chosen to investigate the effect of integrating the mevalonate pathway into the genome of *C. necator* H16, in order to compare this with plasmid-based expression. Generally, plasmid expression is preferred to genome integration, as the larger copy number associated with plasmid expression results in higher product formation (164). To compare the effect of plasmid addiction versus genome integration on mevalonate production, strain Δ*phaCAB*::*phaA-mvaES* was constructed. In

this strain the *phaCAB* operon was replaced with *phaA*, *mvaE*, and *mvaS* under the control of an arabinose-inducible promoter.

Despite encoding only a single copy of the mevalonate production pathway, strain Δ*phaCAB*::*phaA-mvaES* was one of the best performing strains. As mentioned previously, the base plasmid used in the plasmid addiction studies, pMTL71301, has a copy number of 30-40 per cell (M. Ehsaan, personal communication). Almost 9 g/L was achieved in batch fermentation after 188 hours of cultivation and in continuous cultivation mevalonate production peaked at over 7 g/L before decreasing to nearer 4 g/L by the end of the cultivation. The heterologous expression of proteins can exert a large metabolic burden on cells (254). Studies in *E. coli* showed that plasmid-based expression resulted in a significant increase in the intracellular concentration of the stress molecule guanosine tetraphosphate (ppGpp), whereas the concentration in ppGpp was largely unchanged when expression from the genome was used instead (255). It has been shown that ppGpp can activate mutation-generating mechanisms, one way in which synthetic pathways can be lost (248). Therefore, reducing metabolic burden can result in cells with improved fitness, which in turn positively influences production formation (256). It is likely that the reduced metabolic load experienced by strain Δ*phaCAB*::*phaA-mvaES* in comparison to strains using plasmid-based expression was beneficial for the production of mevalonate.

The outcome of the work carried out in this chapter indicated that *C. necator* H16 is suitable for the biosynthesis of mevalonate from CO_2, though further work is needed to generate a stable plasmid for use in

autotrophic cultivation. In particular, the results of the continuous cultivations using plasmid addicted strains indicated either unstable mevalonate production or total loss of mevalonate production, while an integration strain was capable of stable production of mevalonate. Nonetheless, several interesting observations were made which can inform future work.

Using engineered *C. necator* H16, it was possible to produce significant quantities of mevalonate from CO_2. With the aim of producing biodegradable materials containing βMΔVL, a derivative of mevalonate, a next step would be to purify the mevalonate from fermentation broth and convert it to a polymeric material, such as poly(βMΔVL).

Using the plasmid addiction system, co-production of mevalonate and PHB from carbon dioxide was demonstrated. Moreover, the co-production of PHB appeared to be beneficial for mevalonate production, as higher mevalonate titres were achieved in strains with an intact *phaCAB* operon compared to those lacking the *phaCAB* operon. The co-production of PHAs and other chemicals is of great interest as the added value of a second product improves the economics of the process (257,258). Considering that a key factor hindering the commercial viability of PHA-based materials is the cost, the co-production of valuable chemicals alongside PHAs could be important in the drive for more widespread application of PHA-based products. Since the co-production of mevalonate and PHB was facilitated by the use of the plasmid addiction system, continued research into improving plasmid stability is needed. A more appropriate plasmid addiction system would be one in which auxotrophy cannot be relieved, as likely happened

with the *panC*- and *pyrE*-based systems. While the possibility of the emergence of mutations in the mevalonate production pathway was not investigated in the course of this work, future studies could also explore the removal of mutation-generating mechanisms from the genome. A 2006 study described an engineered strain of *E. coli*, referred to as MDS42, in which all insertion sequences had been deleted (259). The authors showed MDS42 was able to produce a toxic fusion protein, while wild-type *E. coli* was not due to the presence of insertion sequences in the coding region of the toxic protein. Subsequent work using MDS42 has shown removal of insertion sequences to be beneficial in improving pathway stability and product titre (260,261). Further engineering of the strain first described, to remove error-prone DNA polymerases, resulted in further decrease in overall mutation rates (262)**.** Additional work could be carried out to more finely tune expression of production pathways, since excessive metabolic loads represent a significant driver of genetic instability at large scale fermentation (256).

Flux towards mevalonate could also be increased by overexpressing *phaA* as well as *mvaE* and *mvaS*. Further work could investigate the applicability of other enzymes which may be able to further boost mevalonate production. For instance, the *atoB* gene from *E. coli*, encoding a β-ketothiolase, has previously been used in the production of mevalonate in engineered strains of *E. coli* (263).

Replacement of the *phaCAB* operon with the *phaA*, *mvaE*, and *mvaS* genes resulted in a strain which performed very well in both batch and continuous fermentation, despite only a single copy of the pathway being

present in each cell. One drawback of this strain was that only mevalonate could be produced, since the mevalonate production pathway replaced the *phaCAB* operon. Future work could investigate neutral sites at which to integrate the mevalonate production pathway such that the resulting strain can produce both mevalonate and PHB using pathways encoded in the genome. It would also be interesting to compare how expression of both mevalonate- and PHB-producing pathways from the genome would affect mevalonate titre, since the results from the plasmid addiction strains showed co-production resulted in higher mevalonate titres.

Chapter 7: General Discussion

7.1 Outcomes of Thesis

The production of poly(3HB-*co*-3HP) with a high 3HP molar fraction from β-alanine was achieved using engineered *C. necator* H16. A systematic approach was used to target bottlenecks at each step of the pathway. Overexpression of a putative β-alanine pyruvate aminotransferase from *C. violaceum* and NADP-dependent 3-hydroxyacid dehydrogenase from *E. coli* under the promoter of the *phaC* gene of *C. necator* H16 resulted in efficient conversion of β-alanine to 3HP. 3HP incorporation into the polymer could be drastically increased by also overexpressing propionyl-CoA transferase from *C. necator* H16 and either PHA synthase from *C. necator* H16 or *C.* sp. USM2. Furthermore, it was shown that strains using PHA synthase from *C.* sp. USM2 produced more polymer than strains using PHA synthase from *C. necator* H16. The final strain, Δ3_CNCM21, was capable of producing poly(3HB-*co*-3HP) containing approximately 80 mol% 3HP when grown in medium containing 50mM β-alanine.

The production of poly(3HB-*co*-3HP) with a range of 3HP molar content was also demonstrated when strain Δ3_CNCM21 was cultivated in medium containing different amounts of β-alanine. Supplementation of the medium with 2mM cysteine could increase the 3HP content of the polymer further. HPLC analysis revealed that the addition of cysteine appeared to increase re-uptake of 3HP from the supernatant. Cultivation of strain Δ3_CNCM21 in this manner resulted in the production of copolymer containing trace to 89 mol% 3HP.

The effect of suppressing 3HB-CoA biosynthesis on 3HP incorporation into the copolymer was also explored. Three strains were generated; a *phaA* knockout, a *phaB1* knockout, and a *phaAB1* double knockout. In each case, increased 3HP incorporation into the polymer was observed. In particular, cultivation of strain Δ3AB1_CNCM21 resulted in the production of a copolymer containing 91 mol% 3HP. A significant increase in PHA titre using the strain in which *phaA* had been deleted, Δ3A_CNCM21, was observed compared to strain Δ3_CNCM21. Specifically, strain Δ3A_CNCM21 produced approximately 1.15 g/L PHA, while strain Δ3_CNCM21 produced only 0.76 g/L PHA.

Lastly, the use of plasmid addiction systems in autotrophic cultivation of *C. necator* H16 was tested. Three knockout strains were generated; Δ*panC*, Δ*panD*, and Δ*pyrE*. However, Δ*panD* did not exhibit auxotrophy, and no mevalonate was detected during the cultivation using the Δ*pyrE* strain. The Δ*panC* strain was cultivated in batch and continuous cultivation. In batch cultivation it was possible to co-produce mevalonate and PHB. In one instance, 14.5 g/L mevalonate and over 10 g/L PHB were produced from CO_2. However, continuous cultivations indicated unstable mevalonate production by strains using the Δ*panC*-based plasmid addiction system, as mevalonate titre was either unstable or was lost completely. In contrast, the integration strain Δ*phaCAB*::phaA-mvaES performed well in both batch and continuous cultivation.

7.2 Limitations and Future Work

The main goal of the work carried out in this thesis was to produce poly(3HB-*co*-3HP) using *C. necator* H16 as the microbial host. While this was successfully achieved, significant future work could be carried out to further improve the strain. Various factors can be addressed which focus on different aspects of the system, resulting in a strain with overall better applicability.

The strategy employed focused on the production of poly(3HB-*co*-3HP) using a partial β-alanine pathway; β-alanine supplied in the medium was converted to 3HP and subsequently incorporated into the polymer. As described earlier, the full β-alanine pathway makes use of excess β-alanine derived from the central metabolism as the precursor to 3HP. Therefore, one of the major directions of future work would be to construct a strain of *C. necator* H16 which overproduces β-alanine from the central metabolism. This would not only remove the need to supplement β-alanine but would also allow the production of poly(3HB-*co*-3HP) from various carbon sources. In this way, waste carbon sources could be more effectively utilized. The work shown in this thesis indicates that β-alanine can be readily converted to 3HP and incorporated into the polymer, if an appropriate pathway is used. The described studies also showed that copolymer composition could be varied depending on the amount of β-alanine supplemented in the medium. It may be possible to control 3HP content in polymers produced by *C. necator* H16 by engineering a range of strains with different degrees of flux directed towards β-alanine.

Another factor which can improve the overall quality of the polymer produced is the specificity of PHA synthase for 3HP. Previously it has been shown that the activity level of PHA synthase has an impact on the molecular weight of the polymer produced (193). Typically, PHAs with higher molecular weights are more desirable than those with low molecular weights (264,265). In this study it proved necessary to overexpress PHA synthase in order to significantly increase the amount of 3HP incorporated into the polymer. Given that the PHA synthase gene was positioned downstream of the promoter of the *trp* gene, and on a plasmid a copy number of 30-40 plasmids per cell, it is likely that the activity of PHA synthase was high and therefore the molecular weight of the polymer low. In order to resolve this issue, a lower copy number plasmid could be used, or it may be possible to engineer the PHA synthase such that it has increased specificity towards 3HP.

Data obtained also showed that 3HP molar content could be increased by additional supplementation of the medium with 2mM cysteine. It was hypothesised that cysteine supplementation would increase the pool of acetyl-CoA available for activation of 3HP to 3HP-CoA, thereby increasing the amount of 3HP which can be added to the polymer. Cultivating strain Δ3_CNCM21 in SGMM + 50mM β-alanine resulted in a copolymer containing approximately 80 mol% 3HP, whereas cultivation in SGMM + 50mM β-alanine + 2mM cysteine resulted in a copolymer containing 89 mol% 3HP. Future work could therefore investigate ways of increasing acetyl-CoA biosynthesis in order to provide more CoA for the activation of 3HP to 3HP-CoA. Increasing the pool of CoA or acetyl-CoA

has been employed previously to improve the production of compounds dependent on these molecules (201,204).

Other data demonstrated that reducing flux towards 3HB-CoA had a significant effect on the 3HP molar fraction of the polymers produced. Various studies have exploited this in order to obtain copolymers with a higher molar fraction of a second monomer. In this case, deletion of *phaA* and *phaB1* greatly reduced the amount of PHB produced by *C. necator* H16 and resulted in a copolymer containing 91 mol% 3HP. Further suppression of 3HB-CoA biosynthesis could result in even higher 3HP content, and it may even be possible to produce poly(3HP) if 3HB-CoA biosynthesis is sufficiently reduced.

Another area which requires further investigation and is not directly related to the biosynthesis of poly(3HB-*co*-3HP) or engineering of the production strain, is greater study of the copolymer itself. While the thermal properties of poly(3HB-*co*-3HP) and the biodegradability have been documented, the mechanical properties of the copolymer remain to be examined. In particular, the elongation at break, Young's modulus, and tensile strength are three basic parameters which must be evaluated in order to determine the usefulness of a polymer for commodity application. Elongation at break determines how much deformation a material can undergo before breaking, Young's modulus and tensile strength describe the overall stiffness and strength of the material, respectively. The influence of changing 3HP molar fraction in a poly(3HP-*co*-4HB) copolymer was previously described and showed significant effects on both the thermal and mechanical properties of the polymer (87). To gain a better understanding of

the properties of poly(3HB-*co*-3HP) and to more accurately determine roles in which this copolymer may be suitable for use, it is essential that the mechanical properties of the copolymer are studied.

Regarding the work carried out to facilitate production of mevalonate from CO_2 as was described in Chapter 6, several different routes of research could be pursued. It was seen that mevalonate could be produced from CO_2 using engineered strains of *C. necator* H16. Since the aim was to produce mevalonate with the intention of using it to produce polymer, subsequent work should focus on conversion of mevalonate to βMΔVL in order to facilitate polymer synthesis. As was shown previously with lactide, it may also be possible to react βMΔVL with different compounds, increasing the range of novel polymers containing a βMΔVL monomer.

It was also shown in the original study by Xiong et al that βMΔVL could be synthesised either biologically or chemically. However, both processes exhibited significant disadvantages. On one hand, the fully biological process resulted in only around 270 mg/L of βMΔVL, despite the ability of the engineered *E. coli* to accumulate ~15 g/L of mevalonate. On the other hand, the chemical process used a very expensive palladium catalyst. Therefore, future work could also investigate protein engineering on the SidI, SidH, and Oye2 enzymes which are responsible for the low conversion of mevalonate to βMΔVL.

The secondary goal Chapter 6 was to investigate the applicability of a plasmid addiction system for use in autotrophically growing strains of *C. necator* H16. A plasmid addiction based on pantothenate auxotrophy

initially appeared to function well in batch cultivation however in continuous cultivation mevalonate production was evidently unstable. Use of the plasmid addiction system however did facilitate co-production of mevalonate and PHB, a phenomenon which is expected to improve the economics of bioprocesses. Additionally, strains which co-produced mevalonate and PHB were able to produce more mevalonate than strains lacking PHB, highlighting another advantage. Both of these facts indicate it is necessary to continue research on developing plasmid addiction systems for *C. necator* H16. Ideally a different plasmid addiction system should be employed since those used in this study did not result in stable plasmid maintenance. Work could be carried out to fine-tune expression, reducing metabolic load on the producer cells. This can simultaneously improve production and reduce the emergence of non-producing cells due to the activity of mutation-generating mechanisms which are activated during stress. Removal of inherent mutation-generating mechanisms would likely also positively impact the performance of *C. necator* H16 in large scale fermentation. Recent research indicates insertion sequences in particular pose a threat to the stability of production pathways in large scale fermentation.

Further investigation into the genomic integration of pathways in *C. necator* H16 should also be carried out. One of the best performing strains generated in the current study was the integration strain, despite only one copy of the mevalonate production pathway being present. Since increased mevalonate titres were observed when the *phaCAB* operon was intact, it would be interesting to find a locus other than the *phaCAB* operon to

integrate the mevalonate production pathway, such that mevalonate and PHB could be co-produced from genomically encoded pathways.

7.3 Conclusions

Previous work had shown that *C. necator* H16 does not efficiently incorporate 3HP into a growing polymer chain and attempts to produce poly(3HB-*co*-3HP) using *C. necator* H16 had resulted in copolymer with a low 3HP molar fraction. Additionally poly(3HB-*co*-3HP) with a wide range of 3HP content had only been achieved in engineered strains of *E. coli*, or by feeding *A. latus* with different concentrations of 3HP. A systematic approach was adopted to improve the ability of *C. necator* H16 to incorporate 3HP into PHB, resulting in a copolymer of poly(3HB-*co*-3HP) with high 3HP molar fraction. Overexpression of both propionyl-CoA transferase and PHA synthase was necessary to achieve this. The molar fraction of 3HP could then be controlled depending on medium composition. Furthermore, deletion of genes contributing to 3HB-CoA biosynthesis was shown to positively influence 3HP content of the copolymer. The use of a plasmid addiction system was also shown to be beneficial for the production of mevalonate from carbon dioxide, though the system used was ultimately not suitable for use in continuous cultivation. The results presented in this thesis indicate numerous different opportunities for further research into the use of *C. necator* H16 as a platform for the production of poly(3HB-*co*-3HP) and for its use in the biosynthesis of other valuable compounds from carbon dioxide in large-scale fermentation.

References

1. IEA. *Key World Energy Statistics 2019*. OECD Publishing.

2. *BP Statistical Review of World Energy 2019*.

3. Rosenzweig C, Iglesias A, Yang XB, Epstein PR, Chivian E. *Climate Change and Extreme Weather Events: Implications for Food Production, Plant Diseases, and Pests*. Global Change and Human Health. 2001;2(2):90–104.

4. Parry ML, Rosenzweig C, Iglesias A, Livermore M, Fischer G. *Effects of climate change on global food production under SRES emissions and socio-economic scenarios*. Global Environmental Change. 2004;14(1):53–67.

5. Heinberg R, Fridley D. *Other Uses of Fossil Fuels: The Substitution Challenge Continues*. In: Our Renewable Future: Laying the Path for 100% Clean Energy. 2016. p. 95–113.

6. Ellen MacArthur Foundation. *The New Plastics Economy: Rethinking the Future of Plastics*. 2016.

7. Geyer R, Jambeck JR, Law KL. *Production, use, and fate of all plastics ever made*. Science Advances. 2017;3(7):25–9.

8. Masnadi MS, El-Houjeiri HM, Schunack D, Li Y, Englander JG, Badahdah A, et al. *Global carbon intensity of crude oil production*. Science. 2018;361(6405):851–3.

9. Center for International Environmental Law. *Plastic & Climate - The Hidden Costs of a Plastic Planet*. 2019.

10. Swift TK, Moore MG, Sanchez E, Rose-Glowacki H. *The Rising Competitive Advantage of U.S. Plastics*. American Chemistry Council. 2015;

11. Material Economics. *The Circular Economy - A Powerful Force for Climate Mitigation*. 2018.

12. Ioakeimidis C, Fotopoulou KN, Karapanagioti HK, Geraga M, Zeri C, Papathanassiou E, Galgani F, Papatheodorou G. *The degradation potential of PET bottles in the marine environment: An ATR-FTIR based approach*. Scientific Reports. 2016;6(October 2015):1–8.

13. Chamas A, Moon H, Zheng J, Qiu Y, Tabassum T, Jang JH, Abu-Omar M, Scott SL, Suh S. *Degradation Rates of Plastics in the Environment*. ACS Sustainable Chemistry and Engineering. 2020;8(9):3494–511.

14. Jambeck J, Geyer R, Wilcox C, Siegler TR, Perryman M, Andrady A, Narayan R, Law KL. *Plastic waste inputs from land into the ocean*. Marine Pollution. 2015;347(6223):768–71.

15. Chiba S, Saito H, Fletcher R, Yogi T, Kayo M, Miyagi S, Ogido M, Fujikura K. *Human footprint in the abyss: 30 year records of deep-sea plastic debris*. Marine Policy. 2018;96(April):204–12.

16. Thompson RC, Olson Y, Mitchell RP, Davis A, Rowland SJ, John AWG, McGonigle D, Russell AE. *Lost at Sea: Where Is All the Plastic?* Science. 2004;304(5672):838.

17. Prata JC, da Costa JP, Lopes I, Duarte AC, Rocha-Santos T. *Environmental exposure to microplastics: An overview on possible human health effects*. Science of the Total Environment. 2020;702:134455.

18. Deng Y, Zhang Y, Lemos B, Ren H. *Tissue accumulation of microplastics in mice and biomarker responses suggest widespread health risks of exposure*. Scientific Reports. 2017;7(March):1–10.

19. Liu A, Richards L, Bladen CL, Ingham E, Fisher J, Tipper JL. *The biological response to nanometre-sized polymer particles*. Acta Biomaterialia. 2015;23:38–51.

20. Brown DM, Wilson MR, MacNee W, Stone V, Donaldson K. *Size-dependent proinflammatory effects of ultrafine polystyrene particles: A role for surface area and oxidative stress in the enhanced activity of ultrafines*. Toxicology and Applied Pharmacology. 2001;175(3):191–9.

21. Beaumont NJ, Aanesen M, Austen MC, Börger T, Clark JR, Cole M, Hooper T, Lindeque PK, Pascoe C, Wyles KJ. *Global ecological, social and economic impacts of marine plastic*. Marine Pollution Bulletin. 2019;142(March):189–95.

22. Plastics Europe. *Plastics - The Facts 2019*.

23. Institute for Bioplastics and Biocomposites. *Biopolymers - Facts and Statistics 2019*.

24. Lee SY. *Bacterial Polyhydroxyalkanoates*. Biotechnology and Bioengineering. 1996;49:1–14.

25. Martin O, Avérous L. *Poly(lactic acid): Plasticization and properties of biodegradable multiphase systems*. Polymer. 2001;42(14):6209–19.

26. Liu H, Xie F, Yu L, Chen L, Li L. *Thermal processing of starch-based polymers*. Progress in Polymer Science (Oxford). 2009;34(12):1348–68.

27. Xu J, Guo BH. *Poly(butylene succinate) and its copolymers: Research, development and industrialization*. Biotechnology Journal. 2010;5(11):1149–63.

28. Siegenthaler KO, Kunkel A, Skupin G, Yamamoto M. *Ecoflex and Ecovio: Biodegradable, Performance-Enabling Plastics*. Advances in

Polymer Science. 2011;245:91–136.

29. Chen T, Cai T, Jin Q, Ji J. *Design and fabrication of functional polycaprolactone*. E-Polymers. 2015;15(1):3–13.

30. Andreeßen C, Steinbüchel A. *Recent developments in non-biodegradable biopolymers: Precursors, production processes, and future perspectives*. Applied Microbiology and Biotechnology. 2019;103(1):143–57.

31. Luzi F, Torre L, Kenny JM, Puglia D. *Bio- and fossil-based polymeric blends and nanocomposites for packaging: Structure-property relationship*. Materials. 2019;12(3).

32. Institute for Bioplastics and Biocomposites. *Biopolymers - Facts and Statistics 2016*.

33. Volanti M, Cespi D, Passarini F, Neri E, Cavani F, Mizsey P, Fozer D. *Terephthalic acid from renewable sources: Early-stage sustainability analysis of a bio-PET precursor*. Green Chemistry. 2019;21(4):885–96.

34. Drumright RE, Gruber PR, Henton DE. *Polylactic Acid Technology*. Advanced Materials. 2000;12(23):1841–6.

35. Farah S, Anderson DG, Langer R. *Physical and mechanical properties of PLA, and their functions in widespread applications — A comprehensive review*. Advanced Drug Delivery Reviews. 2016;107:367–92.

36. Zhao X, Hu H, Wang X, Yu X, Zhou W, Peng S. *Super tough poly(lactic acid) blends: A comprehensive review*. RSC Advances. 2020;10(22):13316–68.

37. Lunt J. *Large-scale production, properties and commercial applications of polylactic acid polymers*. Polymer Degradation and Stability. 1998;59:145–52.

38. Khan B, Bilal Khan Niazi M, Samin G, Jahan Z. *Thermoplastic Starch: A Possible Biodegradable Food Packaging Material—A Review*. Journal of Food Process Engineering. 2017;40(3).

39. Narancic T, Cerrone F, Beagan N, O'Connor KE. *Recent advances in bioplastics: Application and biodegradation*. Polymers. 2020;12(4).

40. Jiang T, Duan Q, Zhu J, Liu H, Yu L. *Starch-based biodegradable materials: Challenges and opportunities*. Advanced Industrial and Engineering Polymer Research. 2020;3(1):8–18.

41. Choi SY, Rhie MN, Kim HT, Joo JC, Cho IJ, Son J, Jo SY, Sohn YJ, Baritugo KA, Pyo J, Lee Y, Lee SY, Park SJ. *Metabolic engineering for the synthesis of polyesters: A 100-year journey from polyhydroxyalkanoates to non-natural microbial polyesters*. Metabolic Engineering. 2020;58(May 2019):47–81.

42. Choi J, Lee SY. *Factors affecting the economics of polyhydroxyalkanoate production by bacterial fermentation*. Applied Microbiology and Biotechnology. 1999;51(1):13–21.

43. Rajagopal D, Sexton SE, Roland-Holst D, Zilberman D. *Challenge of biofuel: Filling the tank without emptying the stomach?* Environmental Research Letters. 2007;2(4).

44. Lemoigne M. *Produits de Deshydration et de Polymerisation de L'acide β-Oxybutyrique*. Bull Soc Chim Biol. 1926;8:770–82.

45. Williamson DH, Wilkinson JF. *The isolation and estimation of the poly-beta-hydroxybutyrate inclusions of Bacillus species.* Journal of general microbiology. 1958;19(1):198–209.

46. Chowdhury AA. *Poly-β-hydroxybuttersäure abbauende Bakterien und Exoenzym*. Archiv für Mikrobiologie. 1963;47(2):167–200.

47. Baptist J, Werber L. *United States Patent Office*. US Patent Office. 3, 044, 942, 1962.

48. Baptist J, Werber L, Werber F. *United States Patent Office*. US Patent Office. 3, 107, 172, 1963.

49. Holmes PA. *Applications of PHB - A microbially produced biodegradable thermoplastic*. Physics in Technology. 1985;16(1):32–6.

50. Kunioka M, Doi Y. *Thermal Degradation of Microbial Copolyesters: Poly(3-hydroxybutyrate-co-3-hydroxyvalerate) and Poly(3-hydroxybutyrate-co-4-hydroxybutyrate)*. Macromolecules. 1990;23(7):1933–6.

51. Shimamura E, Scandola M, Doi Y. *Microbial Synthesis and Characterization of Poly(3-hydroxybutyrate-co-3-hydroxypropionate)*. Macromolecules. 1994;27(16):4429–35.

52. Carraher Jr. CE. *Seymour/Carraher's Polymer Chemistry*. Seymour/Carraher's Polymer Chemistry. 2007.

53. de Koning GJM, Lemstra PJ. *Crystallization phenomena in bacterial poly[(R)-3-hydroxybutyrate]: 2. Embrittlement and rejuvenation*. Polymer. 1993;34(19):4089–94.

54. Koller M, Gasser I, Schmid F, Berg G. *Linking ecology with economy: Insights into polyhydroxyalkanoate-producing microorganisms*. Engineering in Life Sciences. 2011;11(3):222–37.

55. Chanprateep S. *Current trends in biodegradable polyhydroxyalkanoates*. Journal of Bioscience and Bioengineering. 2010;110(6):621–32.

56. Shahhosseini S. *Simulation and optimisation of PHB production in fed-batch culture of Ralstonia eutropha*. Process Biochemistry.

2004;39(8):963–9.

57. Sichwart S, Hetzler S, Bröker D, Steinbüchel A. *Extension of the substrate utilization range of Ralstonia eutropha strain H16 by metabolic engineering to include mannose and glucose*. Applied and Environmental Microbiology. 2011;77(4):1325–34.

58. Ishizaki A, Tanaka K, Taga N. *Microbial production of poly-D-3-hydroxybutyrate from CO2x*. Applied Microbiology and Biotechnology. 2001;57(1–2):6–12.

59. Heinrich D, Raberg M, Steinbüchel A. *Studies on the aerobic utilization of synthesis gas (syngas) by wild type and recombinant strains of Ralstonia eutropha H16*. Microbial Biotechnology. 2018;11(4):647–56.

60. Cruz M V, Paiva A, Lisboa P, Freitas F, Alves VD, Simões P, Barreiros S, Reis MAM. *Bioresource Technology Production of polyhydroxyalkanoates from spent coffee grounds oil obtained by supercritical fluid extraction technology*. 2014;157:360–3.

61. Lee SY, Wong HH, Choi J Il, Lee SH, Lee SC, Han CS. *Production of medium-chain-length polyhydroxyalkanoates by high-cell- density cultivation Pseudomonas putida under phosphorus limitation*. Biotechnology and Bioengineering. 2000;68(4):466–70.

62. Timm A, Steinbuchel A. *Formation of polyesters consisting of medium-chain-length 3-hydroxyalkanoic acids from gluconate by Pseudomonas aeruginosa and other fluorescent pseudomonads*. Applied and Environmental Microbiology. 1990;56(11):3360–7.

63. Kanjanachumpol P, Kulpreecha S, Tolieng V, Thongchul N. *Enhancing polyhydroxybutyrate production from high cell density fed-batch fermentation of Bacillus megaterium BA-019*. Bioprocess and Biosystems Engineering. 2013;36(10):1463–74.

64. Wang F, Lee SY. *Poly(3-hydroxybutyrate) production with high productivity and high polymer content by a fed-batch culture of Alcaligenes latus under nitrogen limitation*. Applied and Environmental Microbiology. 1997;63(9):3703–6.

65. Garcia Lillo J, Rodriguez-Valera F. *Effects of culture conditions on poly(β-hydroxybutyrate acid) production by Haloferax mediterranei*. Applied and Environmental Microbiology. 1990;56(8):2517–21.

66. Doronina N V., Ezhov VA, Trotsenko IA. *Growth of Methylosinus trichosporium OB3b on methane and poly-beta-hydroxybutyrate biosynthesis*. Prikladnaia biokhimiia i mikrobiologiia. 2008;44(2):202–6.

67. Pieja AJ, Sundstrom ER, Criddle CS. *Poly-3-hydroxybutyrate metabolism in the type II Methanotroph Methylocystis parvus OBBP*. Applied and Environmental Microbiology. 2011;77(17):6012–9.

68. Zúñiga C, Morales M, Le Borgne S, Revah S. *Production of poly-β-hydroxybutyrate (PHB) by Methylobacterium organophilum isolated from a methanotrophic consortium in a two-phase partition bioreactor*. Journal of Hazardous Materials. 2011;190(1–3):876–82.

69. Rumah BL, Stead CE, Claxton Stevens BH, Minton NP, Grosse-Honebrink A, Zhang Y. *Isolation and characterisation of Methylocystis spp. for poly-3-hydroxybutyrate production using waste methane feedstocks*. AMB Express. 2021;11(1).

70. Karmann S, Panke S, Zinn M. *Fed-batch cultivations of rhodospirillum rubrum under multiple nutrient-limited growth conditions on syngas as a novel option to produce poly(3-hydroxybutyrate) (PHB)*. Frontiers in Bioengineering and Biotechnology. 2019;7(APR):1–11.

71. Page WJ. *Production of polyhydroxyalkanoates by Azotobacter vinelandii UWD in beet molasses culture*. FEMS Microbiology Letters. 1992;103(2–4):149–57.

72. Miyake M, Erata M, Asada Y. *A thermophilic cyanobacterium, Synechococcus sp. MA19, capable of accumulating poly-β-hydroxybutyrate*. Journal of Fermentation and Bioengineering. 1996;82(5):512–4.

73. Cesário MT, Raposo RS, de Almeida MCMD, van Keulen F, Ferreira BS, da Fonseca MMR. *Enhanced bioproduction of poly-3-hydroxybutyrate from wheat straw lignocellulosic hydrolysates*. New Biotechnology. 2014;31(1):104–13.

74. Shimamura E, Kasuya KI. *Physical Properties and Biodegradability of Microbial Poly(3-hydroxybutyrate-co-3-hydroxyhexanoate)*. Biomacromolecules. 1994;27:878–80.

75. Lee SH, Oh DH, Ahn WS, Lee Y, Choi J, Lee SY. *Production of Poly (3-Hydroxybutyrate- co-3-Hydroxyhexanoate) by High-Cell-Density Cultivation of Aeromonas hydrophila*. Biotechnology and Bioengineering. 2000;67(2):240–4.

76. Bhubalan K, Kam YC, Yong KH, Sudesh K. *Cloning and expression of the PHA synthase gene from a locally isolated Chromobacterium sp. USM2*. Malaysian Journal of Microbiology. 2010;6(1):81–90.

77. Fukui T, Yoshimoto A, Matsumoto M, Hosokawa S, Saito T, Nishikawa H, Tomita K. *Enzymatic Synthesis of Poly-β-Hydroxybutyrate in Zoogloea ramigera*. Archives of Biochemistry and Biophysics. 1976;110:149–56.

78. Monshupanee T, Nimdach P, Incharoensakdi A. *Two-stage (photoautotrophy and heterotrophy) cultivation enables efficient production of bioplastic poly-3-hydroxybutyrate in auto-sedimenting cyanobacterium*. Scientific Reports. 2016;6(November):1–9. Available from: http://dx.doi.org/10.1038/srep37121

79. Panda B, Jain P, Sharma L, Mallick N. *Optimization of cultural and nutritional conditions for accumulation of poly-β-hydroxybutyrate in Synechocystis sp. PCC 6803*. Bioresource Technology. 2006;97(11):1296–301.

80. Khatipov E, Miyake M, Miyake J, Asada Y. *Accumulation of poly-β-hydroxybutyrate by Rhodobacter sphaeroides on various carbon and nitrogen substrates*. FEMS Microbiology Letters. 1998;162(1):39–45.

81. Sharma L, Mallick N. *Accumulation of poly-β-hydroxybutyrate in Nostoc muscorum: Regulation by pH, light-dark cycles, N and P status and carbon sources*. Bioresource Technology. 2005;96(11):1304–10.

82. Peoples OP, Sinskey AJ. *Poly-β-hydroxybutyrate (PHB) biosynthesis in Alcaligenes eutrophus H16. Identification and characterization of the PHB polymerase gene (phbC)*. Journal of Biological Chemistry. 1989;264(26):15298–303.

83. Rehm BHA. *Polyester synthases: Natural catalysts for plastics*. Biochemical Journal. 2003;376(1):15–33.

84. Wang Y, Yamada S, Asakawa N, Yamane T, Yoshie N, Inoue Y. *Comonomer compositional distribution and thermal and morphological characteristics of bacterial poly(3-hydroxybutyrate-co-3-hydroxyvalerate)s with high 3-hydroxyvalerate content*. Biomacromolecules. 2001;2(4):1315–23.

85. Kunioka M, Tamaki A, Doi Y. *Crystalline and Thermal Properties of Bacterial Copolyesters: Poly(3-hydroxybutyrate-co-3-hydroxyvalerate) and Poly(3-hydroxybutyrate-co-4-hydroxybutyrate)*. Macromolecules. 1989;22(2):694–7.

86. Wong YM, Brigham CJ, Rha CK, Sinskey AJ, Sudesh K. *Biosynthesis and characterization of polyhydroxyalkanoate containing high 3-hydroxyhexanoate monomer fraction from crude palm kernel oil by recombinant Cupriavidus necator*. Bioresource Technology. 2012;121:320–7.

87. Meng DC, Shi ZY, Wu LP, Zhou Q, Wu Q, Chen JC, Chen GQ. *Production and characterization of poly(3-hydroxypropionate-co-4-hydroxybutyrate) with fully controllable structures by recombinant Escherichia coli containing an engineered pathway*. Metabolic Engineering. 2012;14(4):317–24.

88. Steinbüchel A. *Perspectives for Biotechnological Production and Utilization of Biopolymers: Metabolic Engineering of Polyhydroxyalkanoate Biosynthesis Pathways as a Successful Example*. Macromolecular Bioscience. 2001;1(1):1–24.

89. Reddy CSK, Ghai R, Kalia VC. *Polyhydroxyalkanoates : an overview*. Bioresource Technology. 2003;87:137–46.

90. Muhammadi, Shabina, Afzal M, Hameed S. *Bacterial polyhydroxyalkanoates-eco-friendly next generation plastic: Production, biocompatibility, biodegradation, physical properties and applications*. Green Chemistry Letters and Reviews. 2015;8(3–4):56–77.

91. Nakamura S, Kunioka M, Doi Y. *Biosynthesis and characterization of bacterial poly(3-hydroxybutyrate-co-3-hydroxypropionate)*. Journal of Macromolecular Science: Part A - Chemistry. 1991;28(1):15–24.

92. Xie CH, Yokota A. *Reclassification of Alcaligenes latus strains IAM 12599T and IAM 12664 and Pseudomonas saccharophila as Azohydromonas lata gen. nov. comb. nov., Azohydromonas australica sp. nov. and Pelomonas saccharophila gen. nov., comb. nov., respectively*. International Journal of Systematic and Evolutionary Microbiology. 2005;55(6):2419–25.

93. Hiramitsu M, Doi Y. *Microbial synthesis and characterization of poly(3-hydroxybutyrate-co-3-hydroxypropionate)*. Polymer. 1993;34(22):4782–6.

94. Ichikawa M, Nakamura K, Yoshie N, Asakawa N, Inoue Y, Doi Y. *Morphological study of bacterial poly(3-hydroxybutyrate-co-3-hydroxypropionate)*. Macromolecular Chemistry and Physics. 1996;197(8):2467–80.

95. Cao A, Ichikawa M, Kasuya KI, Yoshie N, Asakawa N, Inoue Y, Doi Y, Abe H. *Composition fractionation and thermal characterization of poly(3-hydroxybutyrate-co-3-hydroxypropionate)*. Polymer Journal. 1996;28(12):1096–102.

96. Cao A, Ichikawa M, Ikejima T, Yoshie N, Inoue Y. *Thermal and morphological study of fractionated poly(3-hydroxybutyric acid-co-3-hydroxypropionic acid)*. Macromolecular Chemistry and Physics. 1997;198(11):3539–57.

97. Cao A, Kasuya KI, Abe H, Doi Y, Inoue Y. *Studies on comonomer compositional distribution of the bacterial poly(3-hydroxybutyric acid-co-3-hydroxypropionic acid)s and crystal and thermal characteristics of their fractionated component copolyesters*. Polymer. 1998;39(20):4801–16.

98. Arai Y, Cao A, Yoshie N, Inoue Y. *Studies on comonomer compositional distribution and its effect on some physical properties of bacterial poly(3-hydroxybutyric acid-co-3-hydroxypropionic acid)*. Polymer International. 1999;48(12):1219–28.

99. Na Y-H, He Y, Asakawa N, Yoshie N, Inoue Y. *Miscibility and Phase Structure of Blends of Poly(ethylene oxide) with Poly(3-hydroxybutyrate), Poly(3-hydroxypropionate), and Their Copolymers*. Macromolecules. 2002;35(3):727–35.

100. Fukui T, Suzuki M, Tsuge T, Nakamura S. *Microbial synthesis of poly((R)-3-hydroxybutyrate-co- 3-hydroxypropionate) from unrelated carbon sources by engineered cupriavidus necator*. Biomacromolecules. 2009;10(4):700–6.

101. Wang Q, Yang P, Xian M, Yang Y, Liu C, Xue Y, Zhao G. *Biosynthesis of poly(3-hydroxypropionate-co-3-hydroxybutyrate) with fully controllable structures from glycerol*. Bioresource Technology. 2013;142:741–4.

102. Cao A, Arai Y, Yoshie N, Kasuya KI, Doi Y, Inoue Y. *Solid structure and biodegradation of the compositionally fractionated poly(3-hydroxybutyric acid-co-3-hydroxypropionic acid)s*. Polymer. 1999;40(24):6821–30.

103. Nishida H, Suzuki S, Tokiwa Y. *Distribution of poly(β-propiolactone) aerobic degrading microorganisms in different environments*. Journal of Environmental Polymer Degradation. 1998;6(1):43–58.

104. Kasuya KI, Ohura T, Masuda K, Doi Y. *Substrate and binding specificities of bacterial polyhydroxybutyrate depolymerases*. International Journal of Biological Macromolecules. 1999;24(4):329–36.

105. Nishida H, Suzuki S, Konno M, Tokiwa Y. *Microbial utilization of poly(β-propiolactone) by sewage sludge and isolated strains*. Polymer Degradation and Stability. 2000;67(2):291–7.

106. Andreeßen B, Lange AB, Robenek H, Steinbüchel A. *Conversion of glycerol to poly(3-hydroxypropionate) in recombinant escherichia coli*. Applied and Environmental Microbiology. 2010;76(2):622–6.

107. Zhou Q, Shi ZY, Meng DC, Wu Q, Chen JC, Chen GQ. *Production of 3-hydroxypropionate homopolymer and poly(3-hydroxypropionate-co-4-hydroxybutyrate) copolymer by recombinant Escherichia coli*. Metabolic Engineering. 2011;13(6):777–85.

108. Wang Q, Liu C, Xian M, Zhang Y, Zhao G. *Biosynthetic pathway for poly(3-Hydroxypropionate) in recombinant Escherichia coli*. Journal of Microbiology. 2012;50(4):693–7.

109. Wang Q, Yang P, Liu C, Xue Y, Xian M, Zhao G. *Biosynthesis of poly(3-hydroxypropionate) from glycerol by recombinant Escherichia coli*. Bioresource Technology. 2013;131:548–51.

110. Heinrich D, Andreessen B, Madkour MH, Al-Ghamdi MA, Shabbaj II, Steinbüchel A. *From waste to plastic: Synthesis of poly(3-hydroxypropionate) in: Shimwellia blattae*. Applied and Environmental Microbiology. 2013;79(12):3582–9.

111. Andreeßen B, Johanningmeier B, Burbank J, Steinbüchel A. *Influence of the operon structure on poly(3-hydroxypropionate)*

synthesis in Shimwellia blattae. Applied Microbiology and Biotechnology. 2014;98(17):7409–22.

112. Gao Y, Liu C, Ding Y, Sun C, Zhang R, Xian M, Zhao G. *Development of genetically stable Escherichia coli strains for poly(3-hydroxypropionate) production*. PLoS ONE. 2014;9(5):1–9.

113. Wang Q, Yang P, Xian M, Feng L, Wang J, Zhao G. *Metabolic engineering of escherichia coli for poly(3-hydroxypropionate) production from glycerol and glucose*. Biotechnology Letters. 2014;36(11):2257–62.

114. Linares-Pastén JA, Sabet-Azad R, Pessina L, Sardari RRR, Ibrahim MHA, Hatti-Kaul R. *Efficient poly(3-hydroxypropionate) production from glycerol using Lactobacillus reuteri and recombinant Escherichia coli harboring L. reuteri propionaldehyde dehydrogenase and Chromobacterium sp. PHA synthase genes*. Bioresource Technology. 2015;180:172–6.

115. Feng X, Xian M, Liu W, Xu C, Zhang H, Zhao G. *Biosynthesis of poly(3-hydroxypropionate) from glycerol using engineered Klebsiella pneumoniae strain without vitamin B12*. Bioengineered. 2015;6(2):77–81.

116. Meng DC, Wang Y, Wu LP, Shen R, Chen JC, Wu Q, Chen GQ. *Production of poly(3-hydroxypropionate) and poly(3-hydroxybutyrate-co-3-hydroxypropionate) from glucose by engineering Escherichia coli*. Metabolic Engineering. 2015;29:189–95.

117. Sato S, Andreeßen B, Steinbüchel A. *Strain and process development for poly(3HB-co-3HP) fermentation by engineered Shimwellia blattae from glycerol*. AMB Express. 2015;5(1).

118. Lacmata ST, Kuiate JR, Ding Y, Xian M, Liu H, Boudjeko T, Feng X, Zhao G. *Enhanced poly(3-hydroxypropionate) production via β-alanine pathway in recombinant Escherichia coli*. PLoS ONE. 2017;12(3):1–11.

119. Valentin HE, Mitsky TA, Mahadeo DA, Tran M, Gruys KJ. *Application of a propionyl coenzyme A synthetase for poly(3-hydroxypropionate-co-3-hydroxybutyrate) accumulation in recombinant Escherichia coli*. Applied and Environmental Microbiology. 2000;66(12):5253–8.

120. Leal NA, Havemann GD, Bobik TA. *PduP is a coenzyme-a-acylating propionaldehyde dehydrogenase associated with the polyhedral bodies involved in B12-dependent 1,2-propanediol degradation by Salmonella enterica serovar Typhimurium LT2*. Archives of Microbiology. 2003;180(5):353–61.

121. Sun J, Van Den Heuvel J, Soucaille P, Qu Y, Zeng AP. *Comparative genomic analysis of dha regulon and related genes for anaerobic*

glycerol metabolism in bacteria. Biotechnology Progress. 2003;19(2):263–72.

122. Tripathi L, Wu LP, Meng D, Chen J, Chen GQ. *Biosynthesis and characterization of diblock copolymer of P(3-hydroxypropionate)-block-P(4-hydroxybutyrate) from recombinant Escherichia coli*. Biomacromolecules. 2013;14(3):862–70.

123. Borodina I, Kildegaard KR, Jensen NB, Blicher TH, Maury J, Sherstyk S, Schneider K, Lamosa P, Herrgård MJ, Rosenstand I, Öberg F, Forster J, Nielsen J. *Establishing a synthetic pathway for high-level production of 3-hydroxypropionic acid in Saccharomyces cerevisiae via β-alanine*. Metabolic Engineering. 2015;27:57–64.

124. Vivek N, Pandey A, Binod P. *Production and Applications of 1,3-Propanediol*. In: Current Developments in Biotechnology and Bioengineering: Production, Isolation and Purification of Industrial Products. 2016. p. 719–38.

125. Pohlmann A, Fricke WF, Reinecke F, Kusian B, Liesegang H, Cramm R, Eitinger T, Ewering C, Pötter M, Schwartz E, Strittmatter A, Voß I, Gottschalk G, Steinbüchel A, Friedrich B, Bowien B. *Genome sequence of the bioplastic-producing "Knallgas" bacterium Ralstonia eutropha H16*. Nature Biotechnology. 2006;24(10):1257–62.

126. Aragno M, Schlegel HG. *The mesophilic hydrogen-oxidizing (Knallgas) bacteria*. In: The Prokaryotes. 1992. p. 344–84.

127. Cramm R. *Genomic view of energy metabolism in Ralstonia eutropha H16*. Journal of Molecular Microbiology and Biotechnology. 2008;16(1–2):38–52.

128. Schwartz E, Henne A, Cramm R, Eitinger T, Friedrich B, Gottschalk G. *Complete nucleotide sequence of pHG1: A Ralstonia eutropha H16 megaplasmid encoding key enzymes of H2-based lithoautotrophy and anaerobiosis*. Journal of Molecular Biology. 2003;332(2):369–83.

129. Raberg M, Volodina E, Lin K, Steinbüchel A. *Ralstonia eutropha H16 in progress: Applications beside PHAs and establishment as production platform by advanced genetic tools*. Critical Reviews in Biotechnology. 2018;38(4):494–510.

130. Schlegel HG, Gottschalk G, von Bartha R. *Formation and utilization of poly-β-hydroxybutyric acid by Knallgas bacteria (Hydrogenomonas)*. Nature. 1961;191:463–5.

131. Foster JF, Litchfield JH. *A Continuous Culture Apparatus for the Microbial Utilization of Hydrogen Produced by Electrolysis of Water in Closed-Cycle Space Systems*. Biotechnology and Bioengineering. 1964;6(4):441–56.

132. Ammann EC, Reed LL, Durichek JE. *Gas consumption and growth rate of Hydrogenomonas eutropha in continuous culture.* Applied microbiology. 1968;16(6):822–6.

133. Wixom RL, Sheng Y -B, Becker RS. *Utilization of organic nitrogen compounds by Hydrogenomonas eutropha*. Biotechnology and Bioengineering. 1972;14(6):985–1006.

134. Repaske R. *Characteristics of hydrogen bacteria*. Biotechnology and Bioengineering. 1966;8(2):217–35.

135. Repaske R, Repaske AC. *Quantitative requirements for exponential growth of Alcaligenes eutrophus*. Applied and Environmental Microbiology. 1976;32(4):585–91.

136. Repaske R, Mayer R. *Dense autotrophic cultures of Alcaligenes eutrophus*. Applied and Environmental Microbiology. 1976;32(4):592–7.

137. Schwartz E, Voigt B, Zühlke D, Pohlmann A, Lenz O, Albrecht D, Schwarze A, Kohlmann Y, Krause C, Hecker M, Friedrich B. *A proteomic view of the facultatively chemolithoautotrophic lifestyle of Ralstonia eutropha H16*. Proteomics. 2009;9(22):5132–42.

138. Fukui T, Mukoyama M, Orita I, Nakamura S. *Enhancement of glycerol utilization ability of Ralstonia eutropha H16 for production of polyhydroxyalkanoates*. Applied Microbiology and Biotechnology. 2014;98(17):7559–68.

139. González-Villanueva M, Galaiya H, Staniland P, Staniland J, Savill I, Wong TS, Tee KL. *Adaptive laboratory evolution of Cupriavidus necator H16 for carbon co-utilization with glycerol*. International Journal of Molecular Sciences. 2019;20(22):1–19.

140. Brigham CJ, Gai CS, Lu J, Speth DR, Worden RM, Sinskey AJ. *Engineering Ralstonia eutropha for Production of Isobutanol from CO2, H2, and O2*. In: Advanced Biofuels and Bioproducts. 2012. p. 1065–90.

141. Burgdorf T, Lenz O, Buhrke T, Van Der Linden E, Jones AK, Albracht SPJ, Friedrich B. *[NiFe]-hydrogenases of Ralstonia eutropha H16: Modular enzymes for oxygen-tolerant biological hydrogen oxidation*. Journal of Molecular Microbiology and Biotechnology. 2006;10(2–4):181–96.

142. Brigham CJ, Zhila N, Shishatskaya E, Volova TG, Sinskey AJ. *Manipulation of Ralstonia eutropha Carbon Storage Pathways to Produce Useful Bio-Based Products*. In: Reprogramming Microbial Metabolic Pathways. 2012. p. 343–66.

143. Chakravarty J, Brigham CJ. *Solvent production by engineered Ralstonia eutropha: channeling carbon to biofuel*. Applied Microbiology and Biotechnology. 2018;102(12):5021–31.

144. Bi C, Su P, Müller J, Yeh YC, Chhabra SR, Beller HR, Singer SW, Hillson NJ. *Development of a broad-host synthetic biology toolbox for ralstonia eutropha and its application to engineering hydrocarbon biofuel production*. Microbial Cell Factories. 2013;12(1):1–10.

145. Alagesan S, Hanko EKR, Malys N, Ehsaan M, Winzer K, Minton NP. *Functional genetic elements for controlling gene expression in Cupriavidus necator H16*. Applied and Environmental Microbiology. 2018;84(19):1–17.

146. Johnson AO, Gonzalez-Villanueva M, Tee KL, Wong TS. *An Engineered Constitutive Promoter Set with Broad Activity Range for Cupriavidus necator H16*. ACS Synthetic Biology. 2018;7(8):1918–28.

147. Krieg T, Sydow A, Faust S, Huth I, Holtmann D. *CO 2 to Terpenes: Autotrophic and Electroautotrophic α-Humulene Production with Cupriavidus necator*. Angewandte Chemie - International Edition. 2018;57(7):1879–82.

148. Garrigues L, Maignien L, Lombard E, Singh J, Guillouet SE. *Isopropanol production from carbon dioxide in Cupriavidus necator in a pressurized bioreactor*. New Biotechnology. 2020;56:16–20.

149. Volova TG, Kalacheva GS, Steinbüchel A. *Biosynthesis of multi-component polyhydroxyalkanoates by the bacterium Wautersia eutropha*. Macromolecular Symposia. 2008;269(1):1–7.

150. Aboulmagd E, Voss I, Oppermann-Sanio F, Steinbüchel A. *Heterologous Expression of Cyanophycin Synthetase and Cyanophycin Synthesis in the Industrial Relevant Bacteria Corynebacterium glutamicum and Ralstonia eutropha and in Pseudomonas putida*. Biomacromolecules. 2001;1338–42.

151. Voss I, Diniz SC, Aboulmagd E, Steinbüchel A. *Identification of the Anabaena sp. strain PCC7120 cyanophycin synthetase as suitable enzyme for production of cyanophycin in gram-negative bacteria like Pseudomonas putida and Ralstonia eutropha*. Biomacromolecules. 2004;5(4):1588–95.

152. Voss I, Steinbüchel A. *Application of a KDPG-aldolase gene-dependent addiction system for enhanced production of cyanophycin in Ralstonia eutropha strain H16*. Metabolic Engineering. 2006;8(1):66–78.

153. Diniz SC, Voss I, Steinbüchel A. *Optimization of Cyanophycin Production in Recombinant Strains of Pseudomonas putida and Ralstonia eutropha Employing Elementary Mode Analysis and Statistical Experimental Design*. Biotechnology and Bioengineering. 2006;93(4):698–717.

154. Schwamborn M. *Chemical synthesis of polyaspartates: A*

biodegradable alternative to currently used polycarboxylate homo- and copolymers. Polymer Degradation and Stability. 1998;

155. Przybylski D, Rohwerder T, Harms H, Yaneva N, Müller RH. *Synthesis of the building block 2-hydroxyisobutyrate from fructose and butyrate by Cupriavidus necator H16*. Applied Microbiology and Biotechnology. 2013;97(20):8875–85.

156. Przybylski D, Rohwerder T, Dilßner C, Maskow T, Harms H, Müller RH. *Exploiting mixtures of H2, CO2, and O2 for improved production of methacrylate precursor 2-hydroxyisobutyric acid by engineered Cupriavidus necator strains*. Applied Microbiology and Biotechnology. 2015;99(5):2131–45.

157. Xiong M, Schneiderman DK, Bates FS, Hillmyer MA, Zhang K. *Scalable production of mechanically tunable block polymers from sugar*. Proceedings of the National Academy of Sciences of the United States of America. 2014;111(23):8357–62.

158. Zhang C, Schneiderman DK, Cai T, Tai YS, Fox K, Zhang K. *Optically Active β-Methyl-δ-Valerolactone: Biosynthesis and Polymerization*. ACS Sustainable Chemistry and Engineering. 2016;4(8):4396–402.

159. Dalwadi MP, Garavaglia M, Webb JP, King JR, Minton NP. *Applying asymptotic methods to synthetic biology: Modelling the reaction kinetics of the mevalonate pathway*. Journal of Theoretical Biology. 2018;439:39–49.

160. Lu J, Brigham CJ, Gai CS, Sinskey AJ. *Studies on the production of branched-chain alcohols in engineered Ralstonia eutropha*. Applied Microbiology and Biotechnology. 2012;96(1):283–97.

161. Chen JS, Colón B, Dusel B, Ziesack M, Way JC, Torella JP. *Production of fatty acids in Ralstonia eutropha H16 by engineering β-oxidation and carbon storage*. PeerJ. 2015;2015(12):1–18.

162. Lim HN, Lee Y, Hussein R. *Fundamental relationship between operon organization and gene expression*. Proceedings of the National Academy of Sciences of the United States of America. 2011;108(26):10626–31.

163. van Summeren-Wesenhagen P V., Voges R, Dennig A, Sokolowsky S, Noack S, Schwaneberg U, Marienhagen J. *Combinatorial optimization of synthetic operons for the microbial production of p-coumaryl alcohol with Escherichia coli*. Microbial Cell Factories. 2015;14(1):1–10.

164. Kroll J, Klinter S, Schneider C, Voß I, Steinbüchel A. *Plasmid addiction systems: Perspectives and applications in biotechnology*. Microbial Biotechnology. 2010;3(6):634–57.

165. Hägg P, De Pohl JW, Abdulkarim F, Isaksson LA. *A host/plasmid*

system that is not dependent on antibiotics and antibiotic resistance genes for stable plasmid maintenance in Escherichia coli. Journal of Biotechnology. 2004;111(1):17–30.

166. Shaw AJ, Lam FH, Hamilton M, Consiglio A, MacEwen K, Brevnova EE, Greenhagen E, LaTouf WG, South CR, Van Dijken H, Stephanopoulos G. *Metabolic engineering of microbial competitive advantage for industrial fermentation processes*. Science. 2016;353(6299):583–6.

167. Zabriskie DW, Arcuri EJ. *Factors influencing productivity of fermentations employing recombinant microorganisms*. Enzyme and Microbial Technology. 1986;8(12):706–17.

168. Van Melderen L, De Bast MS. *Bacterial toxin-Antitoxin systems: More than selfish entities?* PLoS Genetics. 2009;5(3).

169. Steinle A, Witthoff S, Krause JP, Steinbüchel A. *Establishment of cyanophycin biosynthesis in Pichia pastoris and optimization by use of engineered cyanophycin synthetases*. Applied and Environmental Microbiology. 2010;76(4):1062–70.

170. Budde CF, Riedel SL, Willis LB, Rha CK, Sinskey AJ. *Production of poly(3-hydroxybutyrate-co-3-hydroxyhexanoate) from plant oil by engineered Ralstonia eutropha strains*. Applied and Environmental Microbiology. 2011;77(9):2847–54.

171. Riedel SL, Bader J, Brigham CJ, Budde CF, Yusof ZAM, Rha C, Sinskey AJ. *Production of poly(3-hydroxybutyrate-co-3-hydroxyhexanoate) by Ralstonia eutropha in high cell density palm oil fermentations*. Biotechnology and Bioengineering. 2012;109(1):74–83.

172. Ren Y, Ling C, Hajnal I, Wu Q, Chen GQ. *Construction of Halomonas bluephagenesis capable of high cell density growth for efficient PHA production*. Applied Microbiology and Biotechnology. 2018;102(10):4499–510.

173. Arenas-López C, Locker J, Orol D, Walter F, Busche T, Kalinowski J, Minton NP, Kovács K, Winzer K. *The genetic basis of 3-hydroxypropanoate metabolism in Cupriavidus necator H16*. Biotechnology for Biofuels. 2019;12(1).

174. Bommareddy RR, Wang Y, Pearcy N, Hayes M, Lester E, Minton NP, Conradie A V. *A Sustainable Chemicals Manufacturing Paradigm Using CO2 and Renewable H2*. iScience. 2020;23(6):101218.

175. Song CW, Kim JW, Cho IJ, Lee SY. *Metabolic Engineering of Escherichia coli for the Production of 3-Hydroxypropionic Acid and Malonic Acid through β-Alanine Route*. ACS Synthetic Biology. 2016;5(11):1256–63.

176. Song CW, Lee J, Ko YS, Lee SY. *Metabolic engineering of Escherichia coli for the production of 3-aminopropionic acid*. Metabolic Engineering. 2015;30:121–9.

177. Yuan W, Jia Y, Tian J, Snell KD, Müh U, Sinskey AJ, Lambalot RH, Walsh CT, Stubbe JA. *Class I and III polyhydroxyalkanoate synthases from Ralstonia eutropha and Allochromatium vinosum: Characterization and substrate specificity studies*. Archives of Biochemistry and Biophysics. 2001;394(1):87–98.

178. Liu X-W, Wang H-H, Chen J-Y, Li X-T, Chen G-Q. *Biosynthesis of poly(3-hydroxybutyrate-co-3-hydroxyvalerate) by recombinant Escherichia coli harboring propionyl-CoA synthase gene (prpE) or propionate permease gene (prpP)*. Biochemical Engineering Journal. 2009;43(1):72–7.

179. Park SJ, Kang K-H, Lee H, Park A-R, Yang JE, Oh YH, Song BK, Jegal J, Lee SH, Lee SY. *Propionyl-CoA dependent biosynthesis of 2-hydroxybutyrate containing polyhydroxyalkanoates in metabolically engineered Escherichia coli*. Journal of Biotechnology. 2013;165(2):93–8.

180. Yang JE, Choi YJ, Lee SJ, Kang K-H, Lee H, Oh YH, Lee SH, Park SJ, Lee SY. *Metabolic engineering of Escherichia coli for biosynthesis of poly(3-hydroxybutyrate-co-3-hydroxyvalerate) from glucose*. Applied Microbiology and Biotechnology. 2014;98(1):95–104.

181. Zhuang Q, Qi Q. *Engineering the pathway in Escherichia coli for the synthesis of medium-chain-length polyhydroxyalkanoates consisting of both even- and odd-chain monomers*. Microbial Cell Factories. 2019;18(1):135.

182. Horswill AR, Escalante-Semerena JC. *Characterization of the Propionyl-CoA Synthetase (PrpE) Enzyme of Salmonella enterica: Residue Lys592 Is Required for Propionyl-AMP Synthesis*. Biochemistry. 2002;41(7):2379–87.

183. Lindenkamp N, Schürmann M, Steinbüchel A. *A propionate CoA-transferase of Ralstonia eutropha H16 with broad substrate specificity catalyzing the CoA thioester formation of various carboxylic acids*. Applied Microbiology and Biotechnology. 2013;97(17):7699–709.

184. Volodina E, Schürmann M, Lindenkamp N, Steinbüchel A. *Characterization of propionate CoA-transferase from Ralstonia eutropha H16*. Applied Microbiology and Biotechnology. 2014;98(8):3579–89.

185. Strauss E. *Coenzyme A biosynthesis and enzymology*. Comprehensive Natural Products II: Chemistry and Biology. 2010;7:351–410.

186. Yang JE, Choi YJ, Lee SJ, Kang KH, Lee H, Oh YH, Lee SH, Park

SJ, Lee SY. *Metabolic engineering of Escherichia coli for biosynthesis of poly(3-hydroxybutyrate-co-3-hydroxyvalerate) from glucose*. Applied Microbiology and Biotechnology. 2014;98(1):95–104.

187. Jeon JM, Kim HJ, Bhatia SK, Sung C, Seo HM, Kim JH, Park HY, Lee D, Brigham CJ, Yang YH. *Application of acetyl-CoA acetyltransferase (AtoAD) in Escherichia coli to increase 3-hydroxyvalerate fraction in poly(3-hydroxybutyrate-co-3-hydroxyvalerate)*. Bioprocess and Biosystems Engineering. 2017;40(5):781–9.

188. Sramek SJ, Frerman FE. *Escherichia coli coenzyme A-transferase: Kinetics, catalytic pathway and structure*. Archives of Biochemistry and Biophysics. 1975;171(1):27–35.

189. Liu S-J, Steinbüchel A. *Exploitation of butyrate kinase and phosphotransbutyrylase from Clostridium acetobutylicum for the in vitro biosynthesis of poly(hydroxyalkanoic acid)*. Applied Microbiology and Biotechnology. 2000;53(5):545–52.

190. Martin CH, Dhamankar H, Tseng HC, Sheppard MJ, Reisch CR, Prather KLJ. *A platform pathway for production of 3-hydroxyacids provides a biosynthetic route to 3-hydroxy-γ-butyrolactone*. Nature Communications. 2013;4:1–10.

191. Gao H-J, Wu Q, Chen G-Q. *Enhanced production of d-(−)-3-hydroxybutyric acid by recombinant Escherichia coli*. FEMS Microbiology Letters. 2002;213(1):59–65.

192. Tseng H-C, Martin CH, Nielsen DR, Prather KLJ. *Metabolic Engineering of Escherichia coli for Enhanced Production of (R)- and (S)-3-Hydroxybutyrate*. Applied and Environmental Microbiology. 2009;75(10):3137 LP – 3145.

193. Hiroe A, Tsuge K, Nomura CT, Itaya M, Tsuge T. *Rearrangement of gene order in the phaCAB operon leads to effective production of ultrahigh-molecular-weight poly[(R)-3-hydroxybutyrate] in genetically engineered Escherichia coli*. Applied and Environmental Microbiology. 2012;78(9):3177–84.

194. Arikawa H, Matsumoto K. *Evaluation of gene expression cassettes and production of poly(3-hydroxybutyrate-co-3-hydroxyhexanoate) with a fine modulated monomer composition by using it in Cupriavidus necator*. Microbial cell factories. 2016;15(1):184.

195. Selmer T, Willanzheimer A, Hetzel M. *Propionate CoA-transferase from Clostridium propionicum*. European Journal of Biochemistry. 2002;269(1):372–80.

196. Song JJ, Zhang S, Lenz RW, Goodwin S. *In vitro polymerization and copolymerization of 3-hydroxypropionyl-CoA with the PHB synthase from Ralstonia eutropha*. Biomacromolecules. 2000;1(3):433–9.

197. Bhubalan K, Chuah JA, Shozui F, Brigham CJ, Taguchi S, Sinskey AJ, Rha CK, Sudesh K. *Characterization of the highly active polyhydroxyalkanoate synthase of Chromobacterium sp. strain USM2*. Applied and Environmental Microbiology. 2011;77(9):2926–33.

198. Chen H, Bjerknes M, Kumar R, Jay E. *Determination of the optimal aligned spacing between the shine - dalgarno sequence and the translation initiation codon of escherichia coli m RNAs*. Nucleic Acids Research. 1994;22(23):4953–7.

199. Ringquist S, Shinedling S, Barrick D, Green L, Binkley J, Stormo GD, Gold L. *Translation initiation in Escherichia coli: sequences within the ribosome-binding site*. Molecular Microbiology. 1992;6(9):1219–29.

200. Bhubalan K, Rathi DN, Abe H, Iwata T, Sudesh K. *Improved synthesis of P(3HB-co-3HV-co-3HHx) terpolymers by mutant Cupriavidus necator using the PHA synthase gene of Chromobacterium sp. USM2 with high affinity towards 3HV*. Polymer Degradation and Stability. 2010;95(8):1436–42.

201. Ohtake T, Pontrelli S, Laviña WA, Liao JC, Putri SP, Fukusaki E. *Metabolomics-driven approach to solving a CoA imbalance for improved 1-butanol production in Escherichia coli*. Metabolic Engineering. 2017;41(April):135–43.

202. Heinrich D, Raberg M, Steinbüchel A. *Synthesis of poly(3-hydroxybutyrate-co-3-hydroxyvalerate) from unrelated carbon sources in engineered Rhodospirillum rubrum*. FEMS Microbiology Letters. 2015;362(8):1–9.

203. Vadali R V., Bennett GN, San KY. *Cofactor engineering of intracellular CoA/acetyl-CoA and its effect on metabolic flux redistribution in Escherichia coli*. Metabolic Engineering. 2004;6(2):133–9.

204. Vadali R V., Bennett GN, San KY. *Enhanced isoamyl acetate production upon manipulation of the acetyl-CoA node in Escherichia coli*. Biotechnology Progress. 2004;20(3):692–7.

205. Leonardi R, Zhang YM, Rock CO, Jackowski S. *Coenzyme A: Back in action*. Progress in Lipid Research. 2005;44(2–3):125–53.

206. Lindenkamp N, Peplinski K, Volodina E, Ehrenreich A, Steinbüchel A. *Impact of multiple β-ketothiolase deletion mutations in ralstonia eutropha H16 on the composition of 3-mercaptopropionic acid-containing copolymers*. Applied and Environmental Microbiology. 2010;76(16):5373–82.

207. Lindenkamp N, Volodina E, Steinbüchel A. *Genetically modified strains of Ralstonia eutropha H16 with β- ketothiolase gene deletions for production of copolyesters with defined 3-hydroxyvaleric acid*

contents. Applied and Environmental Microbiology. 2012;78(15):5375–83.

208. Sato S, Maruyama H, Fujiki T, Matsumoto K. *Regulation of 3-hydroxyhexanoate composition in PHBH synthesized by recombinant Cupriavidus necator H16 from plant oil by using butyrate as a co-substrate*. Journal of Bioscience and Bioengineering. 2015;120(3):246–51.

209. Doi Y, Segawa A, Kawaguchi Y, Kunioka M. *Cyclic nature of poly(3-hydroxyalkanoate) metabolism in Alcaligenes eutrophus*. FEMS Microbiology Letters. 1990;67:165–70.

210. Budde CF, Mahan AE, Lu J, Rha C, Sinskey AJ. *Roles of multiple acetoacetyl coenzyme A reductases in polyhydroxybutyrate biosynthesis in Ralstonia eutropha H16*. Journal of Bacteriology. 2010;192(20):5319–28.

211. Jeon JM, Brigham CJ, Kim YH, Kim HJ, Yi DH, Kim H, Rha CK, Sinskey AJ, Yang YH. *Biosynthesis of poly(3-hydroxybutyrate-co-3-hydroxyhexanoate) (P(HB-co-HHx)) from butyrate using engineered Ralstonia eutropha*. Applied Microbiology and Biotechnology. 2014;98(12):5461–9.

212. Insomphun C, Xie H, Mifune J, Kawashima Y, Orita I, Nakamura S, Fukui T. *Improved artificial pathway for biosynthesis of poly(3-hydroxybutyrate-co-3-hydroxyhexanoate) with high C6-monomer composition from fructose in Ralstonia eutropha*. Metabolic Engineering. 2015;27:38–45.

213. Zhang M, Kurita S, Orita I, Nakamura S, Fukui T. *Modification of acetoacetyl-CoA reduction step in Ralstonia eutropha for biosynthesis of poly(3-hydroxybutyrate-co-3-hydroxyhexanoate) from structurally unrelated compounds*. Microbial Cell Factories. 2019;18(1):1–12.

214. Eggers J, Steinbüchel A. *Poly(3-hydroxybutyrate) degradation in Ralstonia eutropha H16 is mediated stereoselectively to (S)-3-hydroxybutyryl coenzyme a (CoA) via crotonyl-CoA*. Journal of Bacteriology. 2013;195(14):3213–23.

215. Brigham CJ, Budde CF, Holder JW, Zeng Q, Mahan AE, Rha CK, Sinskey AJ. *Elucidation of β-oxidation pathways in Ralstonia eutropha H16 by examination of global gene expression*. Journal of Bacteriology. 2010;192(20):5454–64.

216. Peplinski K, Ehrenreich A, Döring C, Bömeke M, Steinbüchel A. *Investigations on the microbial catabolism of the organic sulfur compounds TDP and DTDP in Ralstonia eutropha H16 employing DNA microarrays*. Applied Microbiology and Biotechnology. 2010;88(5):1145–59.

217. Martin VJJ, Piteral DJ, Withers ST, Newman JD, Keasling JD.

Engineering a mevalonate pathway in Escherichia coli for production of terpenoids. Nature Biotechnology. 2003;21(7):796–802.

218. Mata-Gómez LC, Montañez JC, Méndez-Zavala A, Aguilar CN. *Biotechnological production of carotenoids by yeasts: An overview*. Microbial Cell Factories. 2014;13(1):1–11.

219. Steinbüchel A, Schlegel HG. *Excretion of pyruvate by mutants of Alcaligenes eutrophus, which are impaired in the accumulation of poly(β-hydroxybutyric acid) (PHB), under conditions permitting synthesis of PHB.* Applied Microbiology and Biotechnology. 1989;31(2):168–75.

220. Raberg M, Volodina E, Lin K, Steinbüchel A. *Ralstonia eutropha H16 in progress: Applications beside PHAs and establishment as production platform by advanced genetic tools*. Critical Reviews in Biotechnology. 2018;38(4):494–510.

221. Lee C, Chen AF. *Immobilized coenzymes and derivatives*. In: The Pyridine Nucleotide Coenzymes. 1982. p. 189–218.

222. Raetz CRH. *Enzymology, genetics, and regulation of membrane phospholipid synthesis in Escherichia coli*. Microbiological Reviews. 1978;42(3):614–59.

223. Cronan JE, Littel KJ, Jackowski S. *Genetic and biochemical analysis of pantothenate biosynthesis in Escherichia coli and Salmonella typhimurium*. Journal of Bacteriology. 1982;149(3):916–22.

224. Gerdes SY, Scholle MD, D'Souza M, Bernal A, Baev M V., Farrell M, Kurnasov O V., Daugherty MD, Mseeh F, Polanuyer BM, Campbell JW, Anantha S, Shatalin KY, Chowdhury SAK, Fonstein MY, Osterman AL. *From genetic footprinting to antimicrobial drug targets: Examples in cofactor biosynthetic pathways*. Journal of Bacteriology. 2002;184(16):4555–72.

225. Turnbough CL, Switzer RL. *Regulation of Pyrimidine Biosynthetic Gene Expression in Bacteria: Repression without Repressors*. Microbiology and Molecular Biology Reviews. 2008;72(2):266–300.

226. Boeke JD, La Croute F, Fink GR. *A positive selection for mutants lacking orotidine-5'-phosphate decarboxylase activity in yeast: 5-fluoro-orotic acid resistance*. MGG Molecular & General Genetics. 1984;197(2):345–6.

227. Tripathi SA, Olson DG, Argyros DA, Miller BB, Barrett TF, Murphy DM, McCool JD, Warner AK, Rajgarhia VB, Lynd LR, Hogsett DA, Caiazza NC. *Development of pyrF-Based genetic system for targeted gene deletion in clostridium thermocellum and creation of a pta mutant*. Applied and Environmental Microbiology. 2010;76(19):6591–9.

228. Sakaguchi K, Funaoka N, Tani S, Hobo A, Mitsunaga T, Kano Y, Suzuki T. *The pyrE Gene as a Bidirectional Selection Marker in Bifidobacterium Longum 105-A*. Bioscience of Microbiota, Food and Health. 2013;32(2):59–68.

229. Schneider JC, Jenings AF, Mun DM, McGovern PM, Chew LC. *Auxotrophic markers pyrF and proC can replace antibiotic markers on protein production plasmids in high-cell-density Pseudomonas fluorescens fermentation*. Biotechnology Progress. 2005;21(2):343–8.

230. Ehsaan M, Kuehne SA, Minton NP. *Clostridium difficile Genome Editing Using pyrE Alleles*. In: Clostridium difficile: Methods and Protocols. 2016. p. 35–52.

231. Hoppensack A, Rehm BHA, Steinbüchel A. *Analysis of 4-phosphopantetheinylation of polyhydroxybutyrate synthase from Ralstonia eutropha: Generation of β-alanine auxotrophic Tn5 mutants and cloning of the panD gene region*. Journal of Bacteriology. 1999;181(5):1429–35.

232. Hidese R, Mihara H, Kurihara T, Esaki N. *Pseudomonas putida PydR, a RutR-like transcriptional regulator, represses the dihydropyrimidine dehydrogenase gene in the pyrimidine reductive catabolic pathway*. Journal of Biochemistry. 2012;152(4):341–6.

233. Dasu VV, Nakada Y, Ohnishi-Kameyama M, Kimura K, Itoh Y. *Characterization and a role of Pseudomonas aeruginosa spermidine dehydrogenase in polyamine catabolism*. Microbiology. 2006;152(8):2265–72.

234. Herrmann G, Seimer T, Jessen HJ, Gokarn RR, Selifonova O, Gort SJ, Buckel W. *Two beta-alanyl-CoA:ammonia lyases in Clostridium propionicum*. FEBS Journal. 2005;272(3):813–21.

235. Schmitt U, Jahnke K, Rosenbaum K, Cook PF, Schnackerz KD. *Purification and characterization of dihydropyrimidine dehydrogenase from Alcaligenes eutrophus*. Archives of Biochemistry and Biophysics. 1996;332(1):175–82.

236. Müller J, MacEachran D, Burd H, Sathitsuksanoh N, Bi C, Yeh YC, Lee TS, Hillson NJ, Chhabra SR, Singer SW, Beller HR. *Engineering of Ralstonia eutropha H16 for autotrophic and heterotrophic production of methyl ketones*. Applied and Environmental Microbiology. 2013;79(14):4433–9.

237. Schlegel HG, Lafferty R, Krauss I. *The isolation of mutants not accumulating poly-β-hydroxybutyric acid*. Archiv für Mikrobiologie. 1970;71(3):283–94.

238. Raberg M, Voigt B, Hecker M, Steinbüchel A. *A closer look on the polyhydroxybutyrate- (PHB-) negative phenotype of Ralstonia eutropha PHB-4*. PLoS ONE. 2014;9(5):1–11.

239. Peplinski K, Ehrenreich A, Döring C, Bömeke M, Reinecke F, Hutmacher C, Steinbüchel A. *Genome-wide transcriptome analyses of the "Knallgas" bacterium Ralstonia eutropha H16 with regard to polyhydroxyalkanoate metabolism*. Microbiology. 2010;156(7):2136–52.

240. Liu Q, Ouyang S ping, Kim J, Chen GQ. *The impact of PHB accumulation on l-glutamate production by recombinant Corynebacterium glutamicum*. Journal of Biotechnology. 2007;132(3):273–9.

241. Xu M, Qin J, Rao Z, You H, Zhang X, Yang T, Wang X, Xu Z. *Effect of Polyhydroxybutyrate (PHB) storage on l-arginine production in recombinant Corynebacterium crenatum using coenzyme regulation*. Microbial Cell Factories. 2016;15(1):1–12.

242. Nicolas C, Kiefer P, Letisse F, Krömer J, Massou S, Soucaille P, Wittmann C, Lindley ND, Portais JC. *Response of the central metabolism of Escherichia coli to modified expression of the gene encoding the glucose-6-phosphate dehydrogenase*. FEBS Letters. 2007;581(20):3771–6.

243. Kang Z, Gao C, Wang Q, Liu H, Qi Q. *A novel strategy for succinate and polyhydroxybutyrate co-production in Escherichia coli*. Bioresource Technology. 2010;101(19):7675–8.

244. Better M. *araB EXPRESSION SYSTEM IN Escherichia coli*. Gene Expression Systems. ACADEMIC PRESS; 1999. 95–107 p.

245. Porter RD, Black S, Pannuri S, Carlson A. *Use of the Escherichia coli ssb gene to prevent bioreactor takeover by plasmidless cells*. Nature Biotechnology. 1990;8(1):47–51.

246. Wright O, Stan GB, Ellis T. *Building-in biosafety for synthetic biology*. Microbiology (United Kingdom). 2013;159(PART7):1221–35.

247. Meinander NQ, Hahn-Hägerdal B. *Fed-batch xylitol production with two recombinant Saccharomyces cerevisiae strains expressing XYL1 at different levels, using glucose as a cosubstrate: A comparison of production parameters and strain stability*. Biotechnology and Bioengineering. 1997;54(4):391–9.

248. Foster PL. *Stress-induced mutagenesis in bacteria*. Critical Reviews in Biochemistry and Molecular Biology. 2007;42(5).

249. Tompkins JD, Nelson JL, Hazel JC, Leugers SL, Stumpf JD, Foster PL. *Error-prone polymerase, DNA polymerase IV, is responsible for transient hypermutation during adaptive mutation in Escherichia coli*. Journal of Bacteriology. 2003;185(11):3469–72.

250. Reynolds AE, Felton J, Wright A. *Insertion of DNA activates the cryptic bgl operon in E. coli K12*. Nature. 1981;293:625–9.

251. Zelder O, Hauer B. *Environmentally directed mutations and their impact on industrial biotransformation and fermentation processes*. Current Opinion in Microbiology. 2000;3(3):248–51.

252. Hoffmann F, Rinas U. *Stress induced by recombinant protein production in Escherichia coli.* Advances in Biochemical Engineering/Biotechnology. 2004;89:73–92.

253. Rugbjerg P, Myling-Petersen N, Porse A, Sarup-Lytzen K, Sommer MOA. *Diverse genetic error modes constrain large-scale bio-based production*. Nature Communications. 2018;9(1).

254. Glick BR. *Metabolic load and heterologous gene expression*. Vol. 13, Biotechnology Advances. 1995. p. 247–61.

255. Mairhofer J, Scharl T, Marisch K, Cserjan-Puschmann M, Striedner G. *Comparative transcription profiling and in-depth characterization of plasmid-based and plasmid-free Escherichia coli expression systems under production conditions*. Applied and Environmental Microbiology. 2013;79(12):3802–12.

256. Rugbjerg P, Sommer MOA. *Overcoming genetic heterogeneity in industrial fermentations*. Nature Biotechnology. 2019;37(8):869–76.

257. Hori K, Marsudi S, Unno H. *Simultaneous production of polyhydroxyalkanoates and rhamnolipids by Pseudomonas aeruginosa*. Biotechnology and Bioengineering. 2002;78(6):699–707.

258. Mothes G, Schubert T, Harms H, Maskow T. *Biotechnological coproduction of compatible solutes and polyhydroxyalkanoates using the Genus Halomonas*. In: Engineering in Life Sciences. 2008. p. 658–62.

259. Pósfai G, Plunkett G, Fehér T, Frisch D, Keil GM, Umenhoffer K, Kolisnychenko V, Stahl B, Sharma SS, De Arruda M, Burland V, Harcum SW, Blattner FR. *Emergent properties of reduced-genome Escherichia coli*. Science. 2006;312(5776):1044–6.

260. Lee J, Sung B, Kim M, Blattner FR, Yoon B, Kim J, Kim S. *Metabolic engineering of a reduced-genome strain of Escherichia coli for L-threonine production*. Microbial Cell Factories. 2009;8(1):2.

261. Park MK, Lee SH, Yang KS, Jung SC, Lee JH, Kim SC. *Enhancing recombinant protein production with an Escherichia coli host strain lacking insertion sequences*. Applied Microbiology and Biotechnology. 2014;98(15):6701–13.

262. Csörgo B, Fehér T, Tímár E, Blattner FR, Pósfai G. *Low-mutation-rate, reduced-genome Escherichia coli: An improved host for faithful maintenance of engineered genetic constructs*. Microbial Cell Factories. 2012;11:1–13.

263. Wang J, Niyompanich S, Tai Y-S, Wang J, Bai W, Mahida P, Gao T, Zhang K. *Engineering of a Highly Efficient Escherichia coli Strain for Mevalonate Fermentation through Chromosomal Integration*. Applied and Environmental Microbiology. 2016;82(24):7176–84.

264. Hahn SK, Chang YK, Kim BS, Chang HN. *Optimization of microbial poly(3-hydroxybutyrate) recover using dispersions of sodium hypochlorite solution and chloroform*. Biotechnology and Bioengineering. 1994;44(2):256–61.

265. Aoyagi Y, Doi Y, Iwata T. *Mechanical properties and highly ordered structure of ultra-high-molecular-weight poly[(R)-3-hydroxybutyrate] films: Effects of annealing and two-step drawing*. Polymer Degradation and Stability. 2003;79(2):209–16.

266. Matsumoto K, Kageyama Y. *Increased production and molecular weight of artificial polyhydroxyalkanoate poly(2-hydroxybutyrate) above the glass transition temperature threshold*. Frontiers in Bioengineering and Biotechnology. 2019;7(JUL):1–5.

267. Lee SY, Lee KM, Chang HN, Steinbuchel A. *Comparison of Recombinant Escherichia coli Strains for Synthesis and Accumulation of Poly-(3-hydroxybutyric Acid) and Morphological Changes*. Biotechnology and Bioengineering. 1994;44(11):1337–47.

268. de Souza Pinto Lemgruber R, Valgepea K, Tappel R, Behrendorff JB, Palfreyman RW, Plan M, Hodson MP, Simpson SD, Nielsen LK, Köpke M, Marcellin E. *Systems-level engineering and characterisation of Clostridium autoethanogenum through heterologous production of poly-3-hydroxybutyrate (PHB)*. Metabolic Engineering. 2019;53(January):14–23.

269. Hein S, Söhling B, Gottschalk G, Steinbüchel A. *Biosynthesis of poly(4-hydroxybutyric acid) by recombinant strains of Escherichia coli*. FEMS Microbiology Letters. 1997;153(2):411–8.

270. Jung YK, Lee SY. *Efficient production of polylactic acid and its copolymers by metabolically engineered Escherichia coli*. Journal of Biotechnology. 2011;151(1):94–101.

271. Shen XW, Yang Y, Jian J, Wu Q, Chen GQ. *Production and characterization of homopolymer poly(3-hydroxyvalerate) (PHV) accumulated by wild type and recombinant Aeromonas hydrophila strain 4AK4*. Bioresource Technology. 2009;100(18):4296–9.

272. Lv L, Ren YL, Chen JC, Wu Q, Chen GQ. *Application of CRISPRi for prokaryotic metabolic engineering involving multiple genes, a case study: Controllable P(3HB-co-4HB) biosynthesis*. Metabolic Engineering. 2015;29:160–8.

273. Yoon J, Chang W, Oh SH, Choi SH, Yang YH, Oh MK. *Metabolic engineering of Methylorubrum extorquens AM1 for poly (3-hydroxybutyrate-co-3-hydroxyvalerate) production using formate*.

International Journal of Biological Macromolecules. 2021;177:284–93.

274. Insomphun C, Mifune J, Orita I, Numata K, Nakamura S, Fukui T. *Modification of β-oxidation pathway in Ralstonia eutropha for production of poly(3-hydroxybutyrate-co-3-hydroxyhexanoate) from soybean oil*. Journal of Bioscience and Bioengineering. 2014;117(2):184–90.

275. Park SJ, Ahn WS, Green PR, Lee SY. *Biosynthesis of poly(3-hydroxybutyrate-co-3-hydroxyvalerate-co-3-hydroxyhexanoate) by metabolically engineered Escherichia coli strains*. Biotechnology and Bioengineering. 2001;74(1):81–6.

276. Shen R, Yin J, Ye JW, Xiang RJ, Ning ZY, Huang WZ, Chen GQ. *Promoter Engineering for Enhanced P(3HB- co-4HB) Production by Halomonas bluephagenesis*. ACS Synthetic Biology. 2018;7(8):1897–906.

277. Jung HR, Jeon JM, Yi DH, Song HS, Yang SY, Choi TR, Bhatia SK, Yoon JJ, Kim YG, Brigham CJ, Yang YH. *Poly(3-hydroxybutyrate-co-3-hydroxyvalerate-co-3-hydroxyhexanoate) terpolymer production from volatile fatty acids using engineered Ralstonia eutropha*. International Journal of Biological Macromolecules. 2019;138:370–8.

278. Cheema S, Bassas-Galia M, Sarma PM, Lal B, Arias S. *Exploiting metagenomic diversity for novel polyhydroxyalkanoate synthases: Production of a terpolymer poly(3-hydroxybutyrate-co-3-hydroxyhexanoate-co-3-hydroxyoctanoate) with a recombinant Pseudomonas putida strain*. Bioresource Technology. 2012;103(1):322–8.

279. Poblete-Castro I, Binger D, Rodrigues A, Becker J, Martins Dos Santos VAP, Wittmann C. *In-silico-driven metabolic engineering of Pseudomonas putida for enhanced production of poly-hydroxyalkanoates*. Metabolic Engineering. 2013;15(1):113–23.

280. Kadoya R, Matsumoto K, Ooi T, Taguchi S. *MtgA deletion-triggered cell enlargement of Escherichia coli for enhanced intracellular polyester accumulation*. PLoS ONE. 2015;10(6):1–11.

281. Yang TH, Kim TW, Kang HO, Lee SH, Lee EJ, Lim SC, Oh SO, Song AJ, Park SJ, Lee SY. *Biosynthesis of polylactic acid and its copolymers using evolved propionate CoA transferase and PHA synthase*. Biotechnology and Bioengineering. 2010;105(1):150–60.

282. Li T, Ye J, Shen R, Zong Y, Zhao X, Lou C, Chen GQ. *Semirational Approach for Ultrahigh Poly(3-hydroxybutyrate) Accumulation in Escherichia coli by Combining One-Step Library Construction and High-Throughput Screening*. ACS Synthetic Biology. 2016;5(11):1308–17.

283. Hu D, Chung AL, Wu LP, Zhang X, Wu Q, Chen JC, Chen GQ.

Biosynthesis and characterization of polyhydroxyalkanoate block copolymer P3HB-b-P4HB. Biomacromolecules. 2011;12(9):3166–73.

284. Tohyama M, Shimizu K. *Control of a mixed culture of Lactobacillus delbrueckii and ralstonia eutropha for the production of PHB from glucose via lactate*. Biochemical Engineering Journal. 1999;4(1):45–53.

285. Tsuge T. *Metabolic improvements and use of inexpensive carbon sources in microbial production of polyhydroxyalkanoates*. Journal of Bioscience and Bioengineering. 2002;94(6):579–84.

286. Singh M, Kumar P, Ray S, Kalia VC. *Challenges and Opportunities for Customizing Polyhydroxyalkanoates*. Indian Journal of Microbiology. 2015;55(3):235–49.

287. Furukawa T, Sato H, Kita Y, Matsukawa K, Yamaguchi H, Ochiai S, Siesler HW, Ozaki Y. *Molecular structure, crystallinity and morphology of polyethylene/ polypropylene blends studied by Raman mapping, scanning electron microscopy, wide angle X-ray diffraction, and differential scanning calorimetry*. Polymer Journal. 2006;38(11):1127–36.

288. Li SY, Dong CL, Wang SY, Ye HM, Chen GQ. *Microbial production of polyhydroxyalkanoate block copolymer by recombinant Pseudomonas putida*. Applied Microbiology and Biotechnology. 2011;90(2):659–69.

289. Doi Y. *Microbial Polyesters*. New York: VCH Publishers; 1990.

290. Doi Y, Kitamura S, Abe H. *Microbial Synthesis and Characterization of Poly(3-hydroxybutyrate-co-3-hydroxyhexanoate).* Macromolecules. 1995;28(14):4822–8.